Chapter 1.0, INTRODUCTION

This thesis involves research investigations which have included two different areas of polymer science. The first has been concerned with the synthesis and characterization of high performance poly(arylene ether)s, which are engineering thermoplastics well known to be important in a wide variety of applications such as structural resins, gaskets, tubing, and microelectronic components. Furthermore, light weight structural thermoplastics are often preferred relative to their metallic or ceramic counterparts. Poly(arylene ether)s (PAE) have received considerable attention as a consequence of a wide range of physical and chemical properties resulting from the variation in structure of the backbone, and were synthesized *via* nucleophilic aromatic substitution step growth or condensation polymerization of an activated dihalide with an aromatic bisphenol.

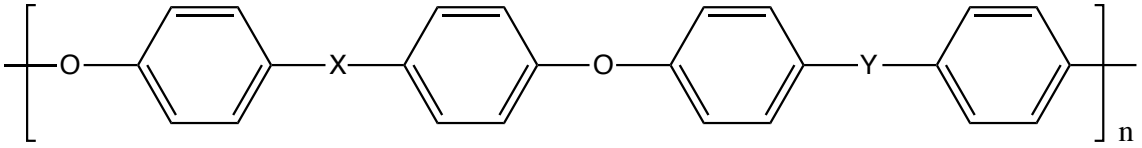

Figure 1.1 A generic representation of poly(arylene ether) backbone structure

Figure 1.1 represents a PAE where X is commonly a carbonyl or sulfone moiety derived from the activated dihalide and Y is a connecting unit that could be, for example, a similar functional group, isopropylidene, or a chemical bond. Utilizing the aryl phosphine oxide moiety as the activating group X contributes to several high performance characteristics. Thus, poly(arylene ether phosphine oxide)s (PEPO)s display high thermal stability, inherent flame resistance and have also shown potential as high temperature matrix resins and/or adhesives. This thesis will describe new research studies which have been directed towards the synthesis of novel PEPOs and the investigations of their molecular weights, thermal behavior, dynamic mechanical properties, stress-strain behavior, and flame resistance.

Hydrolytically stable phosphorus containing monomers, specifically 4,4'-bis(fluorophenyl)methylphosphine oxide (BFPMPO), 4,4'-bis(hydroxyphenyl)methylphosphine oxide (BOHPMPO), and 4,4-bis(hydroxyphenyl)phenylphosphine oxide (BOHPPO) have been synthesized and used in nucleophilic aromatic substitution polycondensation to prepare poly(arylene ether phosphine oxide)s. The synthesis and characterization of these novel polymers are described herein. It was determined that by incorporating the phenyl or methyl phosphine oxide moiety into a polymeric backbone certain properties of the resulting poly(arylene ether) were substantially improved, such as an increase in T_g, thermal stability in air, modulus, and char yield

compared with control poly(arylene ether sulfone)s. The high char yields obtained for these polymers in air along with observed intumescence and cone calorimetry measurements indicates that these materials have improved fire resistance.

This research also focused on comparing the degradation behavior of a commercial polyether sulfone, Victrex, with a phosphorus containing poly(arylene ether phosphine oxide sulfone). Through GC-MS connected to an on-line pyrolysis unit it was possible to analyze the degradation mechanisms. Thermal degradation was studied under both inert and air environments and their volatile products and residual char have been analyzed.

The second part of this thesis focused on the synthesis and characterization of novel poly(arylene ether ionomers) which have not previously been prepared and on their potential use in second-order nonlinear optics. Poly(arylene ether)s can be designed to be optically clear materials with excellent hydrolytic and thermal stability as well as good electrical and mechanical properties as introduced above. It was thus of interest to investigate these materials in second order non-linear optical applications (1). Previously, poly(arylene ether)s have been doped with a variety of compatible chromophores, but the resulting blends showed a considerably depressed Tg, compared to the base polymeric material (2). Chromophores have now been ionically attached to a high performance polymeric backbone using an ion exchange reaction to attempt to avoid this plasticizing effect. The systems described in this thesis show no depression of Tg and preliminary results regarding low temperature corona poling and subsequent stable second harmonic generation of these materials indicate that they may have promise in nonlinear optical applications.

Chapter 2.0, BACKGROUND

2.1 Aromatic Substitution Mechanisms

Poly(arylene ether)s (PAE)s have been synthesized using a variety of different methods, including nucleophilic aromatic substitution (3-10), ring opening of arylene ether cyclics (11,12, 13, 14), silyl ether displacement (15), electrophilic substitution (16-18) and catalytic coupling (20-22). This review chapter will focus on nucleophilic aromatic substitution routes, with emphasis on applications to the synthesis of poly(arylene ether)s. Aromatic electrophiles may undergo nucleophilic substitution reactions *via* different fundamental reaction mechanisms including S_N1, aryne, $S_{RN}1$, S_NAr (18-25). Each of these reaction mechanisms will be reviewed.

2.1.1 S_N1

The S_N1 mechanism for aromatic substitution can be illustrated below to begin with a loss of nitrogen, to form an aromatic cation, followed by nucleophilic attack of a suitable reagent on the reactive cation (26, 29-31).

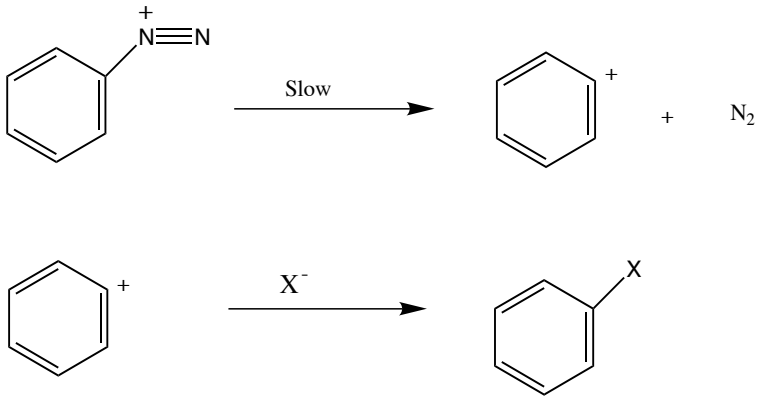

Figure 2.1.1.1 General Mechanism of S_N1 aromatic substitution

The rate of this reaction is affected by different substituents on the aromatic ring (26, 32). For example, it is usually proposed that electron donating groups can stabilize the diazonium cation through the donation of elections by both induction and/or resonance, depending on their position on the aromatic ring. Substituents in the meta position are only capable of stabilizing through induction whereas substituents in the ortho or para position may stabilize the cation *via* both induction and resonance as shown in Figure 2.1.1.2 (26, 29, 32). The effect of substituents on

the rate of diazonium salt decomposition is complicated and is the product of electronic and inductive effects (32). As shown in Figure 2.1.1.1, the positive charge moves from the nitrogen to the aromatic ring, hence inductively electron donating substituents would increase the reaction rate. As illustrated in Table 2.1.1.1, the reaction rate increases as the ability of a *m*-substituent to inductively donate electrons increases due to stabilization of the aryl cation (32, 33).

Table 2.1.1.1 Experimentally observed rate constants (10^{-7} sec^{-1}) for the decomposition of alkyl benzenediazonium ions (33)

Substituent	Ortho	Meta	Para
-OH	6.8	9100	0.93
$-OCH_3$	-----	3400	0.11
$-CH_3$	3700	3400	91
-H	740	740	740
-Cl	0.14	31	1.4
$-NO_2$	0.37	0.69	3.1

However, the same trend is not observed for para or ortho substituents. For example, the order of the rate constants for *p*-substituents is as follows OCH_3<Cl<NO_2<CH_3<H. This confusing order is a direct result of both the resonance and inductive contributions. As shown in Figure 2.1.1.2, *p*-substituents, such as methoxy that are able to donate electrons through resonance thus strengthening the Ar-N bond thereby decreasing rate of the rate controlling aryl cation formation (26, 29, 32). Electron donating substituents such as methyl donate primarily through induction, and therefore, have little effect on the Ar-N bond strength and increase the rate of reaction. Conversely, electron withdrawing substituents (e.g., Cl and NO_2) would be expected to destabilize the cation, thus retarding the reaction.

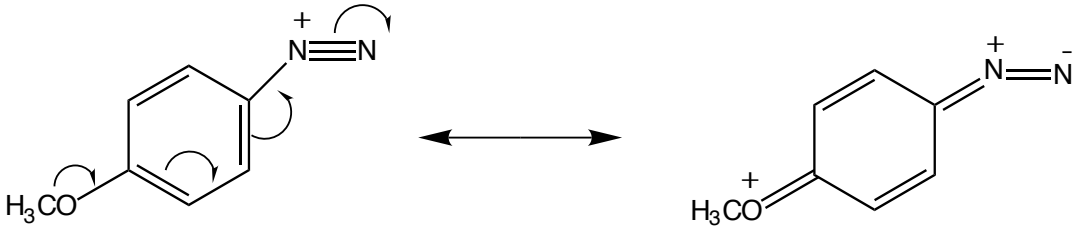

Figure 2.1.1.2 Stabilization of azonium cation through resonance

2.1.2 Aryne

Nucleophilic aromatic substitution may also occur *via* an aryne mechanism (26, 34, 35). This mechanism generally takes place on non-activated aryl halides in the presence of a strong base such as potassium amide. The first step of the reaction involves the elimination of a proton and leaving group to form an aryne. Subsequent attack of a nucleophile yields the substitution product. This mechanism is illustrated in Figure 2.1.2.1.

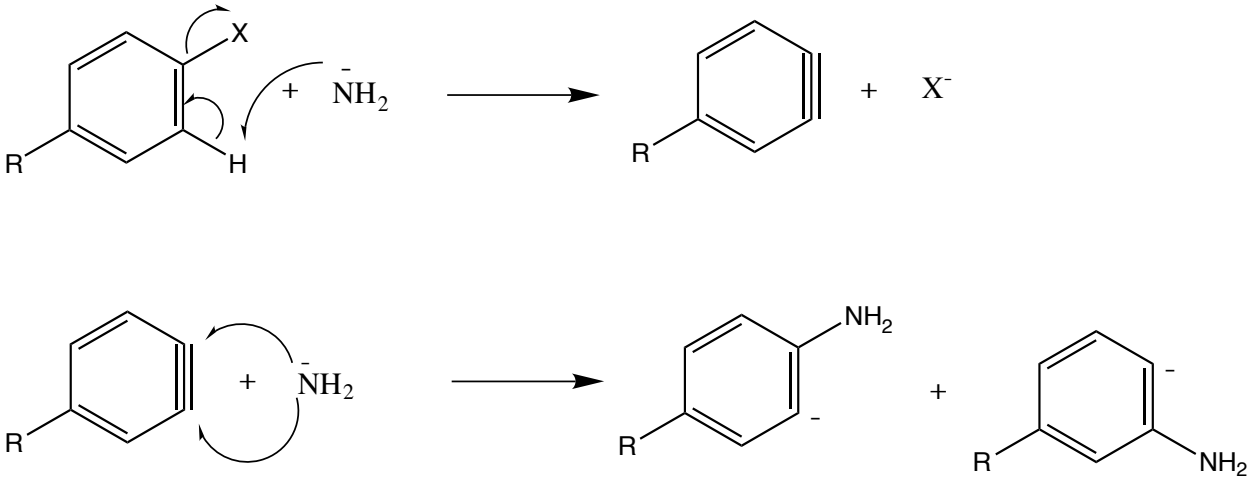

Figure 2.1.2.1 Nucleophilic substitution *via* an aryne mechanism

The aryne mechanism yields two products that result from nucleophilic attack at both aryne carbons (34) and the rate of reaction is governed by two factors. Firstly, the rate at which the proton is removed is important (26). When X=fluorine, the proton is easier to remove than when X=iodine, which stems from the electron withdrawing nature of fluorine. As illustrated in Figure 2.1.2.2 fluorine can create a larger partial positive charge on its adjacent carbon than iodine, which allows the proton to be more easily removed.

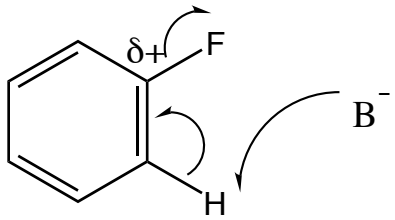

Figure 2.1.2.2 Mechanism for nucleophilic substitution *via* an aryne mechanism

Second, is the ease at which the C-X bond may be broken (26). Iodine is a better leaving group than fluorine because a weaker C-I bond is easier to break than a C-F bond. The combination of

these two factors leads to the following order for the relative reactivity of halogens as leaving groups Br>I>Cl>F in an aryne mechanism.

While the S_N1 and aryne mechanisms for nucleophilic aromatic substitution are important, these mechanisms do currently not play a major role in the synthesis of poly(arylene ether)s. Poly(arylene ether ketones) have been prepared by the electrophilic substitution (36) of, for example, diphenyl ether with terephthaloyl chloride, but the majority of poly(arylene ether)s are synthesized *via* an S_NAr mechanism. However, this nucleophilic aromatic substitution reaction may have a $S_{RN}1$ side reaction in many cases that can limit the molecular weight of the macromolecule (5, 7, 24, 28, 26-33, 34). The rest of this section will concentrate on two reaction pathways for the synthesis of poly(arylene ether); S_NAr and $S_{RN}1$. Figure 2.1.2.3 represents a PAE where X is usually a carbonyl, sulfone (22), or, more recently phosphine oxide (37, 38) and Y is a connecting unit that could be a similar functional group, isopropylidene, or a chemical bond, etc. as discussed earlier.

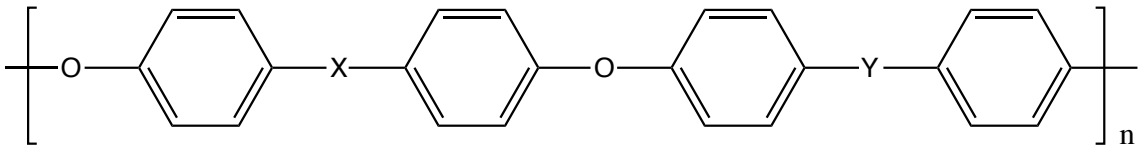

Figure 2.1.2.3 A generic representation of poly(arylene ether) backbone structure

2.1.3 $S_NA R$

The principal method for nucleophilic aromatic substitution step growth polymerization follows the S_NAr mechanism (26, 29, 34). Figure 2.1.3.1 illustrates the basic chemistry of an S_NAr reaction. The first usually rate determining step, involves nucleophilic attack of a phenate on the activated dihalide to form a Meisenheimer complex. Next, this intermediate eliminates a halogen anion by product and forms an ether linkage.

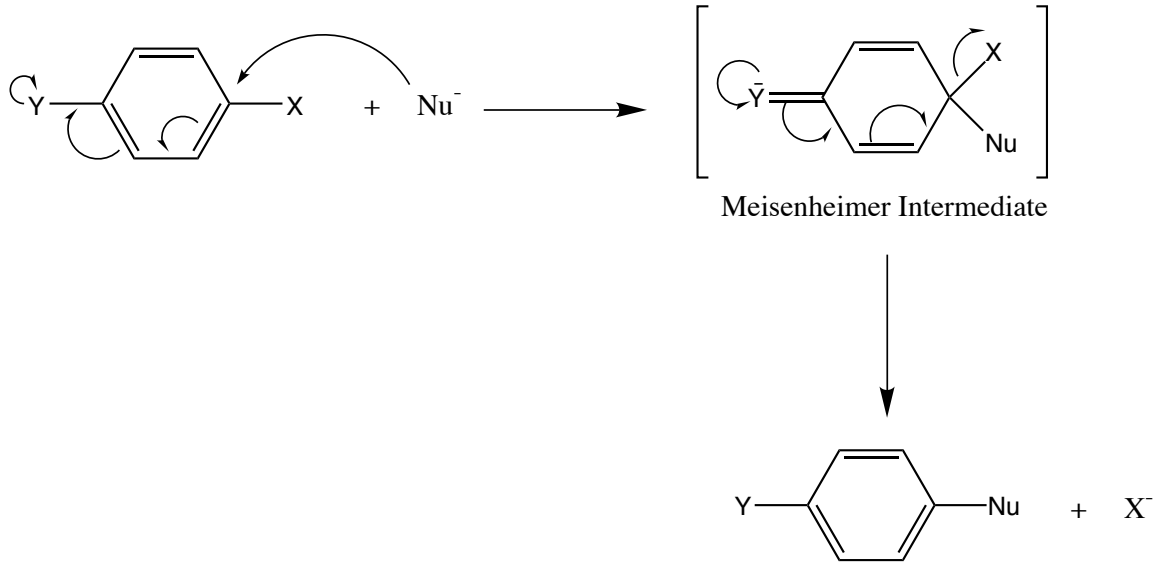

Figure 2.1.3.1 Illustration of the S_NAr mechanism

The successful synthesis of PAEs that achieved high molecular weight *via* nucleophilic aromatic substitution was first reported by Johnson *et al*. in 1965 (39). This reaction involves the nucleophilic addition of a bisphenate to an activated dihalide utilizing an aprotic dipolar solvent (DMSO) *via* S_NAr chemistry under anhydrous conditions. The low water concentrations reduced the possibility of molecular weight limiting halide hydrolysis reactions. Figure 2.1.3.2 illustrates the S_NAr mechanism as it applies to poly(arylene ether) synthesis where X is fluorine or chlorine, Z is an electron withdrawing moiety, and M is a metal ion, usually sodium or potassium. In this reaction the electron withdrawing group on the bisarylhalide monomer activates the aromatic ring towards nucleophilic attack by lowering the energy of the Meisenheimer complex by stabilizing the negative charge and the halide plays a critical role in stabilizing the initial addition product. (26, 28)

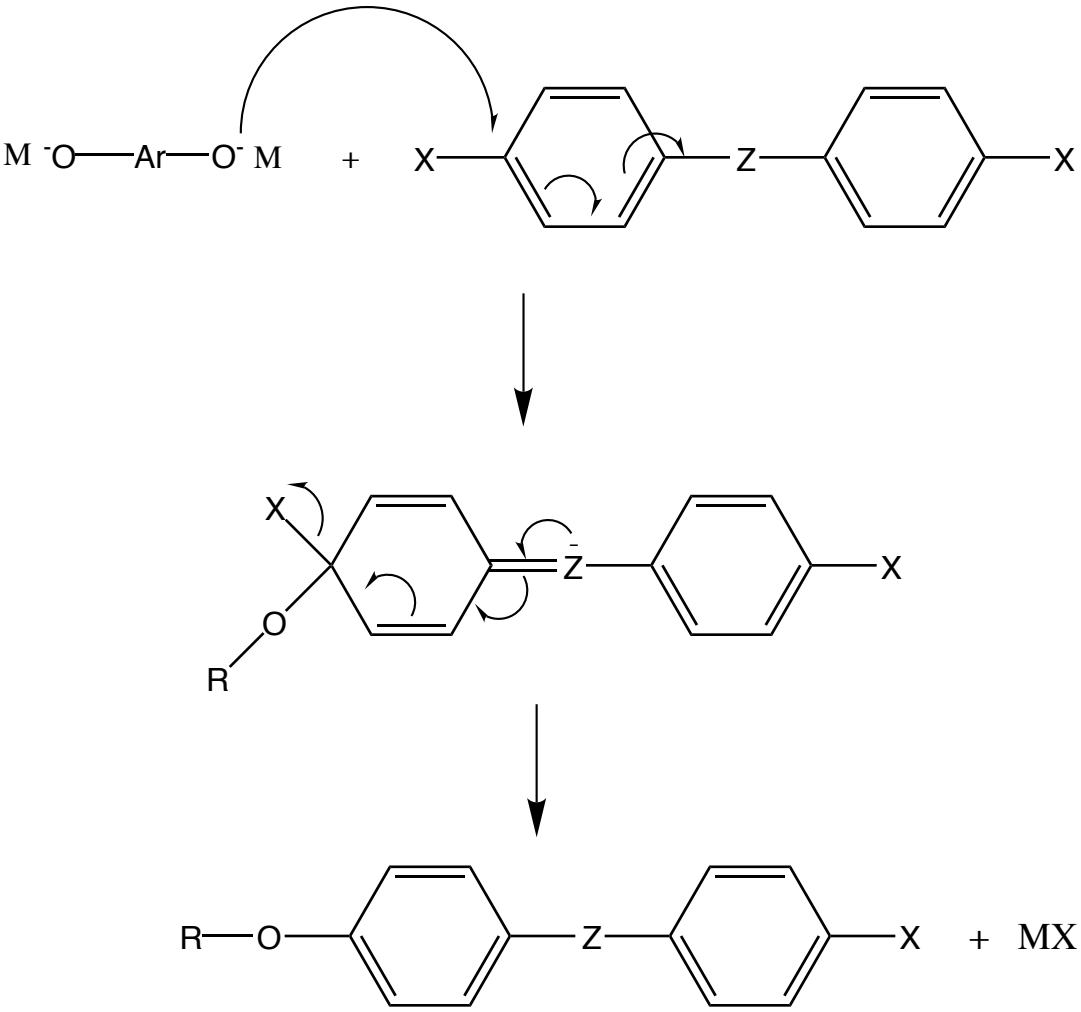

X = F or Cl

Z = Electron withdrawing group

M = K^+ or Na^+

Figure 2.1.3.2 S_NAr mechanism for the synthesis of poly(arylene ether)s

The leaving group of the activated dihalide monomer is important and is usually fluorine or chlorine. For similar monomers, a fluorine containing activated dihalide is more reactive than a chlorine containing one (26, 29). The halogen activates the C_{ipso} towards nucleophilic attack by withdrawing electrons, thereby creating a δ+ charge on the C_{ipso}. Fluorine is a stronger electron withdrawing atom than chlorine and similar dihalide monomers containing fluorine instead of chlorine are observed to be more reactive. The effect of the leaving group upon the rate of reaction is F>Cl>Br>>I (26). In addition, fluorine containing monomers are reported to be less likely to undergo $S_{RN}1$ side reactions than their chlorine counterparts (24, 28, 39). This side reaction can limit the molecular weight in a step growth polymerization and is discussed in detail in section 2.1.4. Figure 2.1.3.2 illustrates that both bisphenol hydroxyls form diphenoxy species that then attacks the activated dihalide, which is not always the case. Thus, when potassium hydroxide is used as the base the diphenolate species may be formed (3-6, 39, 40-47, 48-53), but the weak base potassium carbonate tends to generate initially only a single phenoxide species which reacts prior to the second phenolate formation (54, 55).

2.1.4 $S_{RN}1$

Poly(arylene ether sulfone)s, poly(arylene ether ketone)s, and poly(arylene ether phosphine oxide)s are usually synthesized by the reaction of an activated dihalide with a bisphenate. As shown in Figure 2.1.4.1, the activated dihalide may contain fluorine or chlorine. However, if the activating moiety is a carbonyl then a drastic difference in the molecular weight is obtained, which is a function of the halide utilized (24, 28, 39, 56). In general, fluorine allows for high molecular weight polymer to be obtained. However, if chlorine is utilized, then low molecular weight in often observed. If the lower molecular weight were due to the decreased reactivity of the activated dihalide then a longer reaction time should yield higher molecular weight, but this is often not the case. Therefore, it is generally accepted that this difference in molecular weight is due to reductive elimination of chlorine from the activated dihalide through a $S_{RN}1$ mechanism. In order to understand this reasoning, it is necessary to analyze the $S_{RN}1$ mechanism.

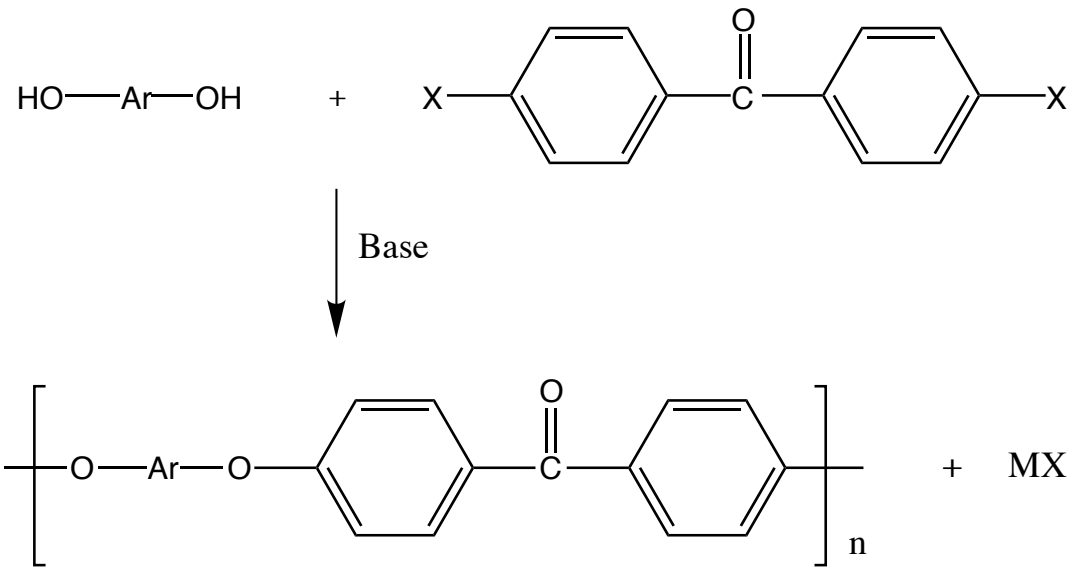

Where X = F or Cl

Figure 2.1.4.1 Synthesis of poly(arylene ether ketone)s utilizing two different activated dihalides

The $S_{RN}1$ mechanism is comprised of three steps, which are illustrated in Figure 2.1.4.2 and consist of; initiation, propagation, and termination (26, 28, 29, 57, 58). In step 1 a radical anion is formed from the aryl halide *via* electron transfer. This may occur through an electron transfer from a radical anion or, possibly by another chemical reaction. The radical anion dissociates into an aryl radical and a halogen anion (step 2). Step 3 consists of a reaction between the aryl radical and a nucleophile, forming another radical anion. Then the radical undergoes electron transfer, which can further propagate the chain. However, as shown in steps 5 and 6, instead of propagating the aryl radical can also undergo termination. This may involve hydrogen abstraction by either an aryl radical or aryl anion to terminate the propagating chain. (28)

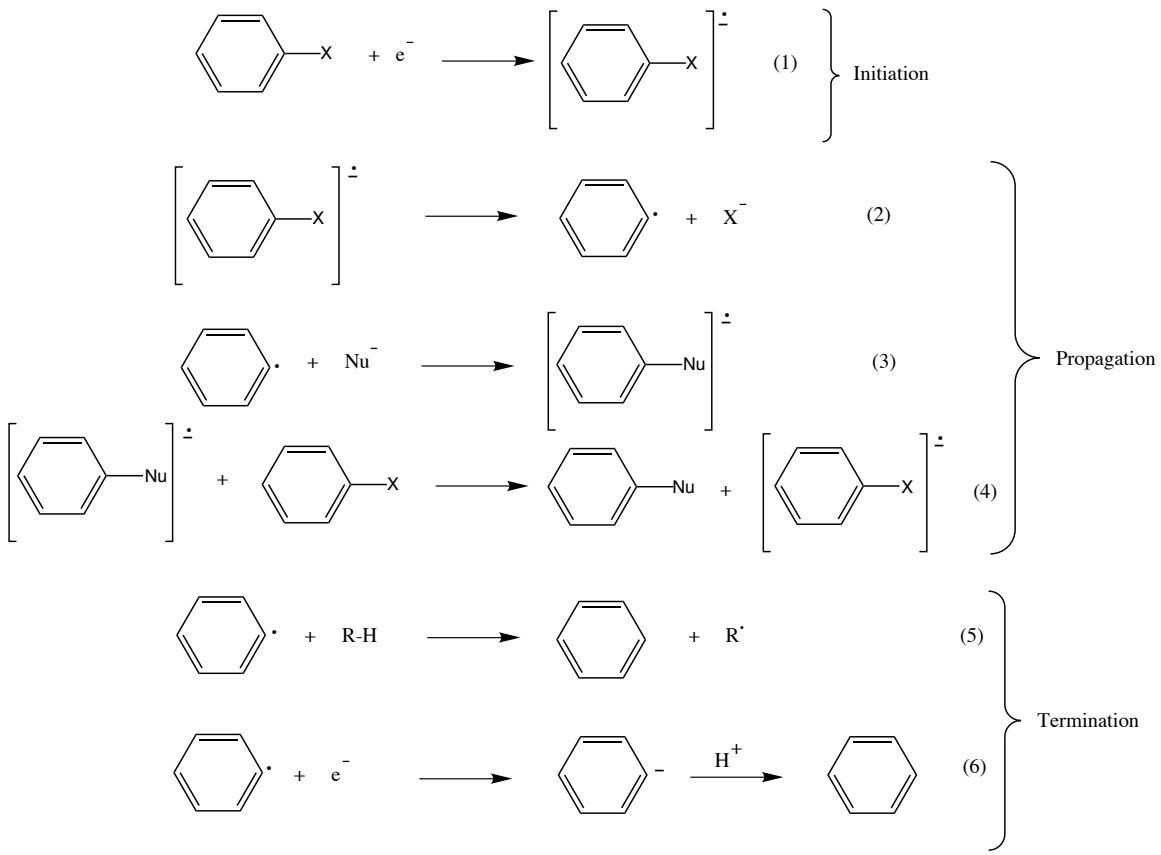

Figure 2.1.4.2 A proposed mechanism for $S_{RN}1$ aromatic substitution reaction (28)

With this background Percec and Clough (28, 59) proposed a possible $S_{RN}1$ side reaction that would either endcap a polymer chain with a non-reactive endgroup and/or upset the stoichiometry of the reaction. Either of these results would result in low molecular weight polymers. In this $S_{RN}1$ side reaction the activated halide undergoes single electron transfer (SET) with a bisphenate. The radical anion may also propagate by combining with the phenoxy radical, thus forming an ether linkage. However, this radical anion may also dissociate into an aryl radical and a halogen anion leading to chain termination. This latter side reaction is illustrated in Figure 2.1.4.3.

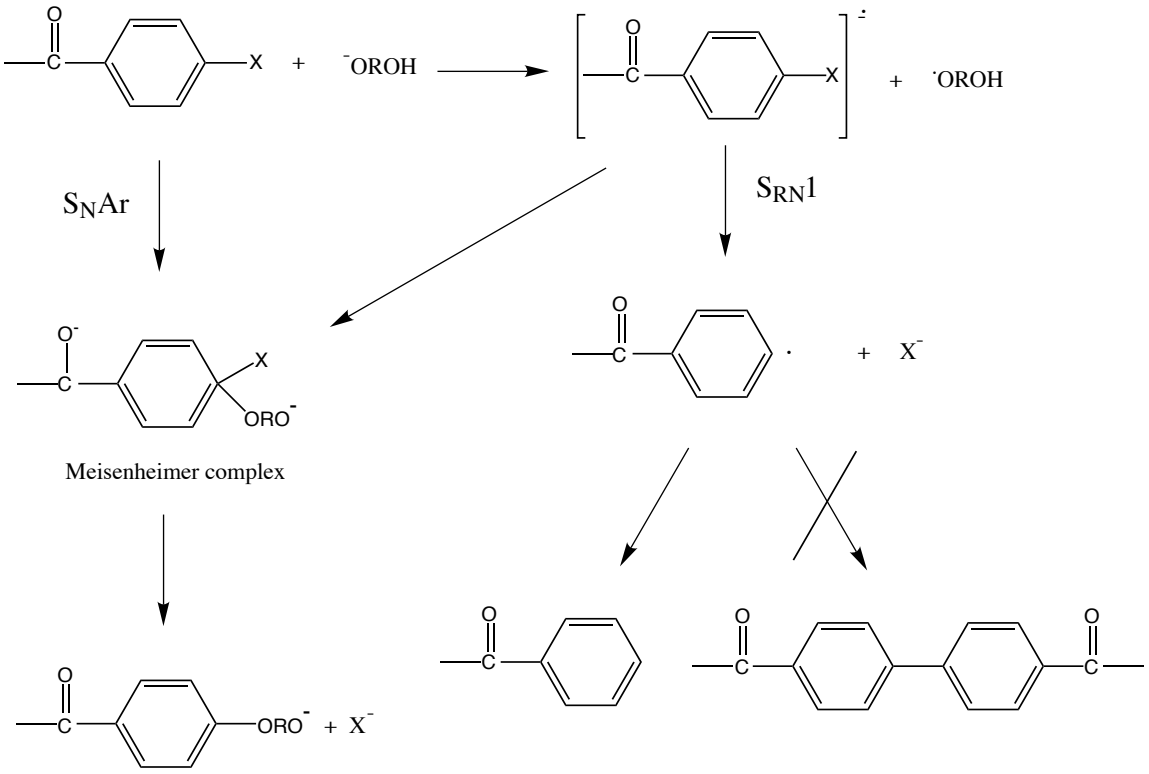

Figure 2.1.4.3 Possible $S_{RN}1$ side reaction during nucleophilic aromatic substitution (28)

This $S_{RN}1$ side reaction pathway was confirmed by Mohanty *et al.* who successfully suppressed the $S_{RN}1$ reaction through the addition of a radical scavenger, which allowed them to obtain high molecular weight poly(arylene ether) even with 4,4'-dichlorobenzophenone activated dihalide (24). There are other methods for eliminating the $S_{RN}1$ pathway, which include using a more reactive nucleophile and by selecting a solvent that does not favor the single electron transfer (SET) route (24, 28).

2.2 Overview of Phosphorus Chemistry

2.2.1 Introduction

Excellent books are now available on the fundamental features of organophosphorus chemistry (60, 61). Moreover, the incorporation of phosphorus into polymers has been discussed (37, 62-64). Figure 2.2.1.1 illustrates various classes of organophosphorus compounds. The focus of this section will be to give an overview of different synthetic routes for the synthesis of hydrolytically stable carbons bonded to phosphorus, such as phosphines and phosphine oxides.

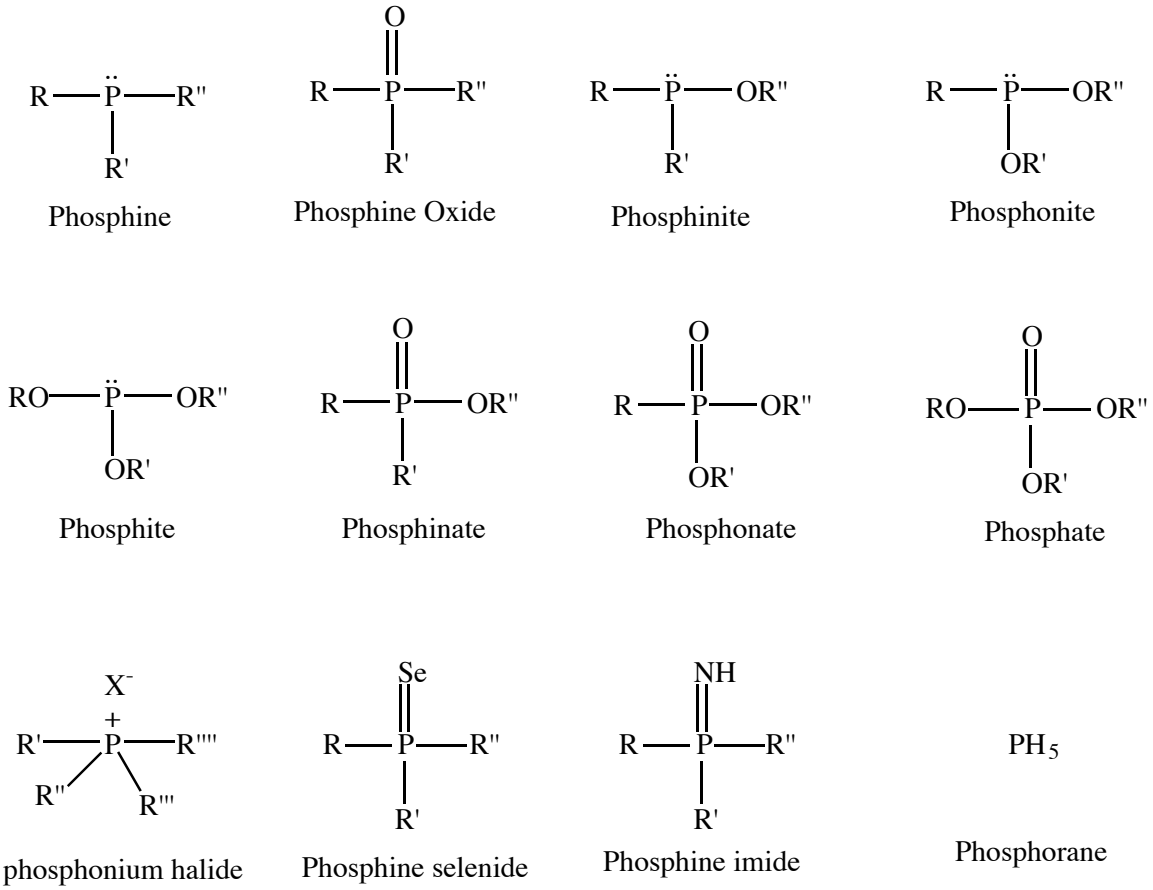

Figure 2.2.1.1 Nomenclature for selected classes of phosphorus compounds

Phosphorus compounds have found many important commercial applications including fertilizer in the form of $CaHPO_4$, along with detergents, animal feed, fire retardants, and even in the pharmaceutical industry. Trivalent phosphorus compounds have also been utilized as antioxidants and stabilizers in rubbers and plastics (60, 61).

2.2.2 Synthetic Routes for the Synthesis of Phosphines and Phosphine Oxides

Phosphines may be synthesized using a variety of techniques including Grignard and organolithium reagents. The synthesis of phosphines using Grignard chemistry starting with phosphorus trichloride follows the form of the equation below (60).

$$PCl_3 + 3RMgX \longrightarrow R_3P + 3MgXCl$$

The phosphorus halide is added to the preformed Grignard reagent in this reaction. After hydrolysis the product is usually separated using ether and purified (65, 66). Grignard syntheses allows for high yields with non-sterically hindered phosphines and primary or aryl Grignard reagents (60, 66-71). Organolithium compounds are the reagents of choice if steric hindrance is important. Attempted syntheses using secondary or tertiary halides produce only low yields of tertiary phosphine (66). This Grignard chemistry can also be applied to the synthesis of phosphine oxides; for example, Kormachev *et al.* (71, 73) showed that dialkylaryl and alkylaryl phosphine oxides could be synthesized using alkyl Grignard reagents, as illustrated by the equations below.

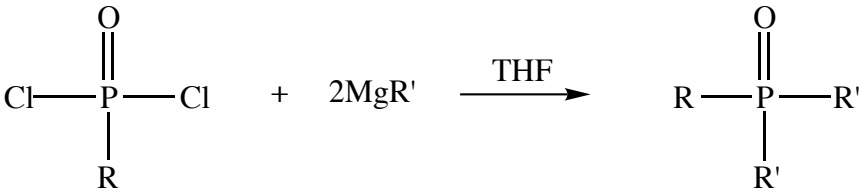

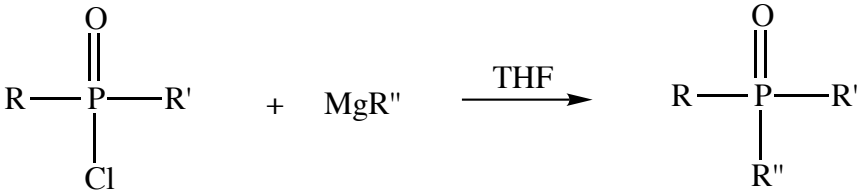

A wide variety of phosphines and phosphine oxides have been synthesized utilizing Grignard chemistry and only a selected few are shown in Figure 2.2.2.1.

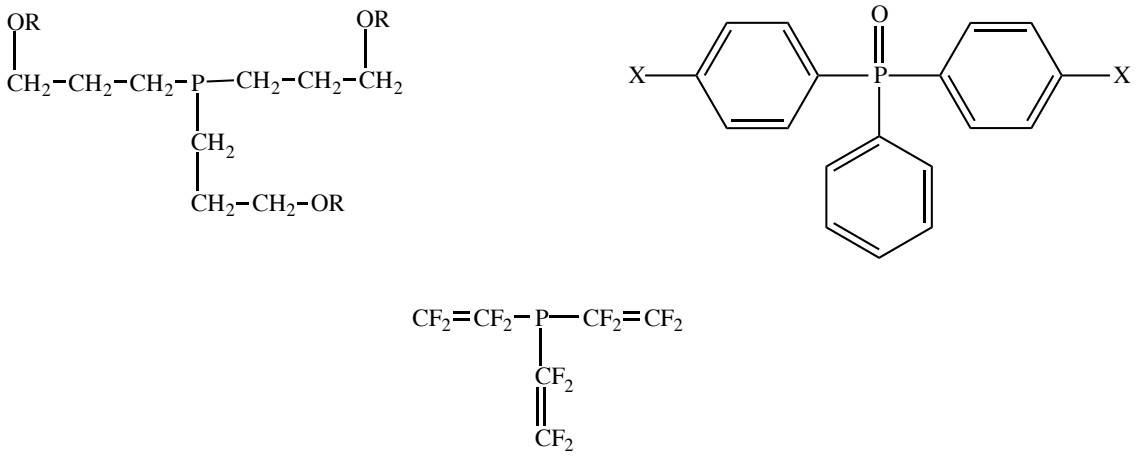

Figure 2.2.2.1 Examples of phosphorus containing compounds synthesized *via* Grignard chemistry

Phosphines may also be synthesized using organolithium reagents (70, 74-76). The synthesis of phosphines using organolithium reagents follows the form of the equation below.

$$3RLi + PCl_3 \longrightarrow R_3P + LiCl$$

Organolithium compounds undergo similar reactions as Grignard reagents; however, they are much more reactive since the carbanion derived from a C-Li bond is more basic than that of the C-Mg bond (74). The organolithium route is preferred for the synthesis of sterically hindered phosphines such as tri-tert-butylphosphine (70). A wide variety of sterically hindered phosphines have been synthesized using organolithium chemistry and several examples are shown in Figure 2.2.2.2.

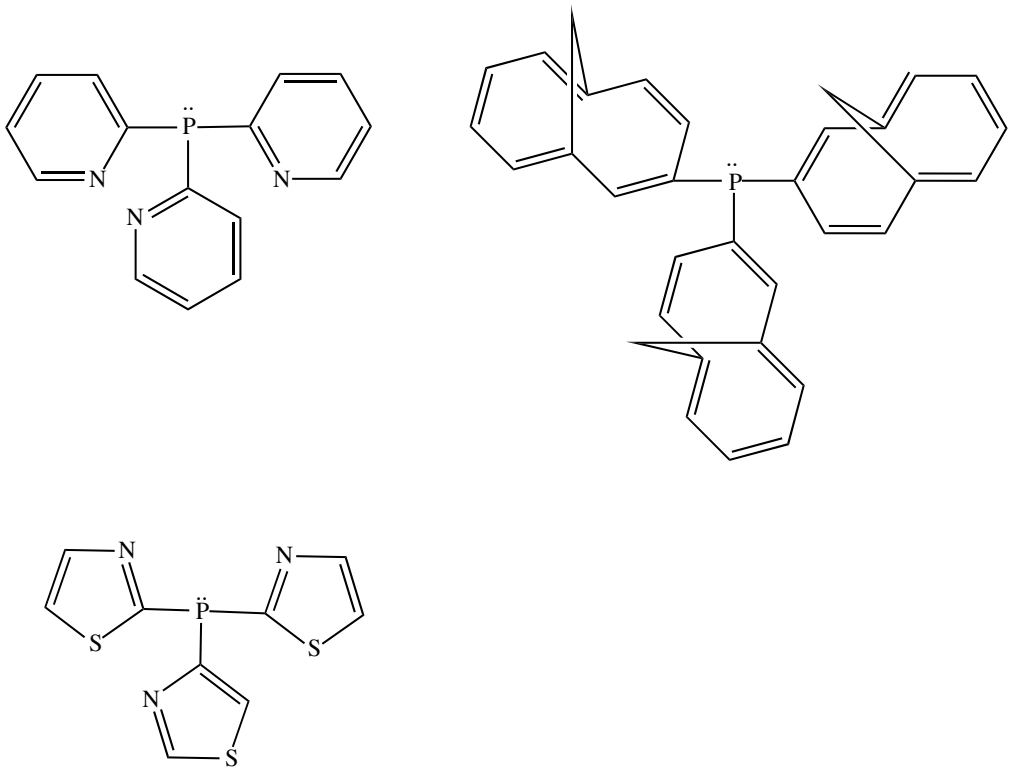

Figure 2.2.2.2 Selected sterically hindered phosphines synthesized using organolithium reagents (60)

In addition, various phosphines and phosphine sulfides may be synthesized *via* electrophilic substitution using Friedel-Crafts chemistry. In this electrophilic synthesis, the starting material is generally a mono-di-or tri-halophosphine or phosphine sulfide. In the case of thiophosphorus trichloride ($PSCl_3$) it is possible to perform sequential additions of benzene or substituted benzene reagents to prepare compounds of the structure bis(R)R'phosphine sulfide (61, 77-80). Therefore, it is possible to prepare such a compound from thiophosphorus trichloride by first reacting $P(S)Cl_3$ with a slight excess of R and then subsequently with excess R'. This reaction has been studied in detail by Weiss and Kliener (78), who demonstrated that bis(chlorophenyl)tolylphosphine sulfide could be synthesized from the reaction of 1 mole of $PSCl_3$ in the presence of 1.79 moles of $AlCl_3$ and 2.2 moles of chlorobenzene, refluxed in cyclohexane for 8 hours, followed by subsequent addition of toluene (3 mol) and further refluxing for 5 hours. The reaction gave the desired product in about 80% yield as shown in Figure 2.2.2.3. Similar work has also been carried out by Wescott in our group for involving the synthesis of 4,4'-bis(fluorophenyl)phenylphosphine sulfide using analogous chemistry (77).

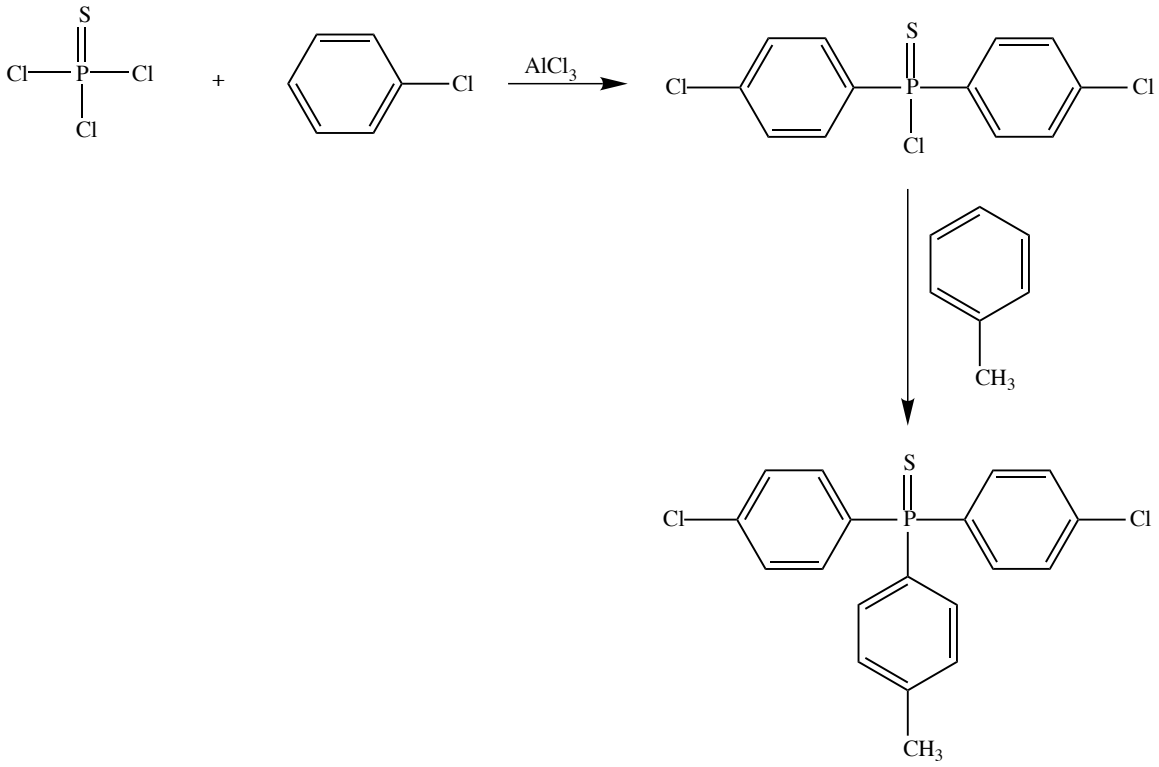

Figure 2.2.2.3 Illustration of the synthesis of a trisubsituted phosphine sulfide *via* subsequent addition of reagents

Wescott was then able to oxidize the phosphine sulfide to a phosphine oxide using hydrogen peroxide in an acetic acid solvent (77). This provides an alternative route the synthesis of 4,4'-bis(fluorophenyl)phenylphosphine oxide to the one described in section 3.2.7 of this thesis.

Conversely, trichlorophosphine appears to be less reactive than trichlorophosphine sulfide and does not easily undergo electrophilic substitution to give a tri-substituted product. Reactions of PCl_3 in the presence of benzene and $AlCl_3$ give only dichlorophenylphosphine and diphenylchlorophosphine (81). This illustrates the lower reactivity of trichlorophosphine towards electrophilic substitution compared with the analogous phosphine sulfide. This is probably due to the partial positive charge created on phosphorus due to the electron withdrawing effect of sulfur. The analogous oxides usually give very low yields, possibly due to complexation with the Lewis acid *eg*. $AlCl_3$.

2.2.3 Nucleophilic Reactions of Phosphines

Phosphines may also behave as reactive nucleophiles that are more reactive than analogous amines and can form quarternary phosphonium salts, which may be the final product or an intermediate in a reaction step, as shown in Figure 2.2.3.1 (60).

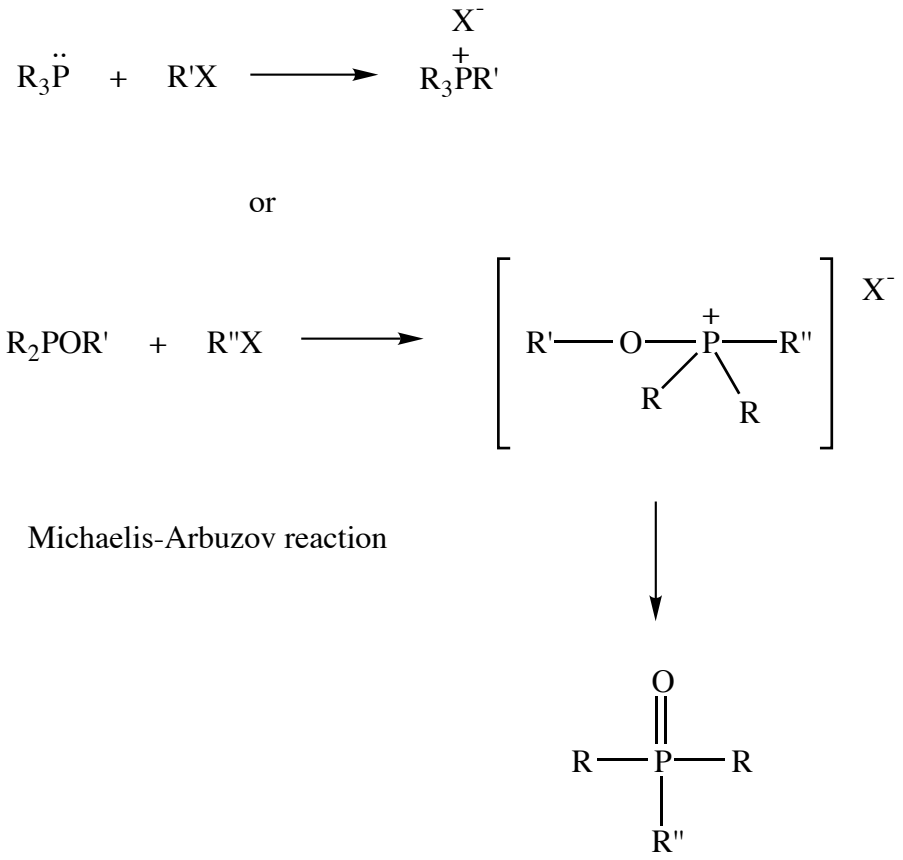

Figure 2.2.3.1 Example of nucleophilic attack of phosphines to produce phosphonium salts and phosphine oxides (60)

The phosphine has been shown to react with an alkyl halide *via* an S_N2 mechanism, leading to inversion of configuration at the carbon, since the backside attack takes place as shown in Figure 2.2.3.2 (82).

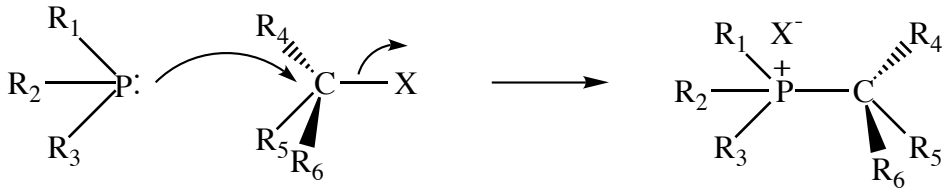

Figure 2.2.3.2 Mechanism for trialkyl phosphine nucleophilic attack and inversion of configuration

The rate of this nucleophilic attack is dependent on many factors, including electronic, steric, and solvent effects (60). For solution reactions the reaction rates of phosphines increase in the presence of electron donating substituents on the phosphorus, even in the presence of bulky electron donating substituents (83). Thus, contrary to amines, where steric factors are dominant, (e.g. primary amine is generally more reactive than a secondary amine) the nucleophilicity of phosphines follows their basicities. This is probably due to the larger size of phosphorus atom with respect to nitrogen. Since nitrogen is a smaller atom, bulky substituents would more easily hinder nucleophilic attack (60).

In addition to electronic and steric effects, solvent effects also play a large role in the reactivity of phosphines. Maccarone *et al*. (84) studied the effects of solvent on the rate of reaction for the reaction between benzyl chloride and triphenyl phosphine in 18 solvents. As shown in Scheme 2.2.3.2, this reaction is well designed for solvation studies. Not only is there a single reaction product, but there should be a large solvent effect upon the rate because the starting material is uncharged and the product is an ionic species. It was determined that the major contribution to the solvent effect on reactivity was the dielectric constant of the solvent for the reaction. The reaction rate increased with dielectric constant due to solvent stabilization of the activated complex.

Trivalent phosphorus is a versatile intermediate to a series of other derivatives, some of which are discussed above. Scheme 2.2.3.1 illustrates the versatility of phosphorus chemistry.

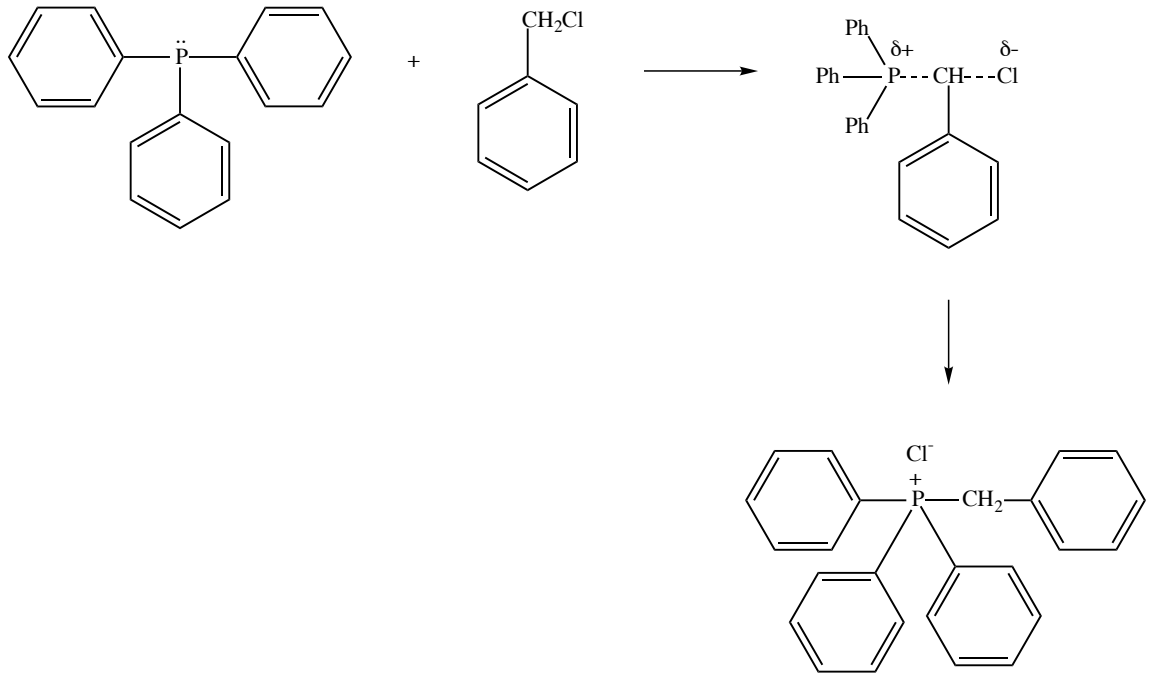

Figure 2.2.3.3 Reaction of triphenyl phosphine with benzyl chloride (84)

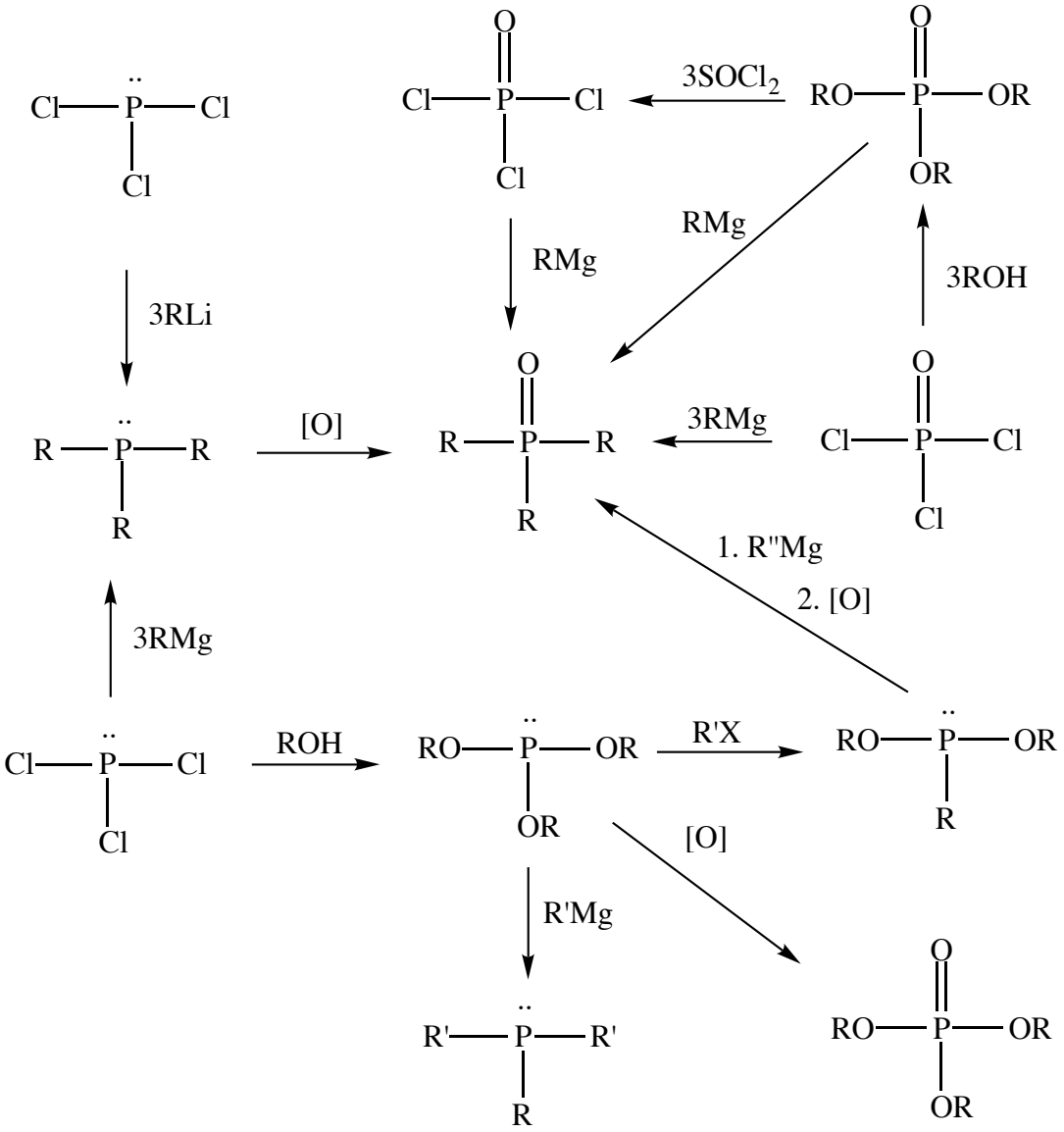

Scheme 2.2.3.1 Trivalent phosphine as a versatile intermediate for many other phosphorus compounds

2.3 Flame Resistance in Polymeric Materials

2.3.1 Modification of Polymers to Improve Flame Resistance

Organic polymers are one of the most versatile and widely utilized class of materials used today. They are utilized in many applications ranging from adhesives, aircraft interiors, and electronic components (85). However, except for a limited number of so called inherently flame resistant

polymers such as polytetrafluoroethylene (Teflon), polyvinyl chloride, etc. thermoplastics are not very flame resistant. The flame resistance of polymers has been improved using two different techniques. Firstly, by physically blending flame retardant additives such as Sb_2O_3 in combination with brominated aromatics (38, 86-90) or various phosphates with the polymer. Secondly, by incorporating flame retardant structures into a polymeric backbone (26, 37, 91-94). Flame retardant additives used in synthetic polymers include organic halogen and organic phosphorus compounds (83). A flame retardant additive interferes with one or more of the steps of the combustion cycle, which include; heating of the polymeric material, its subsequent degradation and the further combustion of volatiles that may be generated (87, 88, 91, 95, 96).

A flame retardant additive may function at one or more of these three steps; it is preferred that the additive function at more than one step. Thus, it may inhibit combustion at step 1 by forming a glass-like coating, which should preferably have low thermal conductivity, on the surface of the material upon exposure to heat. The additive may also degrade endothermically, thereby absorbing energy from the polymer (86-88, 90-95, 96). During the ignition stage these flame retardant additives may also deactivate highly reactive radical propagating species that result from chain scission during the combustion process (97), as is illustrated below in Figure 2.3.1.1 (96).

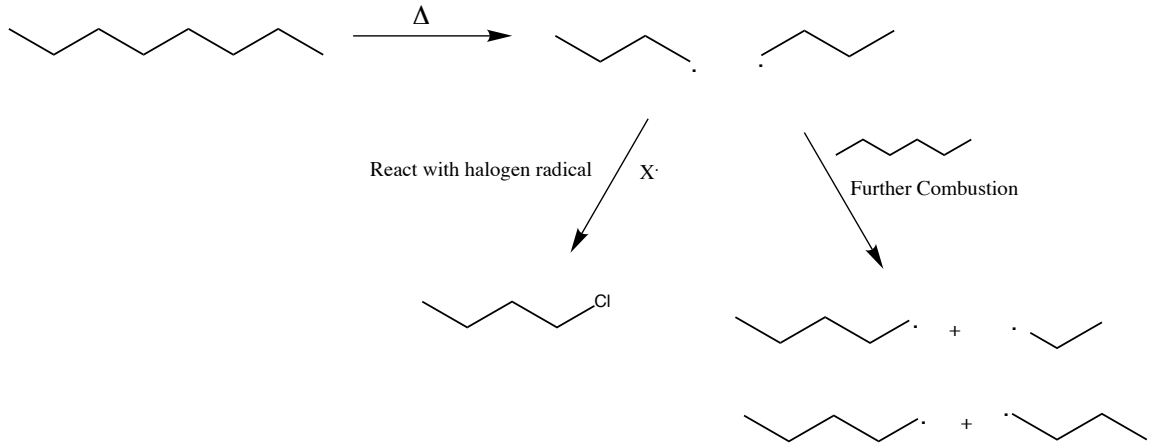

Figure 2.3.1.1 Illustration of how halogens can interrupt the combustion cycle

The flame retardant additive behaves in a similar manner as in the second stage by reacting with radicals during the combustion of volatiles to quench the propagating nature of the fire.

The effectiveness of the halogen depends on many factors, including the halogen used, the polymeric structure and the concentration of halogen. The effectiveness of the halogen follows the order Br>Cl>F and generally large amounts of halogen (between 15-30 wt. %) are required (87, 90, 98). Those halogens bonded to aliphatic carbons are better flame retardants than aromatic

halogens (87). This is probably due to that fact that aliphatic halogens degrade at a lower temperature *via* a radical mechanism than aromatic halogens. However, there are problems with physically blended flame retardant additives including compatibility issues, such as the additive leaching out over time, and the fact that the decomposition temperature of the fire retardant needs to be appropriate for a specific polymeric material. Clough (98) studied the aging effects of ethylene-propylene rubber (EPR) containing various amounts of halogen-hydrocarbon additives combined with Sb_2O_3 and discovered a significant loss of both the halogen additive and the Sb_2O_3 due to aging.

In order to avoid this problem with aging one may add halogens bonded to the backbone of the thermoplastic. This is particularly true for polyolefins (99) and epoxies (91, 100). This incorporation has resulted in an increased char yield and a higher limiting oxygen index which is one of the often used measurement methodologies (91). Commercially, tetrabromobisphenol-A or its diglycidylether are often used to cure epoxies for use in printed circuit boards and other applications where fire resistance is needed (100).

The disadvantage with halogen based flame retardants is the fact that upon combustion toxic gases of the form HX are emitted. Phosphorus or nitrogen containing additives, and others are being investigated as a possible way to overcome this problem (37, 38, 86-88, 95). A survey of phosphorus and nitrogen containing flame retardant additives is listed in Table 2.3.1.1.

Table 2.3.1.1 Examples of phosphorus and nitrogen containing flame retardant additives

Class of Additive	Structure	Reference
Phosphine Oxide	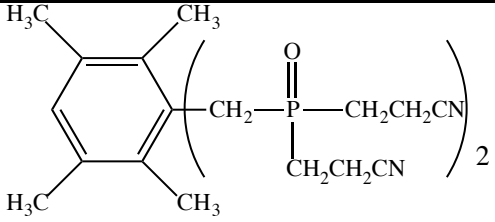	92, 101
Triphenylphosphine Oxide	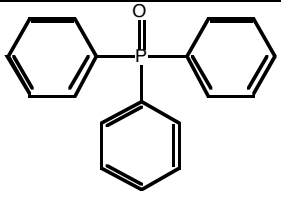	86

Triarylphosphates	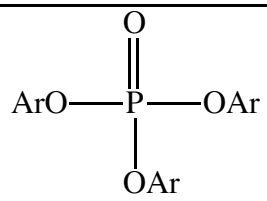	86
Vinylphosphonates	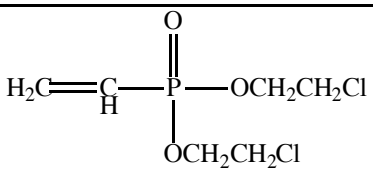	86
Polyphosphazenes	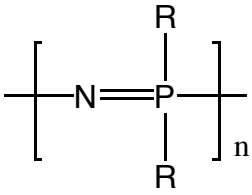	86
Phosphonium Salts	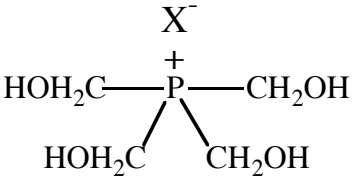	86
Red Phosphorus	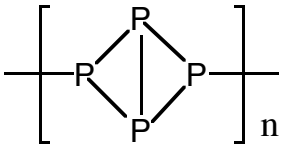	95
Phosphine Sulfide	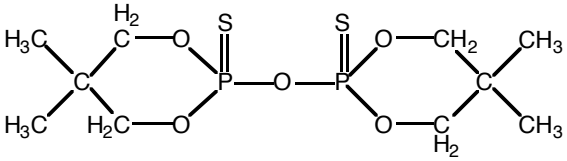	102
Cyanamide	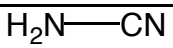	86
Dicyanamide	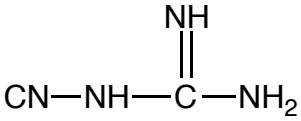	86
Urea	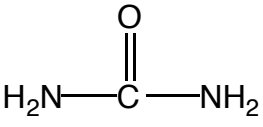	86

Thiourea	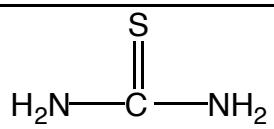	86
Ammonium salt	NH_4SCN	86

Phosphorus containing flame retardants can be either gas phase or condensed phase active. For example, trimethylphosphate, triphenylphosphate, triphenylphosphine oxide, as well as the halogens previously discussed exhibit vapor phase inhibition. A proposed mechanism for the vapor phase inhibition of phosphine oxide flame retardant additives is provided in Figure 2.3.1.2 (103).

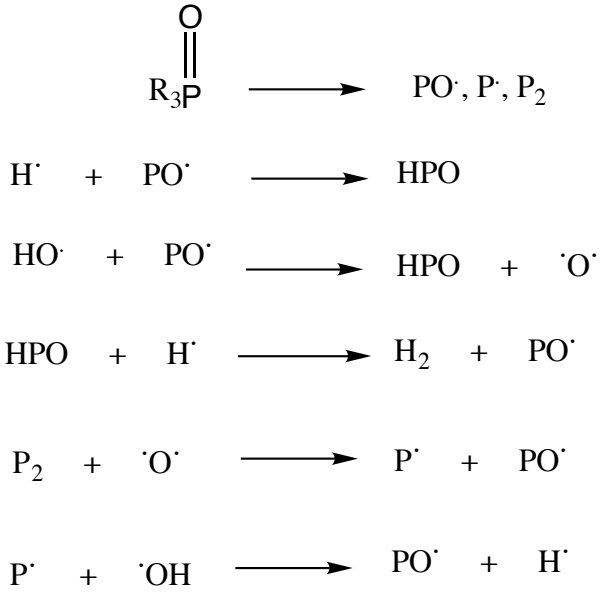

Figure 2.3.1.2 Illustration of the vapor phase inhibition mechanism of phosphorus containing flame retardants (103)

This mechanism produces two radical scavengers; a hydrogen radical and an oxygen radical. These radicals can combine with radicals produced during chain scission and inhibit the propagation of the flame front. A similar idea is shown in Figure 2.3.1.1.

Inagaki *et al.* (104) have shown that there is a linear correlation between the weight percent phosphorus and the limiting oxygen index (LOI) for cotton samples treated with phosphorus containing flame retardants. The LOI is an empirical technique developed to estimate the amount of oxygen in an oxygen/nitrogen atmosphere that is required to sustain a blue flame, therefore, the higher LOI indicates that a material may be more flame resistant (99). In general, these studies

show that as the amount of phosphorus is increased the LOI increased linearly within the range tested.

Phosphorus containing fire retardants may also behave as condensed phase inhibitors (91,103). Condensed phase inhibition involves changes in the polymer substrate to promote crosslinking and the formation of a char which serves two purposes. Firstly, it behaves as an insulating layer protecting the underlying polymer from the heat and flames. Secondly, it can act as a barrier preventing oxygen from reaching the uncombusted polymer, therefore inhibiting further combustion. Figure 2.3.1.3 below illustrates how phosphorus can behave as a condensed phase flame retardant. Organophosphorus compounds containing P-O-C bonds can thermally or hydrolytically degrade to phosphorus acids. These acids are known to react with cellulose to form a phosphorus ester.

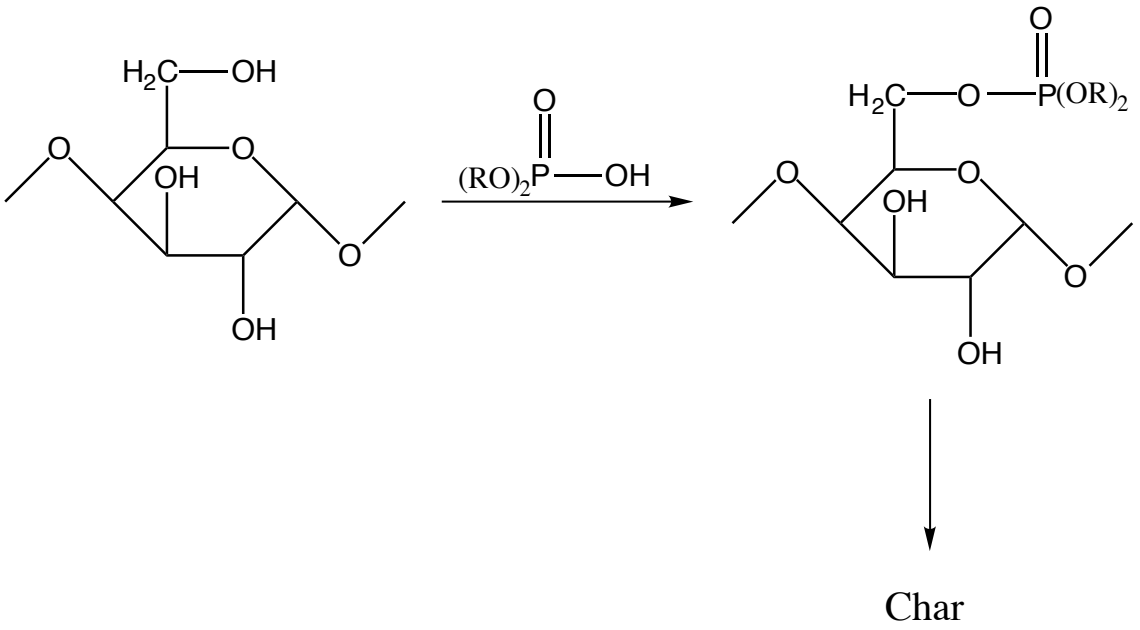

Figure 2.3.1.3 Illustration of how a phosphorus flame retardant may induce char (103)

The phosphorus acid can also catalyze dehydration of an organic species leading to increased unsaturation and increased char formation. When a phosphorus aryl compound is incorporated into a backbone of a polymer, studies show that the phosphorus forms a char consisting of a phosphorus anhydride type structure which inhibits combustion *via* a condensed phase mechanism (91). The condensed mechanism is the one of choice because it offers the advantages of a material with lower flammability without the release of toxic gases such as HX and does not require as large a loading as is essential for the vapor phase mechanism. Table 2.3.1.2 shows a variety of polymers that have phosphorus incorporated within their backbone.

Table 2.3.1.2 Illustration of the variety of polymers containing phosphorus

Polymer Class	Polymer Structure	Reference
Polyphosphazines	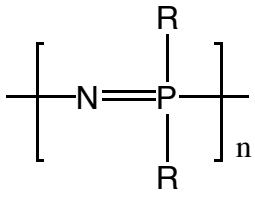	105-110
Polyphosphine	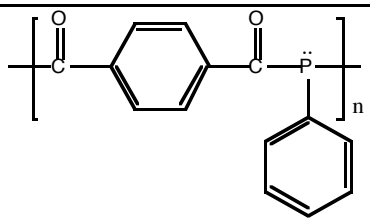	111
Polyphosphonite	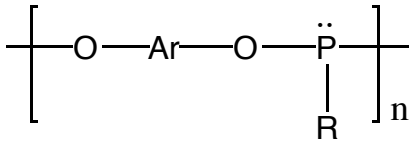	112-114
Polyphosphonate	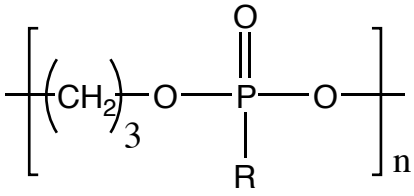	112
Polyphosphonate	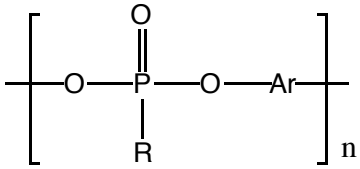	115-117
Phosphorus amide	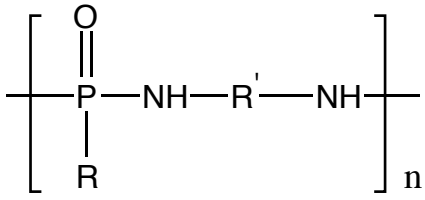	118-125
Polyimide	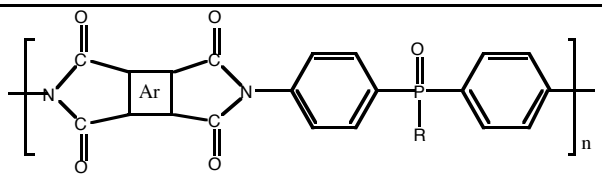	126, 127

Poly(arylene ether)	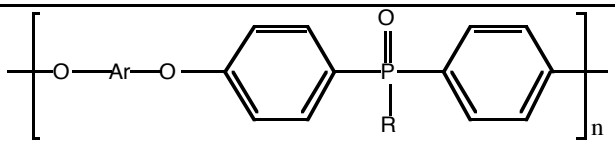	37, 38, 128
Polyamide	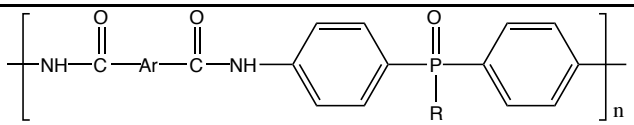	129
Polycarbonate	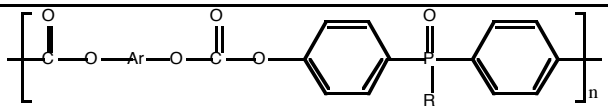	130
Polyester	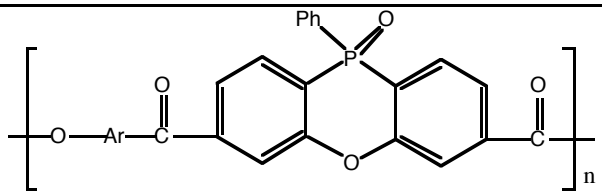	131
Epoxies	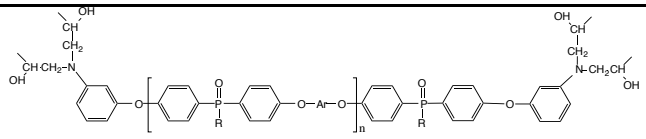	132

Another area of interest is the mechanism of char formation and how to induce high char yields in polymers in order to enhance flame resistance. Figure 2.3.1.4 illustrates a proposed mechanism for char formation (96). In this mechanism, a polymer is thermally decomposed *via* chain scission. After this initial decomposition step, the polymer may either undergo further decomposition or react with another polymer chain to form a crosslinked network. If the polymer undergoes further decomposition it may form small molecular weight volatile byproducts that do not form char and, may in fact, feed the combustion process. However, if after initial decomposition the polymer radical reacts with another polymer chain the polymer may form a crosslinked char. This mechanism would help explain why the char of many highly aromatic polymers contain graphitic structures on the surface.

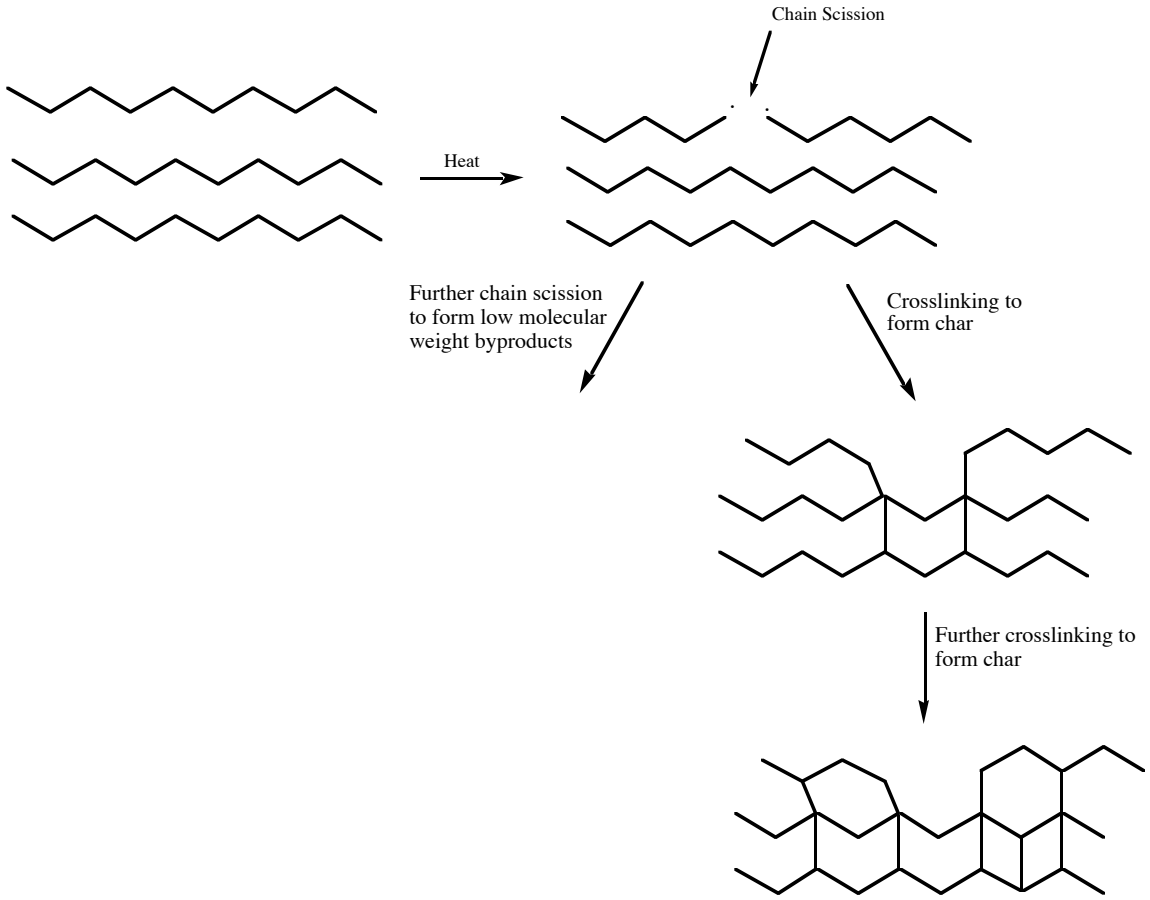

Figure 2.3.1.4 Possible mechanism for char formation (96)

These char forming condensed phase reactions are important in fire resistant polymers such as poly 2,6-dimethyl-1,4-phenylene oxide (PPO) and phenolic resins. Fenimore and Martin (132) illustrated that the high limiting oxygen index of PPO was due to its ability to form char residue upon heating. Table 2.3.1.3 illustrates the effect of aromatic ring upon char formation in non-halogenated polymers. It is evident from the data that as the char yield increases so does the LOI.

Table 2.3.1.3 Effect of aromatic rings upon the char yield of non-halogenated polymers (88)

Polymer	Structure	Oxygen Index	Char Yield
Poly(vinyl alcohol)	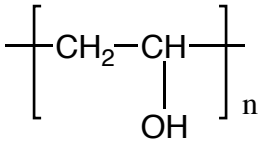	22	0
Poly(methyl methacrylate)	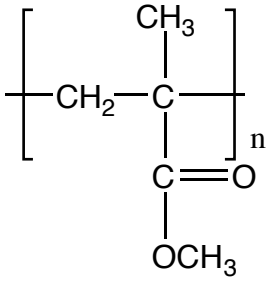	17	0
Polystyrene	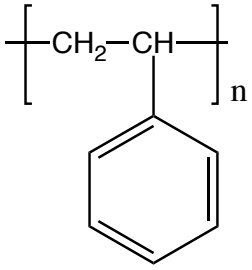	18	0
Poly(benzimidazole)	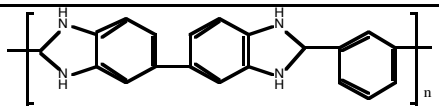	-----	58
Poly(phenylene oxide)	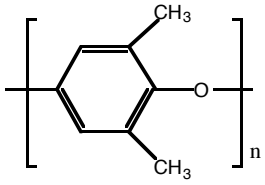	28	40
Phenolic Resin	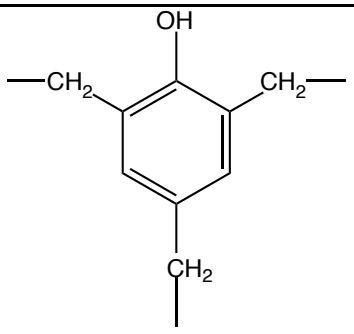	35	60.4

2.3.2 Methods for Testing Flammability

The combustion of polymeric materials is a complex process which includes environment, ignition, flame growth, fire retardants, and "burn out" to name a few. A single flammability test is thus only a partial indicator of how the material may behave in a "real" fire. Many tests have been developed to characterize each aspect of a materials combustion behavior. The areas combustion behavior of interest to researchers in include; ease of ignition, flame spread, ease of extinction, smoke obscuration, smoke toxicity and heat release rate (91, 96, 133).

Ease of ignition may be measured by subjecting a specimen to an ignition source for a specified amount of time (91, 96). The ignition source may be at a specific temperature or heat flux and if the material ignites it fails the test. The angle to which the sample is exposed to the ignition source and the heat flux of the source are the two main variables in this test. For materials that have low melting or softening points, the surface melt may flow away from the ignition source (96). If the softening temperature is below the ignition temperature the material may simply flow away from the ignition source and avoid ignition. Significant differences in horizontal vs vertical tests are observed. If a material can withstand exposure to a heat source without ignition the fire will not occur and combustion is prevented; thus ease of ignition is extremely important. However, this resistance to ignition generally coincides with an increase emission of smoke and toxic gases such as carbon monoxide (96). This is to be expected since most flame retardants work by inhibiting the combustion process resulting in partially burned or combusted products.

The characteristic of the flame after ignition is also important, including how fast the flame spreads. This is especially important in materials that may cover a wall or the interiors of aircraft (91, 96). In general, if a material ignites easily then its flame will spread rapidly. This is easy to understand if one views the propagating flame front as an advancing ignition. There are many types of analyses to characterize how a flame spreads. They consist of igniting a specimen with a specific orientation to the product exhaust (i.e. product exhaust carried into specimen flames) and analyzing visually how the flame spreads over the surface of the test specimen. Flame spread depends upon ignition temperature, orientation, thermal properties of the polymer, and flame heat flux (96). The orientation of the sample is an extremely important variable in a flame spreading experiment. For example, a flame will spread up to an order of magnitude faster up a vertically orientated sample ignited at the bottom than it will that same sample ignited at the top. This is because the heat is transferred more efficiently ahead of the burning zone if the flame propagation is in an upwards direction (96).

The heat release rate is another factor in characterizing the flammability of polymeric materials. It is currently regarded by many as the most important variable in fire resistance. Although most

deaths in a fire occur due to inhalation of toxic gases, the heat release rate is the best predictor of a fire hazard (133). Heat release rate is usually analyzed utilizing cone calorimetry. The cone calorimeter applies a specific heat flux to a sample and measures the ignitability, heat release rate, and toxic gases emitted (133). The ignitability is measured by determining how long a sample can withstand exposure to a specific heat flux before ignition occurs. After ignition, the heat release rate is measured as a function of time using an oxygen compensation method. The oxygen compensation method involves calculating the heat release rate from the amount of oxygen consumed by the polymer during combustion (133). From the heat release rate, it is also possible to monitor the heat release behavior through the combustion cycle from ignition to burn out.

Another important issue in determining the flammability of a material is that a material quickly extinguish after ignition. This is generally analyzed by determining a materials limiting oxygen index (91). The limiting oxygen index (LOI) is the minimum percentage of oxygen in an oxygen/nitrogen environment that is required to sustain combustion (99). Thus, if a material has a high LOI it is considered easier to extinguish than a material with a low LOI. A material is considered flammable if its LOI is <27 (99). The limiting oxygen indices for some commercially important polymers are listed below in Table 2.3.1.1.

Table 2.3.2.1 Effect of polymer structure upon its limiting oxygen index (99)

Polymer	Structure	Oxygen Index
Polyethylene	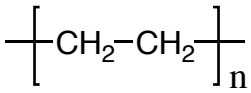	18
Polystyrene	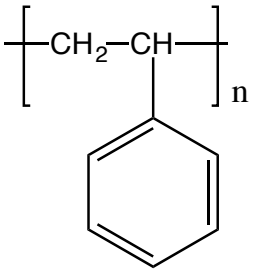	19
Poly(ethylene therphthalate)	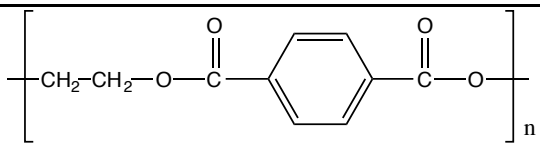	21

Nylon 6,6	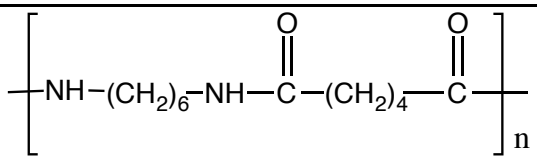	23
Polycarbonate	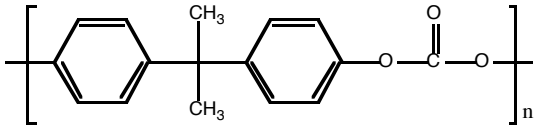	27
Polysulfone	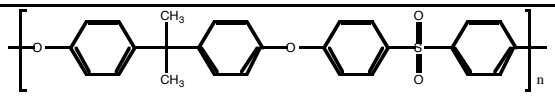	30
Poly(vinyl chloride)	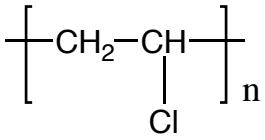	42
Poly(tetrafluoro ethylene)	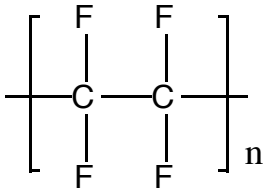	95

In addition to how a material behaves thermally when exposed to heat, it is also important to determine the amount of smoke that is emitted upon combustion. Obviously, in a fire it is desirable to have as little smoke as possible. Smoke can cause loss of visibility, loss of breath and panic among people trapped in a fire. The structure-property relationships between a thermoplastic and smoke are not well understood. It appears to be extremely dependent upon the conditions of combustion (96).

2.4 Non-linear Optical Polymers

One of the characteristics of electromagnetic radiation is that its transmission through a transparent material could be predicted solely based on the wavelength of light and the material through which it was passing. According to the classic equations of Maxwell, this transmission of electromagnetic radiation through a substrate is independent of its intensity (134). However with the advent of intense focused beams of light generated through lasers new phenomena are observed with the transmission of electromagnetic radiation through a medium, such as an inorganic crystal or polymeric film.

Electromagnetic radiation is made up of electric and magnetic components that oscillate at 90° angles to each other (134-137). A polarized model of electromagnetic radiation is shown in Figure 2.4.1.

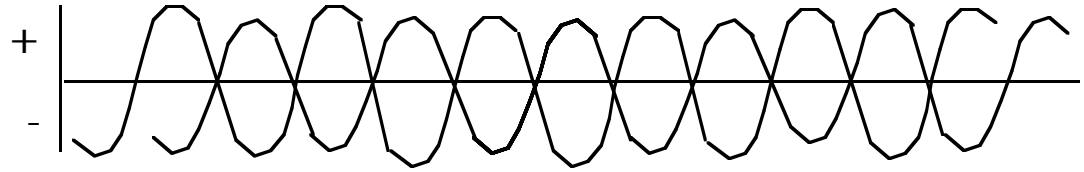

Figure 2.4.1 Illustration of polarized electromagnetic radiation

Faraday showed that a magnetic field affects the way in which light propagates through glass (134), thereby altering the refractive index of the glass by interacting with the magnetic portion of electromagnetic radiation. Kerr later showed a similar effect in the 1870s by applying an electric field to carbon disulfide (134, 137). This applied electric field alters the medium and changes the way it interacts with the electric part of the electromagnetic radiation, slowing its propagation through glass, hence changing the refractive index of the substrate. This electric field induced change in refractive index is known as the Kerr effect (or quadratic electro-optic effect) and an important non-linear optical effect in materials (135, 137). This effect went relatively unnoticed until 1960, with the advent of lasers and the observation by Franken of second harmonic generation in quartz (137, 138). These events were at the forefront of nonlinear optics becoming one of the most exciting physics topics in recent literature. Non-linear optics and photonics have risen as new areas of science and technology because of many potential applications, including second harmonic generation, the electro-optic effect, and all optical processing and switching *via* intensity refractive index.

In order for a material to exhibit large order non-linear optical effects it must possess electrons which are able to delocalize in response to an applied electric field (134, 137, 139). This may be achieved using certain inorganic crystals such as $LiNbO_3$ (135, 137, 138, 140) or a conjugated organic molecule with electron donating and electron withdrawing groups on opposite ends of the molecule (137, 140). In an inorganic crystal, the loosely bound valence electrons redistribute in response to an electric field. By contrast, in an organic molecule it is the π electrons that redistribute, providing charge transfer resonance along the direction of the dipole.

The non-linear response of NLO materials can be described by the following polarization equation where P is the bulk polarization and E is the electric field strength (137, 1, 141).

$$P = \chi^{(1)}\cdot E + \chi^{(2)}\cdot EE + \chi^{(3)}\cdot EEE + ...$$

The coefficient $\chi^{(2)}$ which relates the polarization to the square of the field strength is called the second order non-linear susceptibility of the medium. Its magnitude describes the strength of the second order process. The third term, $\chi^{(3)}$, describes the third order nonlinear susceptibility and so on for higher order processes. This literature review briefly focuses on second order processes such as second-harmonic generation (SHG) since this has been the most actively studied for polymeric materials. Since the second order polarization is proportional to the field squared, $\chi^{(2)}$, and SHG is zero in a randomly oriented medium because of the cancellation of the polarizations (137). Hence to make a material capable of SHG, molecules must be oriented noncentrosymmetrically. In one important case, this is accomplished using electric field poling for polymeric NLO materials (137, 1, 141).

In the case of nonlinear optical polymers where the hyperpolarizable molecule (chromophore) is attached to a polymeric backbone, these polymers are generally amorphous, isotropic and not suited for nonlinear optics. However, by exposing these polymers to an electric field at temperatures above their T_g, the chromophores can be aligned along their dipoles (135, 137, 141, 142). Next, the polar order is "locked" in by cooling the polymers below their T_g in the presence of an electric field. As shown in Figure 2.4.2, the polymer no longer has a center of symmetry and the chromophores are said to be ordered noncentrosymmetric.

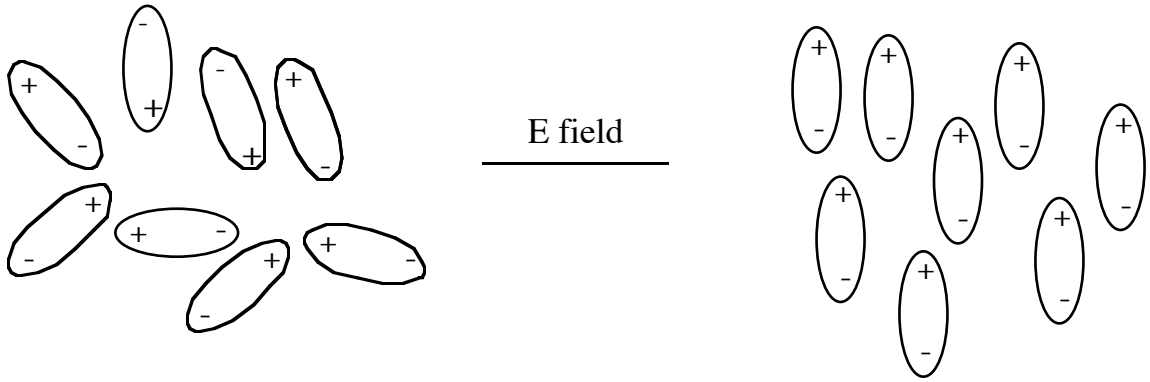

Figure 2.4.2 Illustration of the effect of electric field poling of chromophores

The chromophores, which are responsible for the nonlinear optical behavior, possess two components which contribute to their nonlinear optical response. These are hyperpolarizability (β) and the permanent dipole (μ). Hyperpolarizability is the ability of the chromophores to polarize in response to a high energy beam of light, wereras μ determines the degree of alignment by the applied electric field.

The βμ values indicate the ability of the chromophore to generate second harmonics. Larger βμ values correlate with greater second order susceptibility. Table 2.4.1 reviews examples of organic chromophores, along with their respective βμ values (143). The table indicates, for example, that if two cyano groups are utilized as the electron withdrawing group instead of one nitro group, the βμ value is larger. In addition, as the length of the conjugation increases so do the βμ values, due to larger charge distribution.

Table 2.4.1 Examples of chromophores and their respective βμ values (143)

Chemical Structure	Molecular Weight (g/mole)	βμ (10^{-48} esu)
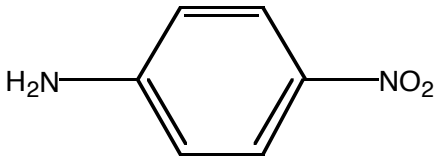	138.1	69
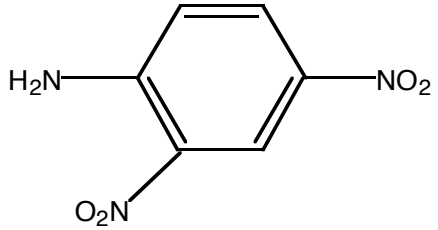	183.1	49
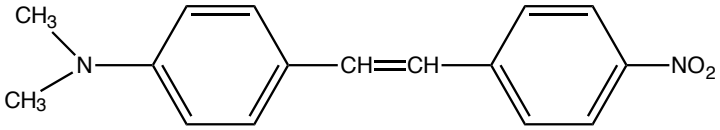	268.1	580

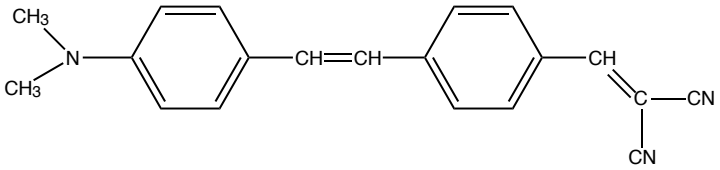	299.4	1100
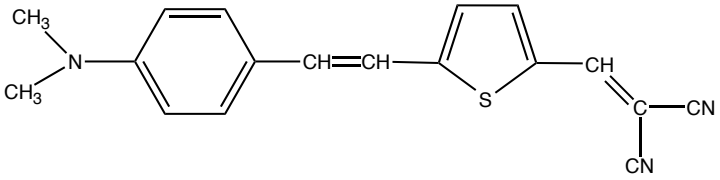	303.4	1300
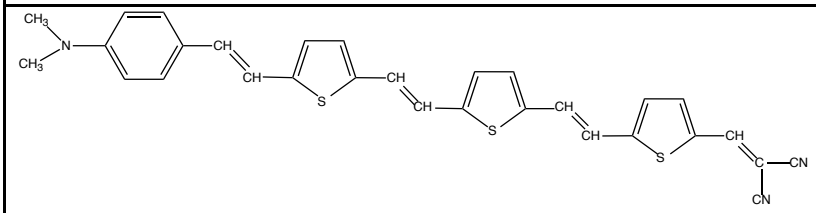	509.7	3800

It is necessary to understand what happens when light passes through a transparent inorganic crystal or polymeric film, to understand why electron redistribution is essential for second harmonic generation. The example below involves an organic chromophore, but may also be applied to an inorganic crystal. One component of light is an alternating electric field and this field interacts with loosely bound π electrons of an organic chromophore. As shown in Figure 2.4.3, these electrons redistribute themselves with the electric field (134, 135, 137). As long as the optical electric field is small, the polarization follows the electric field and the energy of the light remains the same, however, the velocity of the light is slowed, hence, different materials have different refractive indices. Figure 2.4.4 shows a plot of the optical polarization versus the optical electric field. This plot is a straight line and therefore is called linear optics.

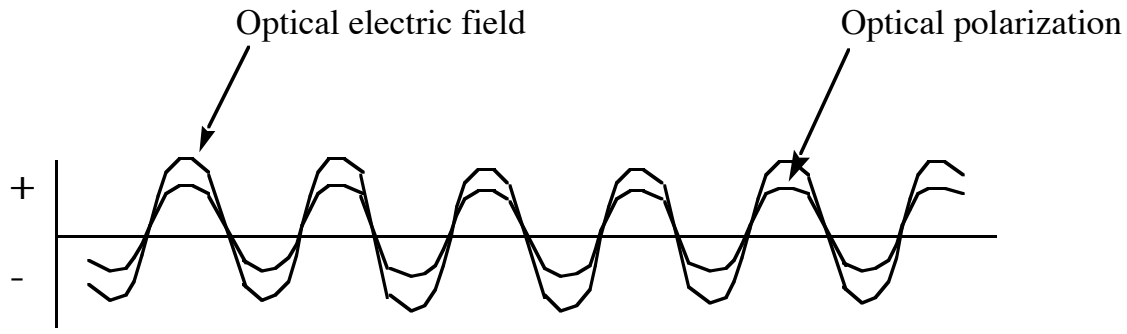

Figure 2.4.3 Response of NLO material to low intensity light (134)

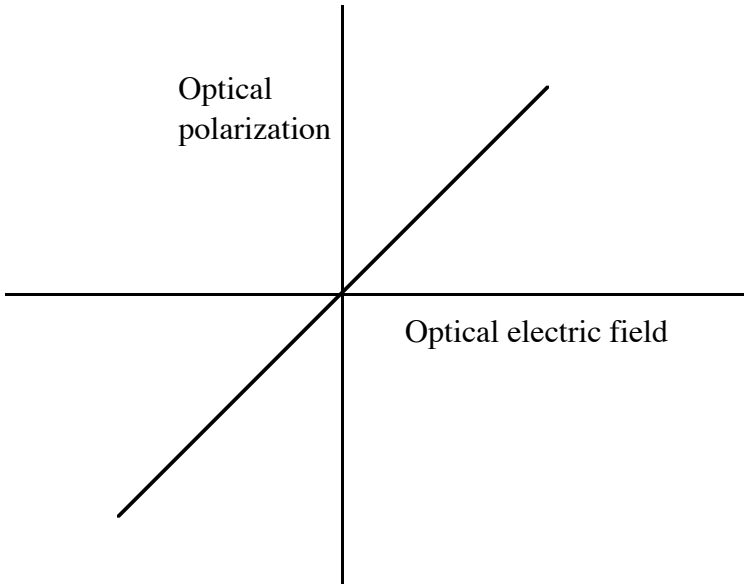

Figure 2.4.4 Plot of optical electric field versus optical polarization for a linear response (134)

On the other hand, if a focused high energy beam of light, such as that generated from a laser is utilized, the situation is much different. The laser light has an electric field that is much greater than that of low energy light. When this focused light enters an NLO material it causes an immense redistribution of electrons and the polarization is not proportional to the optical electric field (134, 135, 141). The π electrons are more easily moved to one side by the electric field of the propagating electro-magnetic radiation, thereby giving a unbalanced polarization wave. This unbalanced polarization is the sum of three components: the wave at frequency (f), the same frequency of the light that created it, a wave at the second harmonic frequency (2f), and a component that corresponds to a steady polarization (134). These three components are illustrated in Figure 2.4.7. The initial wave is transformed into light at the initial frequency plus some second harmonic frequency (134). Figure 2.4.5 illustrates this unbalanced polarization wave. Figure 2.4.6 shows a plot of the optical polarization versus the optical electric field for a non-linear response. This plot is a not a straight line and therefore this field of study is called non-linear optics.

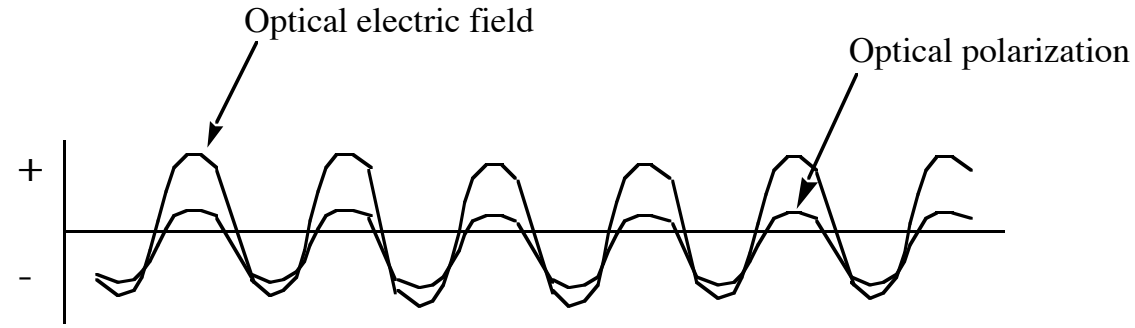

Figure 2.4.5 Illustration of unbalanced polarization (134)

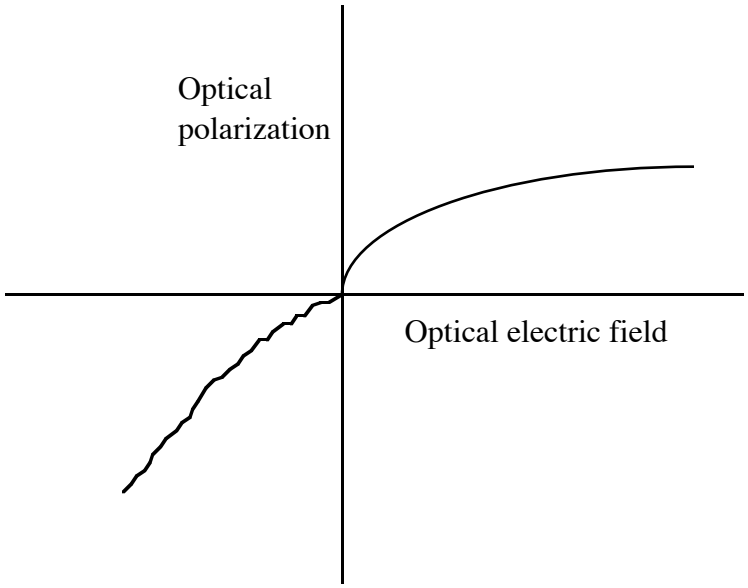

Figure 2.3.6 Plot of optical electric field versus optical polarization for a non-linear response (134)

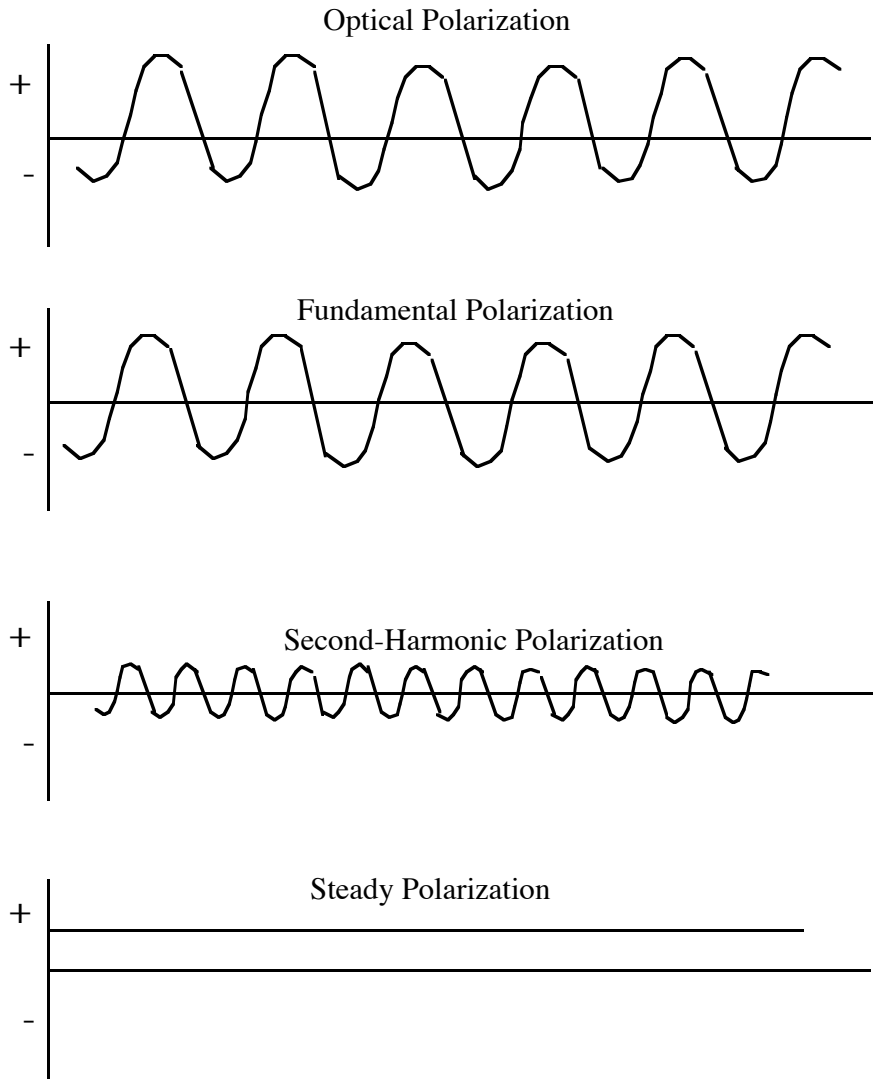

Figure 2.4.7 The components of an unbalanced polarization wave (134)

Second order non-linear optical materials are utilized in many application such as frequency modulation in lasers and wave guides. It is recognized that crystals are better for second harmonic generation due to their high thermal and temporal stability, while organic polymers are more suited for electro-optic wave guide devices because they can be cast into films (135, 137, 138, 144). An area of potential application and vast amounts of research is the use of second order non-linear optical polymers as wave guides for rapid information processing and communications systems (135, 141, 144, 145). Organic polymers offer several advantages compared to existing wave guide technology based on inorganic crystals. Firstly, they can have larger non-linear response (141) and secondly, they can be chemically modified to achieve the desired optical and physical

properties such as refractive index, thermal stability, mechanical properties, and adhesion. A wave guide is a medium in which an optical wave is confined in two dimensions (141, 145, 146) and is formed by a region with a refractive index larger that the surrounding medium. For example, Figure 2.4.8 shows a glass optical fiber that is coated with a cladding whose refractive index is slightly lower than the core fiber. The propagation of the light in the optical fiber may be described as total internal reflection at all interfaces. This concept is illustrated in Figure 2.4.9 below (141).

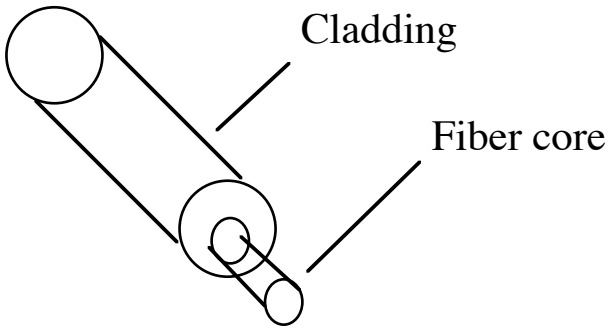

Figure 2.4.8 Illustration of a fiber optic cable (144)

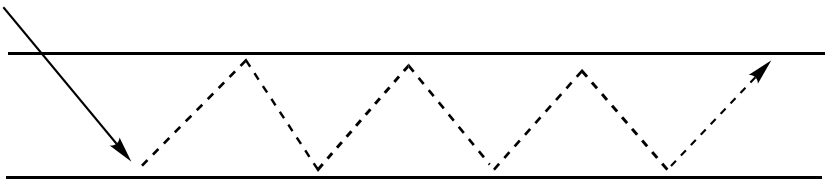

Figure 2.4.9 Illustration of light propagation through a fiber optic cable (141)

In order to fully realize the information carrying capacity of these fibers some questions must be answered. How can the maximum amount of information be put into one channel and how can different information channels be multiplexed and deciphered over short distances? Multiplexing is a means by which many information channels are put into one optical channel to increase the information carrying capacity of the optical fiber. This information then must be separated and redirected into individual channels of information. This is accomplished using wave guides (141-146). In an electro-optic wave guide an electric field is applied to a second order NLO material thereby altering the propagation of the light. This prevents the optical signal from having to be converted into an electronic signal for switching and then back into an optical signal for further distribution. The wide-spread use of electro-optical switching devices has been greatly hindered by the expense of the electro-optic switching material. Polymeric NLO materials shows promise

over current inorganic NLO materials because of their potential lower cost and mechanical properties However, an even greater challenge is to find an all optical means of separating out this information, thereby allow for greater switching speed. This is where third-order nonlinear optics comes into play. A third-order nonlinear optical wave guide allows for optical switching in a completely optical system, eliminating the need for electrical control. The switching action relies on the fact that in a third-order nonlinear optical material the refractive index is dependent on the intensity of the propagating light. Therefore, the light is separated based on intensity dependent changes in refractive indices (144).

Another area of potential application and current research is photonics. Photonics is similar to electronics, except that photonics uses photons instead of electrons to store and transmit information in applications such as optical computing and optical data storage. (141) In an optical computer photons are conducted through channels. To switch the light it is necessary to have a non-linear optical film that allows light propagation to be controlled by applying a laser pulse or electric field (135, 141, 144), thereby directing the propagating light by utilizing a second beam of light. Optical computing and switching offer many potential advantages over electronics. These include femtosecond (10^{-15}) switching and less crosstalk, resulting in faster computing (141). Furthermore, by employing second order non-linear optics it is possible to modify the wavelength of light utilized in optical data storage and retrieval. Modification of the wavelength allows for alteration of the size of the focus spot of the laser used to read an optical disk. The smaller the focus spot the larger the storage capacity of the optical storage disk (141).

Figure 2.4.10 gives examples of non-linear optical devices based on nonlinear optical processes. In many of these applications polymeric organic non-linear optical (NLO) materials are promising compared to current inorganic materials because a greater flexibility in chromophore and polymeric constituents may be achieved by various synthetic techniques.

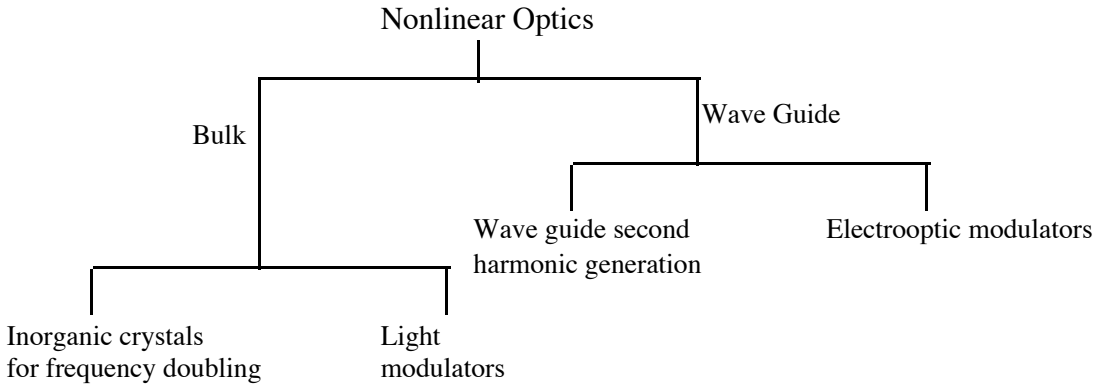

Figure 2.4.10 Examples of potential non-linear optical devices (141)

Polymeric NLO materials can be described as guest-host materials. The polymer is considered the host material and the chromophore the guest. Currently, in the literature there are two basic types of guest-host NLO systems. The first case is where the chromophore is physically blended into the polymeric host (2, 135, 137, 147, 148). The schematic of this system is below in Figure 2.4.11.

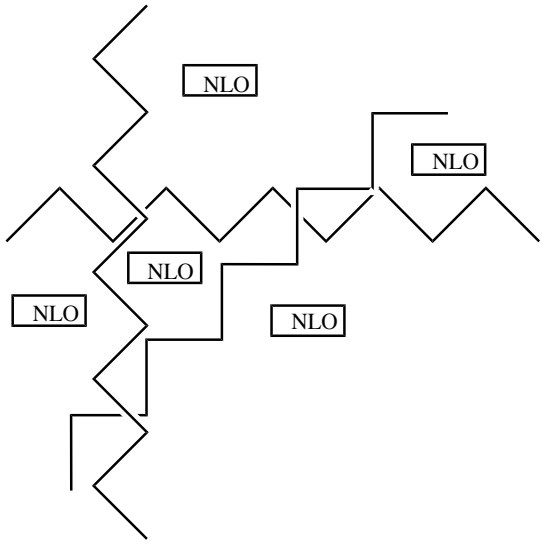

Figure 2.4.11 Schematic of an NLO system where the chromophore is physically blended into a polymeric host.

The desired host polymer should have excellent film forming properties and a high T_g. It should also be miscible with the chromophore. This compatibility is generally aided by the presence of similar or interacting functional groups (2, 148). The advantages of the system is the fact that it is economical and simple (148). However, there are limitations in the amount of chromophore that can be blended into the polymer host since macrophase separation and substantial plasticization will often occur. This type of guest host NLO system has been investigated utilizing many different polymer-chromophore systems including poly(vinylcarbazole) doped with 4-(diethylamino)-(E)-β-nitrostyrene, poly(silane) based systems doped with Coumarin-153 or (e)-β-nitro-(Z)-β-methyl-3-fluoro-4-(N,N-diethylamino)styrene, (135) and poly(arylene ether phosphine oxide) thermoplastic

doped with chromophores such as 4-dimethylamino-4'-nitrostilbene (DANS). (2) These systems and others are illustrated below in Table 2.4.2.

Table 2.4.2 Examples of doped polymer films for second order non-linear optics

Polymeric Host	Chromophore	Reference
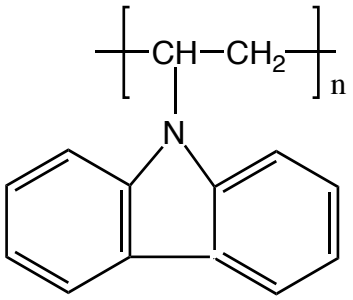	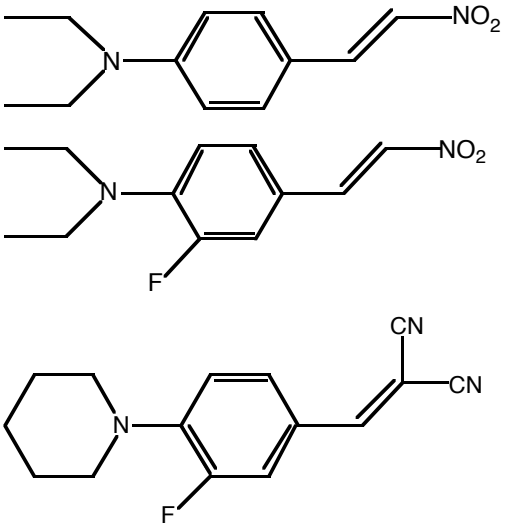	135
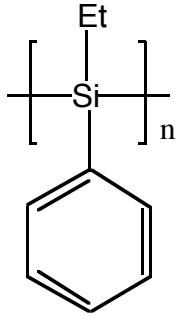	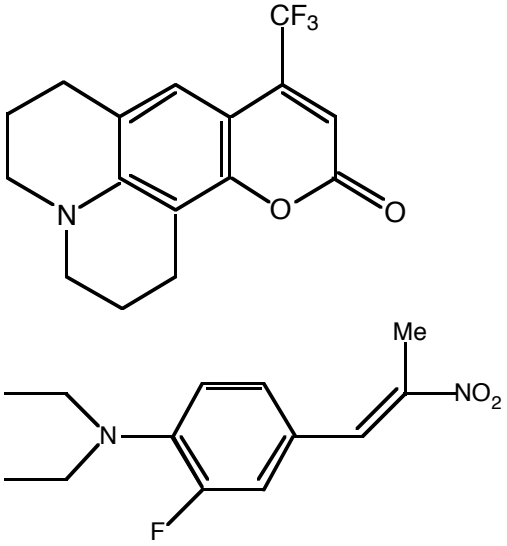	135
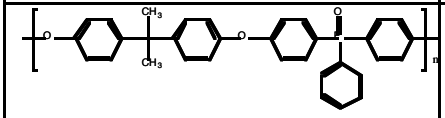	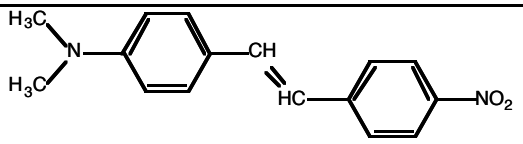	2

	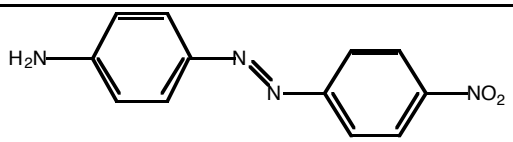	
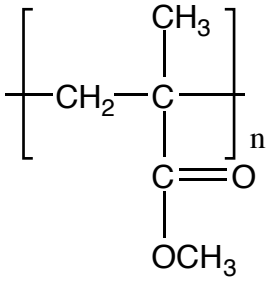	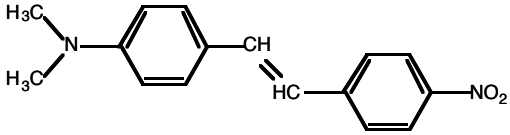 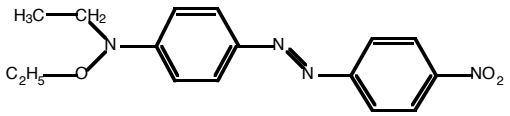	147, 149, 150-153
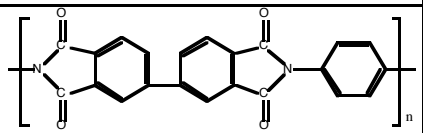	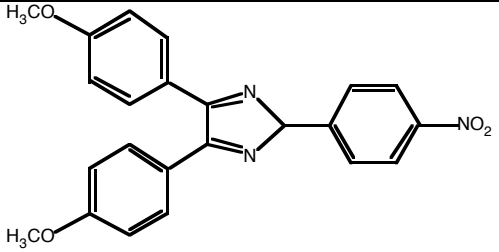 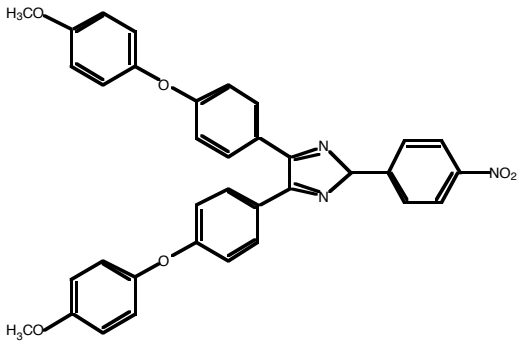	148

Due to the lack of temporal and thermal stability due to plasticization and increased free volume resulting from chromophore incorporation (135), current NLO research focuses on covalently bonding chromophores to the backbone of rigid thermally stable high T_g polymers. Both linear and crosslinked thermoplastics have been utilized in this endeavor. Figure 2.4.12 is a cartoon of a NLO side-chain chromophore covalently bonded to a linear thermoplastic polymer.

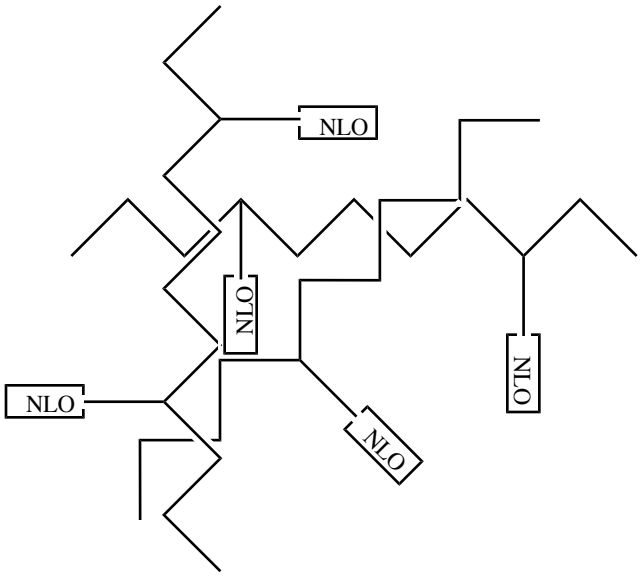

NLO = non-linear optical chromophore

Figure 2.4.12 Schematic of an NLO system where the chromophore is covalently bonded to a linear polymeric host.

This covalently bonded guest-host system has been investigated utilizing various polymeric backbones including polyimides (154), poly(arylene ether)s (155), polyacrylates (156), and polyesters (157). These NLO materials have been synthesized by both reacting with a NLO chromophore during polymerization (158-160) and by derivatizing the polymer with a NLO chromophore post polymerization (155).

Table 2.4.3 Examples of NLO chromophores covalently bonded to the backbone of a linear polymeric host

Structure of NLO Polymer	Reference
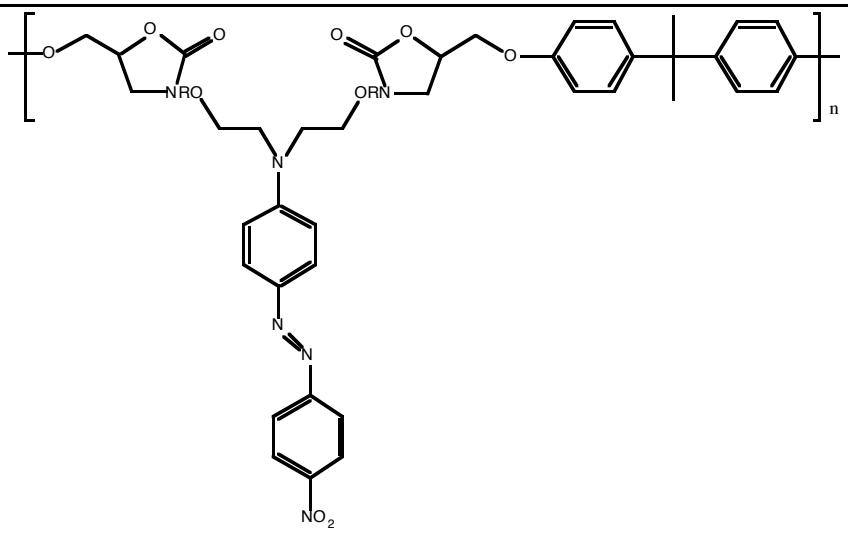	158
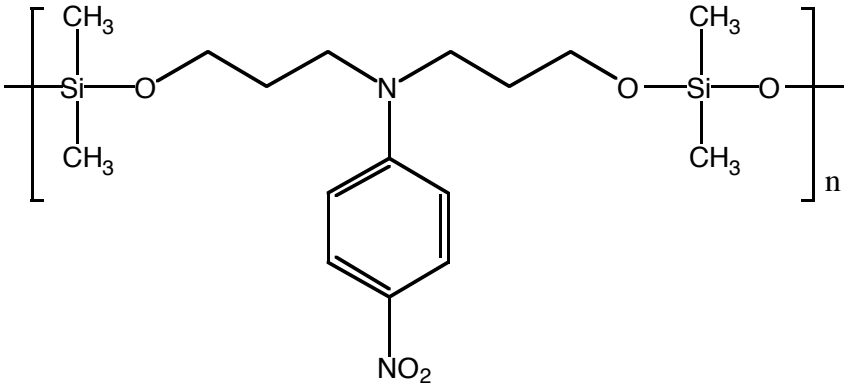	159

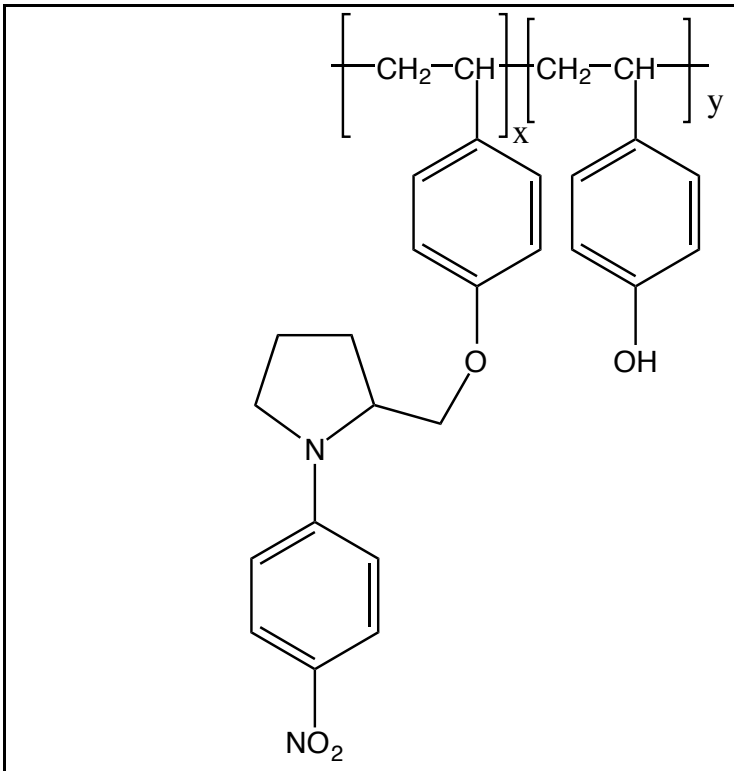	161
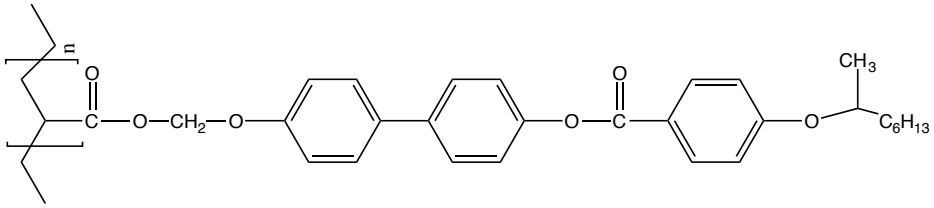	160

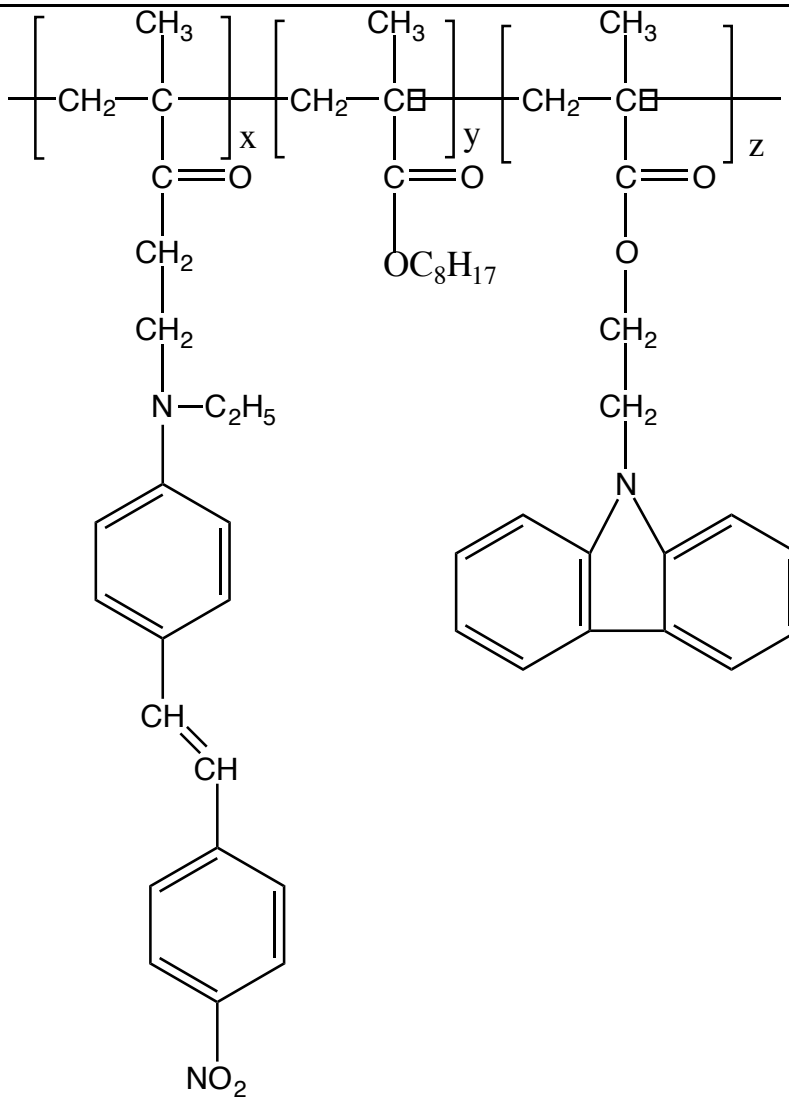	156

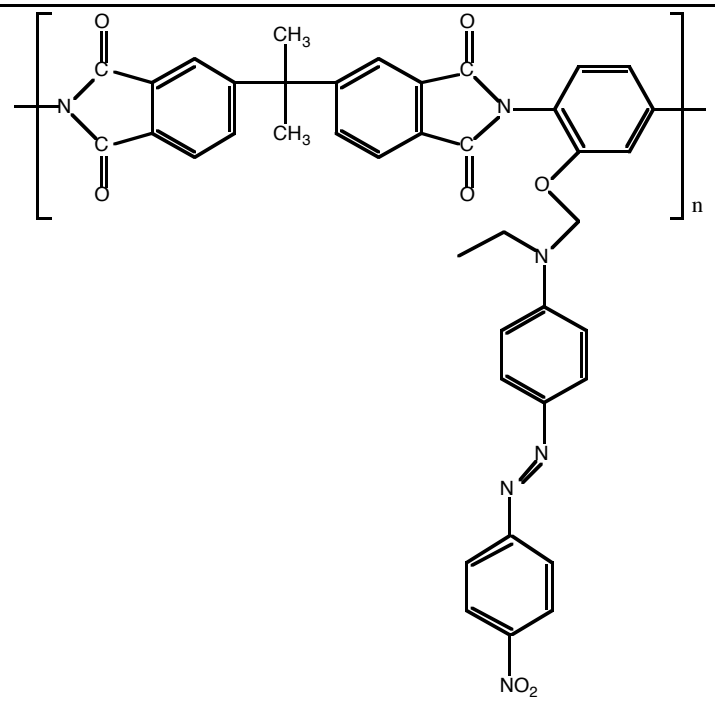	162
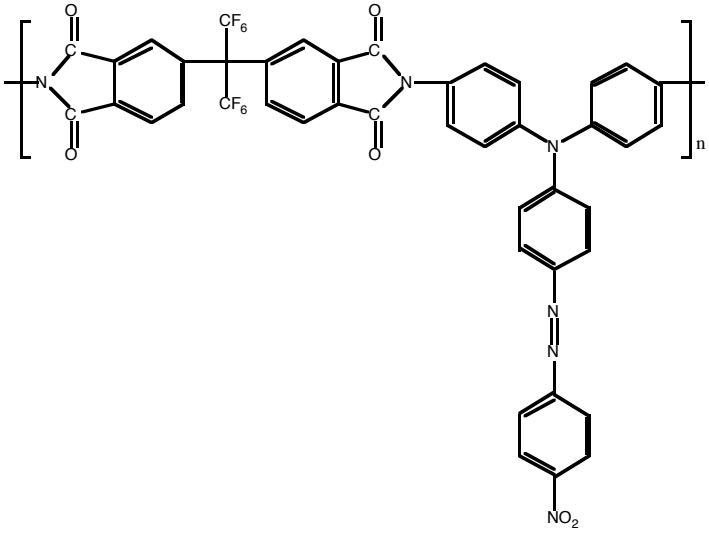	154
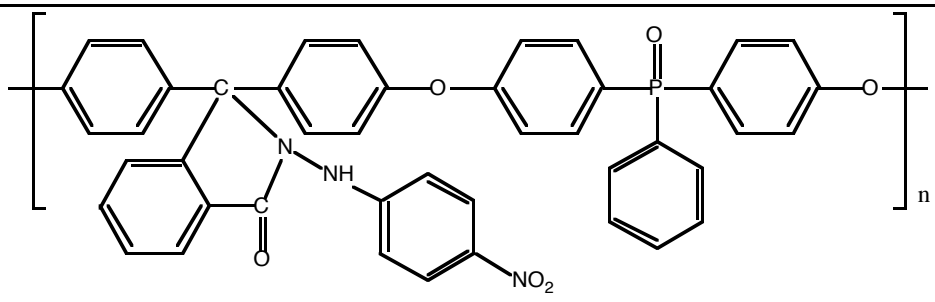	155

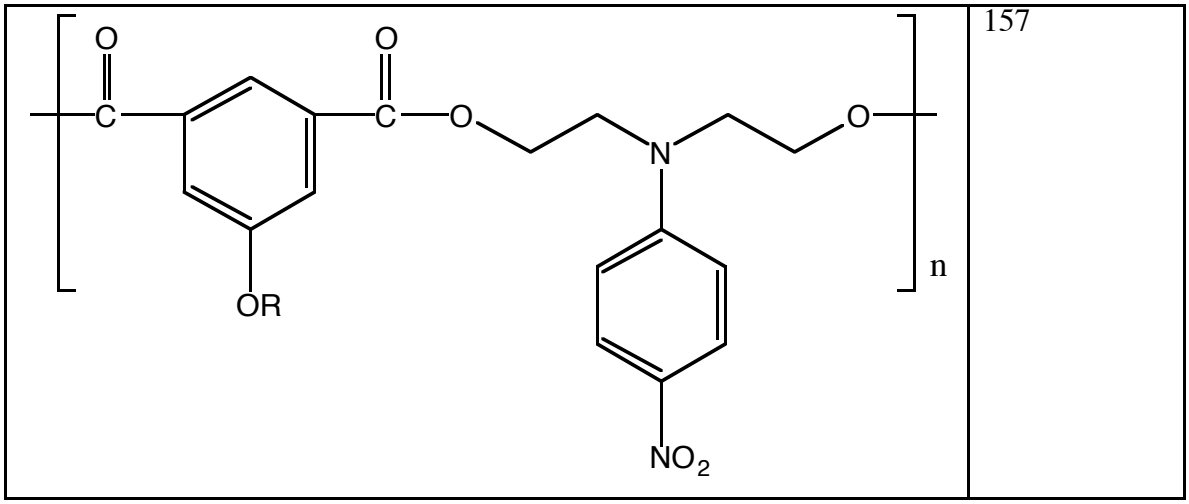

157

These polymers show increased orientation stability after poling compared to the NLO polymers made by simply physically blending the chromophore within a high performance polymer. Some of these materials, such as the polyimide synthesized by Miller et.al (154), show reasonable SHG stability at 25°C and even 100°C. Utilizing this type of chemistry it is possible to avoid plasticization; however, the drawback to these high T_g systems is that in order to obtain SHG stability at high temperatures a polymer with a T_g of between 300-350°C is required for a thermoplastic material. Therefore, the chromophore utilized must also withstand 300-350°C during poling, without degrading. There are only a few chromophores that can withstand these elevated temperature and they do not have high $\beta\mu$ values. That is the main drawback of these high T_g materials.

Another way to integrate chromophores into a linear polymeric host is through main chain incorporation. Main-chain incorporation involves integrating a chromophore within a polymeric backbone as shown in Figure 2.4.13.

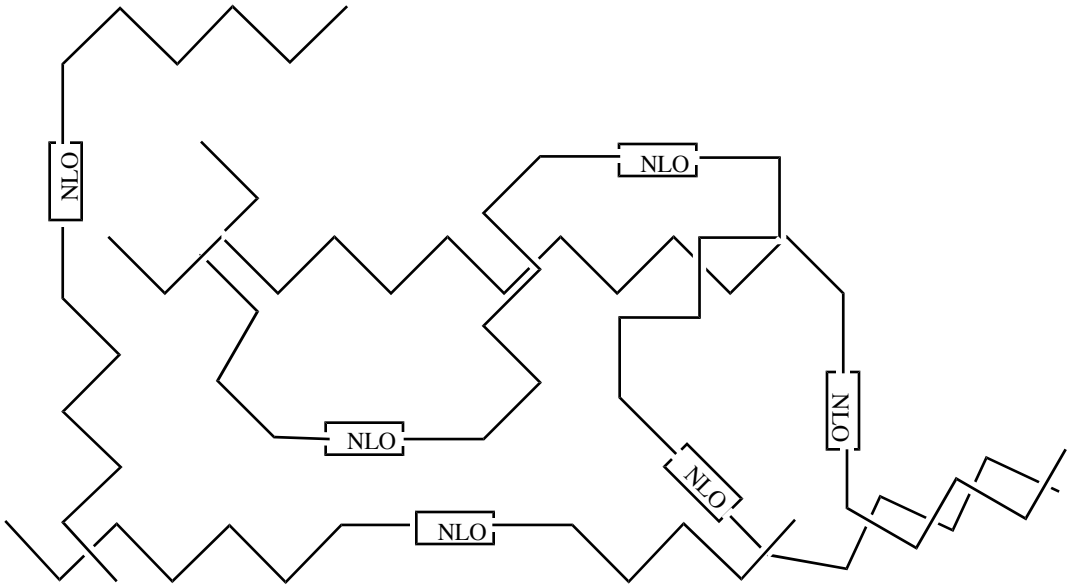

Figure 2.4.13 Schematic of an NLO system of where the chromophore is incorporated within the main-chain of a linear polymeric host

The advantage of main-chain integration with respect to side-chain incorporation is that larger segmental motions of the polymeric backbone are required for poling and relaxation of the main-chain NLO polymer. Consequently, although poling may be more difficult the sub-Tg isotropic reorientation of main-chain chromophores would be suppressed (137). Table 2.3.4 shows examples of main-chain chromophores covalently bonded to linear polymeric hosts.

Table 2.4.4 Examples of main-chain chromophores covalently bonded to linear polymeric hosts

Structure of NLO Polymer	Reference
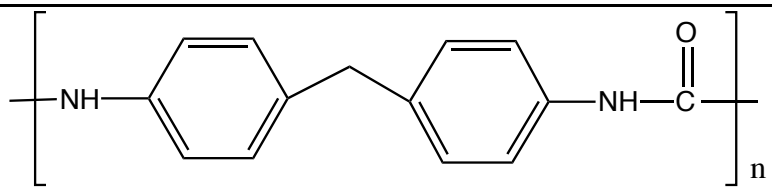	137, 163
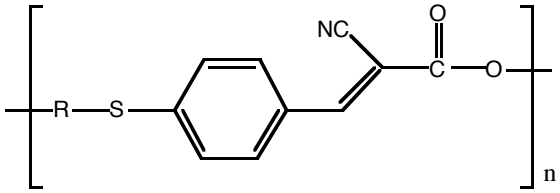	164
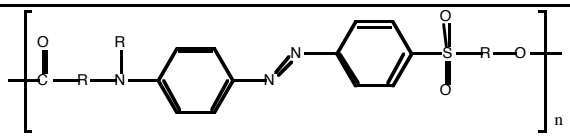	165
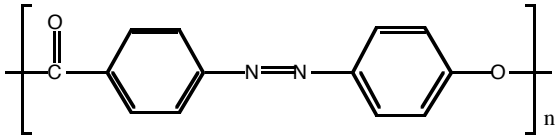	166
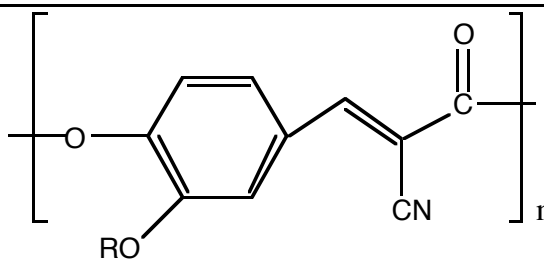	167
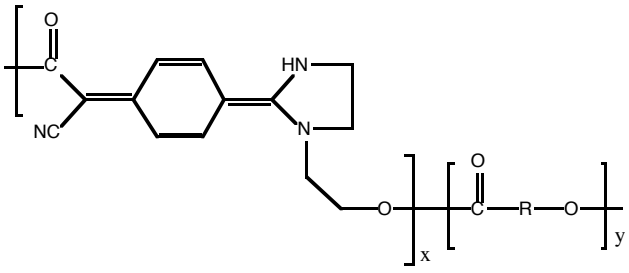	168

In order to improve the temporal and thermal stability of a NLO material, NLO chromophores have also been incorporated into network polymers. In network polymers, relaxation processes which limit the lifetime of second-order nonlinear optical polymers may be inhibited by increasing

the interaction between polymer chains leading to long term temporal and thermal stability due to the partial immobilization of part of a polymer chain (137). Another advantage of network hosts is that since poling requires chromophore mobility the poling must take place before or during cure. Perhaps this could lead to more efficient poling since many of the reactive oligomers utilized are liquids at room temperature. Chromophores may be incorporated into thermoset hosts *via* both side-chain and main-chain incorporation. Figure 2.4.14 and Figure 2.4.15 illustrate this type of incorporation respectively.

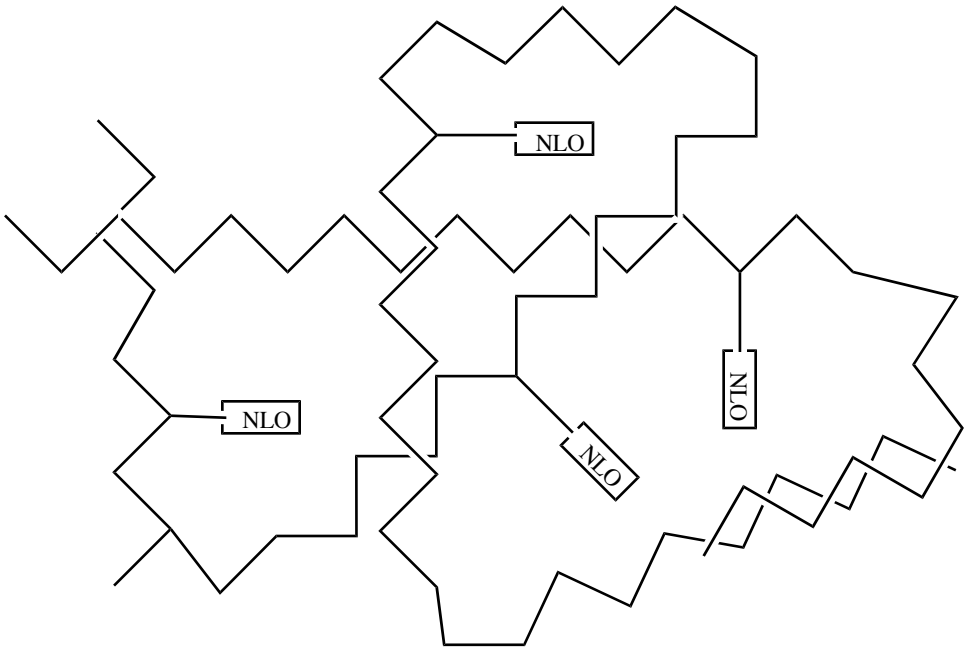

Figure 2.4.14 Incorporation of side-chain NLO chromophore within a crosslinked polymeric NLO material

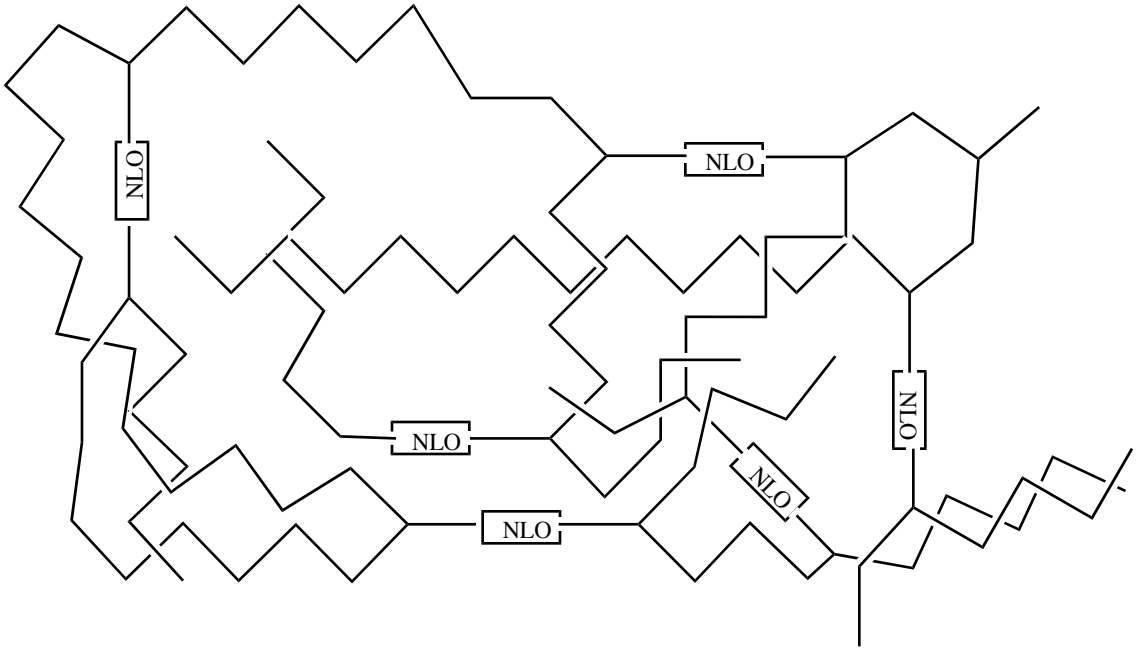

NLO = non-linear optical chromophore

Figure 2.4.15 Schematic of an NLO system of where the chromophore is incorporated within the main-chain of a crosslinked polymeric host

This covalently bonded network guest-host system has been investigated utilizing various polymeric backbones including epoxies and acrylates, and have been cured utilizing both thermal and photochemical initiation. Table 2.4.5 shows examples of both side-chain and main-chain network topologies.

Table 2.4.5 Examples of NLO chromophores covalently bonded to the backbone of a crosslinked polymeric host

Structure of NLO Polymer	Reference
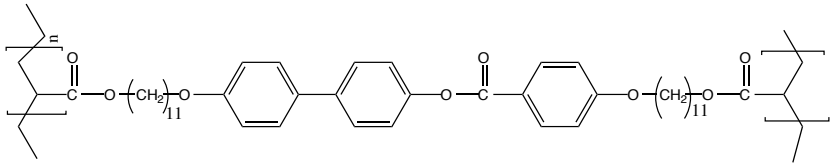	160

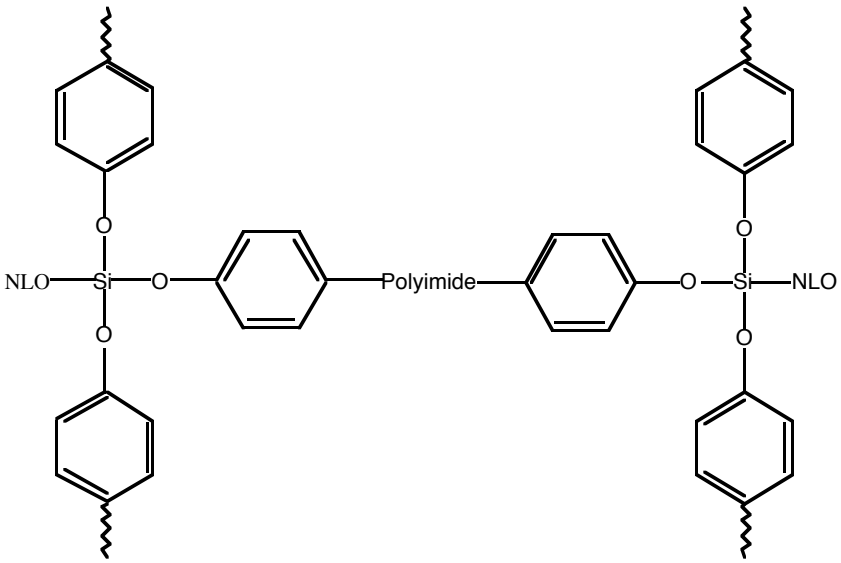 NLO Si O Polyimide O Si NLO O O O O	169
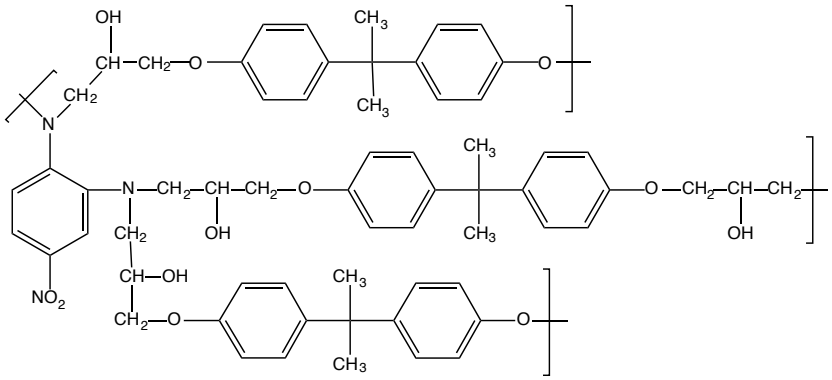 OH CH CH2 O CH3 CH3 CH2 N N CH2 CH CH2 O CH3 CH3 O CH2 CH CH2 CH2 OH OH NO2 CH OH CH2 O CH3 CH3	170

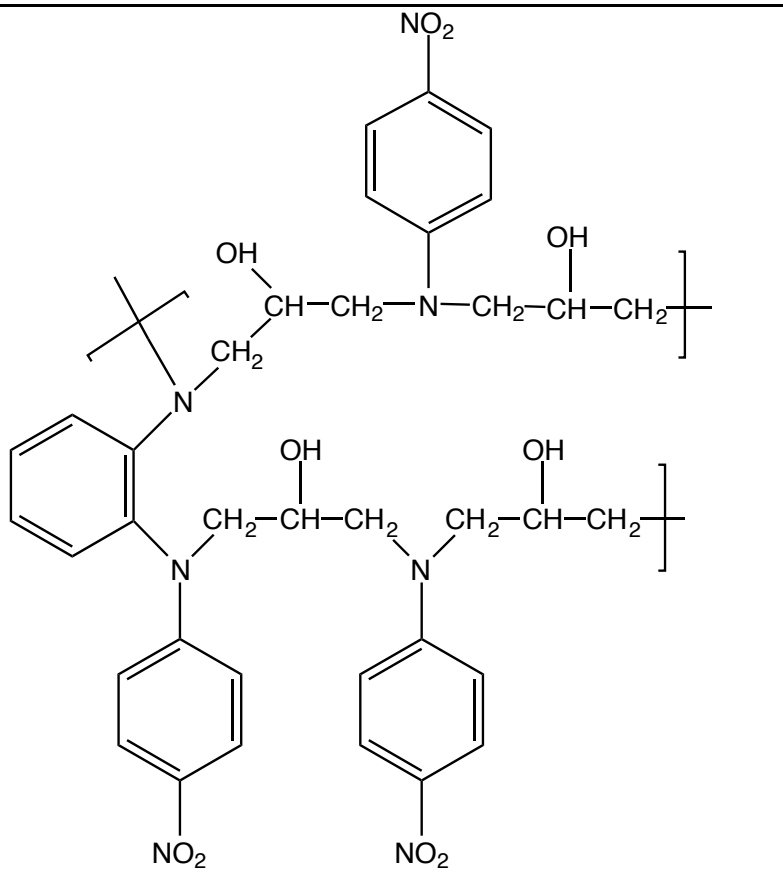

171

Both linear and crosslinked polymeric hosts may possess a high Tg and a rigid nature to minimize relaxation of the chromophore's orientation after poling. However, in general the network hosts show improved orientational stability over their linear counterparts.

Another technique that is starting to receive attention in the literature is the ionic bonding of a chromophore to a polymeric backbone (172). This was accomplished by synthesizing a poly(arylene ether) based on hydroquinone potassium sulfonate 4,4'-difluorobenzophenone or 1,3-bis-(fluorobenzoyl)benzene utilizing nucleophilic aromatic substitution. Acid-base chemistry was then employed to bond a pyridine containing chromophore ionically to the backbone of this poly(arylene ether). This chemistry is shown in Scheme 2.4.1. However, the non-linear optical behavior of this material has yet to be reported.

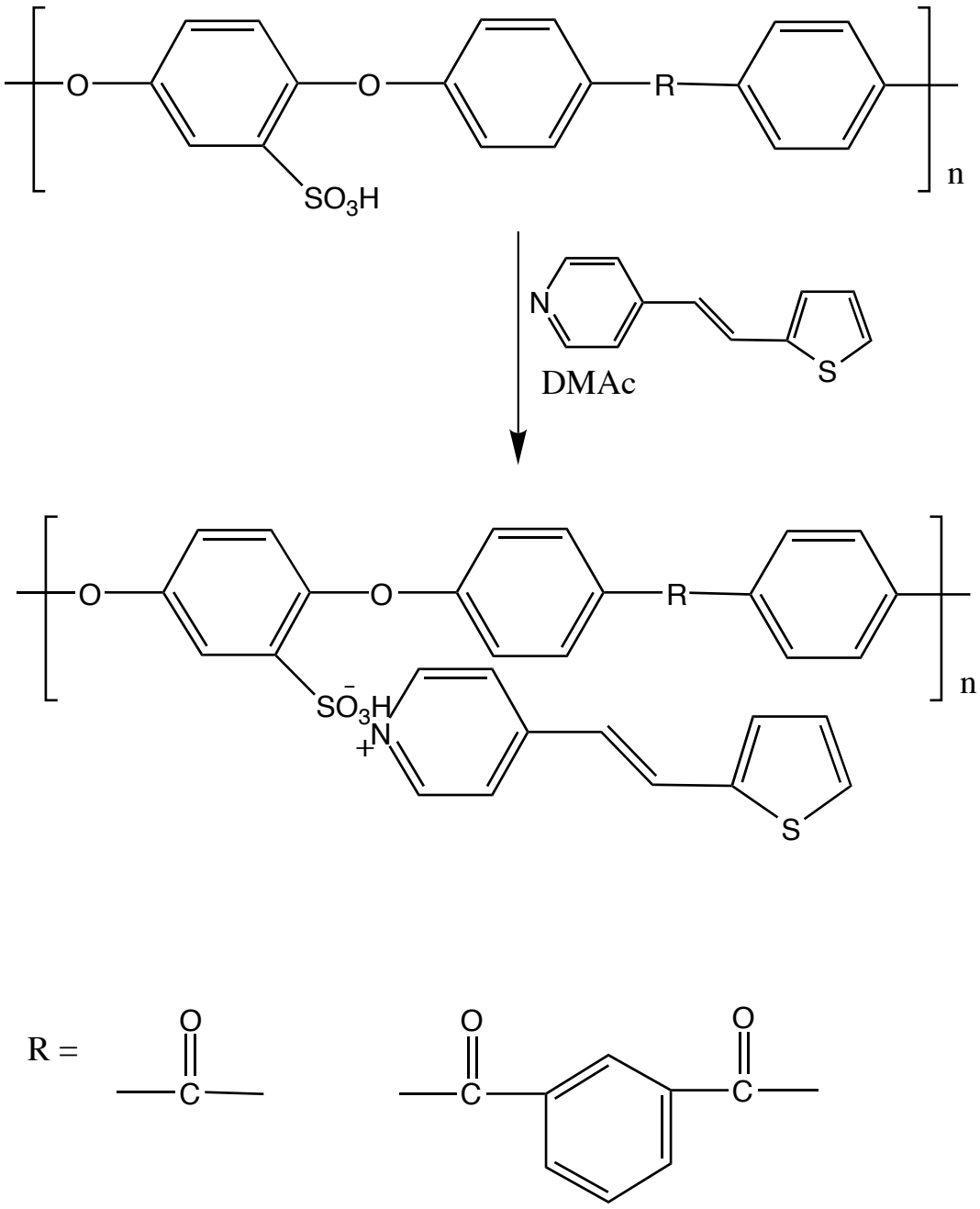

R =

Scheme 2.4.1 Synthesis of poly(arylene ether)s with side chain chromophore (172)

Chapter 3.0, EXPERIMENTAL

3.1 Purification of Solvents

3.1.1 Chlorobenzene

Supplier: Aldrich Chemical Company
Molecular Formula: C_6H_5Cl
Molecular Weight: 112.56 g/mole
Boiling Point: 132°C/760 torr
Chemical Structure:

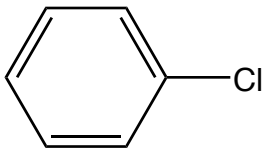

Purification Procedure:

Chlorobenzene was dried over calcium hydride for 24 hours and distilled under reduced pressure at approximately 45°C. The constant boiling fraction was collected and stored in a round bottom flask under nitrogen.

3.1.2 N,N- Dimethylacetamide

Acronym: DMAc
Supplier: Aldrich Chemical Company
Molecular Formula : C_4H_9NO
Molecular Weight: 87.12 g/mole
Boiling Point: 165°C/760 torr
Chemical Structure:

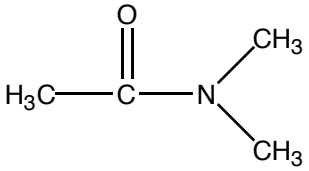

Purification Procedure:

DMAc was dried over phosphorus pentoxide for 24 hours and distilled under reduced pressure at approximately 60°C. The constant boiling fraction was collected and stored in a round bottom flask under nitrogen.

3.1.3 Diphenylsulfone

Acronym: DPS
Supplier: Aldrich Chemical Company
Molecular Formula: $C_{12}H_{10}O_2S$
Molecular Weight: 218.27 g/mole
Melting Point: 127-128°C
Boiling Point: 379°C/760 torr
Chemical Structure:

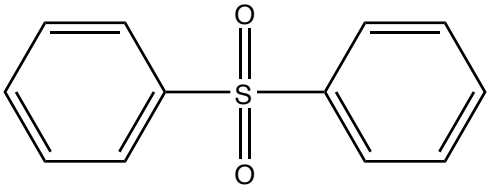

DPS was recrystallized from acetone . The large crystals were crushed using a mortar and pestle and then dried in a vacuum oven at 75°C.

3.1.4 Tetrahydrofuran

Acronym: THF
Supplier: Aldrich Chemical Company
Molecular Formula: C_4H_8O
Molecular Weight: 72.11 g/ mole
Boiling Point: 67°C/760 torr
Chemical Structure:

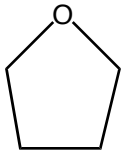

THF was purified by distillation over sodium and benzophenone. The solvent was both distilled and stored under nitrogen.

3.1.5 General Solvents and Reagents:

The following general solvents were used as received from Aldrich Chemical Company: methanol, acetone, toluene, chloroform, DMSO, NMP, cyclohexane, hexanes, and anhydrous diethyl ether.

The following general reagents were used as received from Aldrich Chemical Company: phenylphosphonic dichloride, 1-fluoro-4-bromobenzene, dimethyl methylphosphonate, potassium carbonate, magnesium turnings, anhydrous magnesium sulfate, concentrated sulfuric acid, concentrated hydrochloric acid, bromobenzene, methyl orange, methyl red, phenyl silane, nickel(II)bromide (dried 18 hours at 200°C under vacuum).

The general reagent sodium hydroxide was purchased from Mallinckrodt Chemical Company.

3.2 Synthesis and Purification of Monomers

3.2.1 Bisphenol-A

Acronym: (Bis-A)
Supplier: Dow Chemical Company
Molecular Formula: $C_{15}H_{16}O_2$
Molecular Weight: 228.27 g/mole
Melting Point: 156-157°C
Chemical Structure:

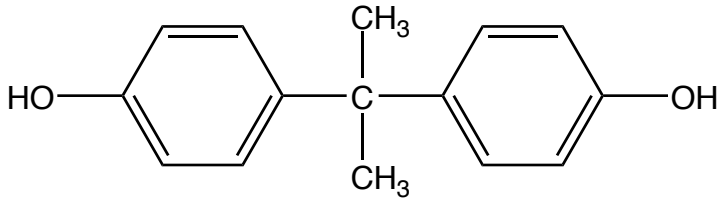

Purification Procedure:

Bis-A needed no further purification except being dried under vacuum at 100°C overnight prior to use. If needed, this monomer can be recrystallized from toluene.

3.2.2 1,1-bis(4-hydroxyphenyl)-1-phenyl-2,2,2-trifluoroethane

Acronym: 3F
Molecular Formula: $C_{20}H_{15}F_3O_2$
Molecular Weight: 344.38 g/mole

Melting Point: 230-231°C

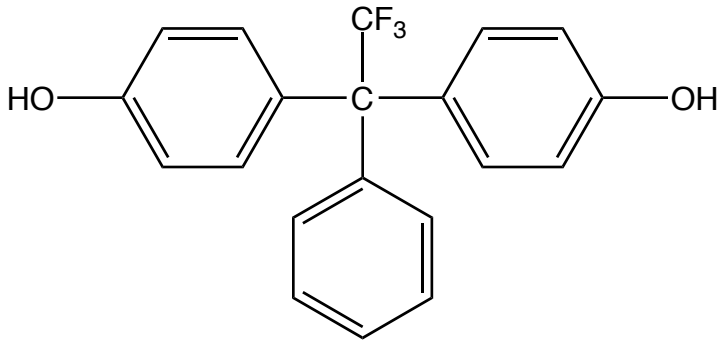

Purification Procedure:

This monomer was obtained from Dr. H. J. Grubbs in our laboratories who synthesized and purified it via previously published procedures (63).

3.2.3 Phenolphthalein [2,2-bis(4-hydroxyphenyl)phthalide]

Acronym: PP

Supplier: Aldrich Chemical Company

Molecular Formula: $C_{20}H_{14}O_4$

Molecular Weight: 318.12 g/mole

Melting Point: 262-263°C

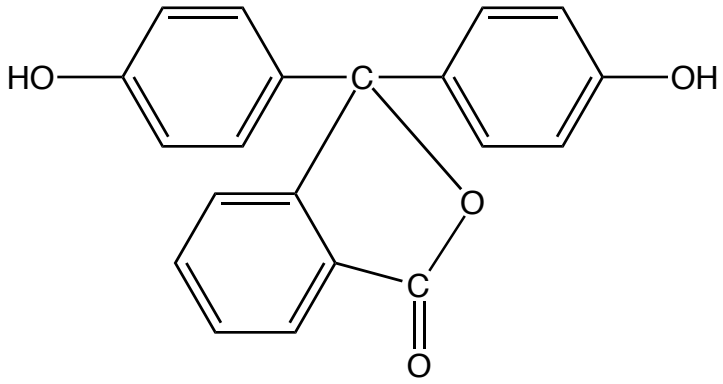

Purification Procedure:

PP needed no further purification except for drying under vacuum prior to use. If needed, this monomer can be recrystallized from methanol.

3.2.4 Hydroquinone

Acronym: HQ

Supplier: Eastman Chemical Company

Molecular Formula: $C_6H_6O_2$

Molecular Weight: 110.11 g/ mole

Melting Point: 173-175°C

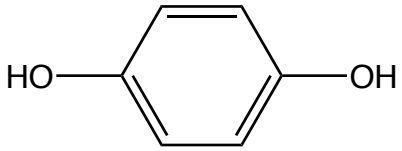

Purification Procedure:

HQ needed no further purification except for drying under vacuum prior to use. If needed, this monomer can be sublimed.

3.2.5 4,4'-Sulfonyldiphenol

Acronym: Bis-S

Supplier: Crown Zellerbach Corporation

Molecular Formula: $C_{12}H_{10}O_4S$

Molecular Weight: 250 g/mole

Melting Point: 245-247°C

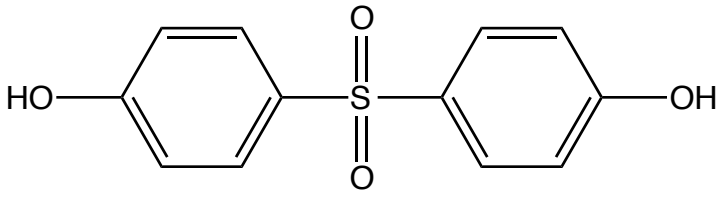

Purification Procedure:

Bis-S was purified by placing 15g of Bis-S and 50mL of hexane in an Erlenmeyer flask. After the solvent was boiling ethyl acetate was added dropwise until Bis-S was completely dissolved. The solution was allowed to cool. The crystals were collected by filtration and then dried in a vacuum oven at 100°C.

3.2.6 4,4'-Bis(fluorophenyl)methylphosphine Oxide

Acronym: BFPMPO

Molecular Formula: $C_{13}H_{12}F_2OP$

Molecular Weight: 252.20 g/mole

Melting Point: 115-116°C

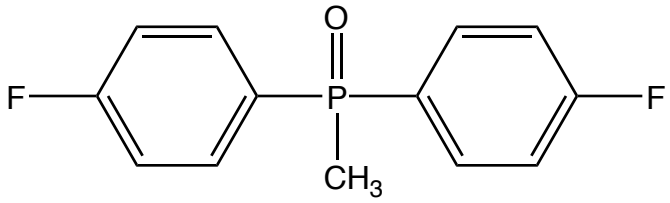

Synthetic Procedure:

BFPMPO was synthesized by reacting 2.1 equivalents of 1-fluoro-4-bromobenzene with 1 equivalent of dichloromethylphosphine oxide *via* Grignard chemistry. For example, 48.2g (2.0 moles) of magnesium turnings (Aldrich 99%) and 1.75 L of freshly distilled THF (Aldrich 99+%) were added to a 3L 3-neck flask equipped with a mechanical stirrer, addition funnel, nitrogen inlet, and condenser. To the solution 352.7g (1.98 moles) p-bromofluorobenzene (Aldrich 99%) was added dropwise at room temperature over a period of 2-3 hours. The mixture was stirred at room temperature overnight. Next, 130.7g (0.98 moles) of methyl phosphonic dichloride was added dropwise at room temperature. The reaction was stirred overnight to give a yellow solution. Aqueous sulfuric acid (10 vol.%) was added until the solution was acidic. Water (0.75L) and diethyl ether (0.10L) were added to the reaction mixture and the THF layer was decanted. The water layer was washed well with THF and diethyl ether and all organic layers combined. The organic layer was then dried over anhydrous magnesium sulfate, filtered, and the filtrate evaporated to afford a light yellow solid. The material was purified by distillation utilizing a Kugelrohr apparatus and subsequent recrystallation from a 1:5 THF/cyclohexane mixture. The resulting material was monomer grade with a melting point of 115-116°C (lit. 112-114°C) (37). The yield of the reaction was 80-85% after purification (38, 128). Elemental analysis for $C_{13}H_{12}F_2OP$: C, 61.9; H, 4.8. Found: C, 62.2, H, 4.5.

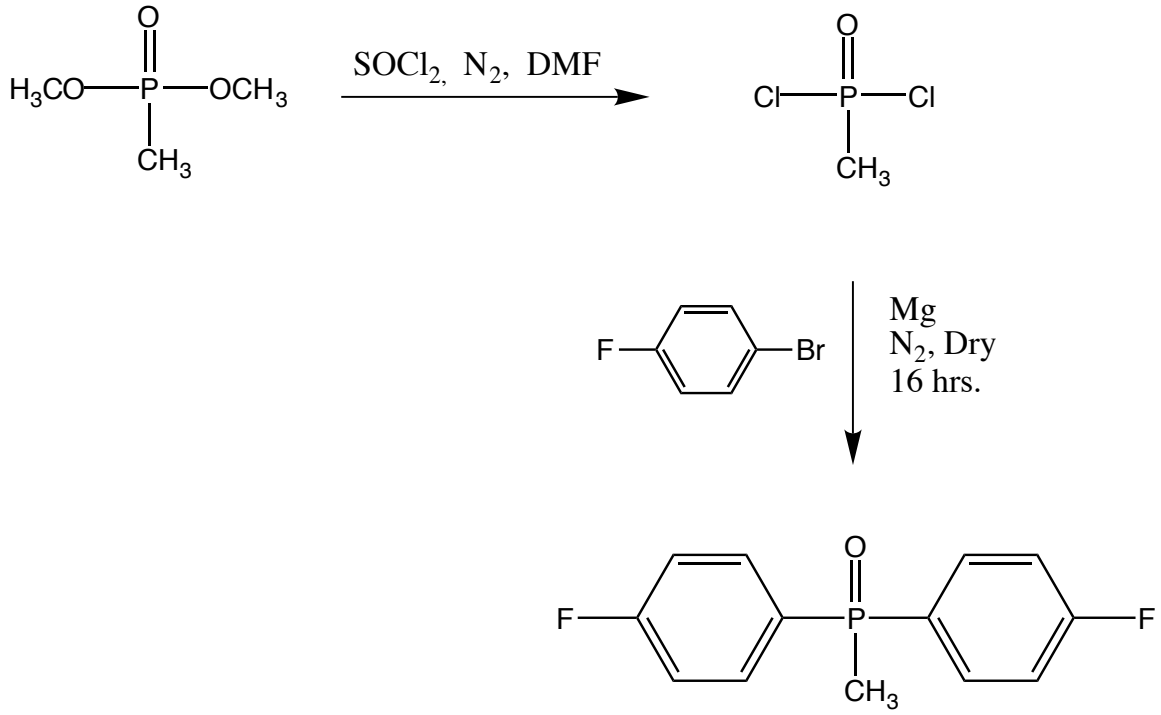

Scheme 3.2.6.1 Synthesis of 4,4'Bis(fluorophenyl)methylphosphine oxide

3.2.7 4,4'-Bis(fluorophenyl)phenylphosphine Oxide

Acronym: BFPPO

Molecular Formula: $C_{18}H_{13}F_2OP$

Molecular Weight: 314.28 g/mole

Melting Point: 130-131°C

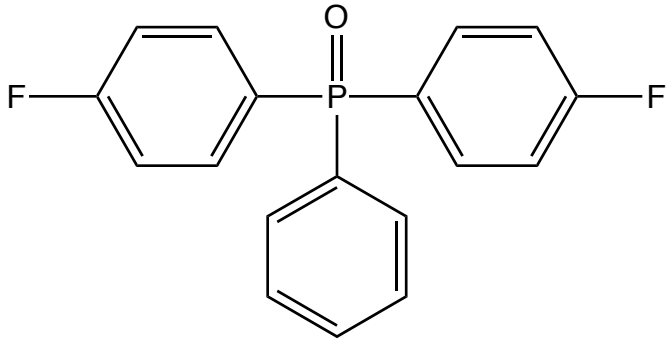

Synthetic Procedure:

BFPPO was synthesized using previously published chemistry similar to that of BFPMPO (57). The melting point of BFPPO synthesized in our laboraory was 130-131°C (lit. 124-126°C) (37). Elemental analysis for $C_{18}H_{13}F_2OP$: C, 68.8; H, 4.2. Found: C, 68.9, H, 4.3.

3.2.8 4,4'-Bis(hydroxyphenyl)methylphosphine Oxide

Acronym: BOHPMPO

Molecular Formula: $C_{13}H_{13}O_3P$

Molecular Weight: 248.22 g/mole

Melting Point: 257-258°C

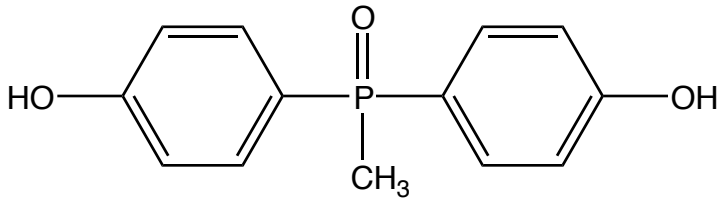

Synthetic Procedure:

BOHPMPO was synthesized by hydrolyzing BFPMPO using 5 moles of potassium hydroxide in DMSO. For example, 10g (0.04 moles) of BFPMPO and 50mL of DMSO (Aldrich 99%) were added to a 100mL 3-neck flask equipped with a mechanical stirrer, nitrogen inlet, and a condenser. To the solution was added a 15N solution of 12.8g (0.2 moles) of potassium hydroxide (Mallinckrodt, 88%) in water. The solution was then raised to reflux (approximately 135°C) and allowed to react for 8 hours. The solution was acidified (HCl) and DMSO removed using a rotovap to afford a pale yellow solid. Water was then added to the solid to remove remaining salt. The product was filtered, dried in a vacuum oven at 150°C overnight, and then purified using fractional recrystallation from a 15 wt % solution of 1:5 v/v ratio of methanol/water. Then resulting material was considered to be monomer grade with a melting point of 257-258°C. The yield of the reaction was 90% after purification (128). Elemental analysis for $C_{13}H_{13}O_3P$: C, 62.9; H, 5.3. Found: C, 62.7, H, 4.9.

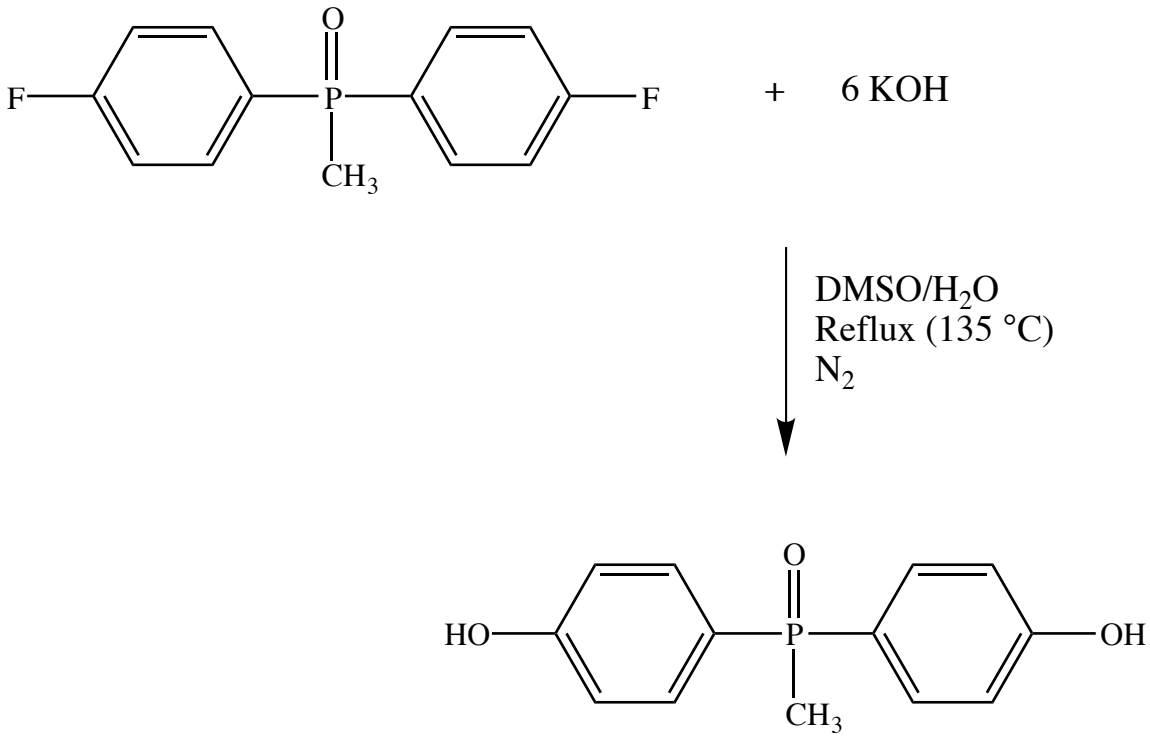

3.2.8.1 Synthesis of 4,4'-bis(hydroxyphenyl)methylphosphine oxide

3.2.9 4,4'-Bis(hydroxyphenyl)phenylphosphine Oxide

Acronym: BOHPPO

Molecular Formula: $C_{18}H_{15}O_3P$

Molecular Weight: 310.30 g/mole

Melting Point: 236-237°C

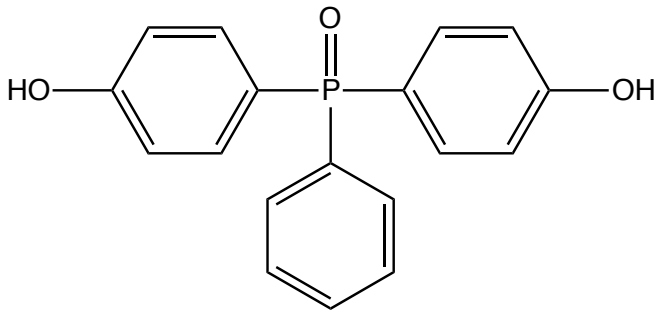

Synthetic Procedure:

BOHPPO was synthesized in a similar manner to BOHPMPO, except that BFPPO was utilized as the starting material instead of BFPMPO. The reaction product was purified by precipitation into acidic water (10% HCl) and subsequent recrystallation from a 1:5 methanol/water solution. The resulting material was monomer grade with a melting point of 236-237°C. The reaction yield was greater than 95% after purification (128). Elemental analysis for $C_{18}H_{15}O_3P$: C, 69.7; H, 4.9. Found: C, 68.9, H, 5.3.

3.3 Polymer Synthesis

3.3.1 High Molecular Weight Poly(arylene ether phosphine oxide)s

High molecular weight poly(arylene ether phosphine oxide)s (PEPO)s were synthesized *via* S_NAR step growth polymerization of BFPMPO with various bisphenols including 1,1-bis(4-hydroxyphenyl)-1-phenyl-2,2,2-trifluoroethane (3F) (63), phenolphthalein (PP) (167), hexafluoro bisphenol-A (6F), and hydroquinone (HQ). The synthesis of a PEPO based on bisphenol-A will be used as an example. To a 500mL 3-neck flask equipped with a mechanical stirrer, nitrogen inlet, and a Dean-Stark trap were added equal molar amounts (0.05 moles) of each monomer followed by potassium carbonate (0.058 moles). Freshly distilled DMAc was introduced to afford a concentration of 15% solids. Toluene was added as an azeotroping agent (50mL) and the reaction temperature was raised to 135-140°C to give a reflux. After four hours the solution temperature was raised to 155°C by the removal of most of the toluene and a slight reflux of toluene was maintained to ensure anhydrous reaction conditions for 16 to 18 hours. After cooling the mixture, chloroform (35mL) was added to dilute the mixture and most of the salts (*eg*. KF, K_2CO_3) were filtered using filter paper. After adding 5mL acetic acid, the polymer was precipitated into an 80:20 methanol/water mixture using a Waring blender. The fibrous polymer was filtered and dried in a vacuum oven at 170°C for 12 hours, redissolved in chloroform (20 % solids), reprecipitated into methanol and again dried under the same conditions. Spectroscopic analysis (^{1}H NMR and ^{31}P NMR) is given in section 4.2 (38, 128).

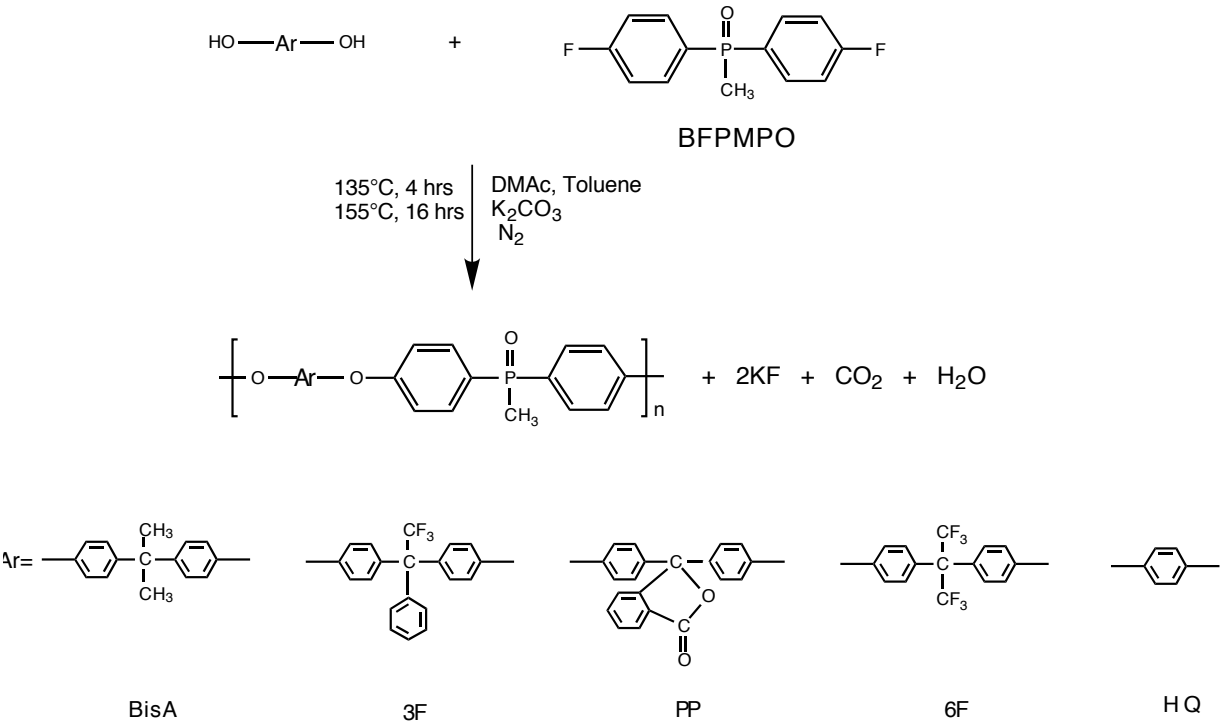

3.3.1.1 Synthesis of high molecular weight poly(arylene ether phosphine oxide)s

3.3.2 High Poly(arylene ether methyl phosphine oxide sulfone)

Acronym: BFPMPO-SO_2

High molecular weight poly(arylene ether methyl phosphine oxide sulfone)s based on BFPMPO was synthesized as follows. To a 3-neck 250 mL high temperature reaction flask equipped with a mechanical stirrer, nitrogen inlet, and nitrogen outlet were added equal molar amounts (0.01 moles) of BFPMPO and Bis-S monomer followed by potassium carbonate (0.015 moles) and 150 wt. % of diphenyl sulfone. The reaction was initially run at 135°C for 1 hour and then at 170°C for 4 hours. These lower temperatures were used to dry the system. The polymerization temperature was then increased to 270°C for 4 hours and finally 320°C for 20 minutes. The short time at 320°C was required to drive the reaction to completion which produced high molecular weight. The reaction flask was then cooled, 100 mL of NMP was added to the flask and the salts filtered off. After adding 5 mL of acetic acid the polymer was precipitated into methanol and dried in a vacuum oven at 170°C overnight. The polymer was redissolved in NMP, reprecipitated into methanol and dried in a vacuum oven at 170-200°C overnight. Spectroscopic analysis (^{1}H NMR and ^{31}P NMR) are given in section 4.2 (38, 128).

The higher temperatures used in this reaction, with respect to the previously mentioned synthesis, were necessary as a consequence of the deactivating effect of the phosphine oxide moiety on the bisphenol monomers.

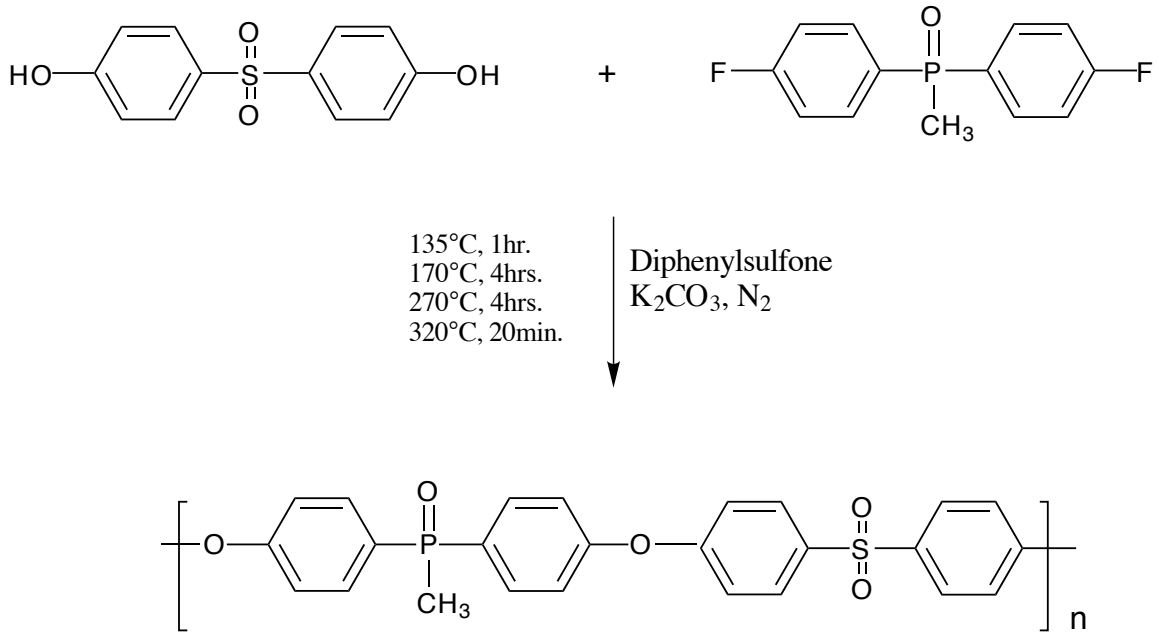

Scheme 3.3.2.1 Synthesis of poly(arylene ether methyl phosphine oxide sulfone)

3.3.3 Synthesis of poly(arylene ether phenyl phosphine oxide sulfone)

Acronym: BFPPO-SO_2

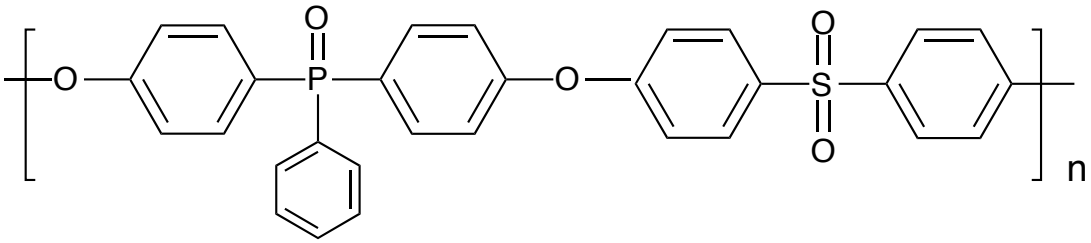

Similar conditions were used as described in the synthesis of poly(arylene ether methyl phosphine oxide sulfone). The only exception was that BFPPO was used as the activated dihalide instead of BFPMPO. Spectroscopic analyses (^{1}H NMR and ^{31}P NMR) are given in section 4.2.

3.3.4 Polyarylene(ether methyl phosphine oxide)

Acronym: BFPMPO-BOHPMPO

High molecular weight poly(arylene ether phosphine oxide) homopolymer based on BFPMPO was synthesized as follows. To a 3-neck 250 mL high temperature reaction flask equipped with a mechanical stirrer, nitrogen inlet, and nitrogen outlet was added equal molar amounts (0.01 moles) BFPMPO and BOHPMPO followed by potassium carbonate (0.015 moles), with 150 wt. % of diphenyl sulfone. The reaction was initially run at 135°C for 1 hour then 170°C for 4 hours. These lower temperatures were used to dry the reaction. The temperature was then increased to 270°C for 4 hours and finally 320°C for 20 minutes. The short time at 320°C was to drive the reaction to completion as discussed earlier. The reaction flask was then cooled and 100 mL of DMAc was added to the flask and the salts filtered off. After adding 5 mL of acetic acid the polymer was precipitated into acetone and dried in a vacuum oven at 170°C overnight. It was redissolved in DMAc, reprecipitated into acetone and dried in a vacuum oven at 170-200°C overnight. Spectroscopic analyses (^{1}H NMR and ^{31}P NMR) confirmed the structure as are given in section 4.2 (38, 128).

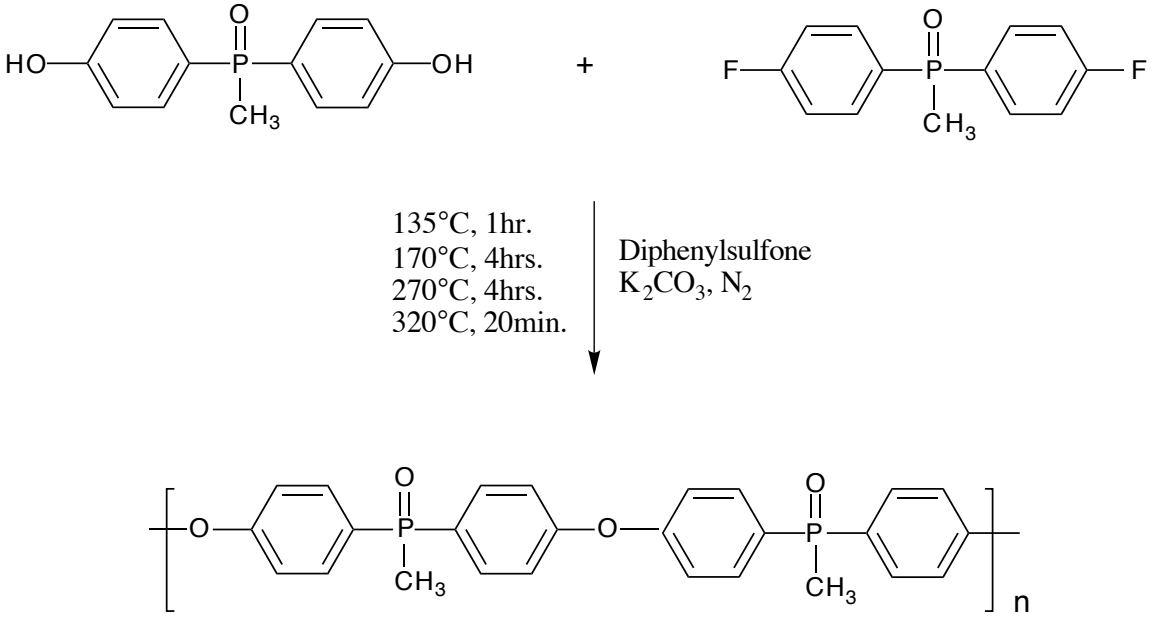

Scheme 3.3.4.1 Synthesis of Poly(arylene ether methyl phosphine oxide)

3.3.5 Poly(arylene ether methyl phosphine oxide phenyl phosphine oxide)

Acronym: BFPMPO-BOHPPO

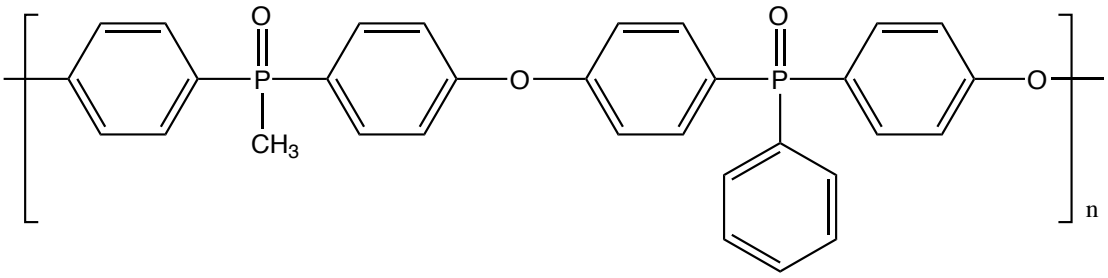

Similar conditions were used as described in the synthesis of poly(arylene ether methyl phosphine oxide). The only exception was that BOHPPO was employed as the bisphenol. Spectroscopic analyses (^{1}H NMR and ^{31}P NMR) are given in section 4.2 (38, 128).

3.3.6 Poly(arylene ether phenyl phosphine oxide)

Acronym: BFPPO-BOHPPO

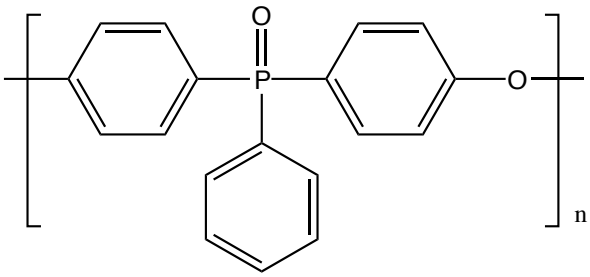

Similar conditions were used as described in the synthesis of poly(arylene ether methyl phosphine oxide). The only exception being that BOHPPO was employed as the bisphenol and BFPPO was the activated dihalide. Spectroscopic analyses (^{1}H NMR and ^{31}P NMR) are given in section 4.2 (38, 128).

3.3.7 Bisphenol-A Based Poly(arylene ether phosphine)

The phosphine oxide moiety of a 30K poly(arylene ether) based on bisphenol-A and BFPPO was partially reduced using phenylsilane (173, 174). The reaction was conducted under nitrogen in a one-neck flask equipped with a magnetic stirrer and a condenser. For example, 69.5g (0.14 moles) of polymer was initially dissolved in chlorobenzene to afford a concentration of 20% solids. After the solution became homogeneous, 39.9g (0.37 moles) of phenylsilane was

introduced to afford an 8:3 molar ratio. The reaction temperature was raised to 110°C for 5 days, following which the solution was precipitated into methanol. The polymer was then redissolved in chloroform, reprecipitated into methanol and dried in a vacuum oven at 150°C. Spectroscopic analyses (^{1}H NMR and ^{31}P NMR) are given in section 4.6.

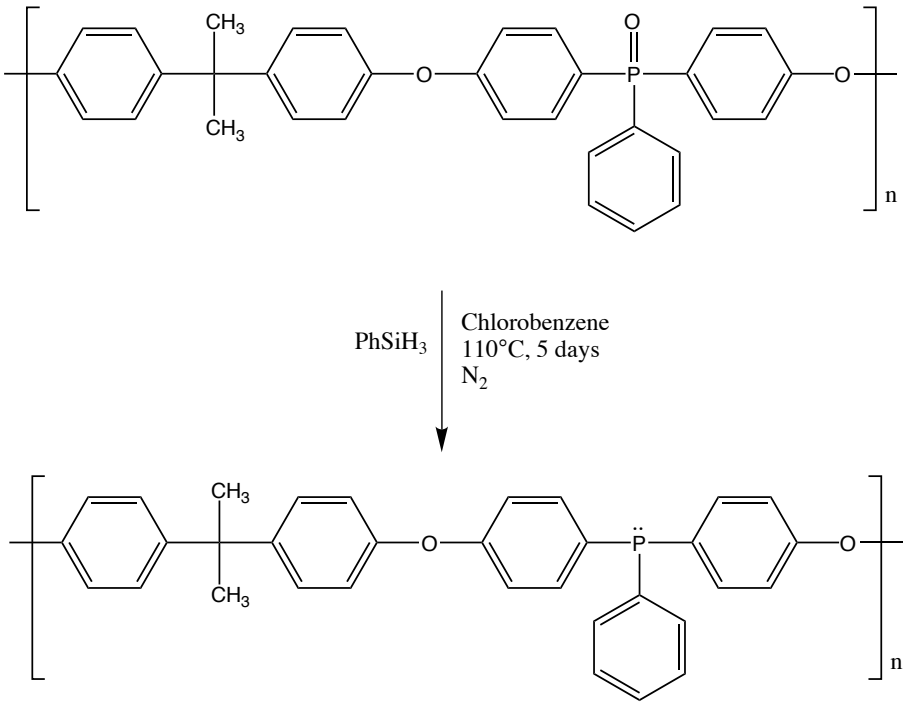

Scheme 3.3.7 Synthesis of bisphenol-A based poly(arylene ether phosphine)

3.3.8 Bisphenol-A Based Poly(arylene ether phosphonium bromide)

Poly(arylene ether phosphonium bromide) ionomers were synthesized using the poly(arylene ether phosphine) described above. The reaction was conducted under nitrogen in a one-neck flask equipped with a magnetic stirrer and a condenser. For example, 11g (23 mmoles) of poly(arylene ether phosphine) was initially dissolved in benzonitrile to which 3.55g (22.6 mmoles) bromobenzene and 2.45g (11.3 mmoles) nickel(II)bromide were added to afford a 2:2:1 ratio of phosphorus:bromobenzene:nickel (II) bromide. The reaction temperature was raised to 210°C for 3 hours. The mixture was then precipitated into deionized water and dried in a vacuum oven at 175°C overnight. During work up of the reaction care was taken to ensure that all $NiBr_2$ was removed (175). This was accomplished by precipitating the phosphonium polymer in deionized water and then filtering. The polymer was then placed into warm deionized water overnight. The polymer was then filtered and the warm water step was repeated two more times. Spectroscopic analyses (^{1}H NMR and ^{31}P NMR) are given in section 4.6.2. The percent conversion of the

phosphine oxide to phosphine could be modified by decreasing the reaction time. This may be useful in controlling the amount of chromophore incorporation with the polymeric backbone (see 3.3.9 below).

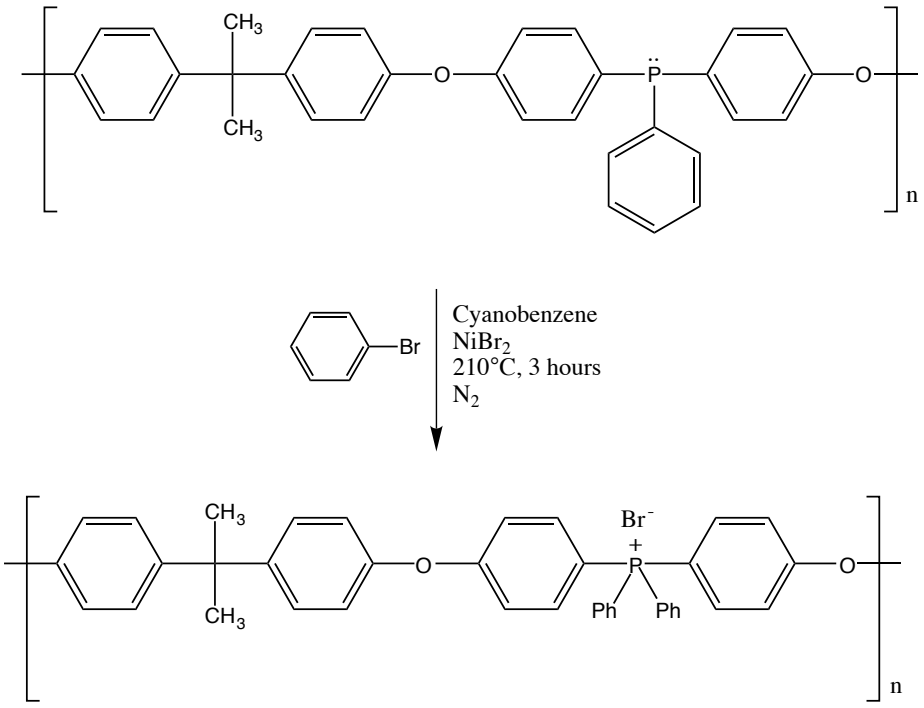

Scheme 3.3.8 Synthesis of Bisphenol-A based poly(arylene ether phosphonium bromide)

3.3.9 Derivatization of Poly(arylene ether phosphonium bromide) ionomer with methyl orange

Poly(arylene ether phosphonium bromide) was reacted with 4-[4-(dimethylamino)phenylazo]benzenesulfonic acid, sodium salt (methyl orange) in order to synthesize an ionomer which might be useful as a second order non-linear optical polymer. The reaction was conducted in a one-neck flask equipped with a magnetic stirrer. For example, 8g (12 mmoles) of poly(arylene ether phosphonium bromide) was dissolved in DMSO. 4.5g (12 mmoles) of methyl orange (predissolved in DMSO) was added to the reaction. The reaction was allowed to continue at room temperature for 1.5 hours. The solution was precipitated into water, filtered, and the precipitate dried in a vacuum oven at 80°C overnight. The red polymer was then redissolved in DMSO and reprecipitated into water and filtered. The polymer was then stirred in deionized water overnight, filtered, and dried in a vacuum oven at 80°C overnight. Spectroscopic analyses (^{1}H NMR and ^{31}P NMR) are given in section 4.6, and confirmed the structure.

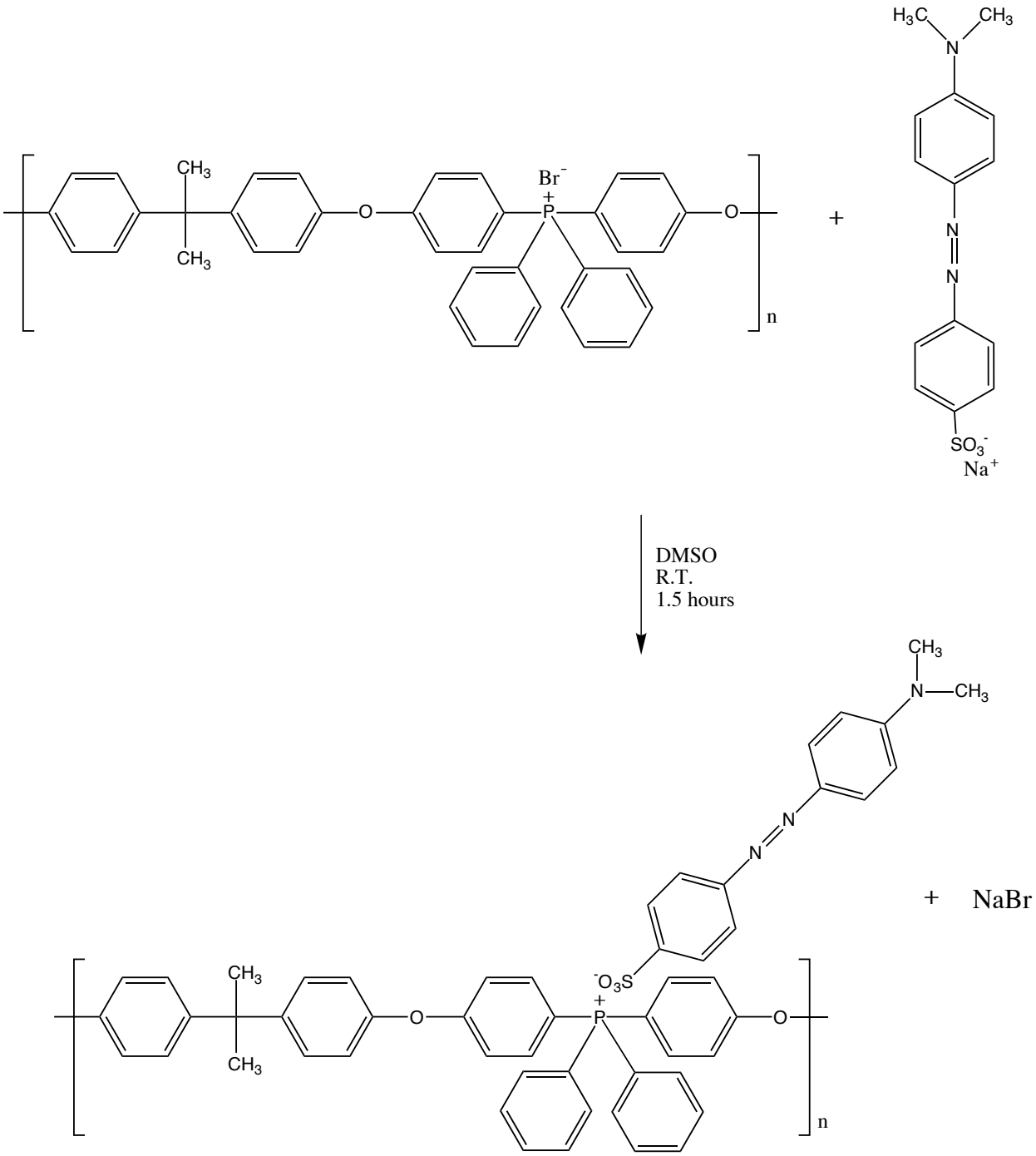

Scheme 3.3.9 Derivatization of Poly(arylene ether phosphonium bromide) with methyl orange

3.3.10 Derivatization of Poly(arylene ether phosphonium bromide) with methyl red

Derivatization of poly(arylene ether phosphonium bromide) with 4-[4-(dimethylamino)phenylazo]benzenecarboxylic acid, sodium salt (methyl red) followed a procedure similar to derivatization with methyl orange, except that methyl red was used instead of methyl orange. Spectroscopic analysis (^{1}H NMR and ^{31}P NMR) is given in section 4.6.

3.4 Commercial Thermoplastics Utilized

Udel from Amoco Chemical and Victrex from ICI were employed as reference polymers throughout this research. Their structures, thermal transitions, and source are outlined in Table 3.4.1 below.

Table 3.4.1 Commercial poly(arylene ether)s utilized

Polymer	T_g, °C	Source
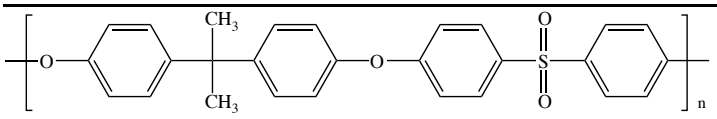	190	Amoco
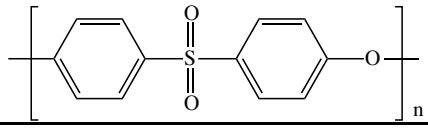	230	ICI

3.5 Characterization Methods

3.5.1. Proton NMR Spectra (^{1}H NMR)

Proton (^{1}H) NMR spectra were measured on a Varian 400 MHz instrument in $CDCl_3$ or DMSO depending on the solubility of the material being analyzed. All $CDCl_3$ spectra were referenced to tetramethylsilane (TMS) at 0 ppm.

3.5.2 Carbon NMR Spectra (^{13}C NMR)

Carbon (^{13}C) NMR spectra were obtained in the same manner as the proton NMR spectra but at a frequency of 100 MHz.

3.5.3 Phosphorus NMR Spectra (^{31}P NMR)

Phosphorus (^{31}P) NMR spectra were obtained in the same manner as the proton NMR spectra but at a frequency of 160 MHz. Deuterated DMSO, chlorobenzene, or $CDCl_3$ were used as the solvent depending on the situation. All spectra were referenced to H_3PO_4 at 0 ppm.

3.5.4 Melting Point of Monomers

Melting points were obtained by placing a ground sample into a capillary tube and heated slowly (2°C/min) to determine a melting range. The formation of a meniscus was taken to be the beginning of the melt.

3.5.5 Intrinsic Viscosity

Intrinsic viscosities were measured at 25°C in a Cannon-Ubbelohde viscometer, typically using chloroform as the polymer solvent. When the polymer was not soluble in chloroform, NMP was used as the solvent. Three low concentration polymer solutions were prepared and the time measured for the polymer solutions (t) and the pure solvent (t_o) to pass through the viscometer was measured. Assuming $t/t_o = \eta/\eta_o$, the specific viscosity was defined as $[\eta]_{sp} = (\eta/\eta_o) - 1$ and the reduced viscosity was defined as $\eta_{red} = \ln(\eta/\eta_o)$. Both (η_{sp}/c) and (η_{red}/c) were plotted with respect to concentration and extrapolated to zero concentration to give the intrinsic viscosity $[\eta]$.

3.5.6 Gel Permeation Chromatography

Molecular weights were analyzed on a Waters 150C ALC/GPC chromatograph equipped with a differential refractive index detector and a Viscotek Model 100 viscosity detector connected in parallel (15). N-methylpyrrolidone (HPLC grade) containing 0.06M LiBr filtered through 0.5 mm Teflon filter served as a mobile phase. The chromatography conditions were as follows: two stainless steel columns (7.8 x 300)mm packed with Waters μStyragel HT 10^3 Å and 10^4 Å, mean particle diameter 10 mm, flow rate 1.0 mL/min, injection volume 200 mL, and a temperature of 60°C for both GPC and detectors. Samples prepared to known concentrations (approx. 3 mg/mL) were dissolved in the mobile phase and filtered through 0.2 mm PTFE disposable filters prior to analysis (176).

3.5.7 Differential Scanning Calorimetry

Differential scanning calorimetry (DSC) was performed using a Perkin Elmer DSC 7 instrument. The glass transition temperatures were obtained from sample which had been pressed and secured in crimped aluminum pans. Scans were run at 10°C/min and the reported T_g values were obtained from the second heat after a quench cool from the first run.

3.5.8 Dynamic Thermogravimetric Analysis

Dynamic thermogravimetric analysis (TGA) was performed on a Perkin Elmer TGA 7 instrument. The heating rate was 10°C/min in air unless otherwise noted. Only polymers of the same physical form were compared. For example, films were compared with films and powders were compared to other powders.

3.5.9 Isothermal Thermogravimetric Analysis

Isothermal thermal gravimetric analysis was also performed on a Perkin Elmer TGA 7 instrument. The analysis was carried out at a specified temperature (e.g., 400°C) in air for 3 hours unless otherwise noted.

3.5.10 Dynamic Mechanical Analysis

Dynamic mechanical analysis was carried out on a Perkin Elmer DMA 7 using 3-point bending mode. The frequency was 1 Hz and the heating rate was 2°C/min. The sample was a 3 mm thick compression molded bar. These samples were compressed in the same manner described in section 3.5.12.

3.5.11 Dielectric Thermal Analysis

Dielectric thermal analysis were performed on a polymer laboratories instrument at frequencies of 4, 10, 33.3, and 100 Khz using a potential of 1 volt. The 20 mm diameter sample of varying thickness below 0.05 mm was heated at a rate of 2°C/min..

3.5.12 Stress-Strain Behavior

The stress-strain behavior was analyzed at room temperature using an Instron 1123 equipped with a strain gauge extensiometer (Instron 2630-013). The dog-bone shape samples (ASTM D-

638 #5) were cut out of a compression molded plaque with thickness ranging from 0.0064 - 0.010 inches. The samples were tested at an average cross head speed of 0.5 in/min (ASTM D-638). Approximately 8 samples were tested and the results were averaged.

3.5.13 Cone Calorimetry

Polymer samples with dimensions of 10 cm x 10 cm x 3 mm were compression molded 70°C above their Tg and measured at the Fire Research Laboratory of the National Institute of Standards and Technology (NIST), under the supervision of Dr. T. Kashiwagi, where they were evaluated in air using cone calorimetry at a constant flux of 40 kW/m^2. The instrument was run in the standard mode of ASTM E 1354. The only exception was that the sample was not mounted on the standard metal holder; rather it was mounted on a silicate board.

3.5.14 Pyrolysis Studies

Samples were pyrolyzed for 6 seconds in either helium or air at 550°C and 700°C in a Pyrojector II (SGE) pyrolysis unit. The Pyrojector was attached to an on line Hewlett Packard gas chromatograph unit connected to a VG 7070E mass spectrometer. This way the polymer could be degraded at a specified temperature and the degradation products separated *via* GC, prior to analysis using mass spectrometry. The conditions for gas chromatography were as follows:
Carrier gas: helium
GC temperature: 25°C (1 min) -150°C (rate = 10°C/min)
Carrier gas pressure: 5 psi
Pressure differential between Pyrojector and column: 7 psi
Column type: 30 meter HP5 column (5% phenylmethylsilicone), 0.32 i.d.
For further clarification of this technique refer to Figure 3.4.14.1.

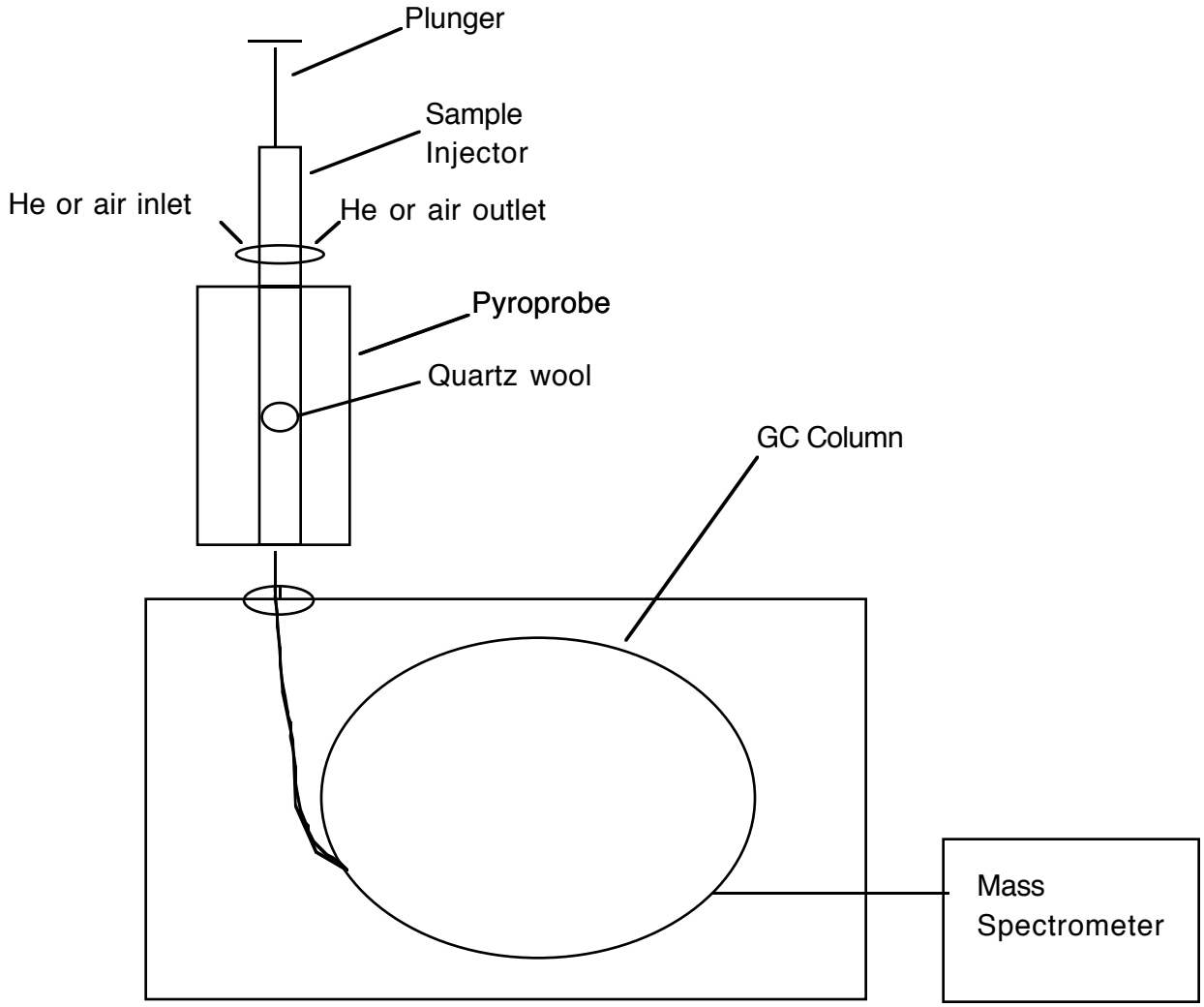

Figure 3.4.14.1 Illustration of pyrolysis GC-MS instrumentation

3.5.15 Refractive Index Measurements

The refractive index of solution cast films were measured using a Metricon Model 2010 Prism Coupler in the bulk mode. The laser used was a low power (0.5 mW nominal) He-Ne (632.8 nm) laser.

Chapter 4.0, RESULTS AND DISCUSSION

4.1 Monomer Synthesis and Characterization

4.1.1 4,4'-Bis(fluorophenyl)methylphosphine Oxide (BFPMPO)

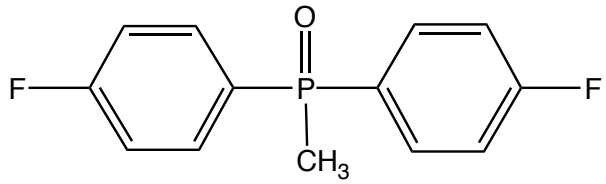

This activated halide monomer was synthesized utilizing Grignard chemistry *via* the reaction of p-bromofluorobenzene and methylphosphonic dichloride as described in section 3.2.6. These reactions were conducted at room temperature, afforded yields of 80-85% after recrystallization in a THF/cyclohexane (1/5 v/v) solution and showed a sharp melting point at 115-116°C. The molecular structure of this material was confirmed using ^{1}H and ^{31}P NMR in $CDCl_3$. These spectra are shown below in Figures 4.1.1.1 and 4.1.1.2. The two different aromatic protons appear at H_a (7.7 ppm) and H_b (7.15 ppm) and the pendant methyl shows a down field peak at 2.0. These protons appear as higher multiplets, due to coupling with phosphorus, which has a spin of 1/2. The protons have an integration ratio of 8 aromatic protons/3 aliphatic protons. The sole phosphorus shows a singlet at 29.2 ppm and the small side peaks equidistant on either side of the major phosphorus peak are side bands. Figure 4.1.1.3 was developed by courtesy of Venkat Vesudevan using molecular modeling and illustrates diphenylmethylphosphine oxide in its lowest energy confirmation.

4.1.2 4,4'-Bis(fluorophenyl)phenylphosphine Oxide (BFPPO)

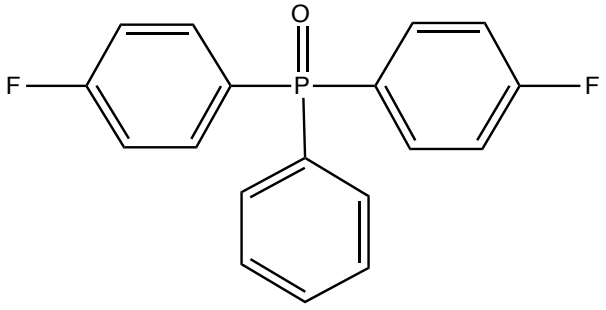

BFPPO was synthesized *via* Grignard chemistry involving p-bromofluorobenzene and phenylphosphonic dichloride as described in section 3.2.7. These reactions were conducted at room temperature and afforded yields of 80-85% after recrystallization in a THF/cyclohexane (1/5 v/v) solution. The melting point was 130-131°C and the structure was confirmed using ^{1}H and ^{31}P

NMR in $CDCl_3$. These spectra are shown below in Figures 4.1.2.1 and 4.1.2.2. There are four different aromatic protons are shown as H_a (7.65 ppm), H_b (7.56 ppm), H_c (7.48 ppm), and H_d (7.16 ppm). The phosphorus gives a singlet at 28.1 ppm which is a little up field from the similar methyl phosphine oxide structure above and is attributed to the phenyl being more electron donating than the methyl in BFPMPO. Figure 4.1.2.3 was also developed by courtesy of Venkat Vesudevan using molecular modeling and illustrates triphenylphosphine oxide in its lowest energy confirmation.

4.1.3 4,4'-Bis(hydroxyphenyl)methylphosphine Oxide (BOHPMPO)

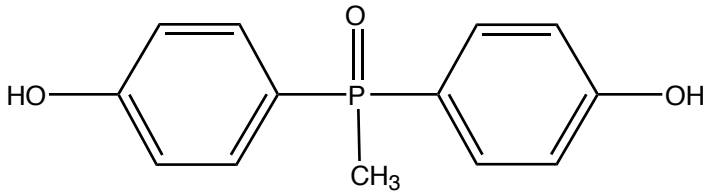

BOHPMPO was synthesized by hydrolyzing BFPMPO with potassium hydroxide in DMSO as described in section 3.2.9. The reaction was conducted for 8 hours at 135°C to afford a yield of 90% monomer grade material. It was necessary to maintain a reaction of 135°C because if the reaction temperature is too low (e.g. 80°C) only the monosubstituted product was obtained. If the reaction temperature is too high it is possible to obtain oligomers as shown in Scheme 4.1.3.1. It is important to avoid these side reactions because separation from the desired product would likely be difficult. The melting point was 257-258°C and the molecular structure of this material was confirmed using ^{1}H and ^{31}P NMR in DMSO. The integration of the aromatic protons to the aliphatic protons yielded a ratio of 8/3 and the integration of the hydroxyl protons to aromatic protons yielded a ratio of 1/4. The phosphorus NMR shows one major peak at 28.2 ppm, which is a 1 ppm up field shift compared to the dihalide adduct BFPMPO, due to the electron donating ability of the phenolic hydroxyls. The other smaller peaks equidistant from the major peak are spinning side bands. These spectra are shown below in Figures 4.1.3.1 and 4.1.3.2.

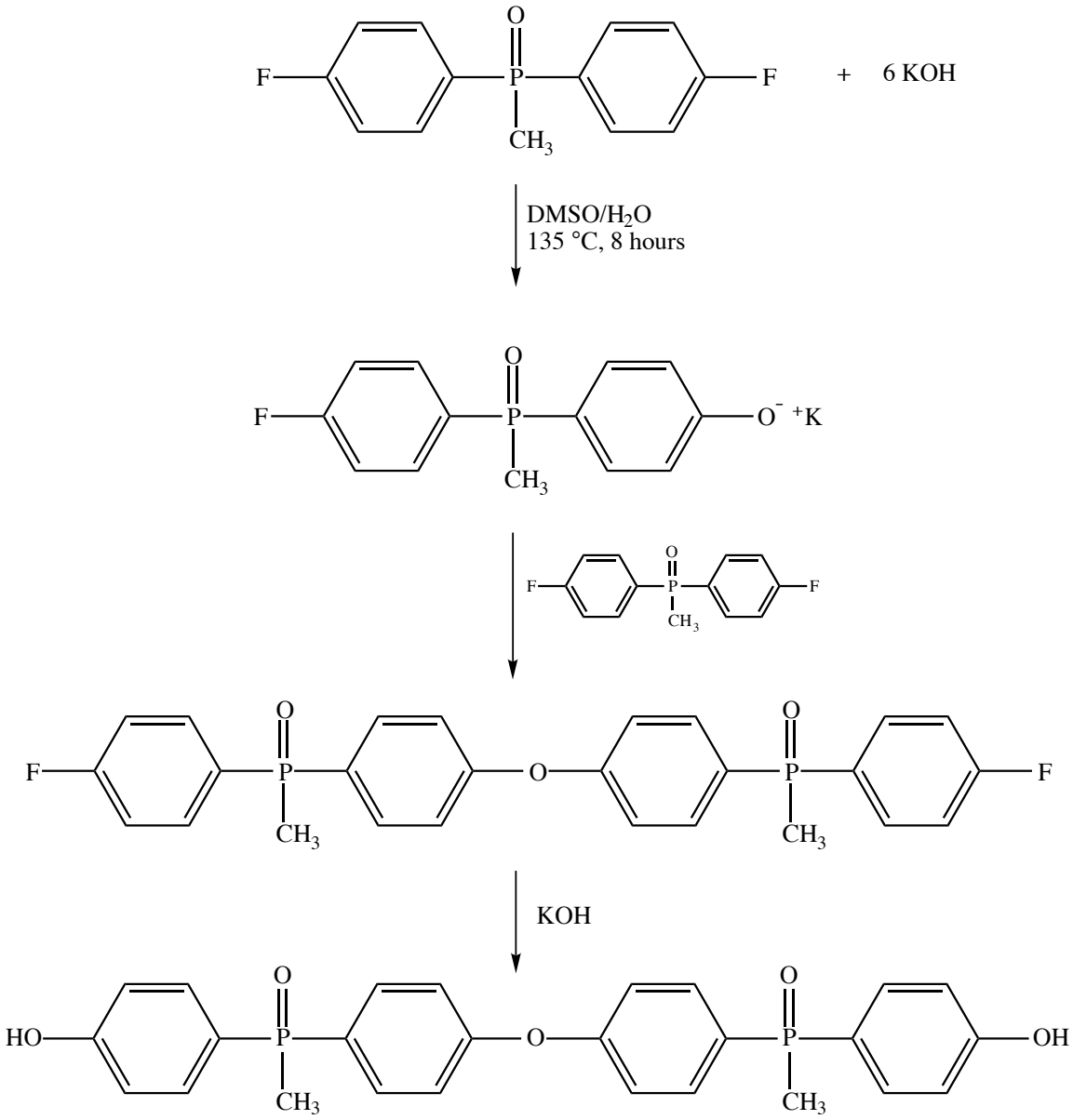

Scheme 4.1.3.1 Possible side reactions resulting in the synthesis of dimers and higher oligomers

4.1.4 4,4'-Bis(hydroxyphenyl)phenylphosphine Oxide (BOHPPO)

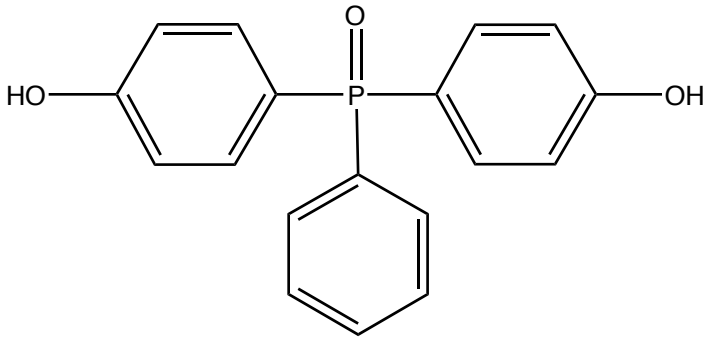

BOHPPO was synthesized by hydrolyzing BFPPO with five moles of potassium hydroxide (section 3.2.9) at 135°C for 8 hours to afford a yield of approximately 95% of monomer grade material, after recrystallization in a methanol water (1/5 v/v) solution (melting point = 236-237°C). The melting point was 236-237°C. The structure of this material was confirmed using ^{1}H and ^{31}P NMR in DMSO. The integration of the hydroxy peaks to aromatic peaks yielded a ratio of 2/13. These spectra are shown below in Figures 4.1.4.1 and 4.1.4.2. These monomers could also be considered in polyester, polycarbonate, and epoxy systems.

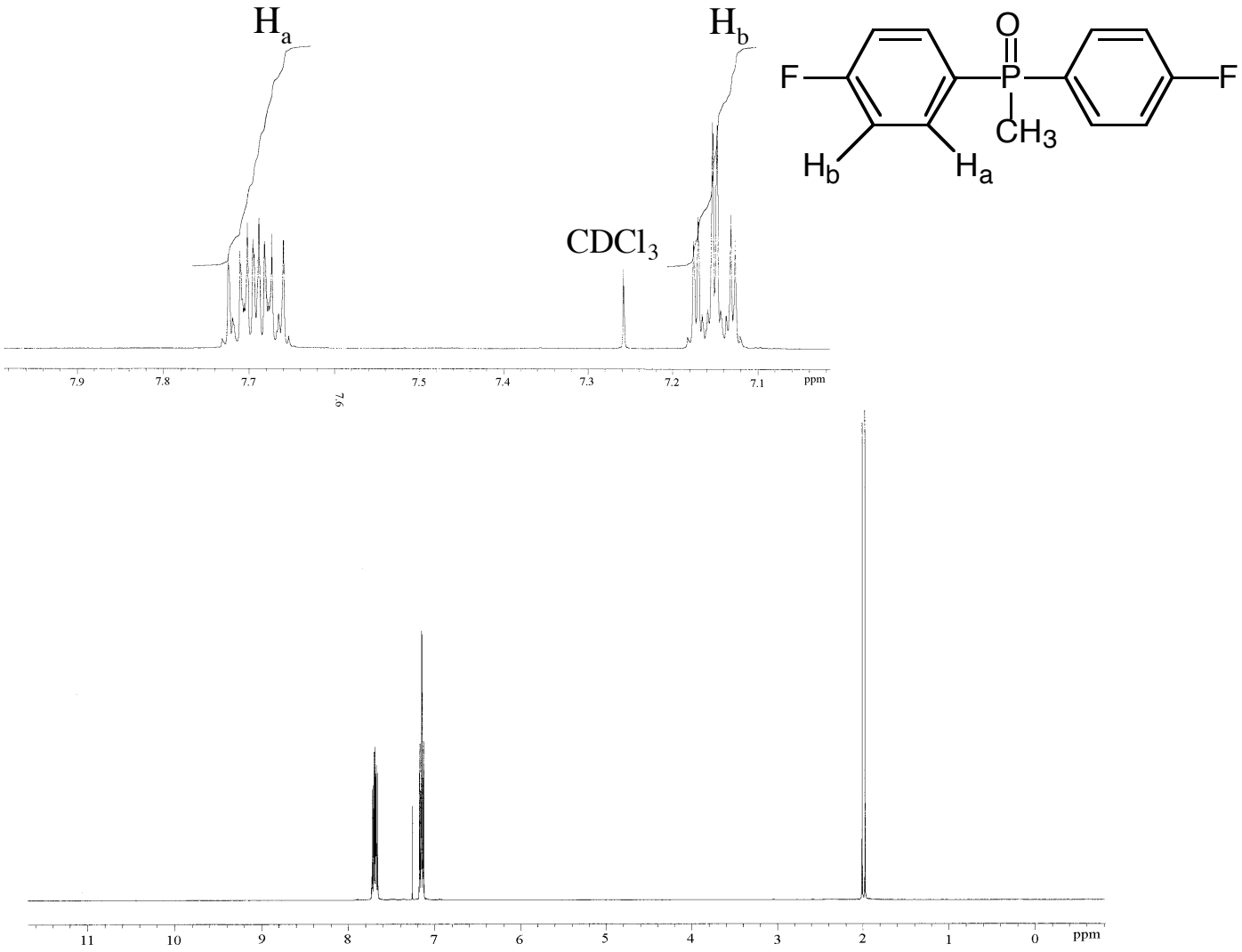

Figure 4.1.1.1 ^{1}H NMR spectrum of 4,4'-bis(fluorophenyl)methylphosphine oxide in $CDCl_3$

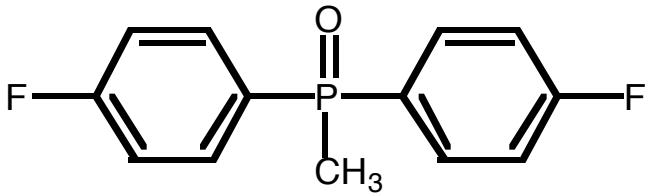

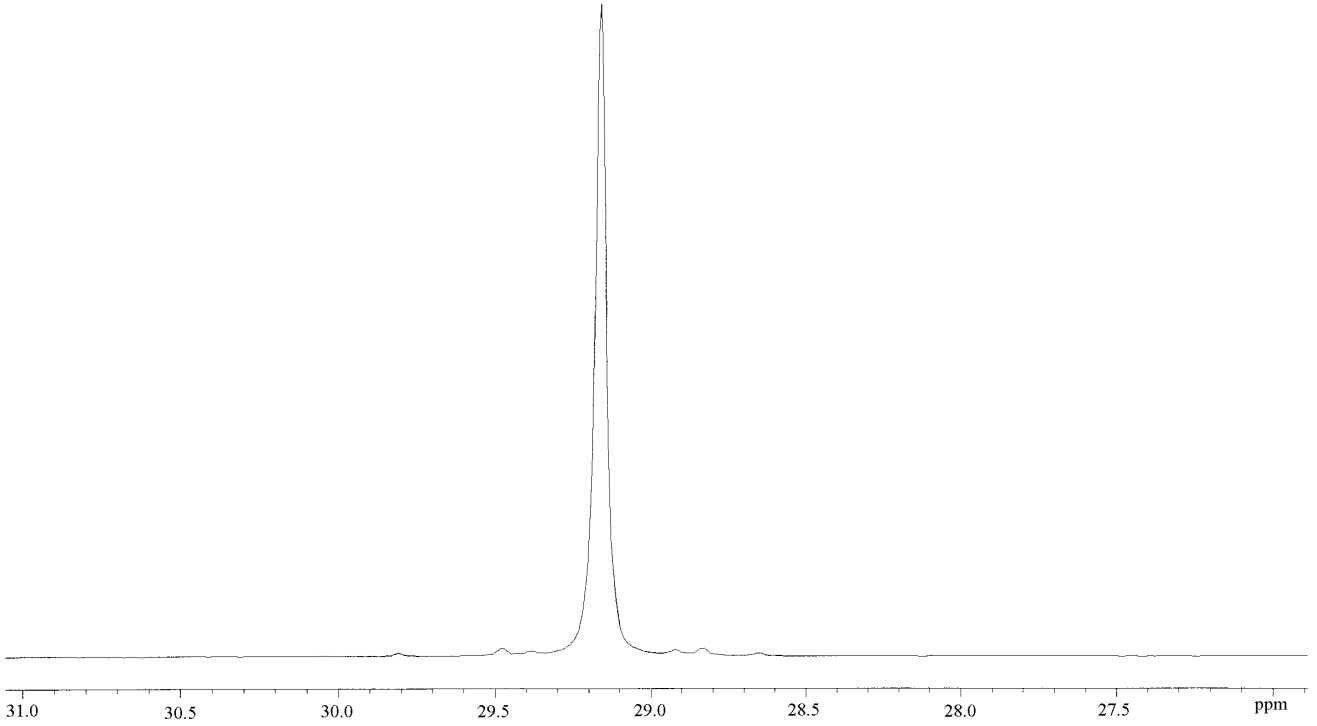

Figure 4.1.1.2 ^{31}P NMR spectrum of 4,4'-(bisfluorophenyl)methylphosphine oxide in $CDCl_3$

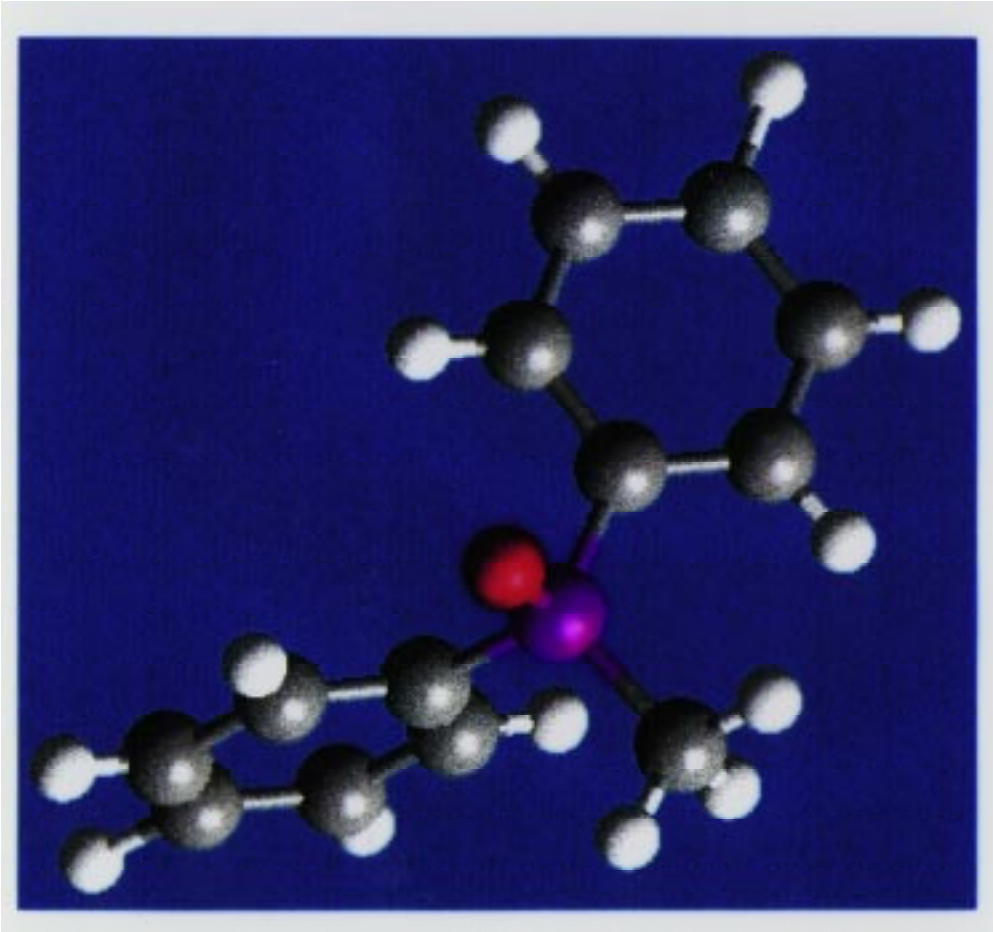

Figure 4.1.1.3 Illustration of diphenylmethylphosphine oxide in its lowest energy conformation

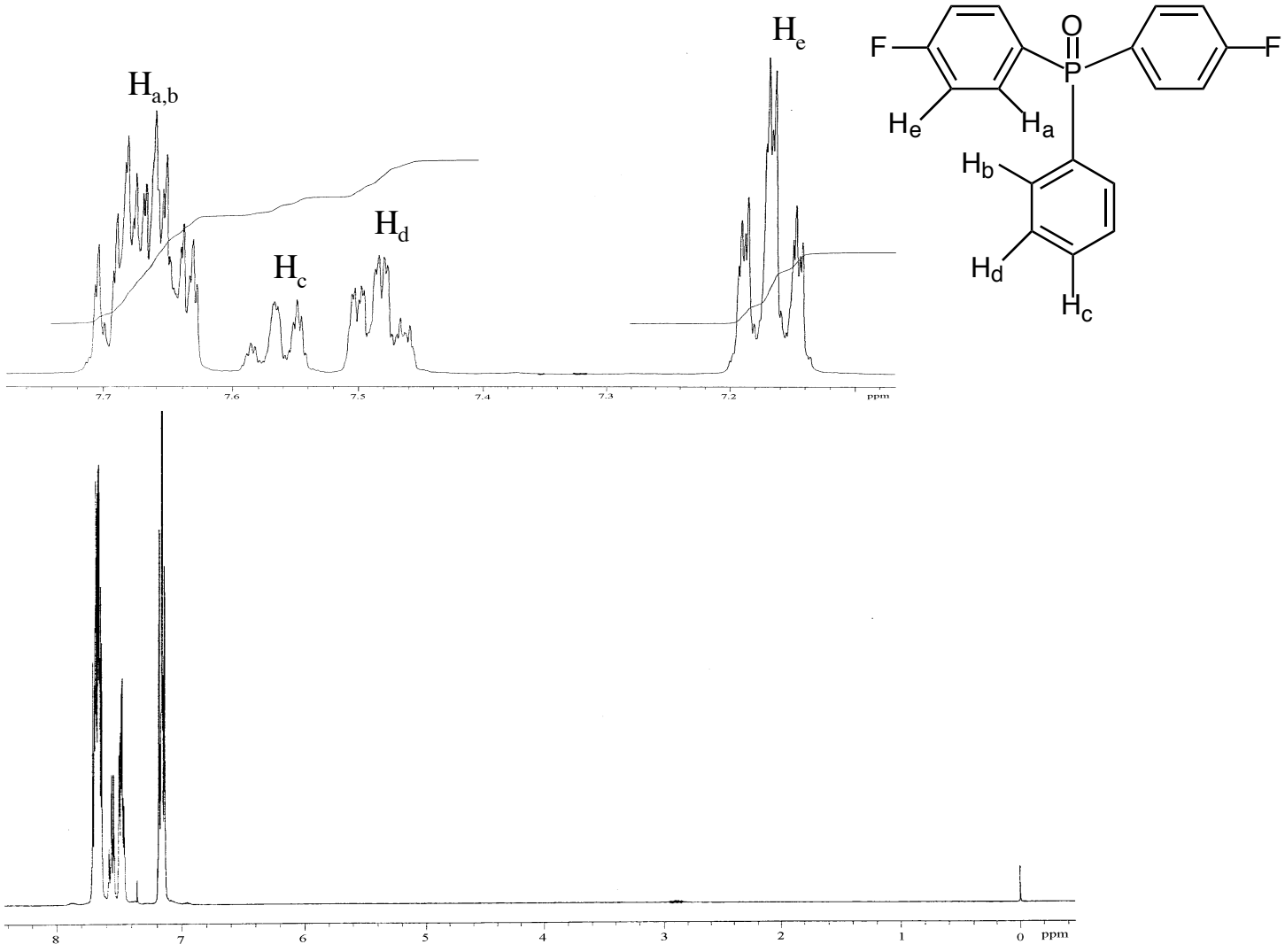

Figure 4.1.2.1 ^{1}H NMR spectrum of 4,4'-bis(fluorophenyl)phenylphosphine oxide in $CDCl_3$

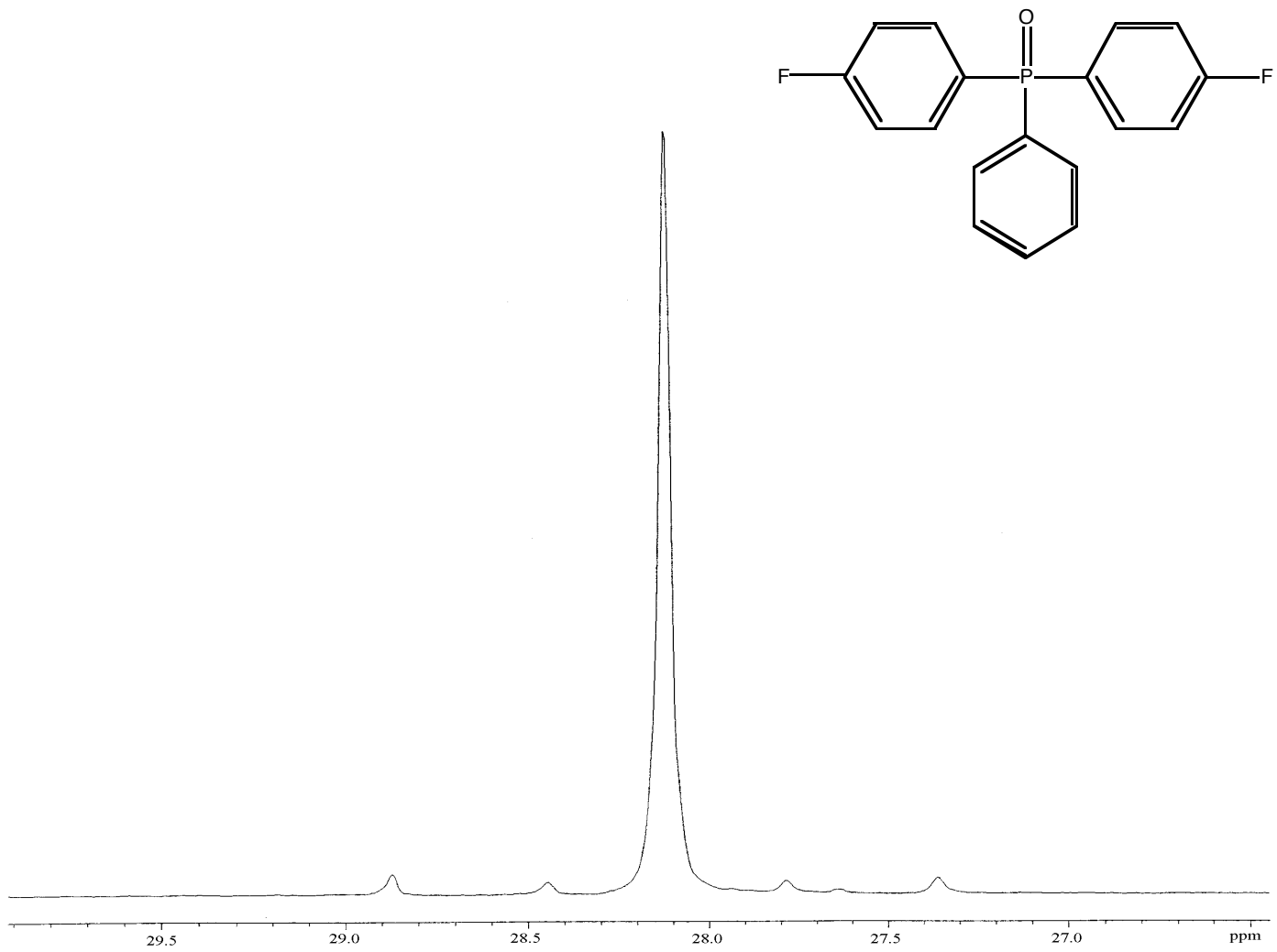

Figure 4.1.2.2 ^{31}P NMR spectrum of 4,4'-bis(fluorophenyl)phenylphosphine oxide in $CDCl_3$

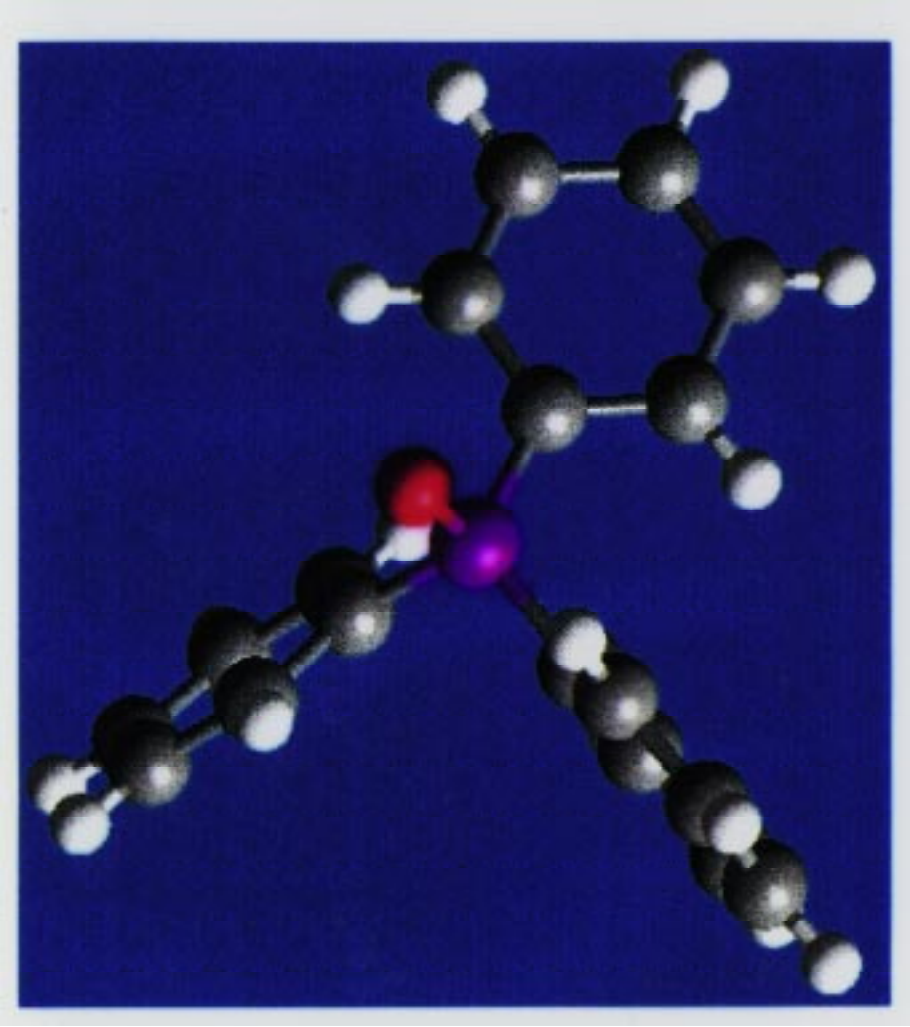

Figure 4.1.2.3 Illustration of triphenylphosphine in its lowest energy conformation

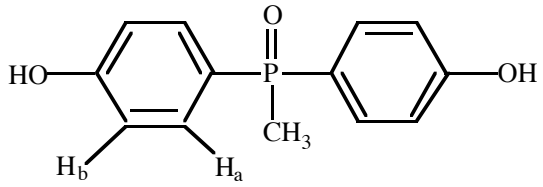

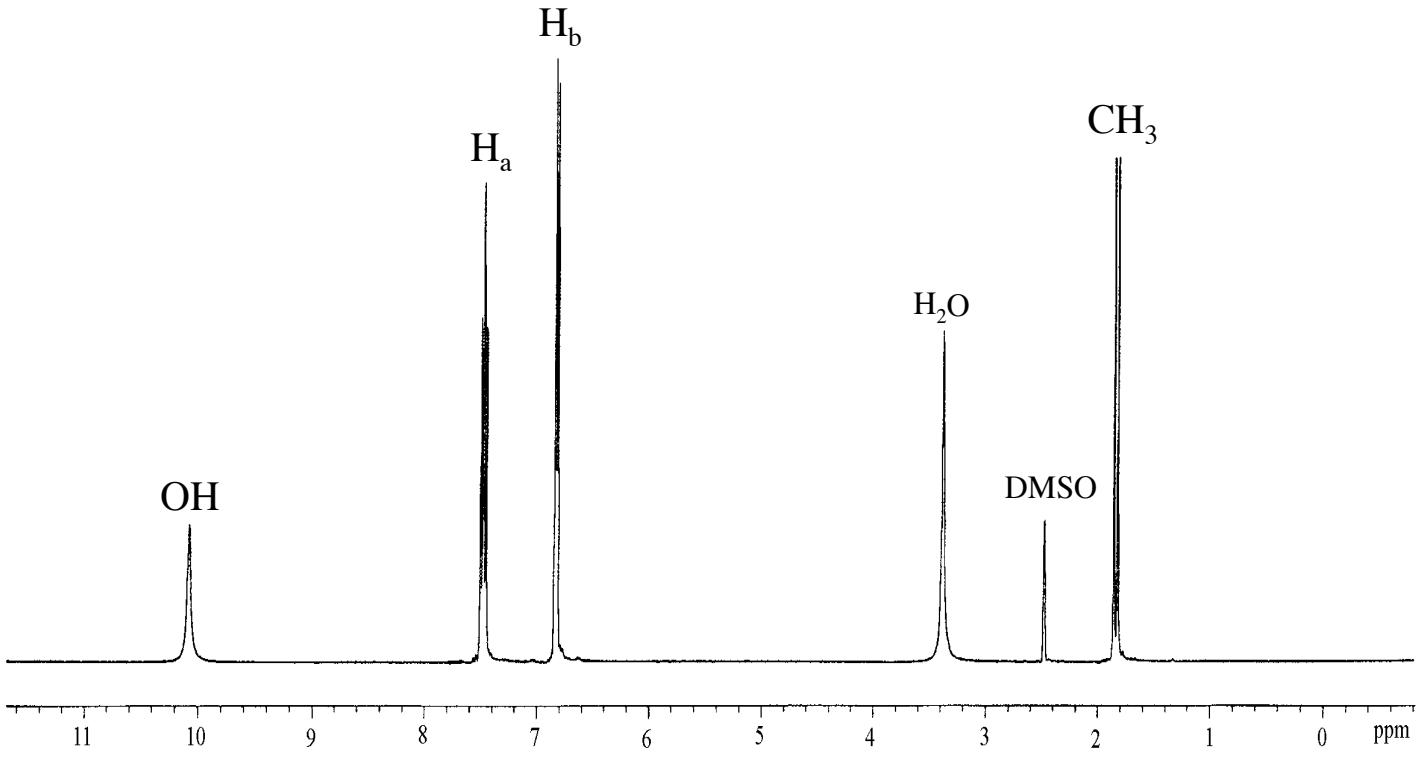

Figure 4.1.3.1 ^{1}H NMR spectrum of 4,4'-bis(hydroxyphenyl)methylphosphine oxide in DMSO

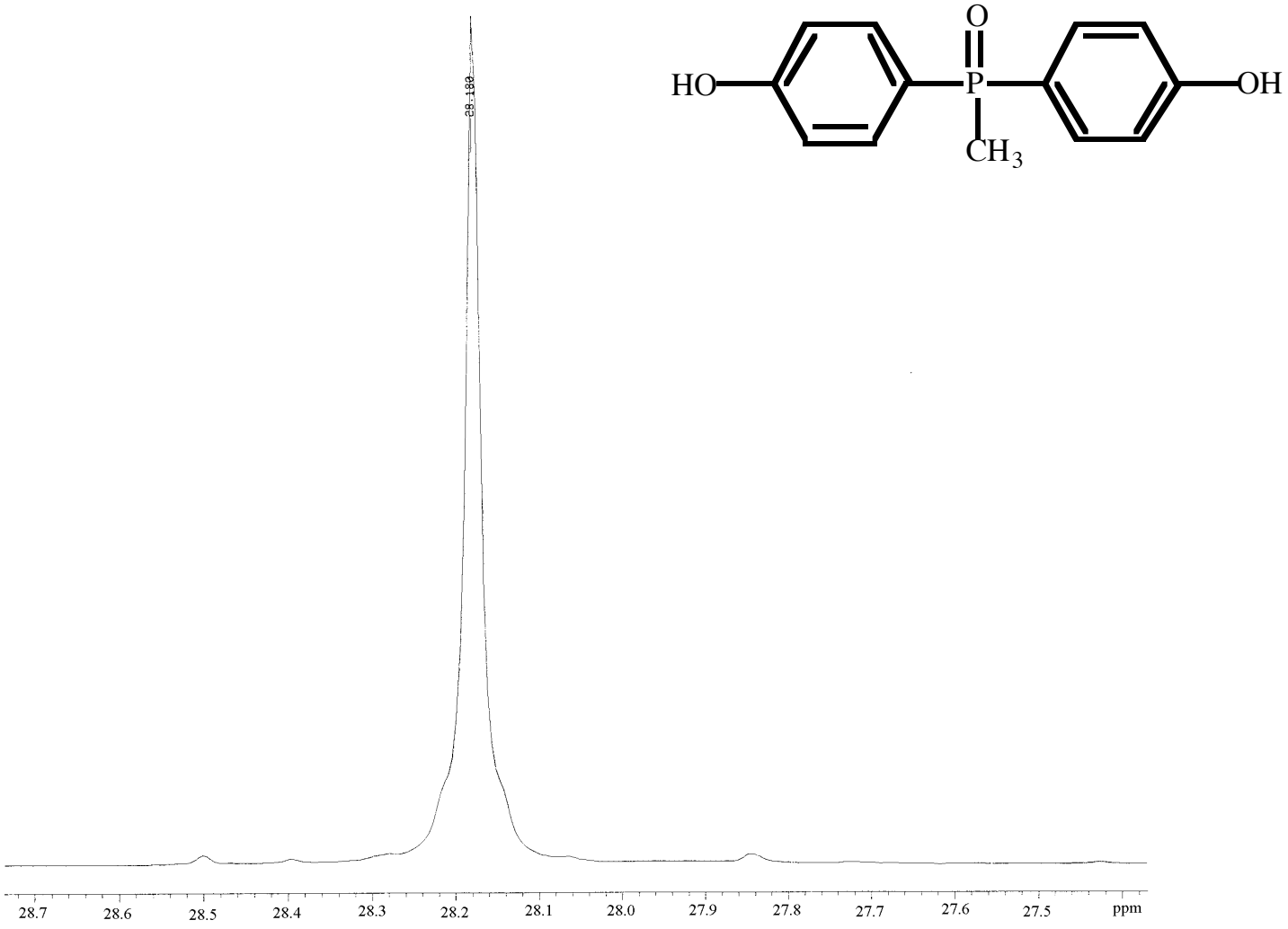

Figure 4.1.3.2 ^{31}P NMR spectrum of 4,4'-bis(hydroxyphenyl)methylphosphine oxide in DMSO

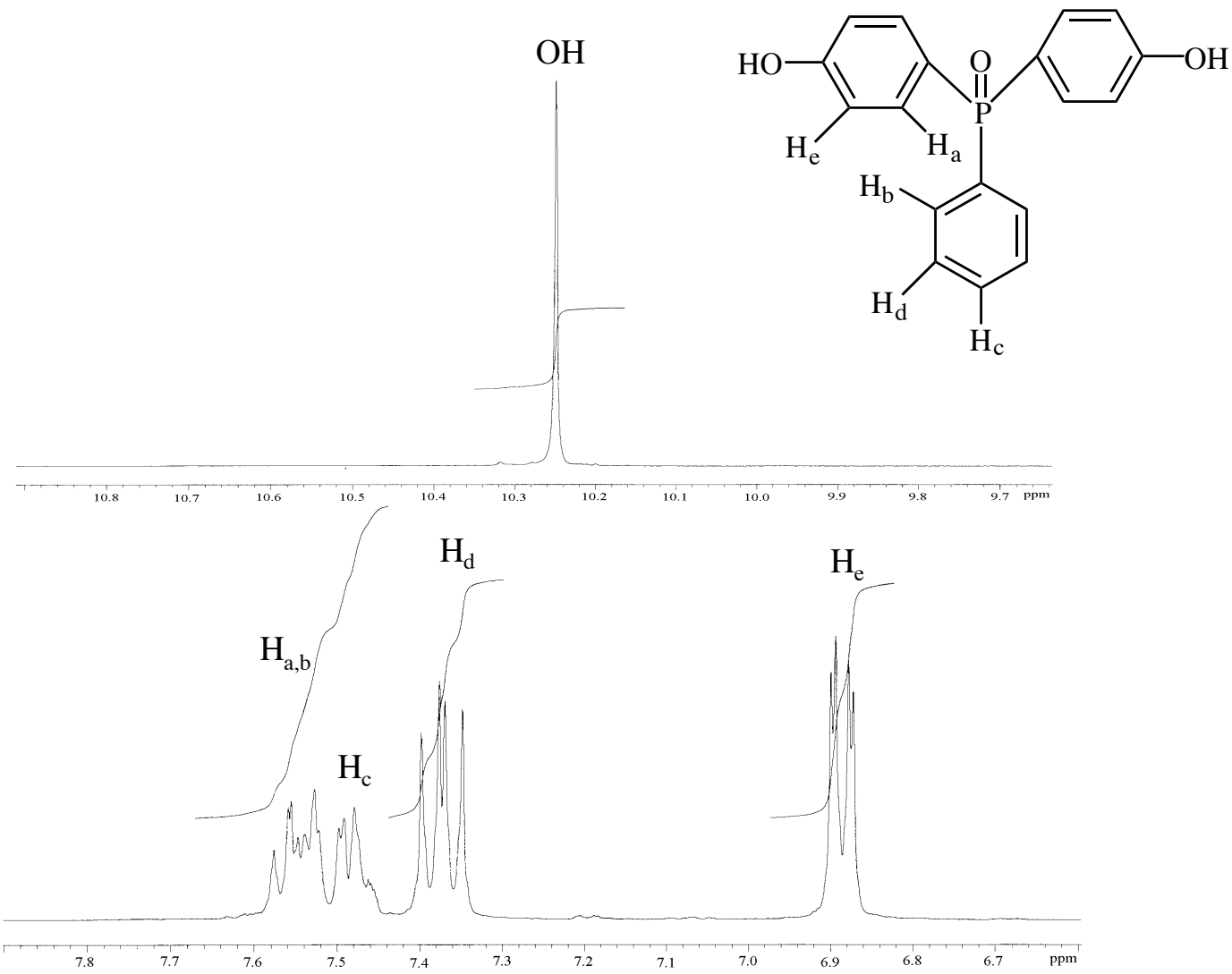

Figure 4.1.4.1 ^{1}H NMR spectrum of 4,4'-bis(hydroxyphenyl)phenylphosphine oxide in DMSO

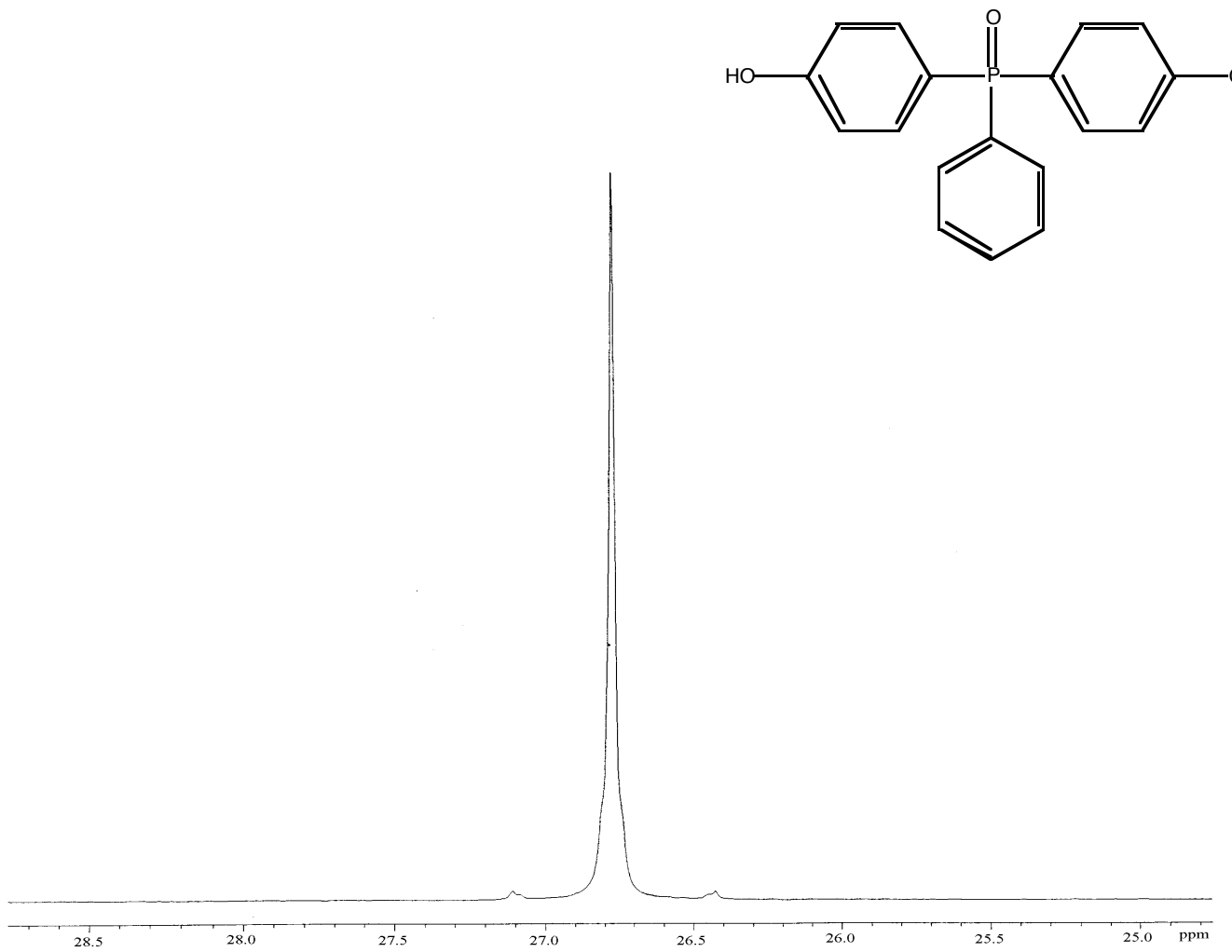

Figure 4.1.4.2 ^{31}P NMR spectrum of 4,4'-bis(hydroxyphenyl)phosphine oxide in DMSO

4.2 Polymer Synthesis and Characterization

4.2.1 High Molecular Weight Poly(arylene ether phosphine oxide)s

Poly(arylene ether)s display high performance features such as high thermal stability, toughness, good flame resistance and have shown potential for high temperature matrix resins and/or adhesive applications. Earlier studies utilizing triphenylphosphine oxide based derivatives as comonomers have been reported (37, 177). Phosphorus has been postulated to be responsible for the lower flammability, relative to some analogous systems, and it was presumed that an increase in phosphorus content would further decrease the flammability of the resulting poly(arylene ether)s. High molecular weight poly(arylene ether phosphine oxide)s (PEPO)s were synthesized *via* nucleophilic aromatic substitution (S_NAR) step growth polymerization of 4,4'-bis(fluorophenyl)methylphosphine oxide (BFPMPO) and bisphenol-A (Bis-A) in the presence of a weak base as shown in scheme 4.2.1.1. Freshly distilled DMAc was used as the solvent. Where possible this solvent was preferred relative to NMP due to side reactions between carbonate anion and NMP as shown in Scheme 4.2.1.1. Analogous problems with DMAc appear to be less frequent.

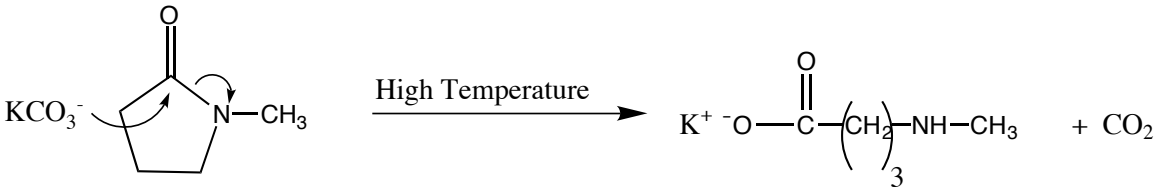

Scheme 4.2.1.1 NMP side reaction under high temperature basic conditions (178)

A reaction temperature of 135°C was employed to remove the by-product water via the toluene azeotrope. The temperature was then raised to 155°C to essentially complete the reaction of the functional groups, so that high molecular weight could be achieved. It was important not to increase the temperature above 155°C to maintain anhydrous refluxing conditions. The methanol precipitated yield of the polymer was always greater than 90%. The molecular structure of these polymers were confirmed by ^{1}H and ^{31}P NMR such as those shown in Figures 4.2.1.1 - 4.2.1.5.

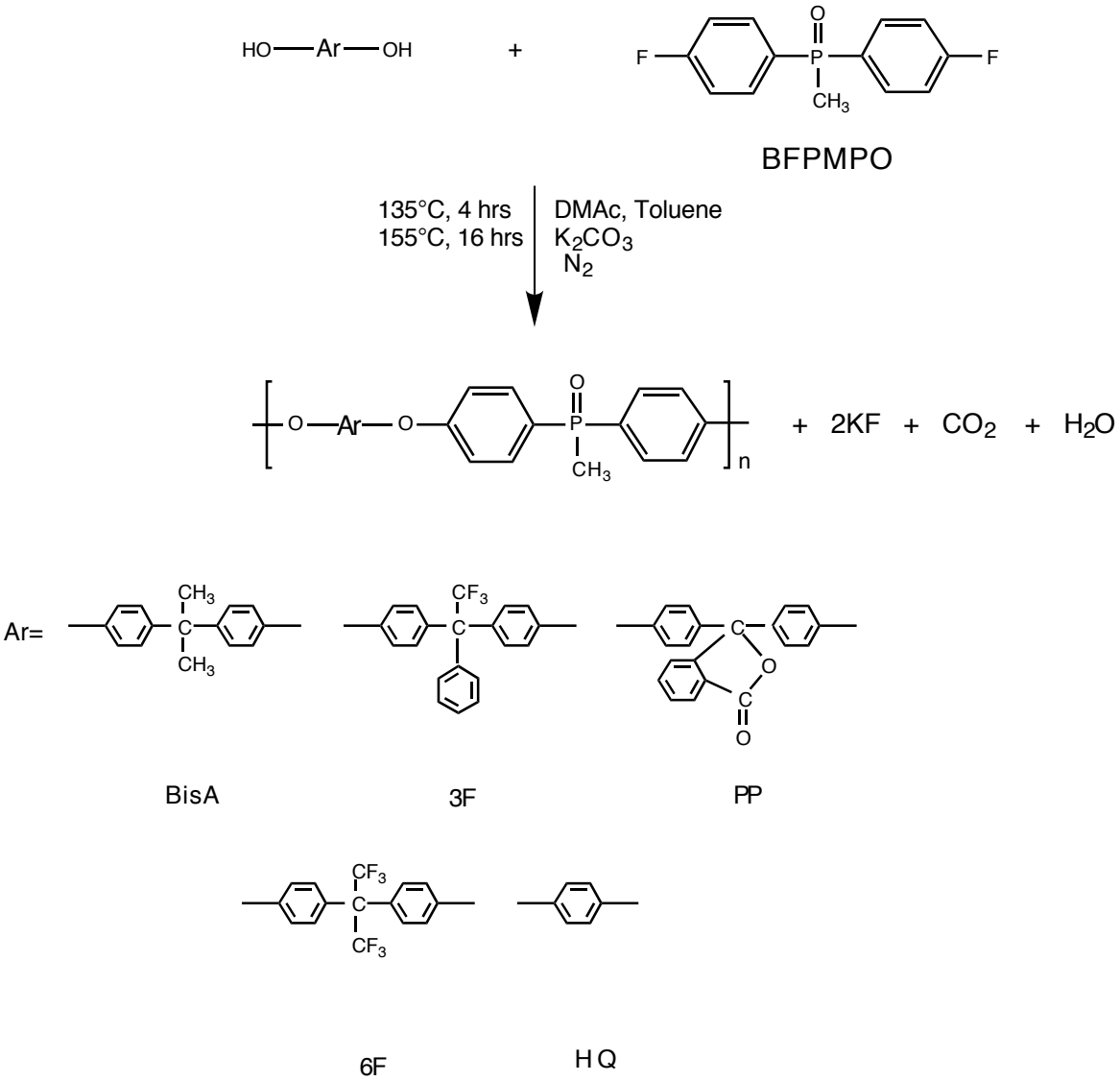

Scheme 4.2.1.2 Synthesis of high molecular weight poly(arylene ether phosphine oxide)s

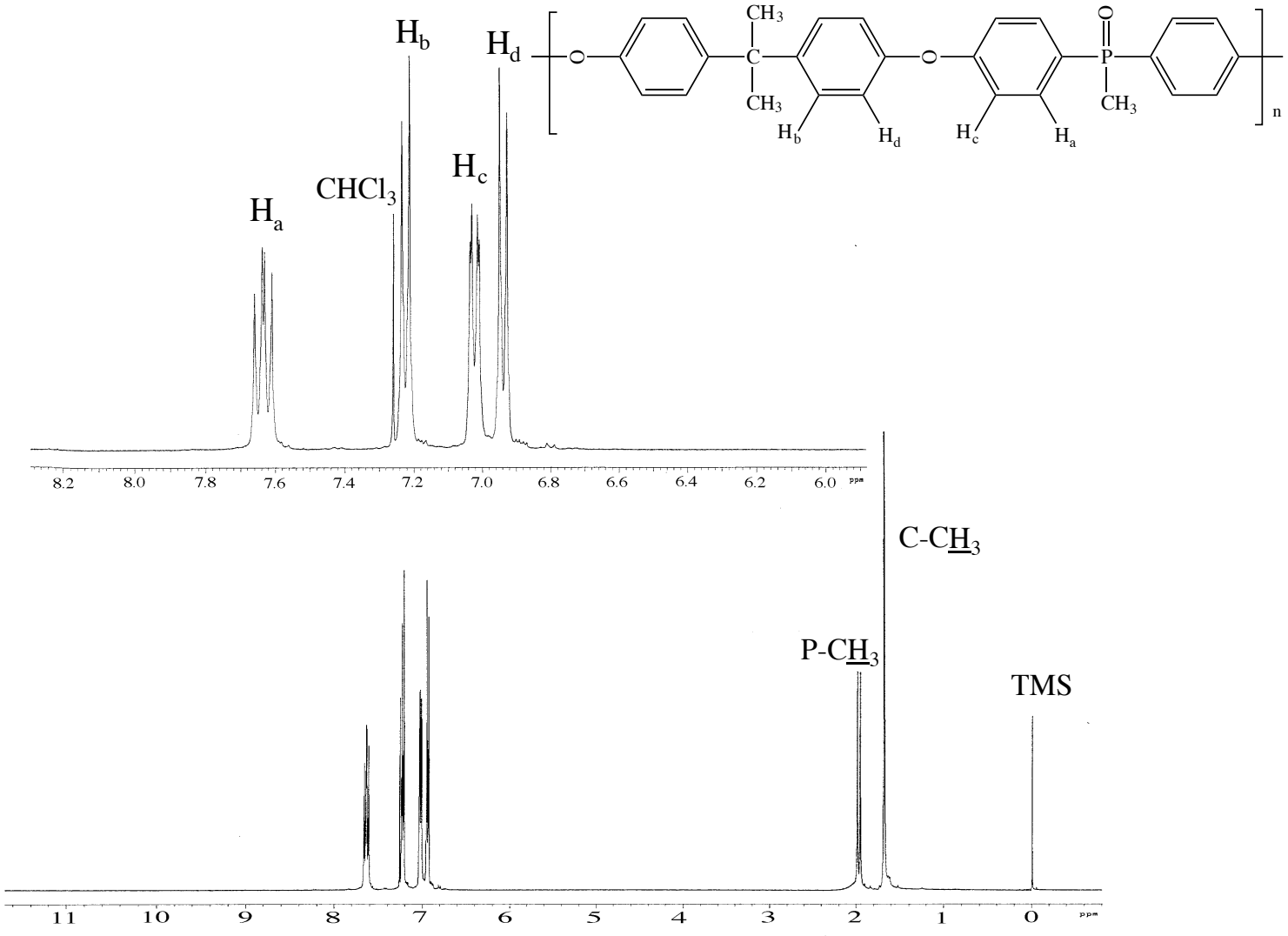

Figure 4.2.1.1 ^{1}H NMR Spectrum of BisA-BFPMPO in $CDCl_3$

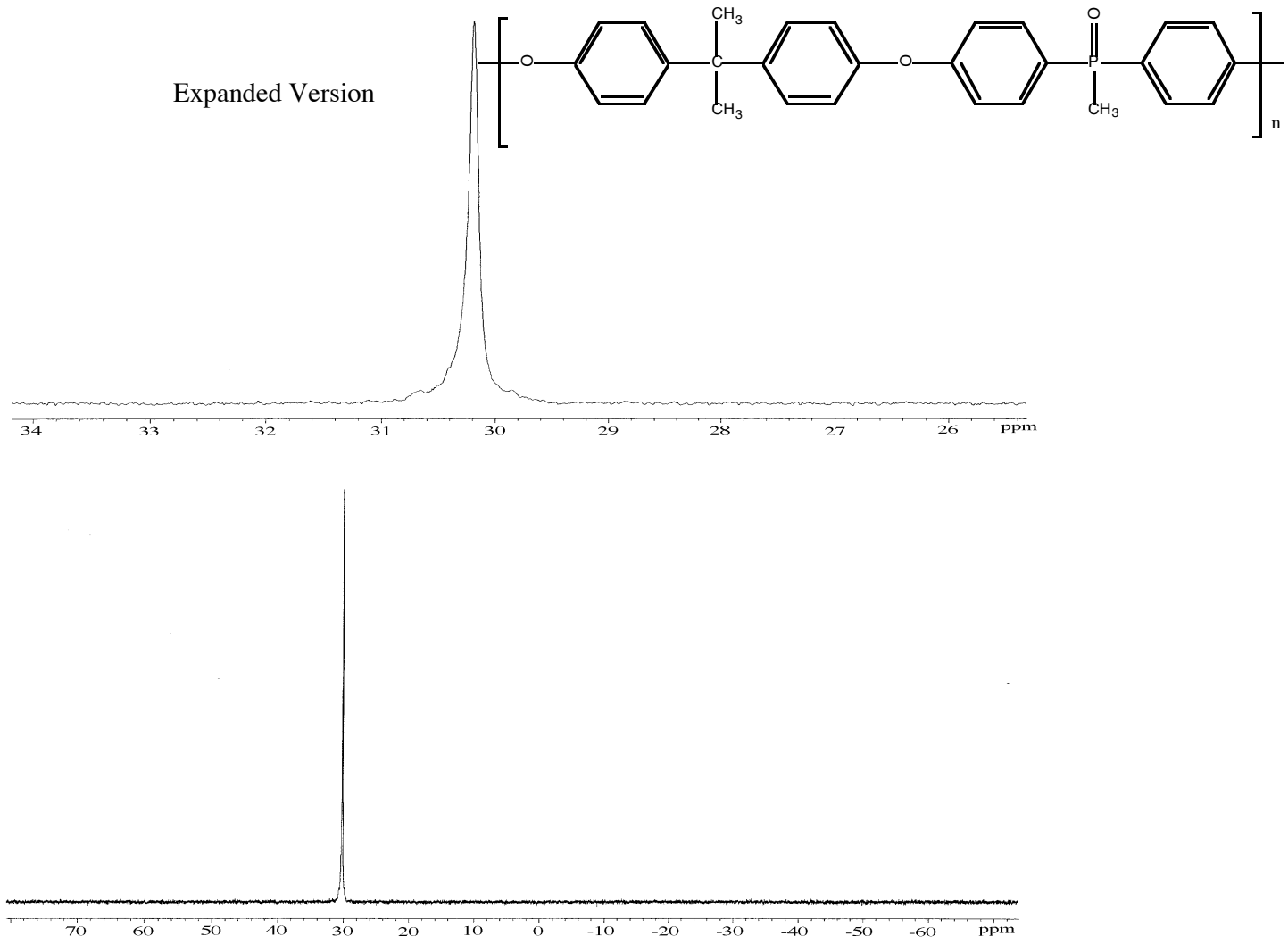

Figure 4.2.1.2 ^{31}P NMR spectrum of BisA-BFPMPO in $CDCl_3$

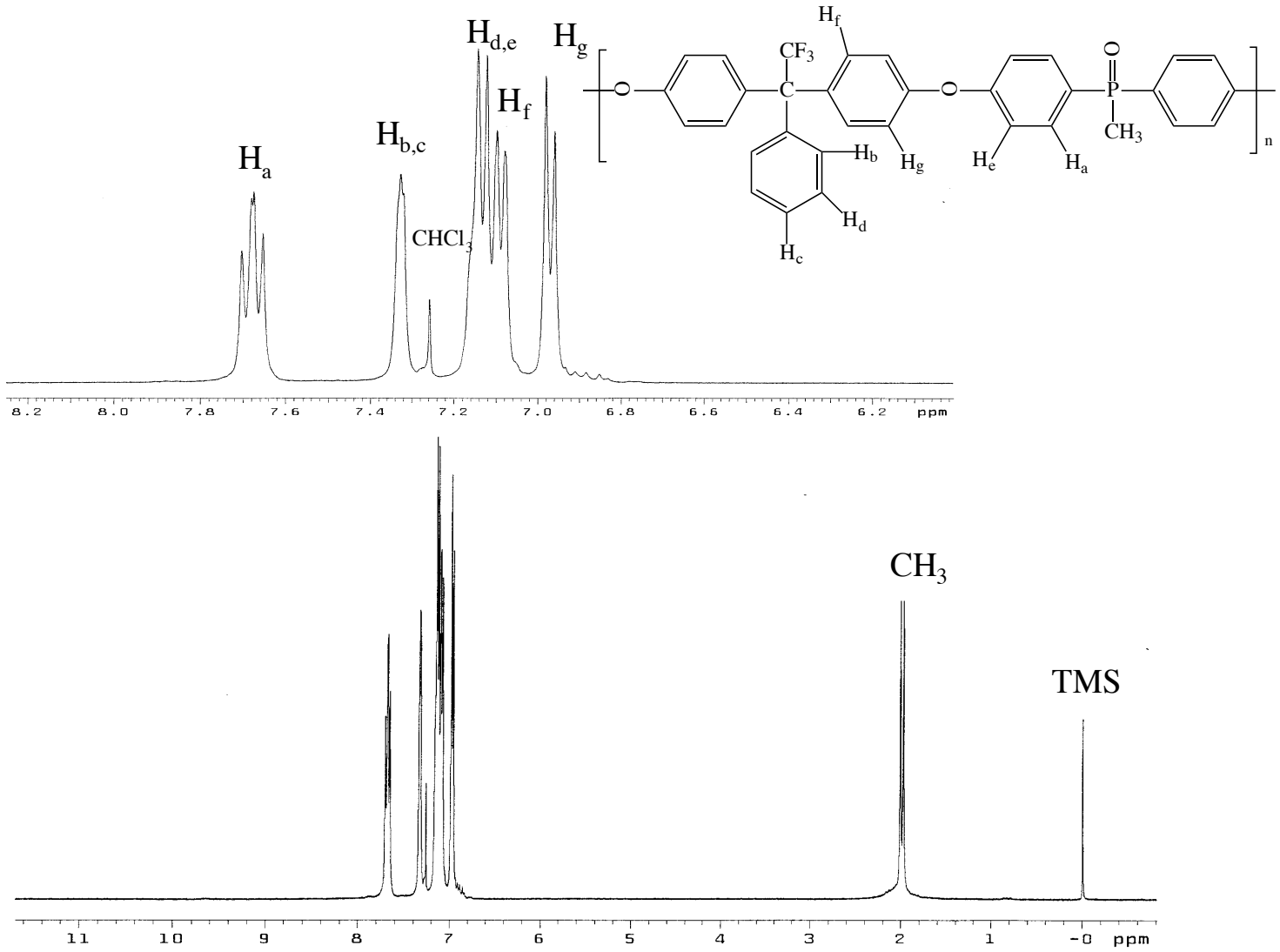

Figure 4.2.1.3 ^{1}H NMR Spectrum of 3F-BFPMPO in $CDCl_3$

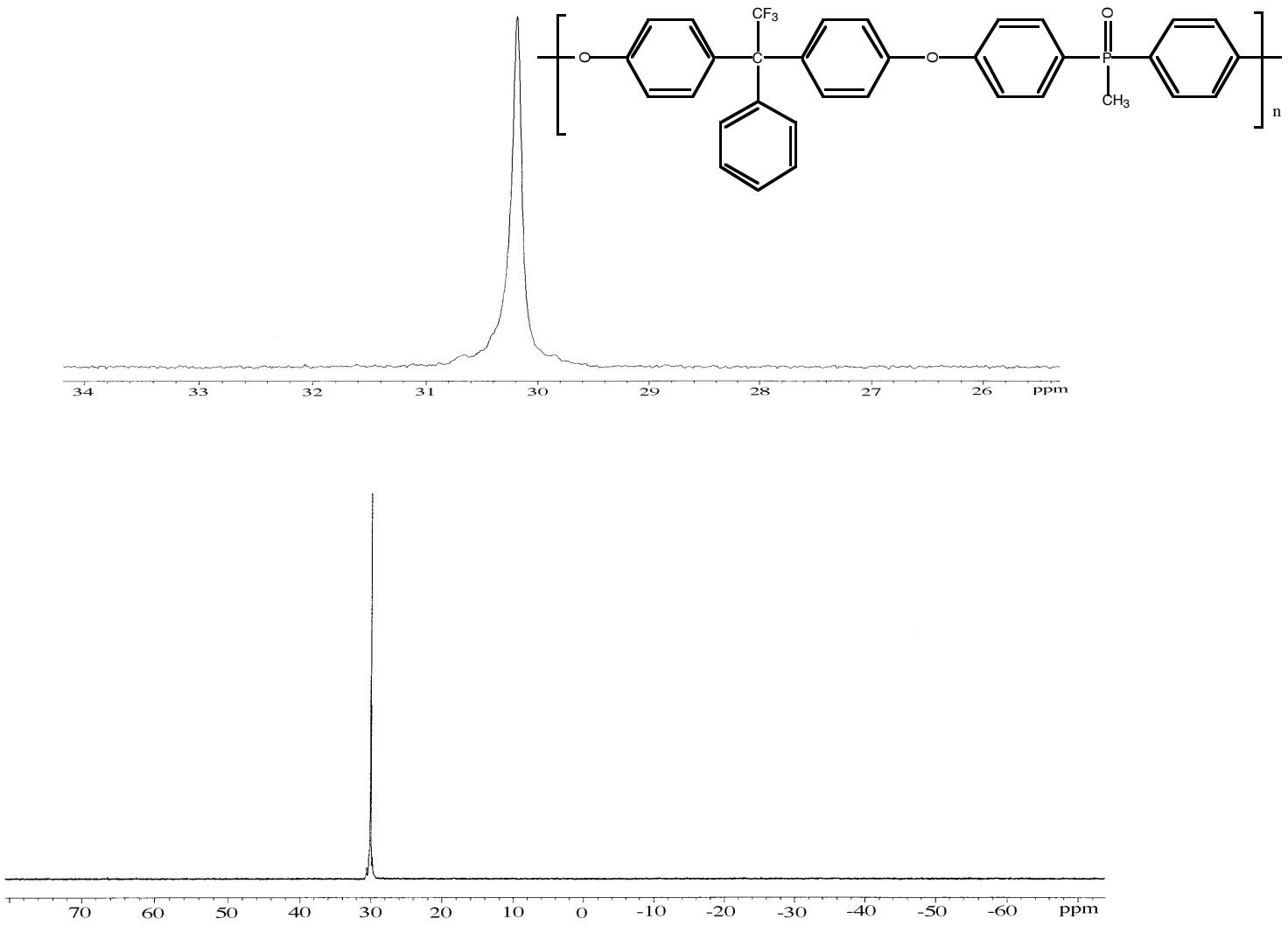

Figure 4.2.1.4 ^{31}P NMR spectrum of 3F-BFPMPO in $CDCl_3$

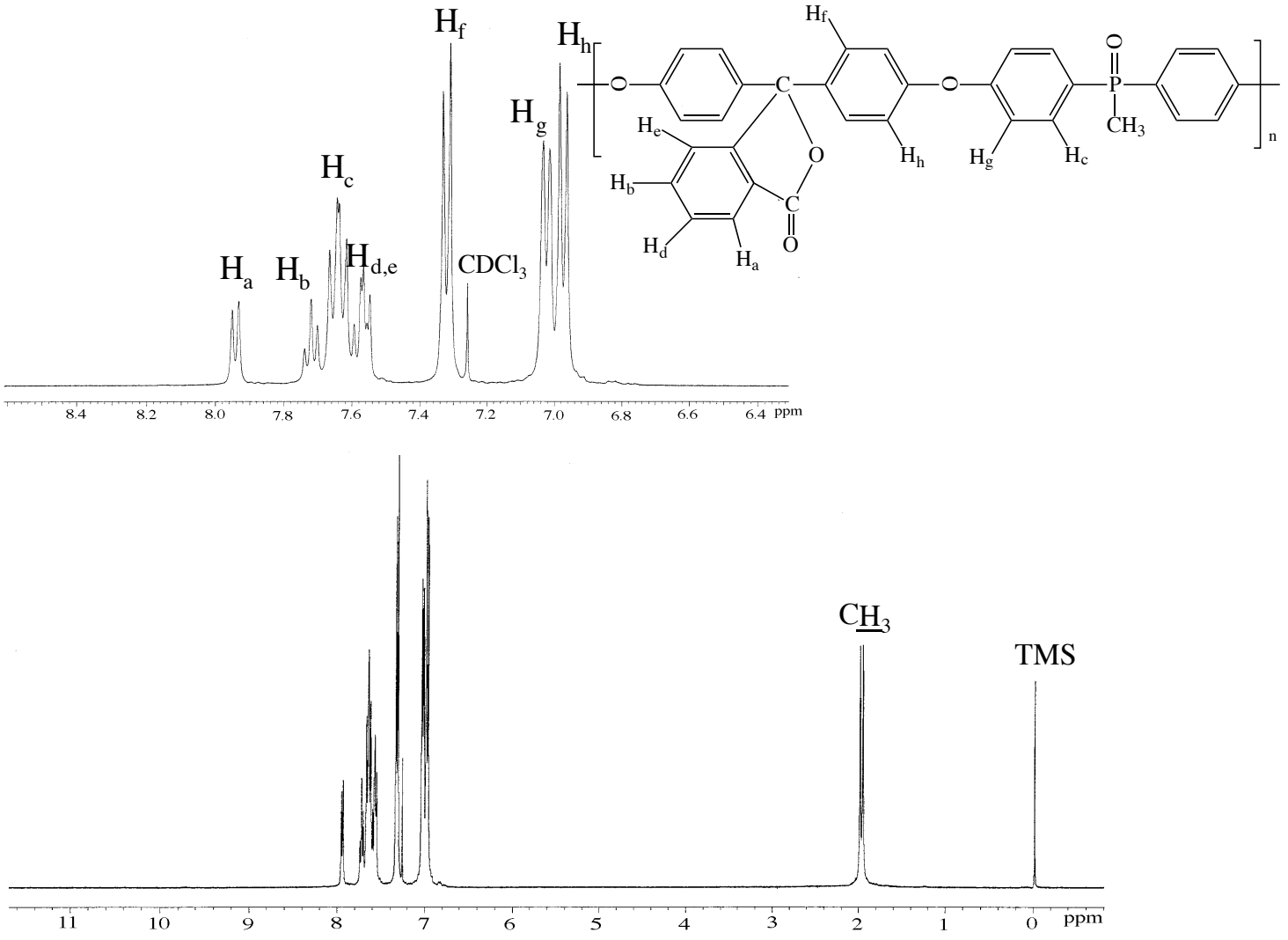

Figure 4.2.1.5 ^{1}H NMR Spectrum of PP-BFPMPO in $CDCl_3$

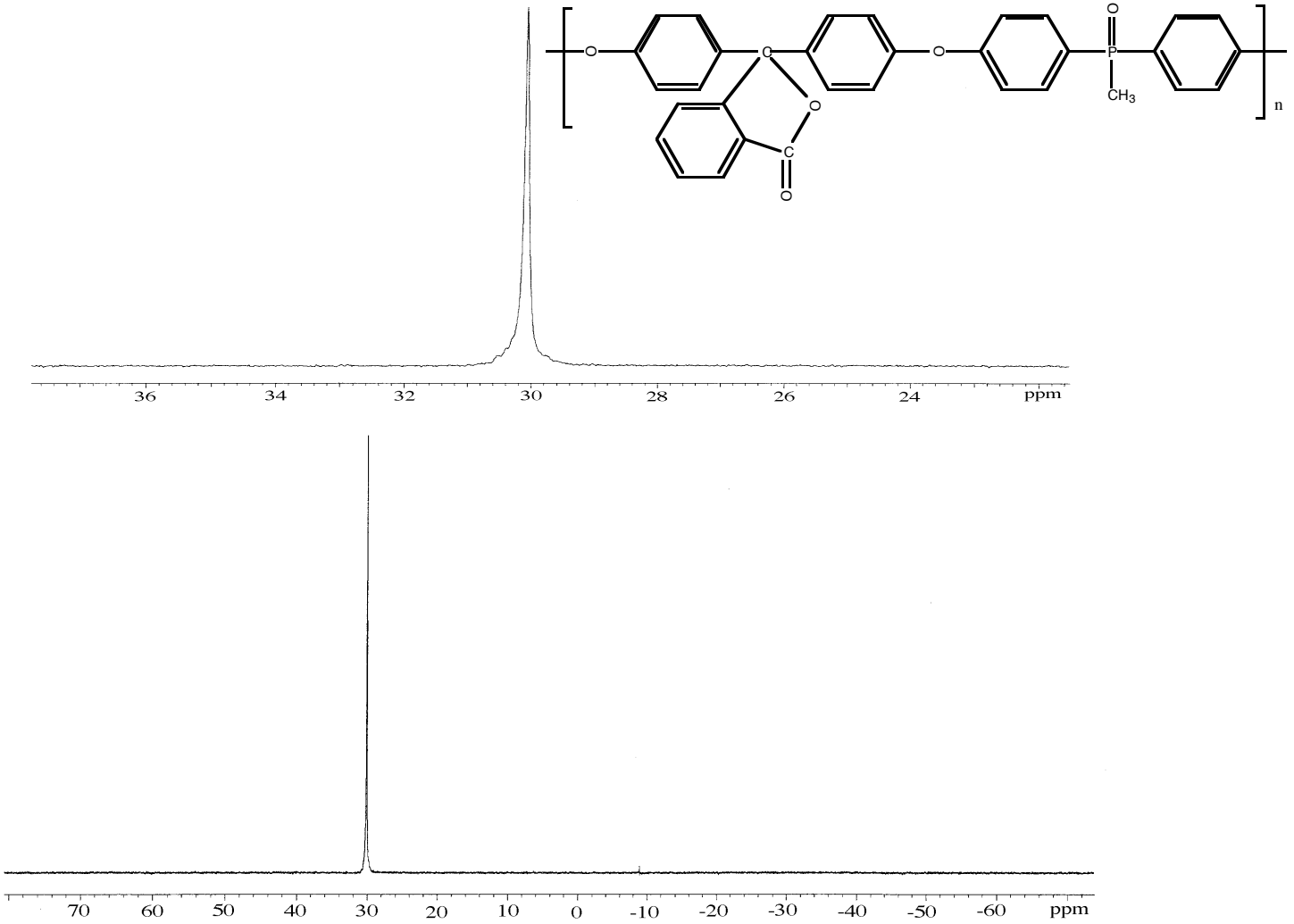

Figure 4.2.1.6 ^{31}P NMR Spectrum of PP-BFPMPO in $CDCl_3$

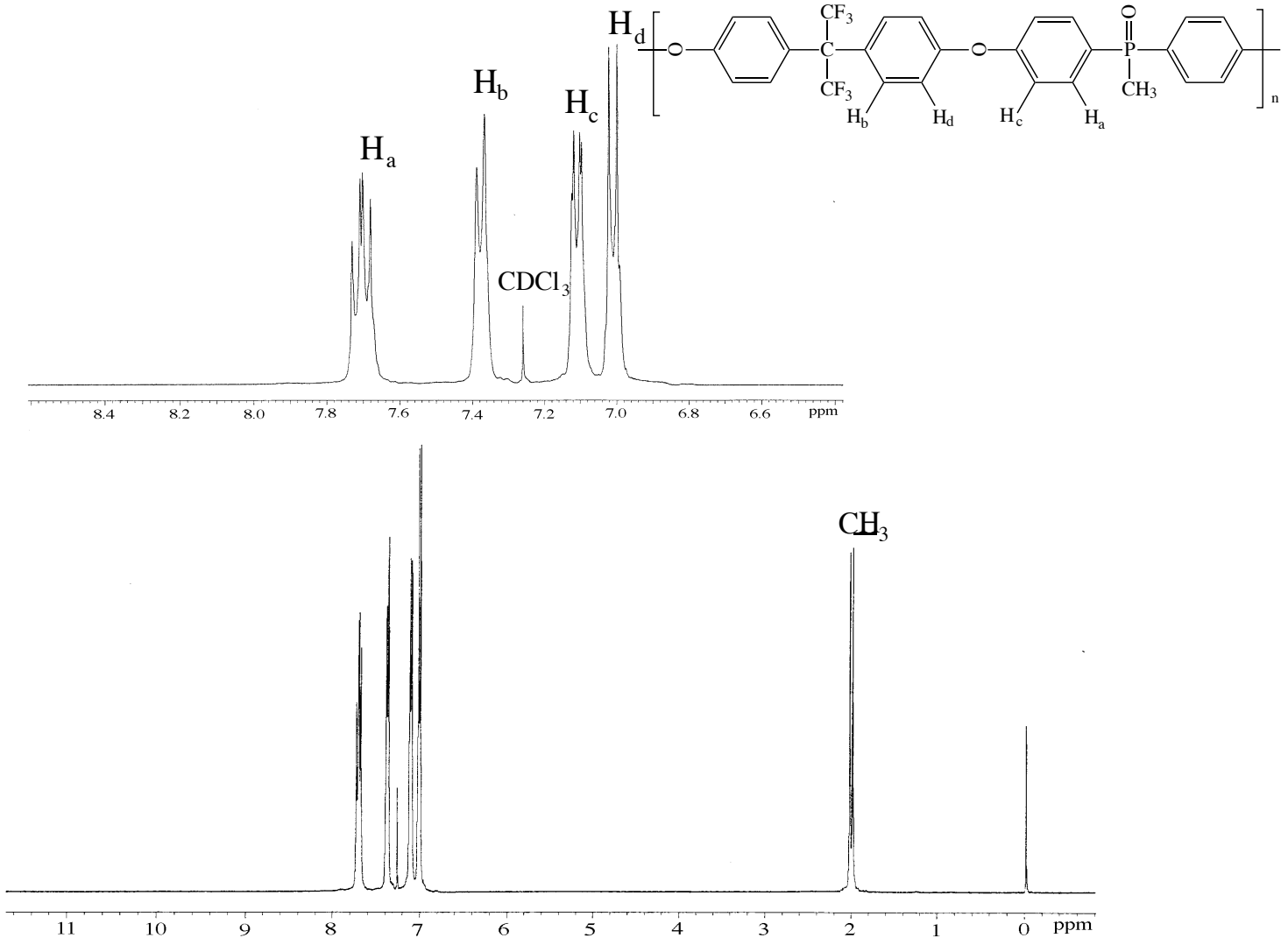

Figure 4.2.1.7 ^{1}H NMR Spectrum of 6F-BFPMPO in $CDCl_3$

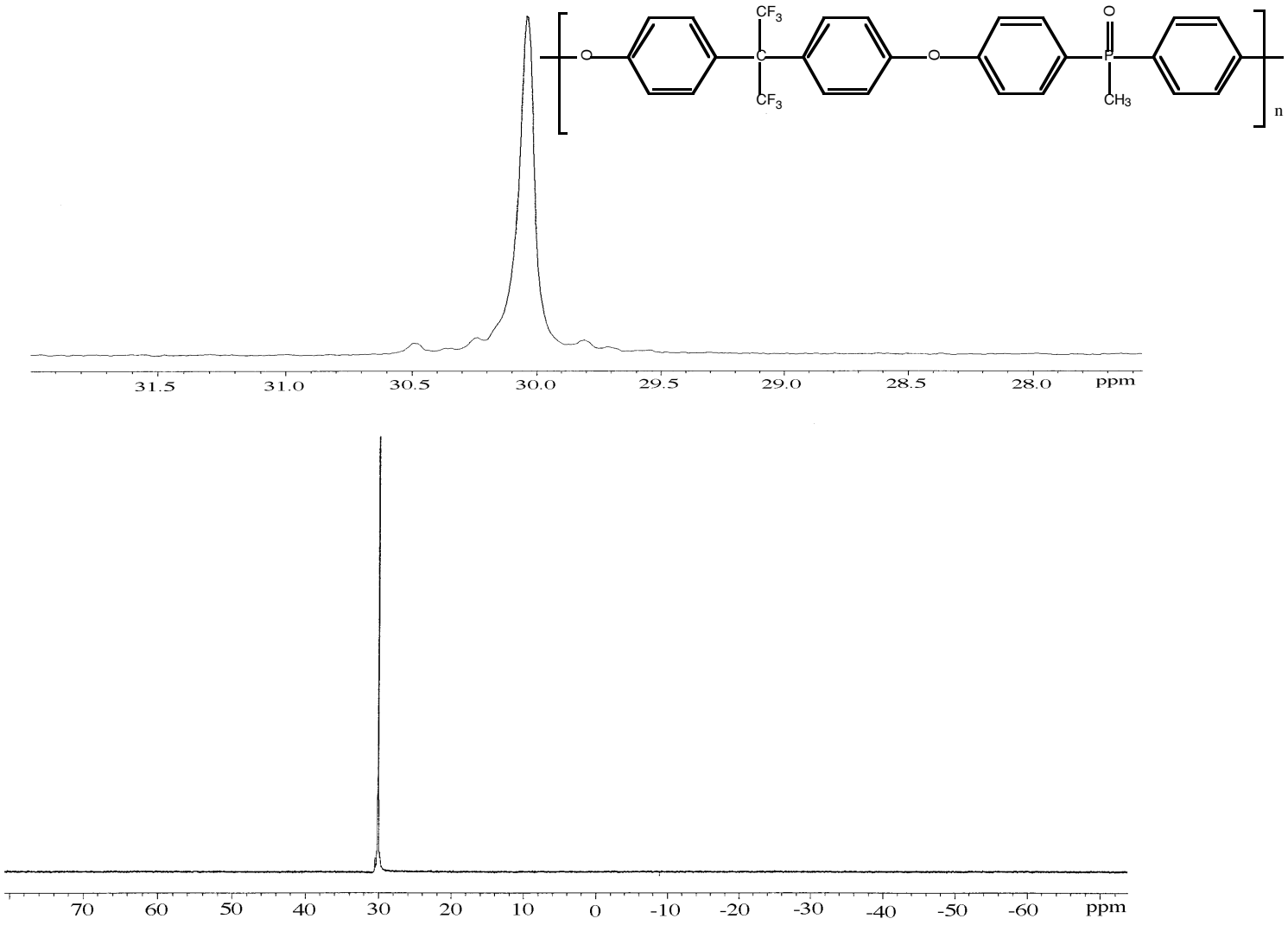

Figure 4.2.1.8 ^{31}P NMR spectrum of 6F-BFPMPO in $CDCl_3$

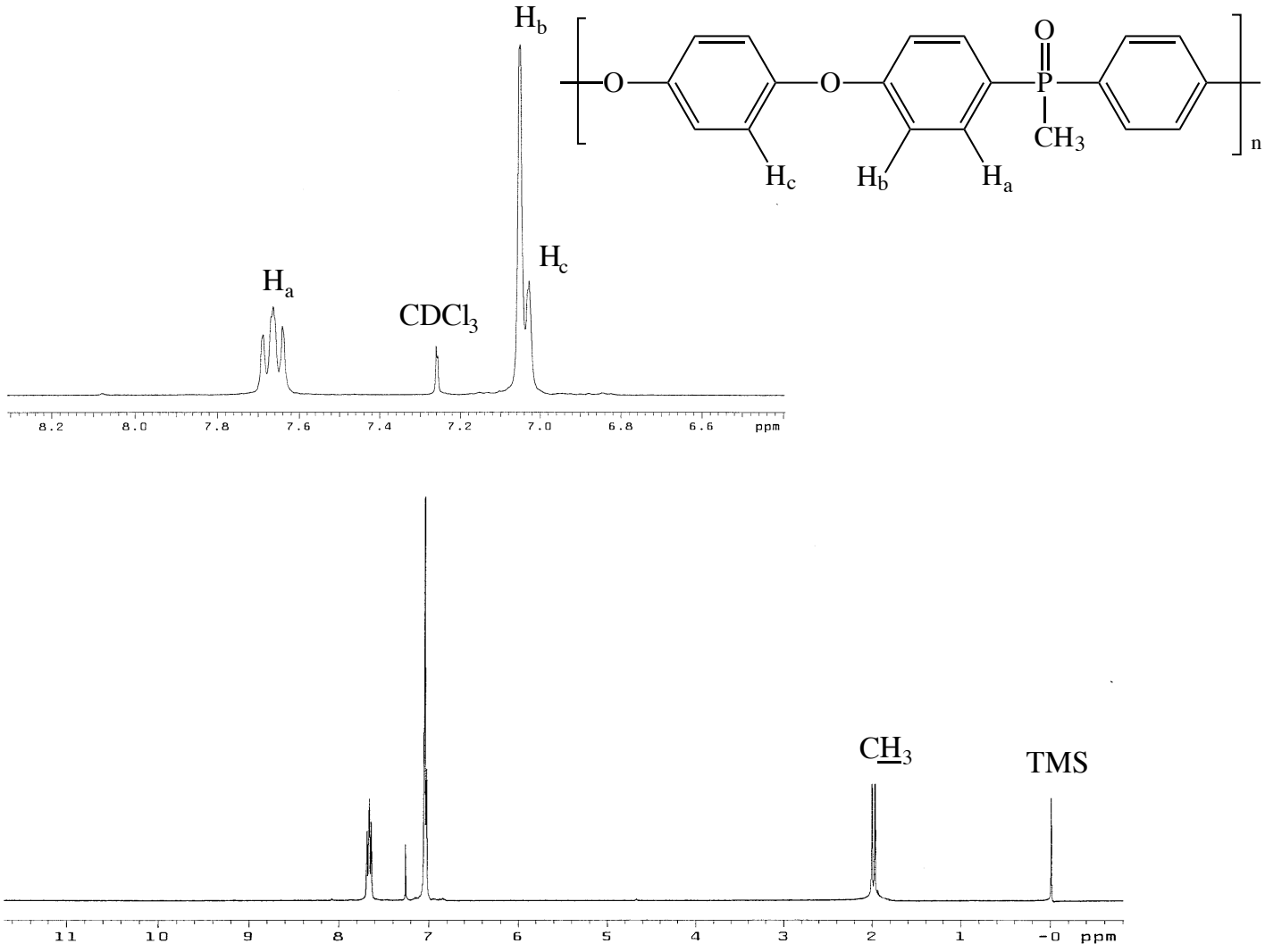

Figure 4.2.1.9 ^{1}H NMR Spectrum of HQ-BFPMPO in $CDCl_3$

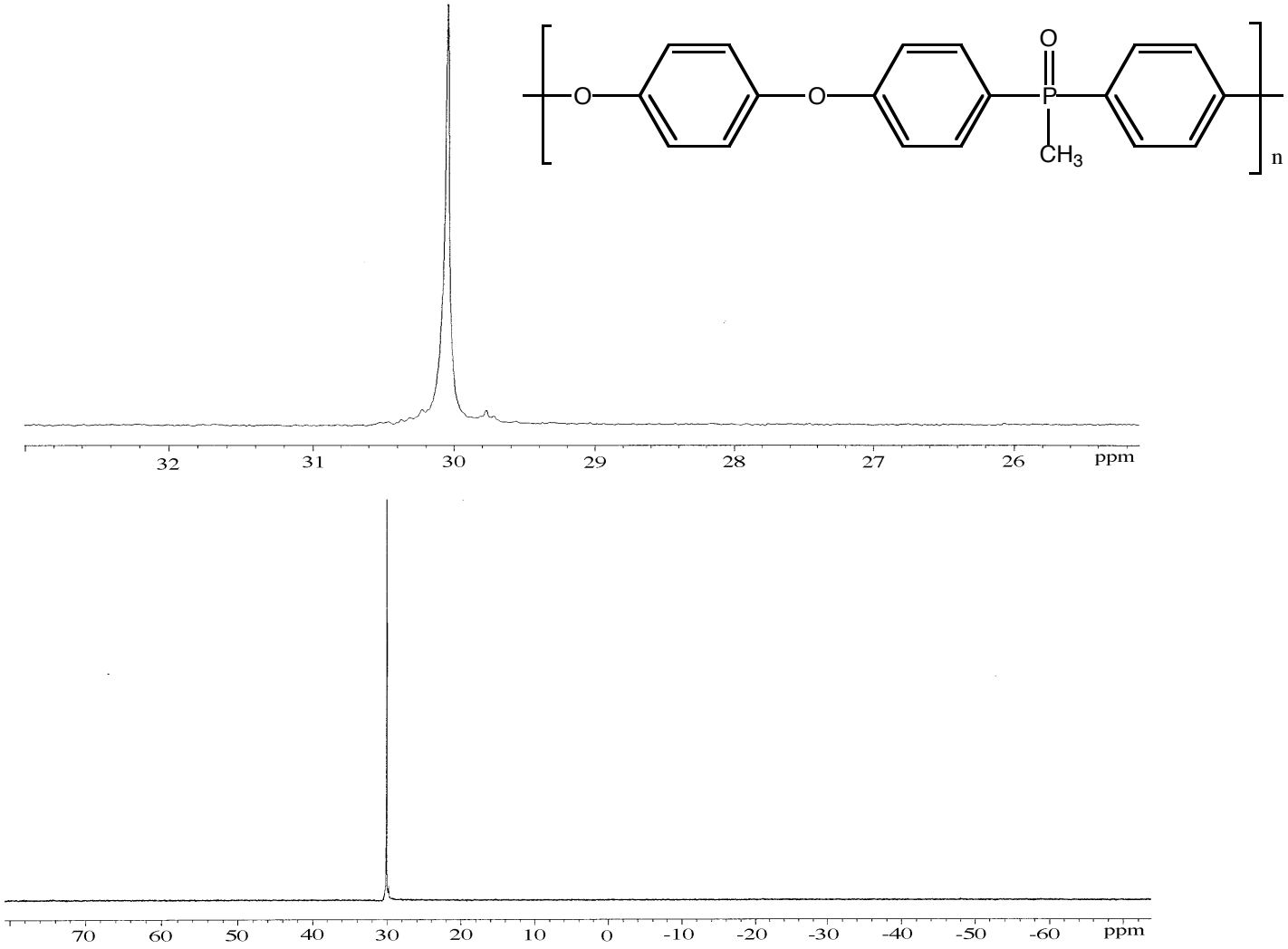

Figure 4.21.10 ^{31}P NMR spectrum of HQ-BFPMPO in $CDCl_3$

4.2.2 High Molecular Weight Poly(arylene ether phosphine oxide sulfone)s

Poly(arylene ether sulfone)s are much more hydrolytically stable compared to polycarbonates, polyesters, polyamides, and even polyimides and display excellent thermal and mechanical properties. They are thus commonly commercially utilized in applications that require high performance hydrolytically stable polymers. High molecular weight poly(arylene ether phosphine oxide sulfone)s were synthesized to investigate the physical behavior of a polymer that contain both the advantageous heteroatom phosphine oxide and sulfone moieties within the polymer backbone. Diphenylsulfone, which has a melting point of 126-128°C, was used as the reaction solvent, as earlier described by workers at ICI (179). The reaction was initially run at 135°C for 1 hour and at 170°C for 4 hours to dry the system. The temperature was then increased to 270°C for 4 hours and finally to 320°C for 20 minutes to achieve high molecular weight, >90% yield. The high reaction temperatures were required as a consequence of the deactivating effect of the electron withdrawing properties of SO_2 moiety, which decreases the nucleophilicity of the resulting phenate, as shown in Scheme 4.2.2.1. The structures were confirmed by ^{1}H and ^{31}P NMR in $CDCl_3$. These spectra are shown in Figures 4.2.2.1 - 4.2.2.4.

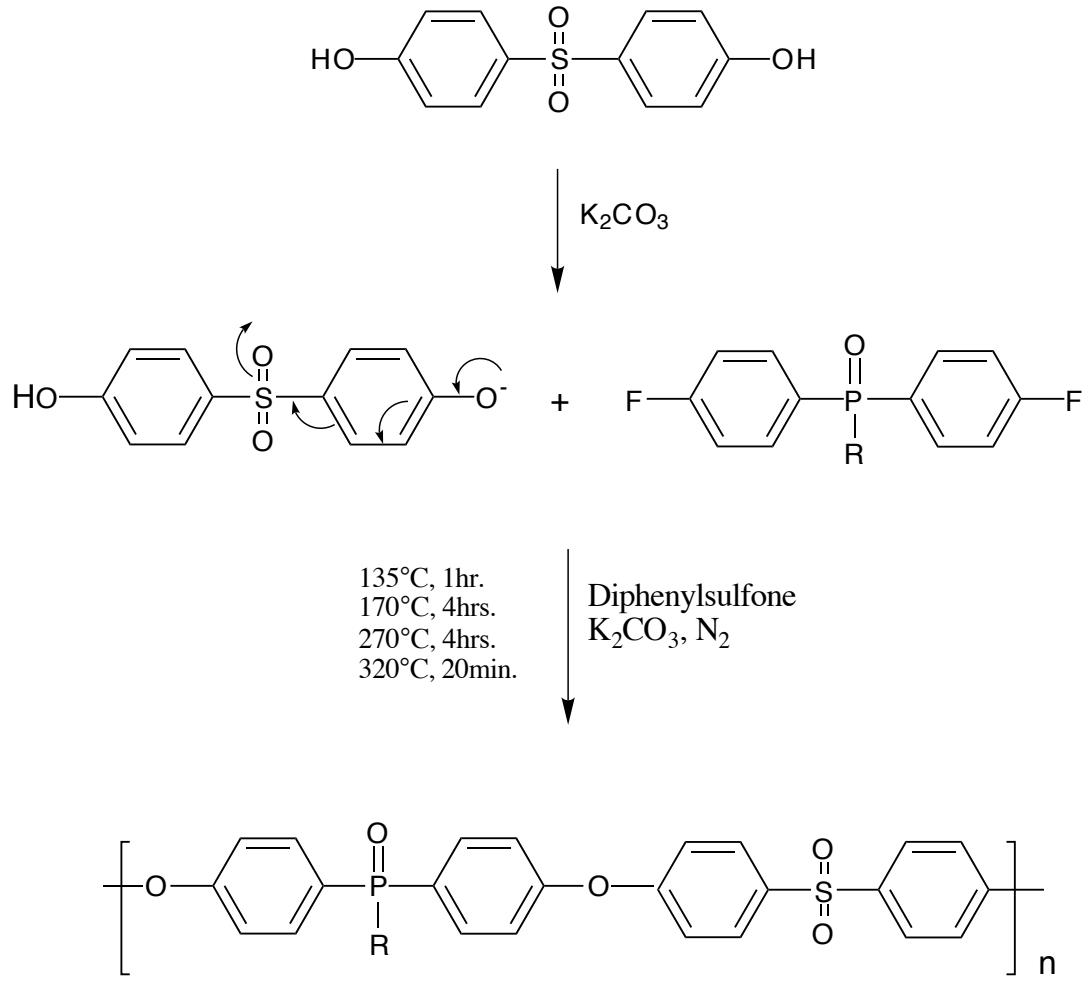

Where R = CH_3 or phenyl

Scheme 4.2.2.1 Synthesis of poly(arylene ether phosphine oxide sulfone)s emphasizing the decreased nucleophilicity of the aryl sulfone phenolate

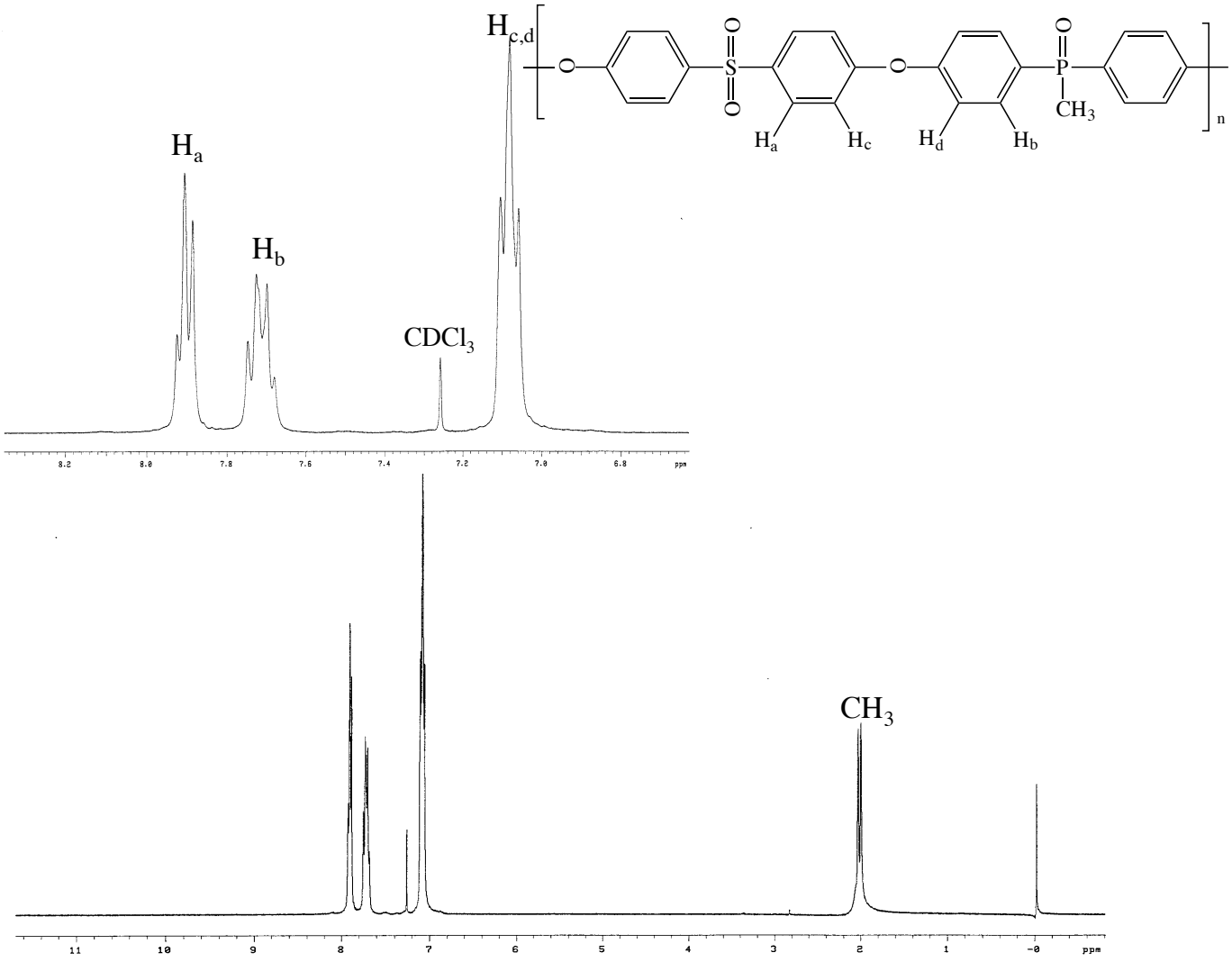

Figure 4.2.2.1 ^{1}H NMR Spectrum of BFPMPO-SO_2 in $CDCl_3$

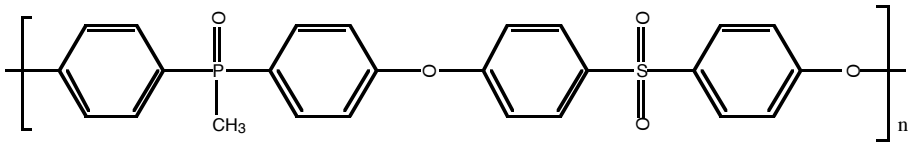

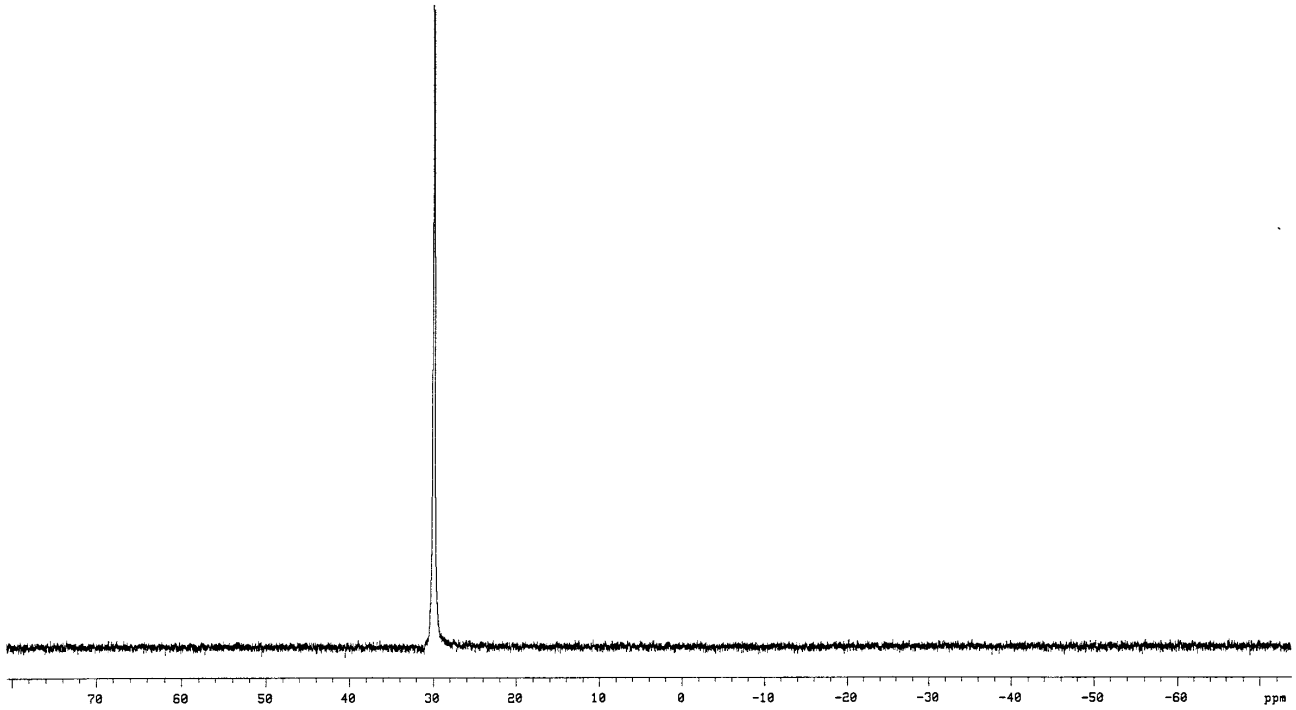

Figure 4.2.2.2 ^{31}P NMR Spectrum of BFPMPO-SO_2 in $CDCl_3$

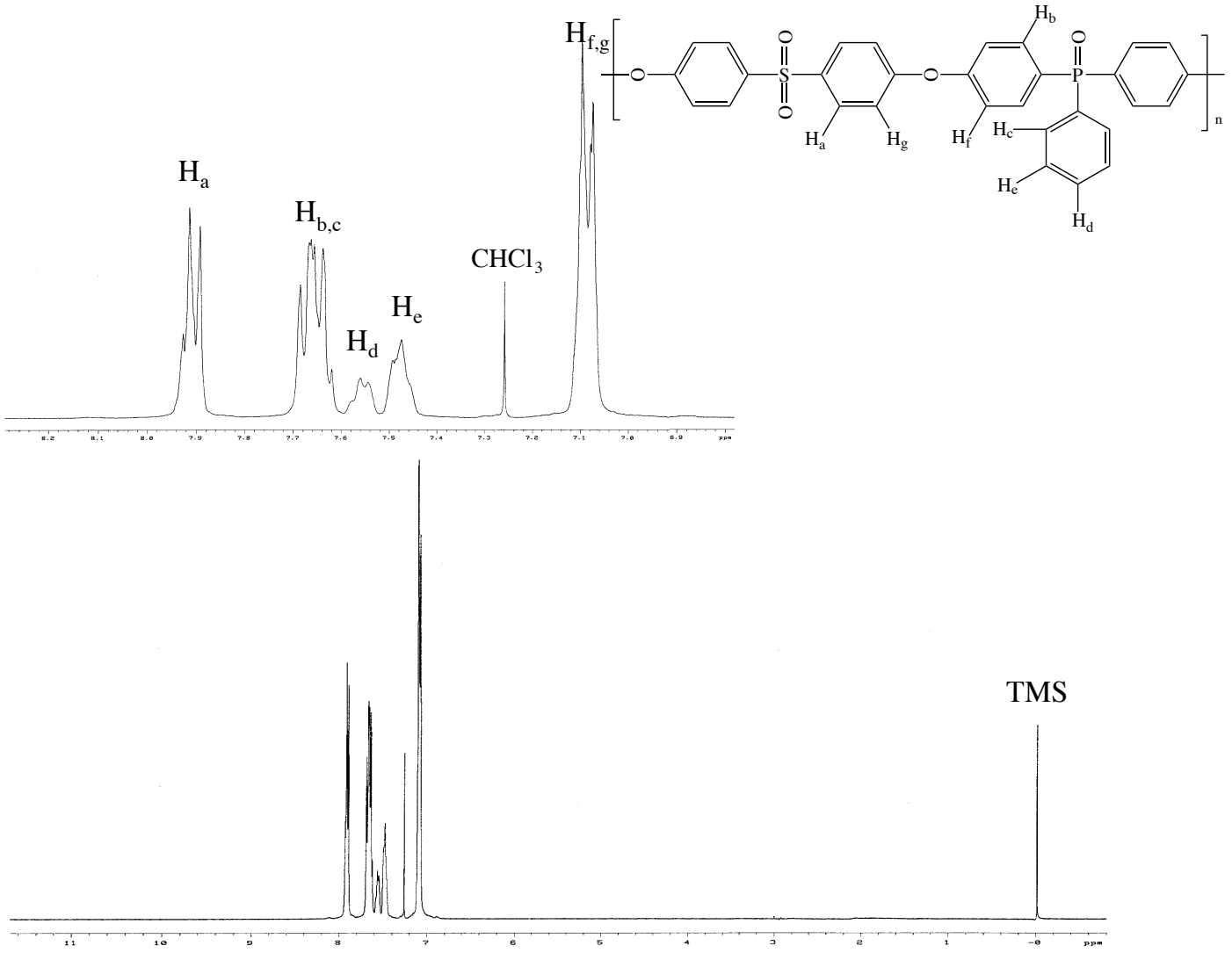

Figure 4.2.2.3 ^{1}H NMR Spectrum of BFPPO-SO_2 in $CDCl_3$

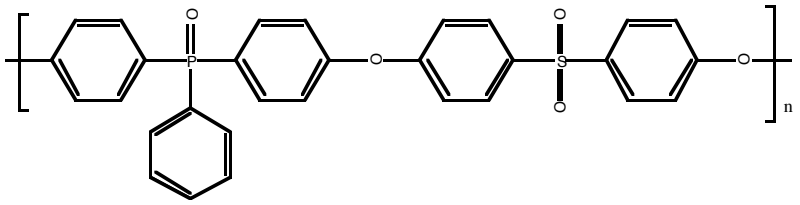

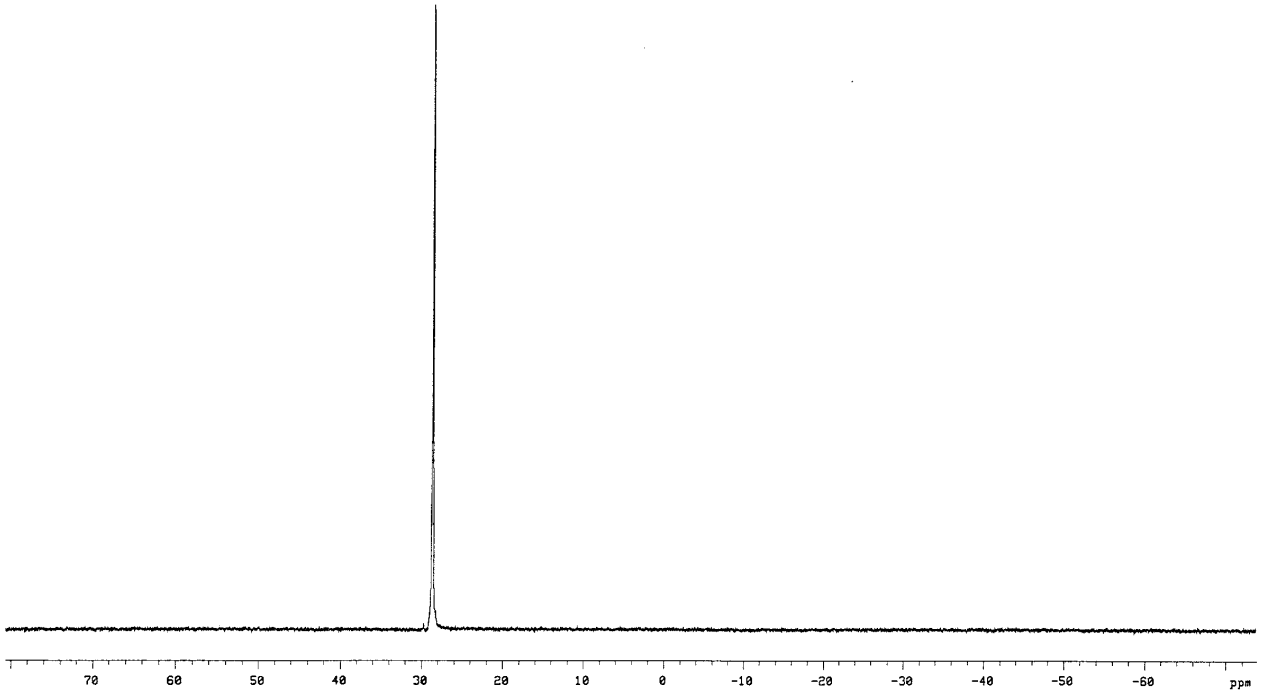

Figure 4.2.2.4 ^{31}P NMR Spectrum of BFPPO-SO_2 in $CDCl_3$

4.2.3 Synthesis of Poly(arylene ether)s With A High Phosphorus Content

Poly(arylene ether)s with a high phosphorus content were synthesized to determine the effect of phosphorus concentration upon polymer properties. These polymers were synthesized using similar procedures as described for the synthesis of poly(arylene ether phosphine oxide sulfone)s. The only difference was that a 4,4'-phosphine oxide containing bisphenol was substituted for 4,4'-bis(hydroxyphenyl)sulfone (Bis-S). The reaction scheme is shown below in Scheme 4.2.3.1. The molecular structures were confirmed by ^{1}H and ^{31}P NMR in $CDCl_3$.

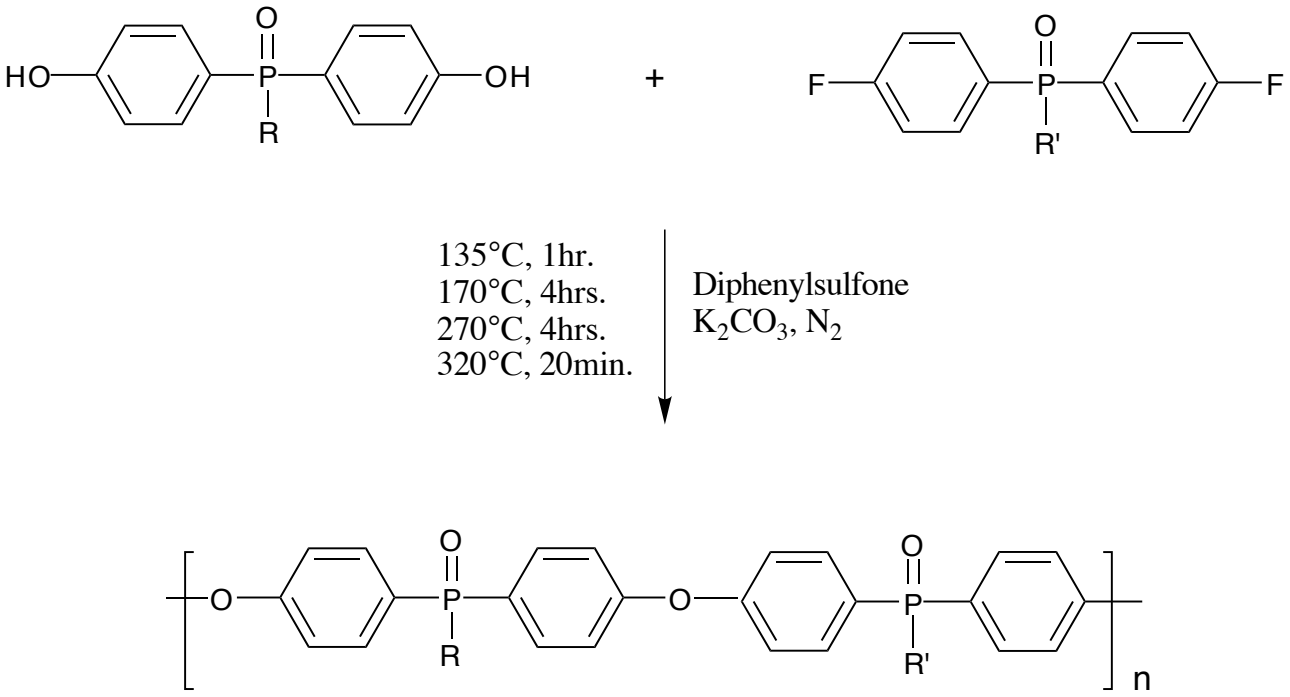

Where R and R' = CH_3 or phenyl

Scheme 4.2.3.1 Synthesis of poly(arylene ether)s with a high phosphorus content

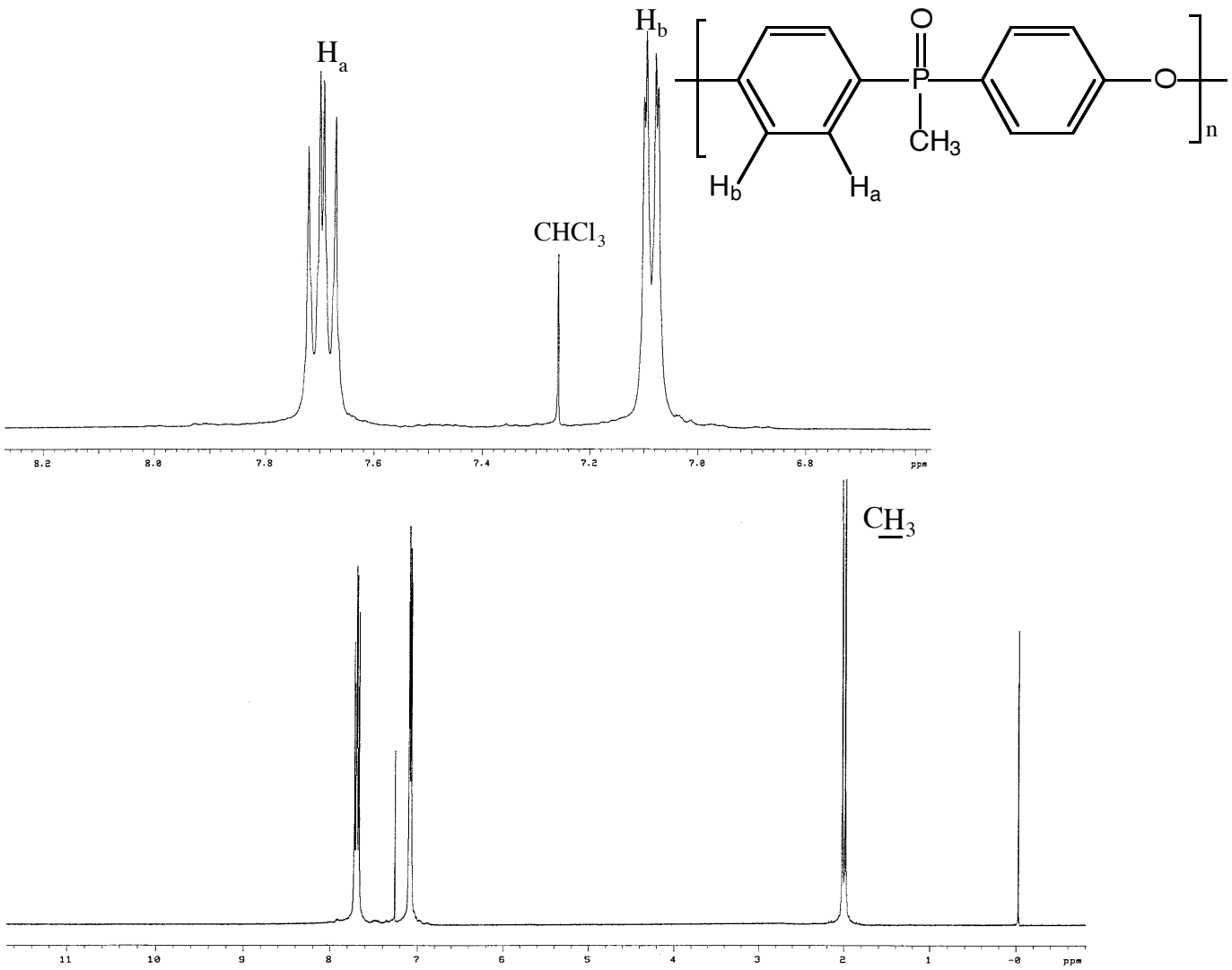

Figure 4.2.3.1 ^{1}H NMR Spectrum of BFPMPO-BOHPMPO in $CDCl_3$

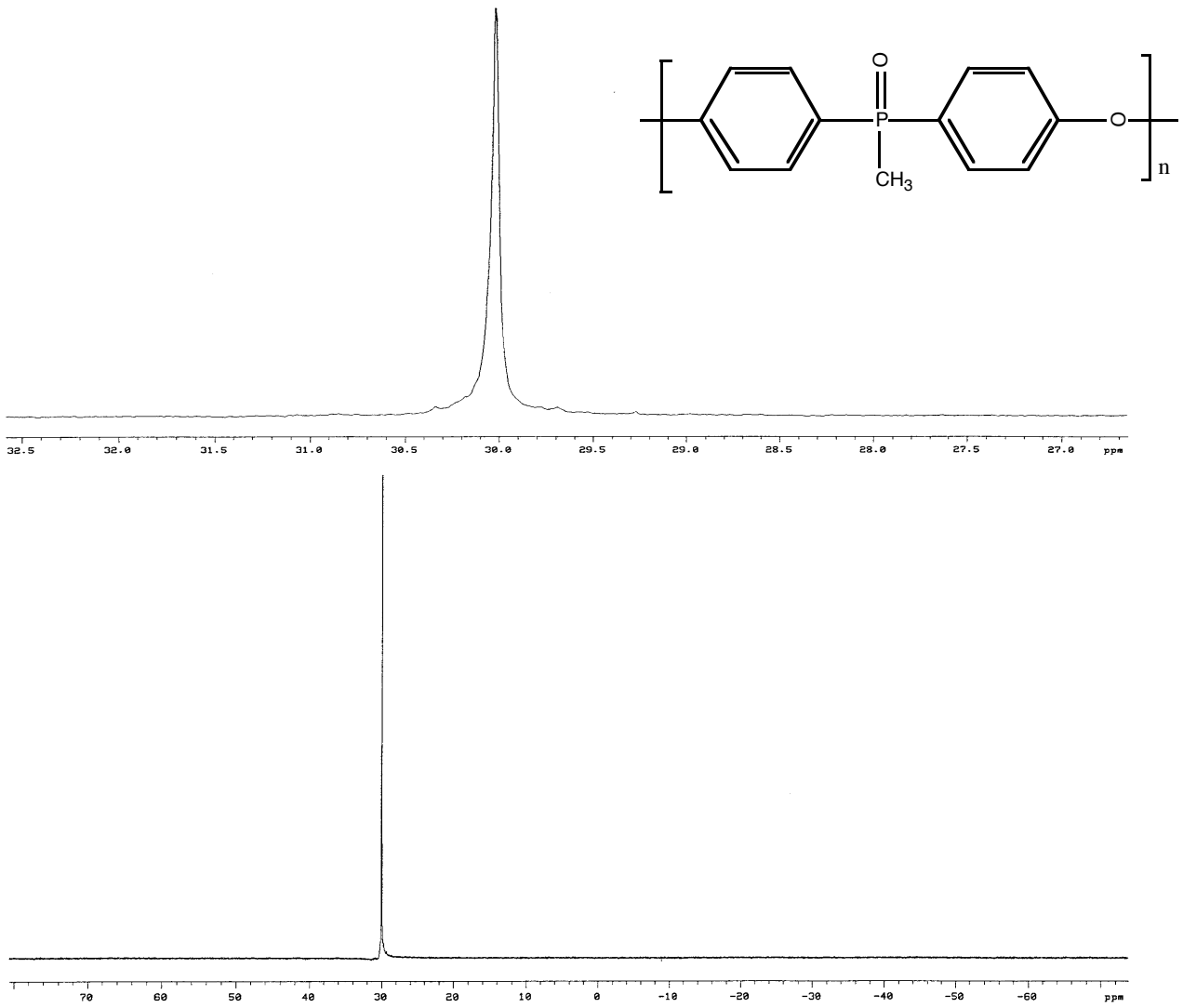

Figure 4.2.3.2 ^{31}P NMR Spectrum of BFPMPO-BOHPMPO in $CDCl_3$

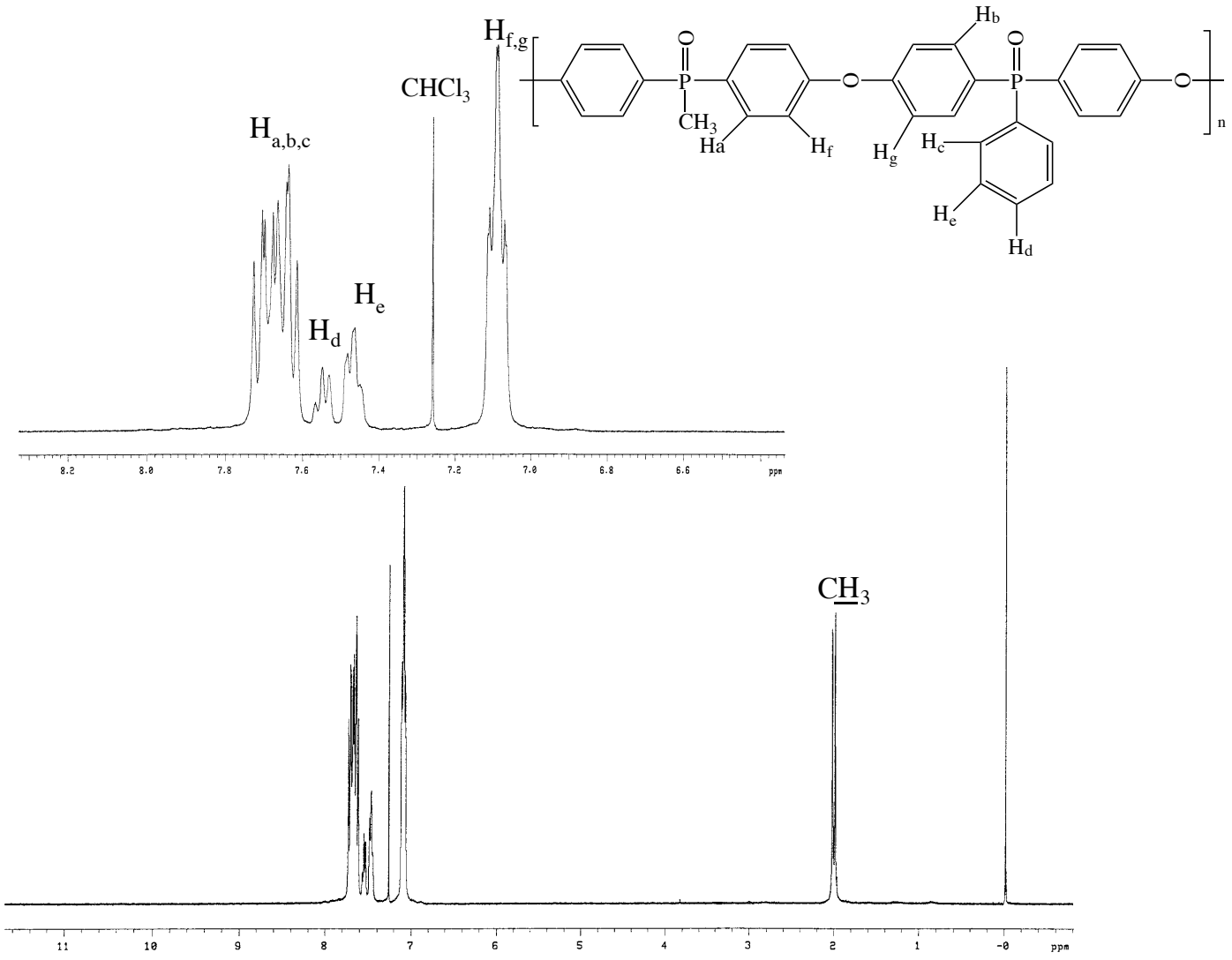

Figure 4.2.3.3 ^1H NMR Spectrum of BFPMPO-BOHPPO in $CDCl_3$

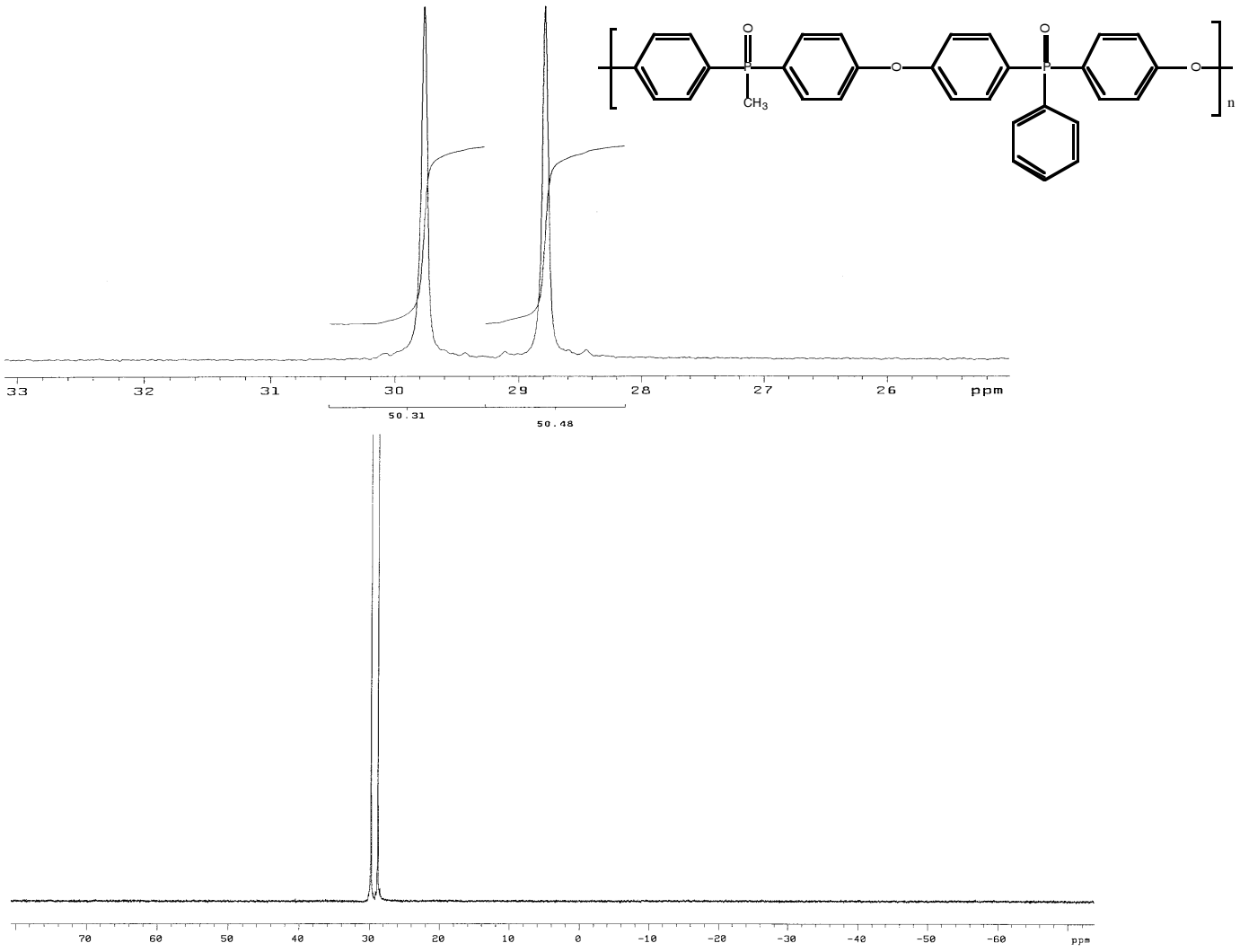

Figure 4.2.3.4 ^{31}P NMR Spectrum of BFPMPO-BOHPPO in $CDCl_3$

Figure 4.2.3.5 provides a reference to the backbone structure of polymers utilized in this thesis. The acronyms of the polymers are listed below their structure. For simplicity, these polymers will be described by these acronyms.

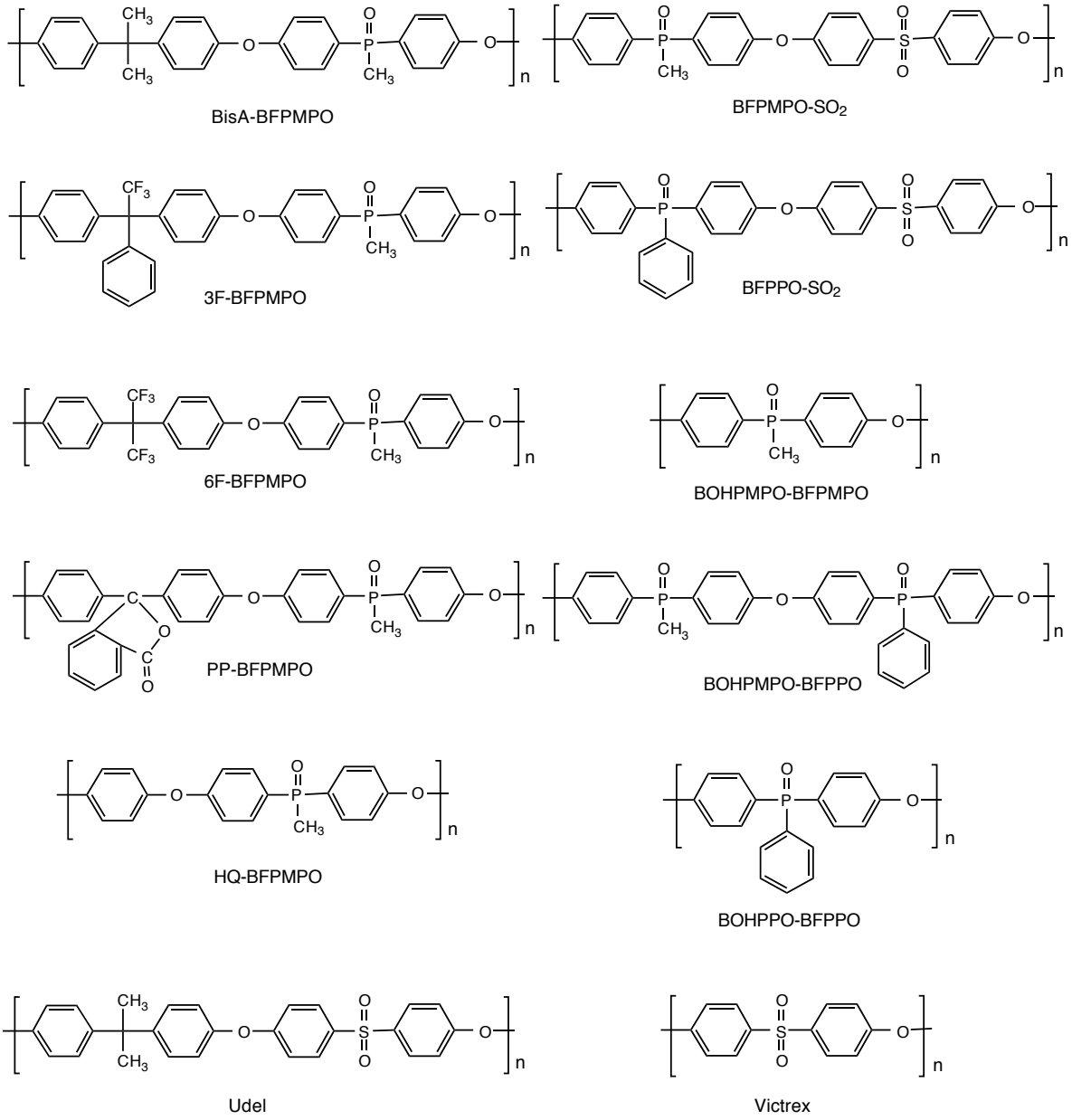

Figure 4.2.3.5 Structure and corresponding acronyms of polymers utilized in this thesis

4.3 Intrinsic Viscosity and GPC Analysis.

Determination of absolute molecular weight averages and distribution of the polymer samples was accomplished using universal calibration GPC (176). Eighteen different polystyrene standards with low polydispersity indices were used to construct a calibration curve. The results for the molecular weight characterization along with intrinsic viscosity data for the aforementioned poly(arylene ether)s are listed in Tables 4.3.1 and 4.3.2 below.

Table 4.3.1 Molecular weight and intrinsic viscosity analysis of poly(arylene etherphosphine oxide)s

Polymer	$[\eta]^{25°C}_{CHCl_3}$	M_n (Kg/mole)	M_w (Kg/mole)	M_w/M_n
BisA-BFPMPO	0.45	27	47	1.7
PP-BFPMPO	0.51	41	72	1.7
3F-BFPMPO	0.57	47	82	1.8
6F-BFPMPO	0.37	21	33	1.6
HQ-BFPMPO	0.85	44	72	1.6
Udel	0.48	23	40	2.3

Table 4.3.2 Molecular weight and intrinsic viscosity analysis of poly(arylene ether phosphine oxide sulfone)s and poly(arylene ether phosphine oxide)s with a high phosphorus content

Polymer	$[\eta]^{25°C}_{CHCl_3}$ dl/gm	M_n (Kg/mole)	M_w (Kg/mole)	M_w/M_n
BFPMPO-BOHPMPO*	0.32			
BFPMPO-BOHPPO	0.33	21	40	1.9
BFPPO-BOHPPO*	0.34			
BFPMPO-SO_2	0.40	29	45	1.6
BFPPO-SO_2	0.41	24	35	1.5
Victrex	0.41	11	22	2.0

* Could not be determined due to insolubility in GPC solvent

From Tables 4.3.1 and 4.3.2 it is shown that the above materials are high molecular weight materials and were considered to be well above their entanglement molecular weight. It is noted that the molecular weight of the experimental polymer samples is, in general, considerably higher than that of the control polysulfones utilized. The relatively narrow molecular weight distribution may be due the fact that these polymers were purified by being precipitated twice. The low molecular weight fraction may have remained in the methanol precipitation medium. This would produce a polydispersity index (M_w/M_n) less than the theoretical value of 2.0. The polymers synthesized using a deactivated bisphenol such as Bis-S (Table 4.3.2) were of somewhat lower molecular weight compared to other polymer systems (Table 4.3.1). It was not certain whether this was due to the reactivity of the bisphenol or reaction times, but when the Bis-S based polymers were allowed to react for a longer time the molecular weight did not increase as might have been anticipated, from a simple second order rate effect.

4.4 Thermal and Mechanical Behavior of Poly(arylene ether phosphine oxide)s

Thermal Analysis. Thermal gravimetric analysis (TGA) was utilized to determine weight loss and, by implication, thermal stability of these polymers in air and nitrogen atmospheres. The

char yield, in air, was also used as a measure of a polymer's anticipated fire resistance. Char yield is an easy and important measurement which correlates the ability to sustain combustion (99). Figure 4.4.1 below illustrates how the char yield may affect polymer combustion. When a polymer is heated to a temperature where it combusts, the degradation reaction may form small molecular weight byproducts and/or highly crosslinked char. It has been proposed that this char may act as a barrier which restricts oxygen reaching the flame front, which promotes quenching the combustion reaction (91). On the other hand, the low molecular weight byproducts generated may be flammable or non-flammable. Clearly, the flammable byproducts are essentially fuel and can undergo further combustion, produce heat which further continues the burning process. A major objective of this thesis research was to investigate whether one could minimize the combustion processes by synthesizing engineering thermoplastics which contain phosphorus and that produce significant char during degradation, thereby disrupting the combustion cycle.

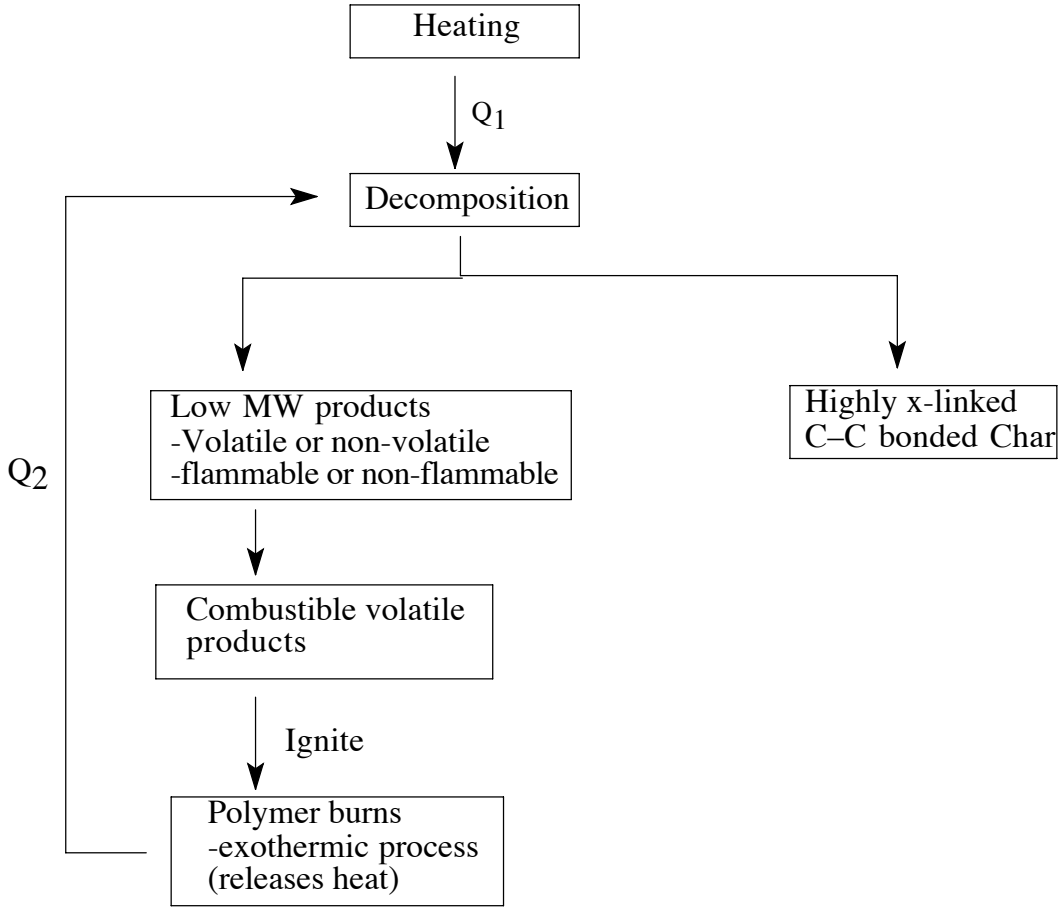

Figure 4.4.1 An illustration of a polymers combustion cycle (91)

The triaryl phosphine oxide polymers have been reported (180) to show an increased char yield over similar ketone and sulfone derivatives. Table 4.4.1 and Figure 4.4.2 illustrates the effect of phosphine oxide upon the TGA char yield in air of various poly(arylene ether)s. Figure 4.4.2 compares two analogous TGA thermograms of analogous poly(arylene ether)s such as BisA-BFPMPO and Udel whose structures are provided below. It is evident from the thermograms that the phosphine oxide containing thermoplastic has a higher char yield at 700°C. Table 4.4.1 also compares the theoretical wt.% phosphorus with the observed char yield. It is evident that the percent phosphorus has a direct influence upon the char yield. The polymer PP-BFPMPO appears to have a higher than expected char yield based on the phosphorus content. This result has also be noted by Lin and Pearce (181) in the case of analogous phenolphthalein based polycarbonates and polyesters and may be due to additional char forming tendencies of the cyclic ester group.

Differential scanning calorimetry (DSC) was used to determine the glass transition temperature (T_g). DSC indicates that these polymers have values up to 260°C and thermal gravimetric analysis shows that they are stable briefly in air over 500°C. It can be seen from Table 4.4.1 that the phenolphthalein based poly(arylene ether phosphine oxide) (PP-BFPMPO) has a 71°C increase in T_g when compared to its analogous BisA derivative. This is probably due to the incorporation of a rigid and polar pendant heterocycle within the polymeric backbone.

Table 4.4.1 Thermal analysis of high molecular weight poly(arylene ether)s

Polymer	$[\eta]^{25°C}_{CHCl3}$ (dl/gm)	TGA (°C)* 5% Wt. loss in air	T_g (°C)**	Char yield*** wt.% in air	%P
Bis A-BFPMPO	0.45	500	192	16	7.0
PP-BFPMPO	0.51	477	263	14	5.8
3F-BFPMPO	0.57	505	229	7	5.6
6F-BFPMPO	0.37	530	208	5	5.7
HQ-BFPMPO	0.85	515	213	26	9.3
Udel	0.48	510	187	0	0

*Scan rate of 10°C/min
**Second heat rate of 10°C/min
***Scan rate of 10°C/min: Yield calculated at 700°C

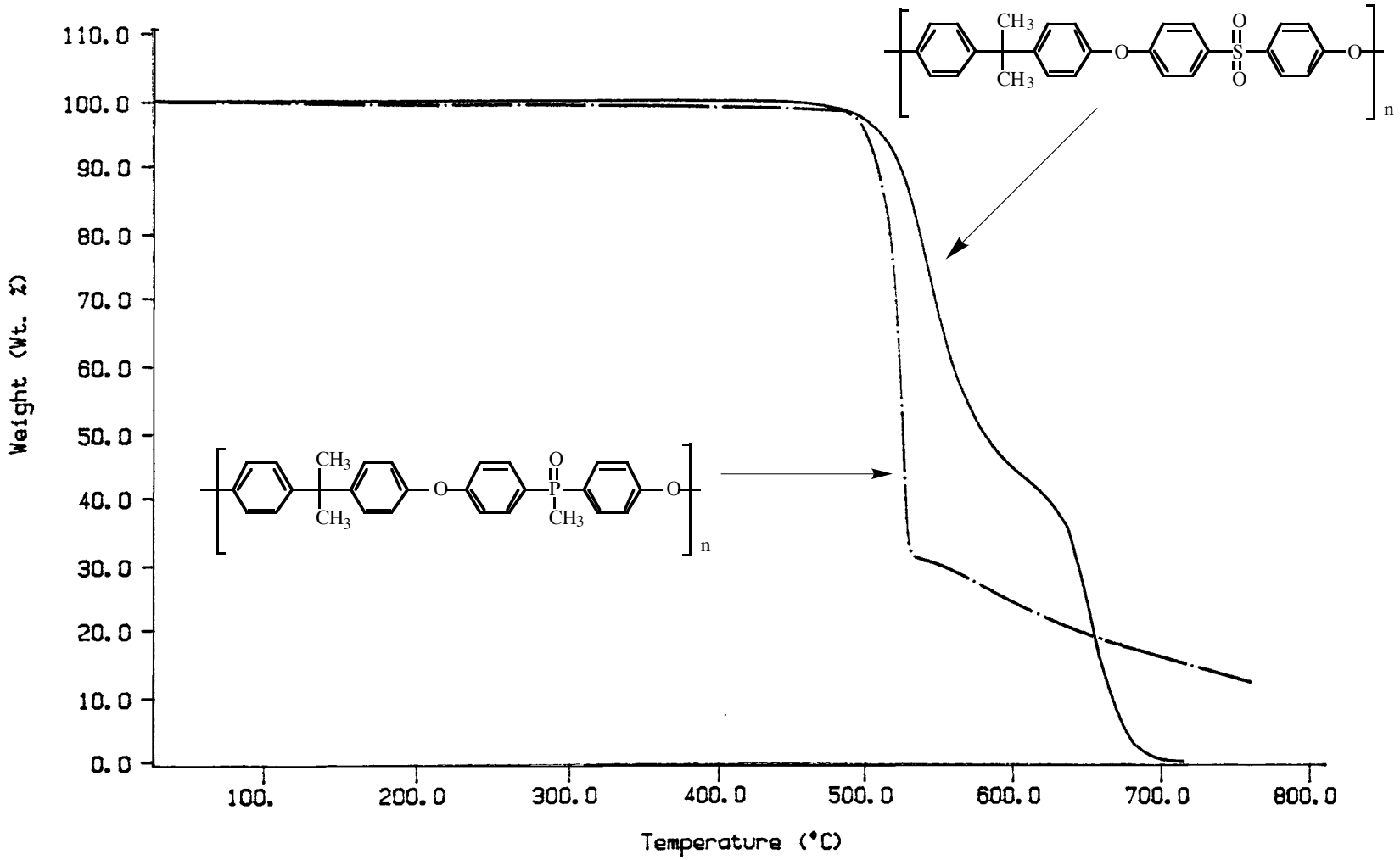

Figure 4.4.2 Comparison of a methyl phosphine oxide with a sulfone conecting link on the thermal stability and char yield of Bisphenol A based poly(arylene ether)s in air (10°C/min.)

The PEPOs also show a significant increase in tensile strength and Young's modulus compared to poly(arylene ether sulfone), possibly due to enhanced intermolecular dipolar forces. When a polymer sample is deformed the polymer molecules must reorient in response to the stress being imposed upon them. Increased intermolecular forces can thus produce a higher modulus at a constant measurement time. Table 4.4.2 illustrates that BisA-BFPMPO has a 15% increase in modulus when compared to the analogous poly(arylene ether sulfone) control. Furthermore, the stiffness and higher concentration of the polar phosphine oxide moieties within the polymer backbone explain the increased modulus of hydroquinone based HQ-BFPMPO.

Table 4.4.2 Room Temperature Stress-Strain Behavior of Compression Molded High Molecular Weight Poly(arylene ether)s

Polymer	Youngs* Modulus (ksi)	Tensile* Strength (ksi)	Strain* (%)
Bis A-BFPMPO	420±45	12.2±0.9	>40
3F-BFPMPO	420±7	13.3±0.9	25±1
6F-BFPMPO	350±14	11.1±0.7	26±3
HQ-BFPMPO	510±35	12.0±1.2	38±3
Udel	360±38	10.2±1.0	>40

*ASTM D638 (0.05 in/min)

The effect of phosphine oxide upon the refractive index and hence optical properties was also a area of interest. Table 4.4.3 illustrates the of phosphine oxide and other backbone modification upon the refractive index values of amorphous thermoplastics.

Table 4.4.3 The effect of the backbone structure on the refractive index of poly(arylene ether)s

Polymer	Refractive Index*
BisA-BFPMPO	1.628
PP-BFPMPO	1.639
3F-BFPMPO	1.612
6F-BFPMPO	1.575
HQ-BFPMPO	1.644
BisA-Phosphonium Bromide	1.664
Udel	1.629

*measured at a wavelength of 632.8 nm

Incorporating a phosphine oxide moiety into a polymeric backbone does not have a significant effect on the refractive index, when compared to the sulfone control. However, by increasing the aromatic nature of the polymer and by incorporating a polarizable halogen in a phosphonium ionomer, the refractive index is increased from 1.628 (BISA-BFPMPO) to 1.664 BisA-Phosphonium bromide). The synthesis and structure of bisA-phosphonium bromide is described in chapter 4.6.2. Conversely, the poly(arylene ether)s that contain fluorine in the polymeric backbone show low polarizability and a decrease in refractive index.

Poly(arylene ether phosphine oxide sulfone)s were synthesized to determine if the aforementioned increase in thermal and mechanical properties could be achieved. These polymers contained both the polar phosphine oxide and sulfone moieties. As can be seen in Table 4.2.4 these phosphine oxide-sulfones materials have substantially improved properties such as: increased modulus, T_g, and char yield over the commercially available polyethersulfone known as Victrex. The increase in T_g of these new polymers is probably due to the increased bulkiness and dipole moment of the phosphine oxide monomer, compared to the sulfone derivative. The effect of phosphine oxide upon thermal stability and char yield is illustrated from the TGA thermograms in Figure 4.4.3. It is evident from these plots that the phosphine oxide moiety increases the char yield (700°C in air) of these poly(arylene ether)s from 15 to 30%. The poly(arylene ether phosphine oxide)s synthesized from partially aliphatic BFPMPO appear to be less thermally stable that those synthesized from wholly aromatic BFPPO. Thus, both BFPPO-SO_2 and Victrex

demonstrate higher thermal stability than BFPMPO-SO2. This no doubt reflects the weaker bond strength of a methyl-phosphorus covalent bond (272 kJ/mole) (92) relative to a phenyl-phosphorus bond (322 kJ/mole) (37).

Table 4.4.4 Thermal and mechanical properties of poly(arylene etherphosphine oxide sulfone)s

Polymer	25°C $[\eta]_{CHCl3}$ (dl/gm)	Char yield* Wt. % in air	TGA (°C)** 5% Wt. loss in air	T_g (°C)***	Youngs**** Modulus (ksi)	Strain**** (%)
BOHPMPO-SO2	0.40	24	514	233	465 ± 7	36 ± 5
BOHPPO-SO2	0.41	30	596	231	476 ± 7.5	25 ± 9
Victrex 3600P	0.41(NMP)	15	561	222	374 ± 16	25 ± 3
Victrex 4100G*****					348	

* Scan rate of 10°C/min: determined at 700°C

** Scan rate of 10 °C/min

***Determined from second scan rate of 10 °C/min

****ASTM D638 (0.05 in/min)

*****Encyclopedia of Polymer science and Engineering 2nd ed.*

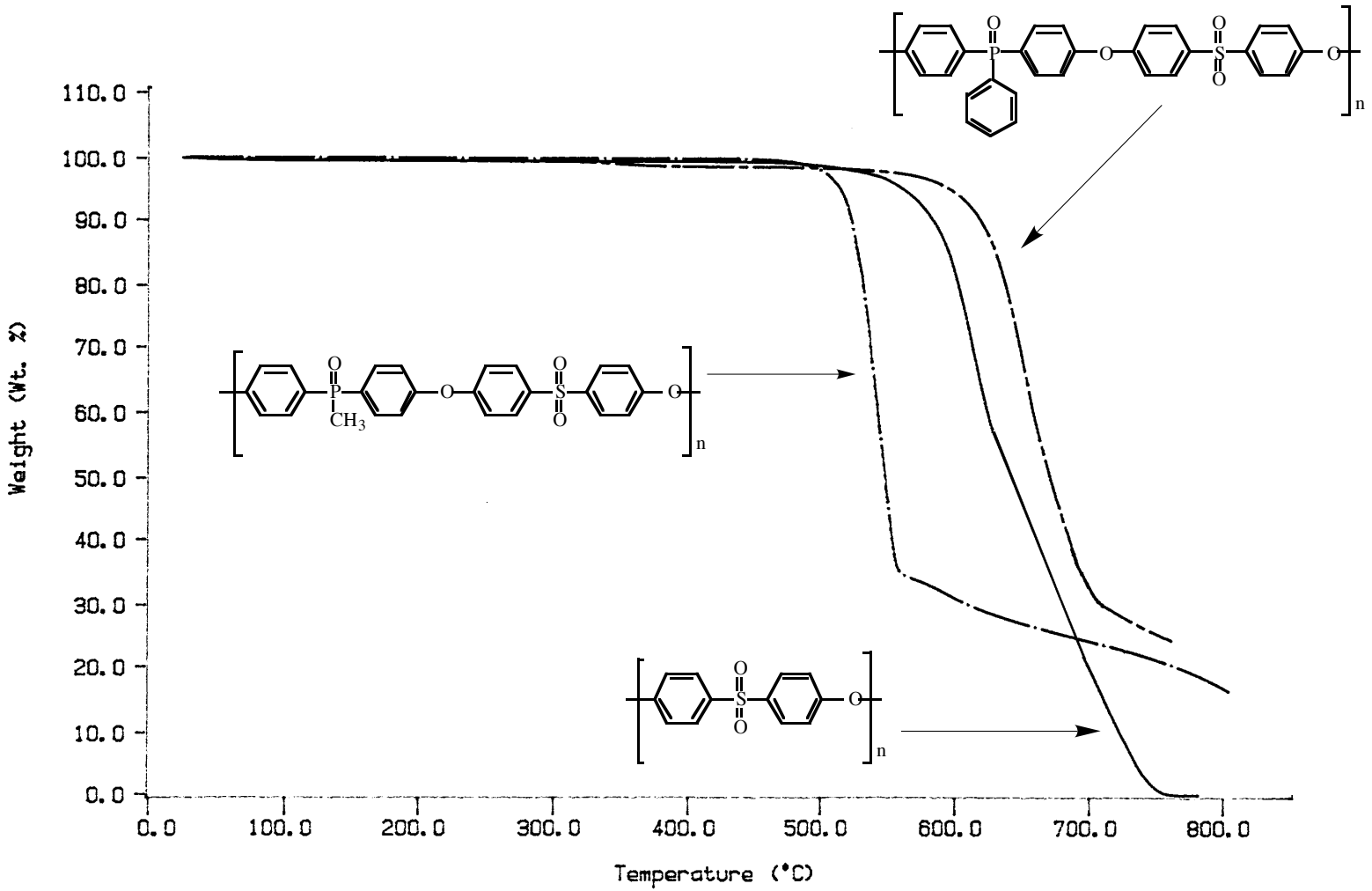

Figure 4.4.3 Effect of methyl or phenyl phosphine oxide on the thermal stability and char yield of poly(arylene ether sulfone)s in air (10°C/min.)

What is most impressive about these phosphine oxide sulfone materials in their increase in modulus and char yields compared to the control polysulfone thermoplastic. By incorporation of a phosphine oxide moiety within the polymeric backbone, Young's modulus of the thermoplastic was increased over 25%. The effect of the polar phosphine oxide moiety upon the modulus is greater in these polymers than in the bisphenol A based thermoplastics. This may be due to the elimination of the flexible sp^3 carbon in the backbone of the bisphenol A based polyethers. That carbon is the "weak link" in the polymer chain, therefore, if the intermolecular interaction between polymer chains is increased, but the weak link still exists, the overall effect of the phosphine oxide group may be minimized. However, when the weak part of the chain is eliminated the overall effect of the polar phosphine oxide moiety upon the modulus in increased. In addition, the high char yields of the phosphine oxide-sulfones after both dynamic and three hours of high temperature isothermal TGA indicates that these polymers may be inherently flame resistant, as described below.

Figure 4.4.4, Figure 4.4.5, and Figure 4.4.6 illustrate the difference in TGA thermograms between the commercially available thermoplastic Victrex and two phosphorus containing thermoplastics, BFPPO-SO_2 and BFPMPO-SO_2. Thus, the polyether sulfones were completely volatilized after a short exposure to 550°C or 600°C. However, the phosphine oxide containing polymers studied showed between a 9 to 18 percent char yield after exposure to 600°C for three hours. This data clearly indicates that the phosphorus within the backbone of the polymer plays a key role in char formation. Furthermore, the char that is formed is extremely thermally stable and shows little weight loss with time at 600°C. Some characteristics of the phosphorus containing char have been investigated and are discussed in Chapter 4.5.

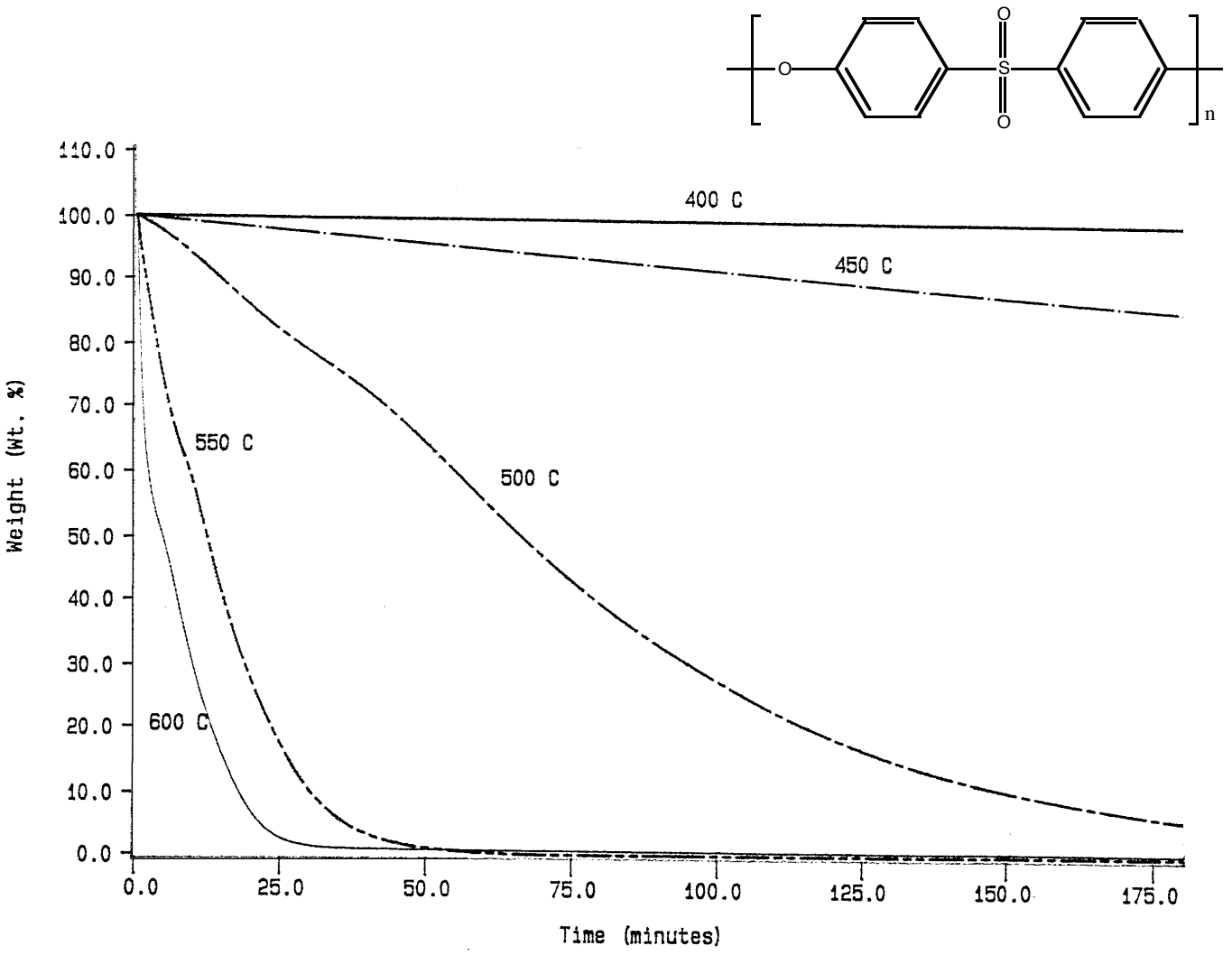

Figure 4.4.4 Isothermal TGA of Victrex polyether sulfone in air for 3 hours at selected temperatures

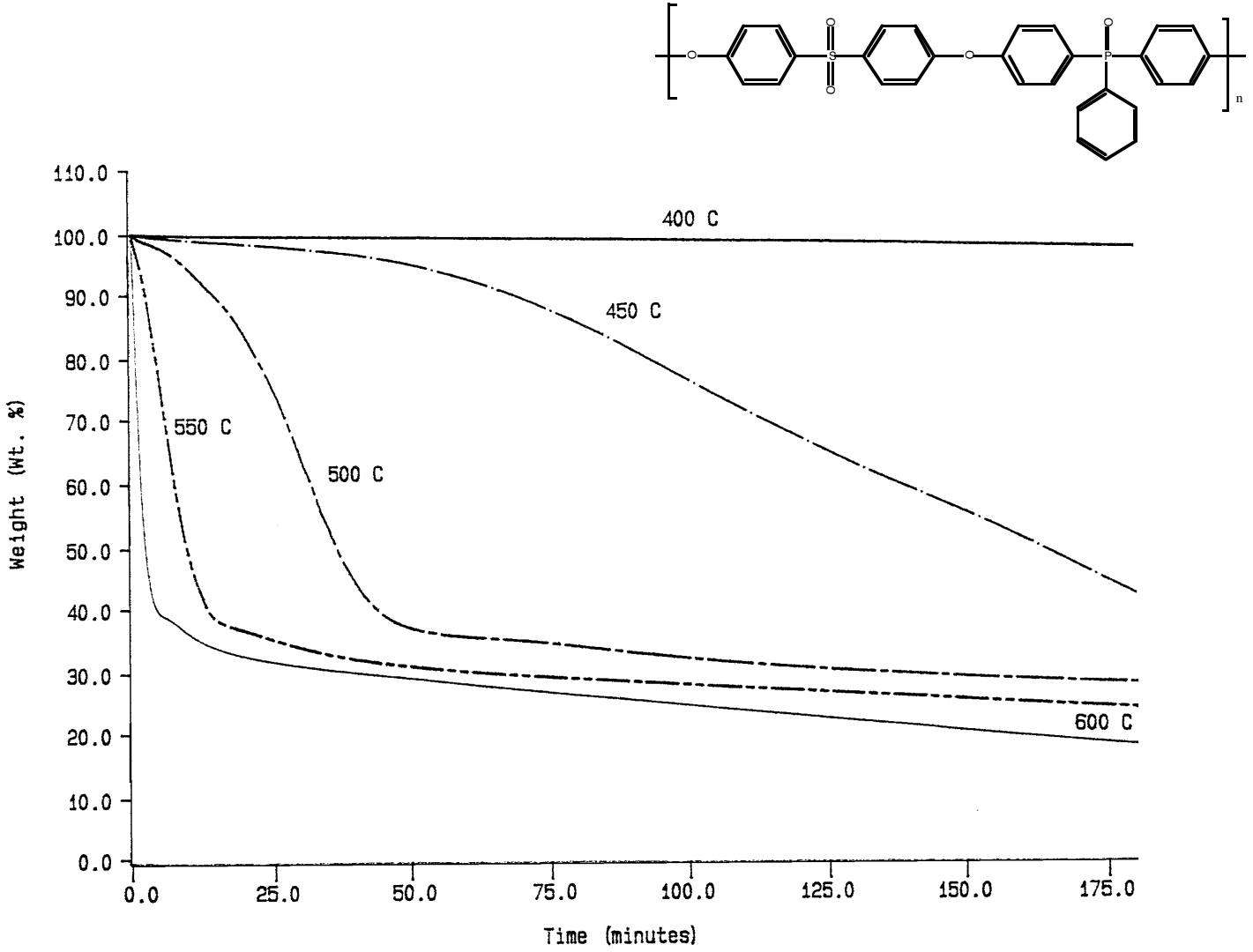

Figure 4.4.5 Isothermal TGA of BFPPO-SO_2 in air for 3 hours at select temperatures

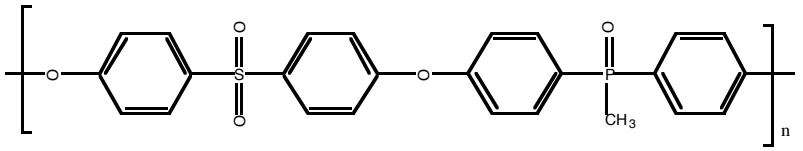

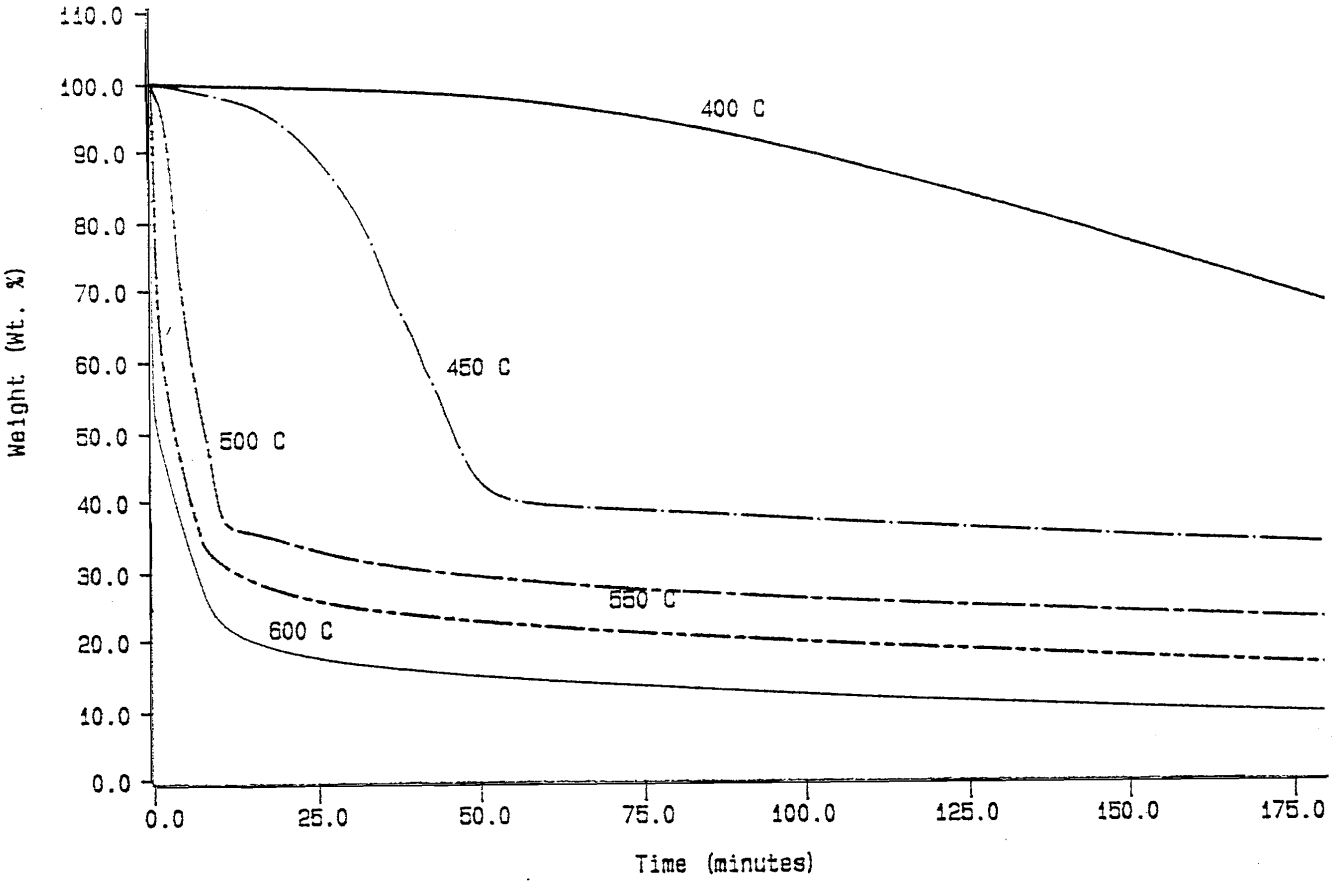

Figure 4.4.6 Isothermal TGA of BFPMPO-SO_2 in air for 3 hours at select temperatures

Table 4.4.5 Influence of temperature, molecular structure, and 3 hour aging on TGA char yields of various poly(arylene ether)s

Polymer	400 °C (%)	450 °C (%)	500 °C (%)	550 °C (%)	600 °C (%)
BFPMPO-SO2	68	33	23	16	9
BFPPO-SO2	98	42	28	24	18
Victrex	99	86	6	0	0

* Determined isothermally using TGA

From TGA analysis all three of these polymers appear to possess enough thermal stability at 400°C to be melt processed without significant degradation within a 45 minute processing time.

Since phosphorus appeared to have a direct influence upon the char yield it was decided to synthesize poly(arylene ether phosphine oxide) that would contain up to 14 mass percent phosphorus. Table 4.4.6 and Figure 4.4.7 shows the thermal data of these high phosphorus content poly(arylene ether)s. The partially aliphatic BFPMPO-BOHPMPO and BFPMPO-BFPPO systems are not as thermally stable as BFPPO-BOHPPO. This is probably due to the fact that the P-Me has a lower bond dissociation energy than P-Ph as mentioned earlier. It was also of interest to show whether the additional mass percent phosphorus or the additional aromatic ring would lead to a higher char yield. The data suggests that the higher aromaticity of the BFPPO-BOHPPO polymer produces a higher char yield.

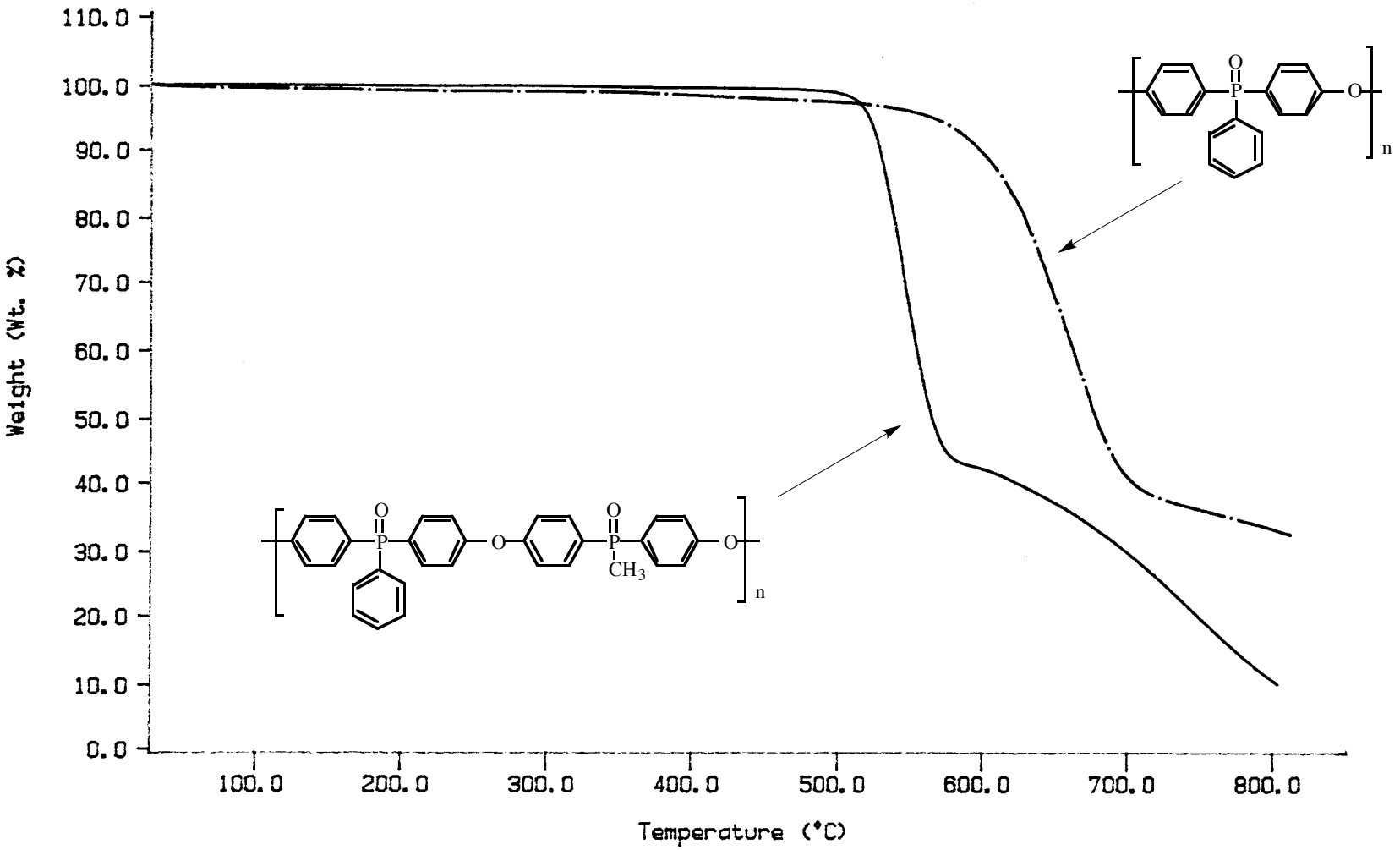

Figure 4.4.7 Effect of pendant methyl moiety upon the thermal stability and char yield of poly(arylene ether phosphine oxide)s (10°C/min.)

In addition to their higher char yields, as shown in Table 4.4.6, these polymers show a 20°C increase in T_g over the control polysulfone and a 10°C increase in Tg over their poly(arylene ether phosphine oxide sulfone) counterpart. The increase in T_g may be due to the high concentration of polar phosphine oxide moieties within the polymeric backbone. The phosphine oxide polymers also have a higher char yield 700°C in air than both the control polysulfone and the phosphine oxide sulfones studied. It is also noted that the phosphine oxide homopolymer with a pendant aromatic ring has the highest char yield, which is consistent with results previously discussed by Lin and Pierce (181).

Table 4.4.6 Thermal properties of poly(arylene ether phosphine oxide)

Polymer	$[\eta]^{25°C}_{CHCl3}$ (dl/gm)	Char Yield* Wt% in air	TGA(°C)* 5% Wt. loss in air	T_g(°C)**
BOHPMPO-BFPMPO	0.32	30	518	238
BOHPMPO-BFPPO	0.33	30	530	238
BOHPPO-BFPPO	0.33	41	567	240

* Scan rate of 10 °C/mi: determined at 700°C
**Determined from second scan rate of 10°C/min

The influence of phosphorus upon the char yield was analyzed by plotting char yield as a function of percent phosphorus and Figure 4.4.8 demonstrates the influence of phosphorus content on the char yield. Indeed, a strong, almost linear correlation between the percent phosphorus and char yield is observed. This is quite revealing, considering that the structure of the polymer backbone is also changing along with the phosphorus concentration: for example the amount of aromatic rings within the polymeric backbone was earlier noted also to affect char yields. Therefore, by considering the generalization derived by van Krevelen (99), who suggested that higher char yields produced higher limiting oxygen index values (LOI), one may conclude that the increased phosphorus content within the backbone of poly(arylene ether)s increases their flame resistance.

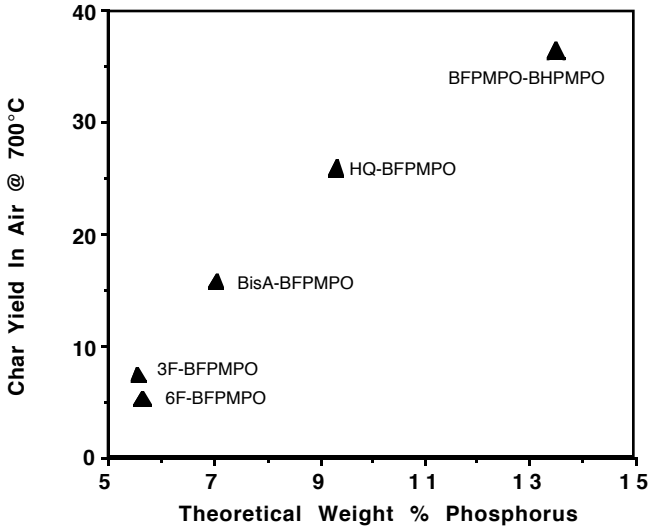

Figure 4.4.8 Influence of percent phosphorus on char yield at 700 °C

The flammability of the phosphine oxide polymers was further examined by cone calorimetry in cooperation with Dr. T. Kashiwagi of the NIST Fire Laboratories (91). Cone calorimetry determines the amount of heat released by a polymer due to combustion under a specific applied heat flux. The results are summarized in Figure 4.4.9 and Table 4.4.7 (38). The Udel control had the highest heat release rate of the samples analyzed, which may be due to the partially aliphatic bisphenol-A structure. The wholly aromatic poly(arylene ether sulfone) Victrex ignited with a longer delay time and had a similar peak heat release to the phosphine oxide containing polymers. However, the phosphine oxide containing polymers did not generate a steady flame during combustion and extinguished shortly after ignition. This is noted in Figure 4.4.9 by the rapid decrease in the heat release rate to approximately zero, after the peak value was reached. This rapid decrease in heat release rate indicates that the poly(arylene ether phosphine oxide sulfone)s did not sustain combustion even under a continuous heat flux of 40Kw/m^2. In essence, these polymers self-extinguished. However, the polymers not containing phosphorus show continued combustion as demonstrated by the long tail on the plot of their heat release rate (76). Table 4.2.5 summarizes the effect upon the peak heat release rate by incorporating phosphorus within the backbone of various polymers (38, 182, 183).

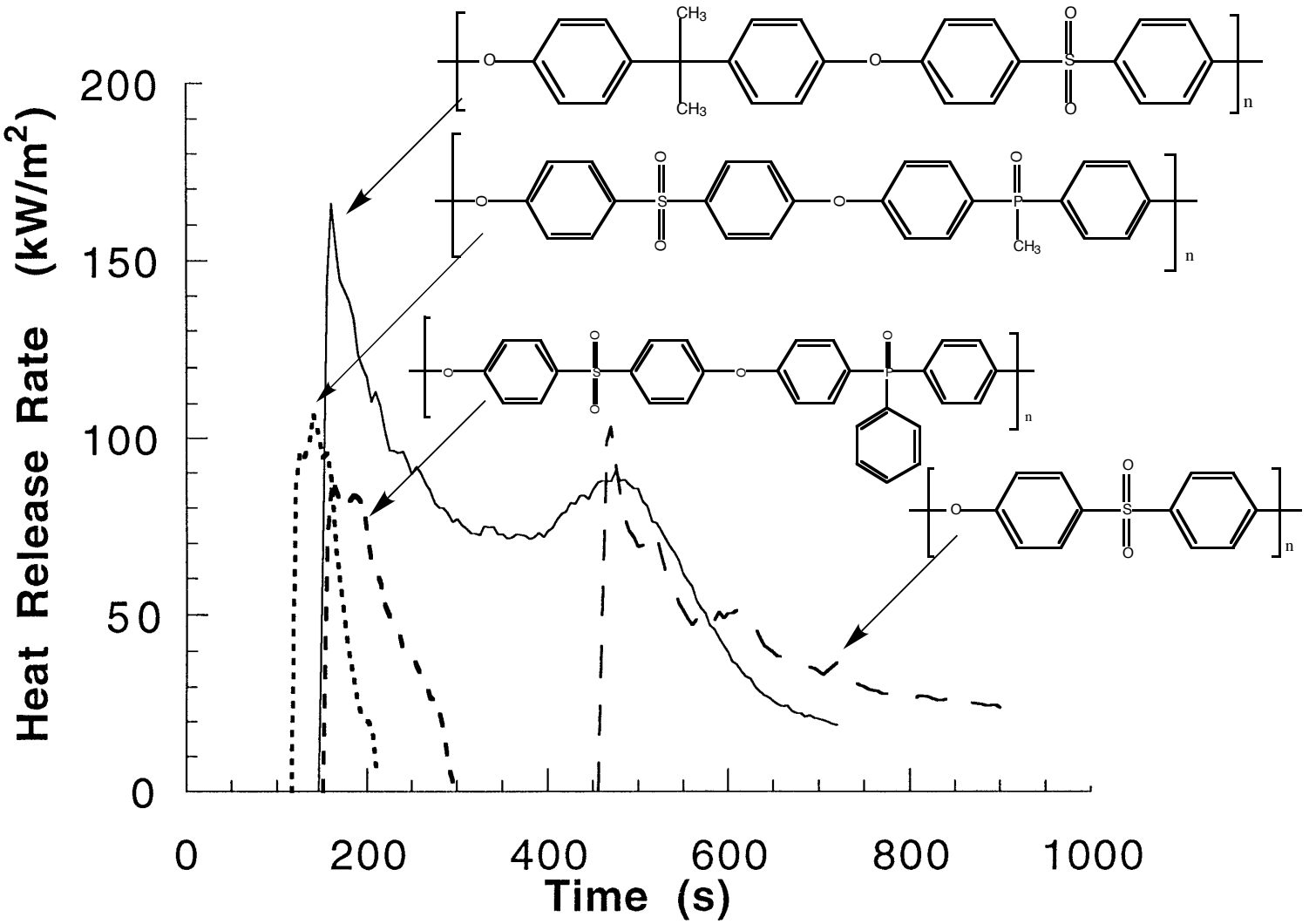

Figure 4.4.9 Effect of phosphine oxide on the heat release rate of poly(arylene ether)s at 40 kW/m^2

Table 4.4.7 Influence of phosphine oxide upon the peak heat release of various polymers (182, 183)

Polymer	Heat Release Rate* kW/m^2
Nylon 6,6	1200
Nylon 6,6 30%PO (3.4 wt.% Phosphorus)	500
BisA-polycarbonate	540
BisA-polycarbonate 10% PO (1.2 wt.% Phosphorus)	420
Ether-sulfone (Victrex)	105
BFPMPO-SO_2 (6.7 wt.% Phosphorus)	105
BFPPO-SO_2 (5.9 wt.% Phosphorus)	85

* Samples tested using cone calorimetry at a flux of 40 kW/m^2

Another way to analyze the heat release rate by averaging of heat release rate over time, *e.g.* 180 seconds. An average heat release rate allows one to generate a combustion time cycle. For example, in a "real-life" fire not every portion of the burning item is undergoing its peak burning. Indeed, some portions could be barely igniting while others are decaying. Therefore, to better analyze how materials behave in a "real life" fire it is necessary to determine the average heat release rate over a period of time. Statistical consideration developed at NIST led to 3 minutes being utilized as the averaging period (133). When considering the 3 minute averaging period, the change in heat release rate of the phosphine oxide sulfones with respect to the two ether sulfones is dramatic. Not only do these polymers show an improved average heat release rate but are also self-extinguishing under the conditions tested.

Incorporation of a phosphine oxide does not appear to alter the important dynamic mechanical sub-ambient damping behavior which is in contrast to their different thermal, mechanical strength, and flammability, of the polymers analyzed . Plots of Tan delta versus temperature are shown below in Figure 4.4.10.

These low temperature beta transitions are often considered to be important to molecular motions which may lead to the impact resistant properties of Victrex and other poly(arylene ether)s.

The relaxation motions may play a role in absorbing the energy of the impact without failure (184). Therefore, the fact that beta transition are observed for the phosphine oxide sulfone polymer at the same temperature as for other analogous system is an additional explanation of why the phosphine oxide sulfones are very ductile.

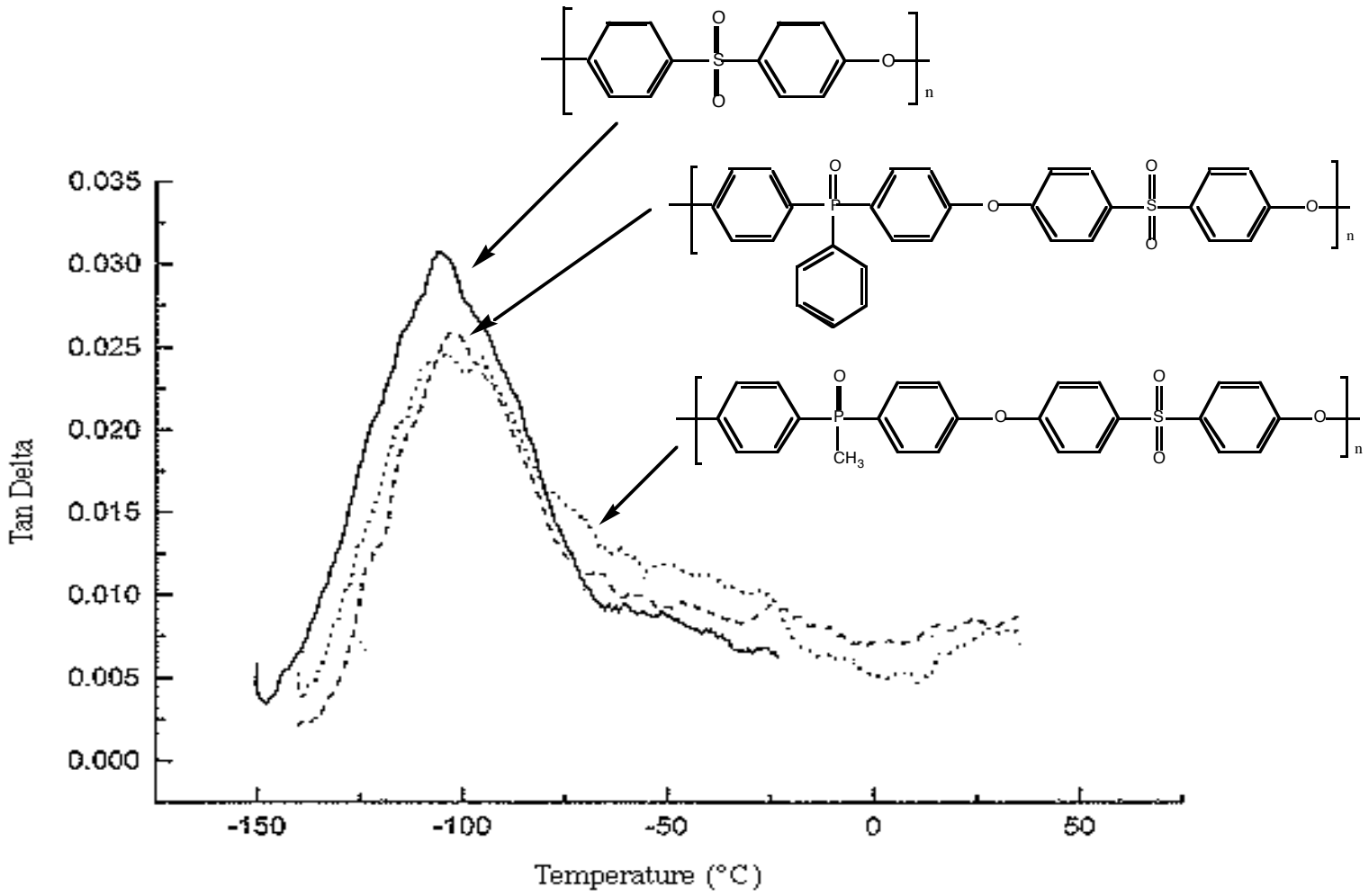

Figure 4.4.10 Phosphorus does not influence the low temperature relaxation of poly(arylene ether)s

The effect of phenyl or methyl phosphine oxide upon the refractive index of highly aromatic poly(arylene ether)s was also a area of interest. Table 4.4.8 illustrates the of phosphine oxide and other backbone modification upon the refractive index of amorphous thermoplastics.

Table 4.4.8 The effect of a phosphine oxide and sulfone groups on the refractive index of poly(arylene ether)s

Polymer	Refractive Index*
BFPMP-BOHPMPO	1.643
BFPMPO-BOHPPO	1.644
BFPMPO-SO_2	1.650
BFPPO-SO_2	1.654
Victrex	1.647

*measured at a wavelength of 632.8 nm

Incorporating a phosphine oxide moiety into a polymeric backbone thus appears to not have a significant effect on the refractive index with respect to the sulfone derivative. Nonetheless, these polymers display excellent thermal and mechanical properties along with high refractive index values and often produce clear transparent films.

4.5 Degradation Studies of Poly(arylene ether)s

Polymer degradation studies were conducted to compare the behavior of the poly(arylene ether phosphine sulfone)s with that to the control poly(ether sulfone) Victrex. It is important to understand how these polymers degrade for several reasons. Firstly, one may learn how to better design polymers that have increased thermal stability. Secondly, the volatile byproducts can be identified, and the composition of the residual char may be further understood. The polymer BFPPO-SO_2 and control Victrex were decomposed in helium at 550 and 700°C, and their volatile byproducts were separated by gas chromatography and analyzed using mass spectrometry, detailed procedures are provided in the experimental. The gas chromatograms are shown below in Figures 4.5.1 through 4.5.4 and every major peak was identified. It is critical when analyzing these polymers to quickly sweep the volatiles through the pyrolysis injector so that further degradation of

the initial volatile reaction product does not occur. If this does occur to a significant extent, then the number of volatile compounds increases dramatically and render interpretation difficult.

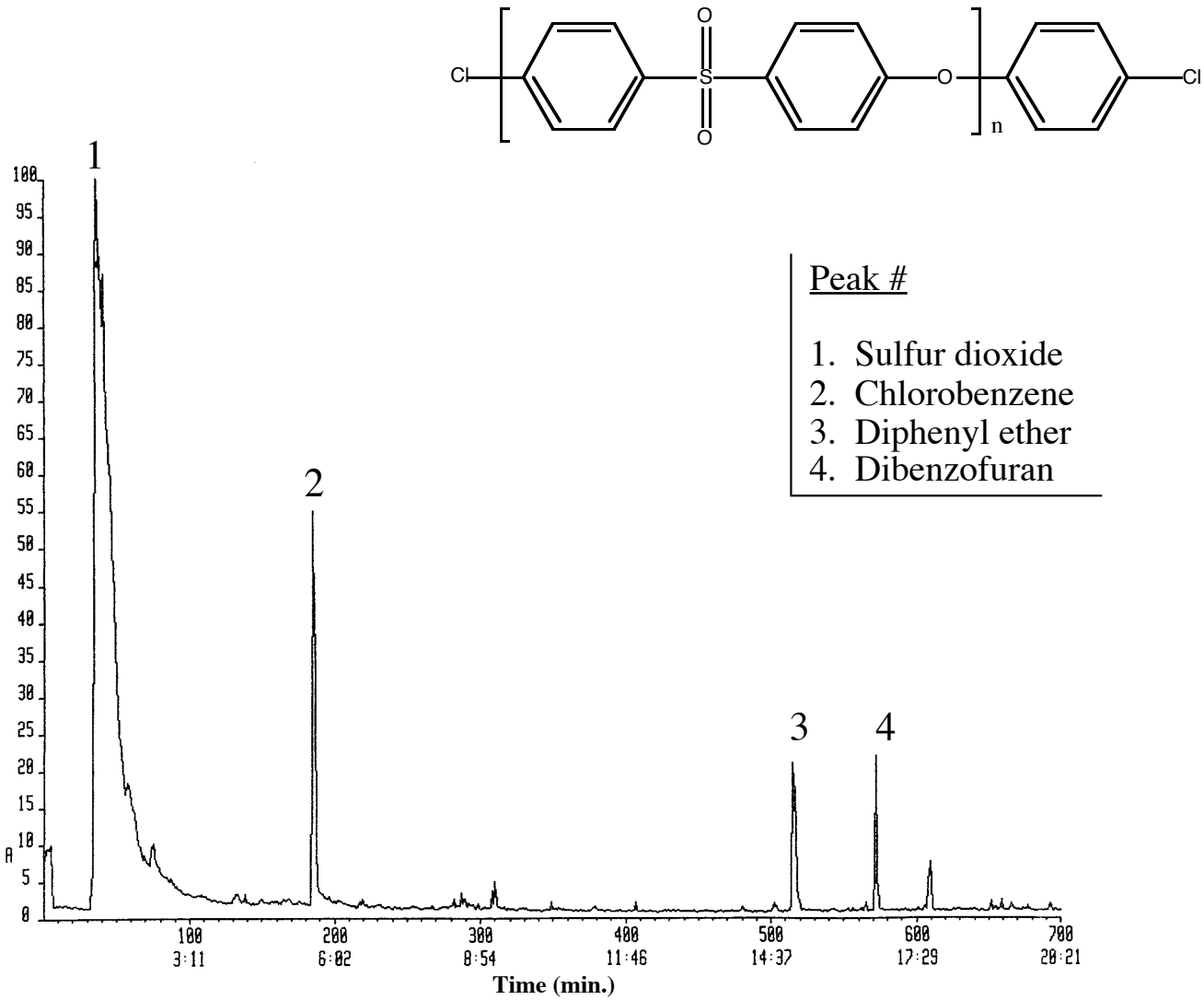

Figure 4.5.1 Gas chromatographic analysis of polyether sulfone (Victrex) degraded at 550°C in a helium atmosphere

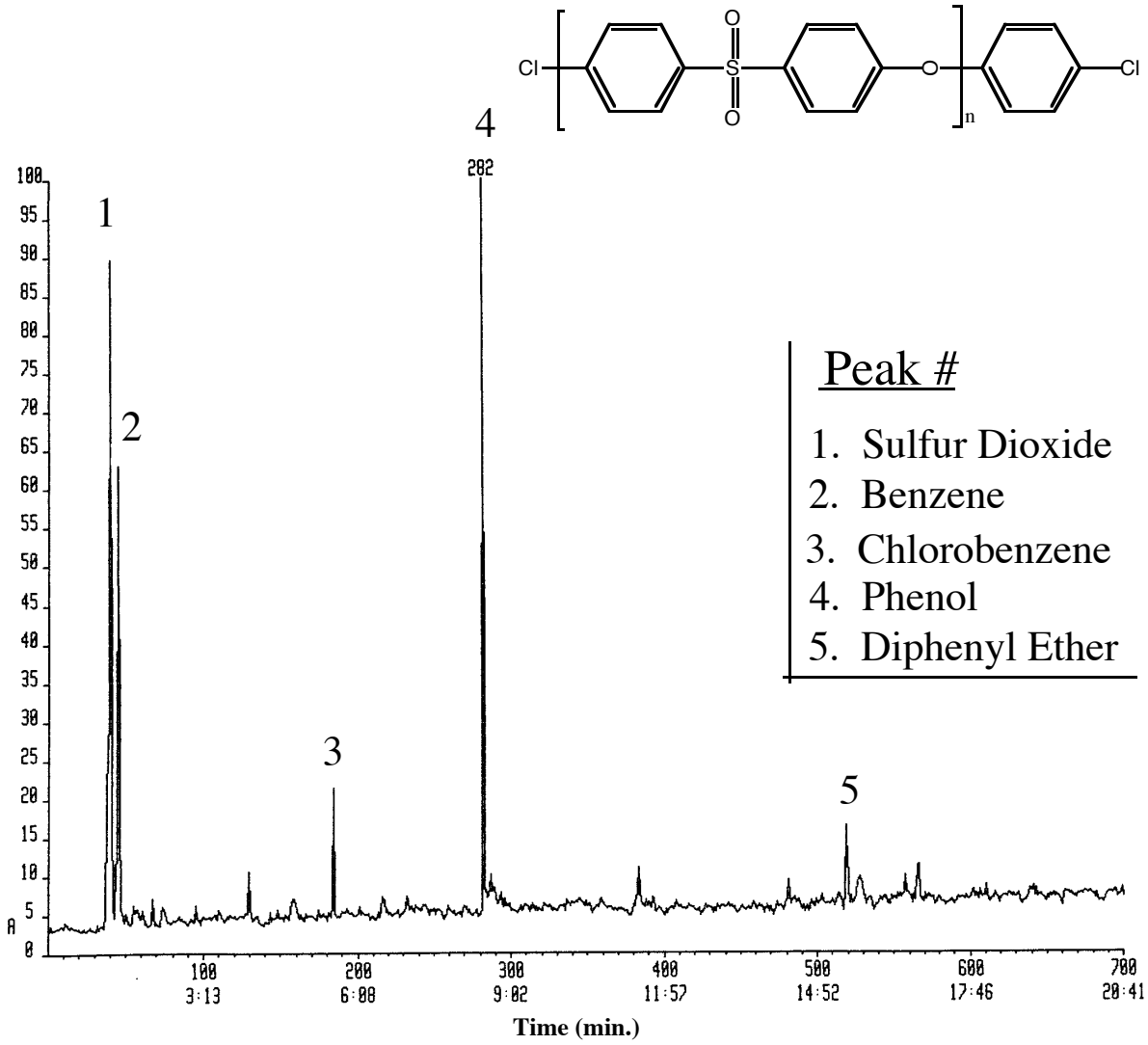

Figure 4.5.2 Gas chromatographic analysis of Victrex degraded at 700°C in a helium atmosphere

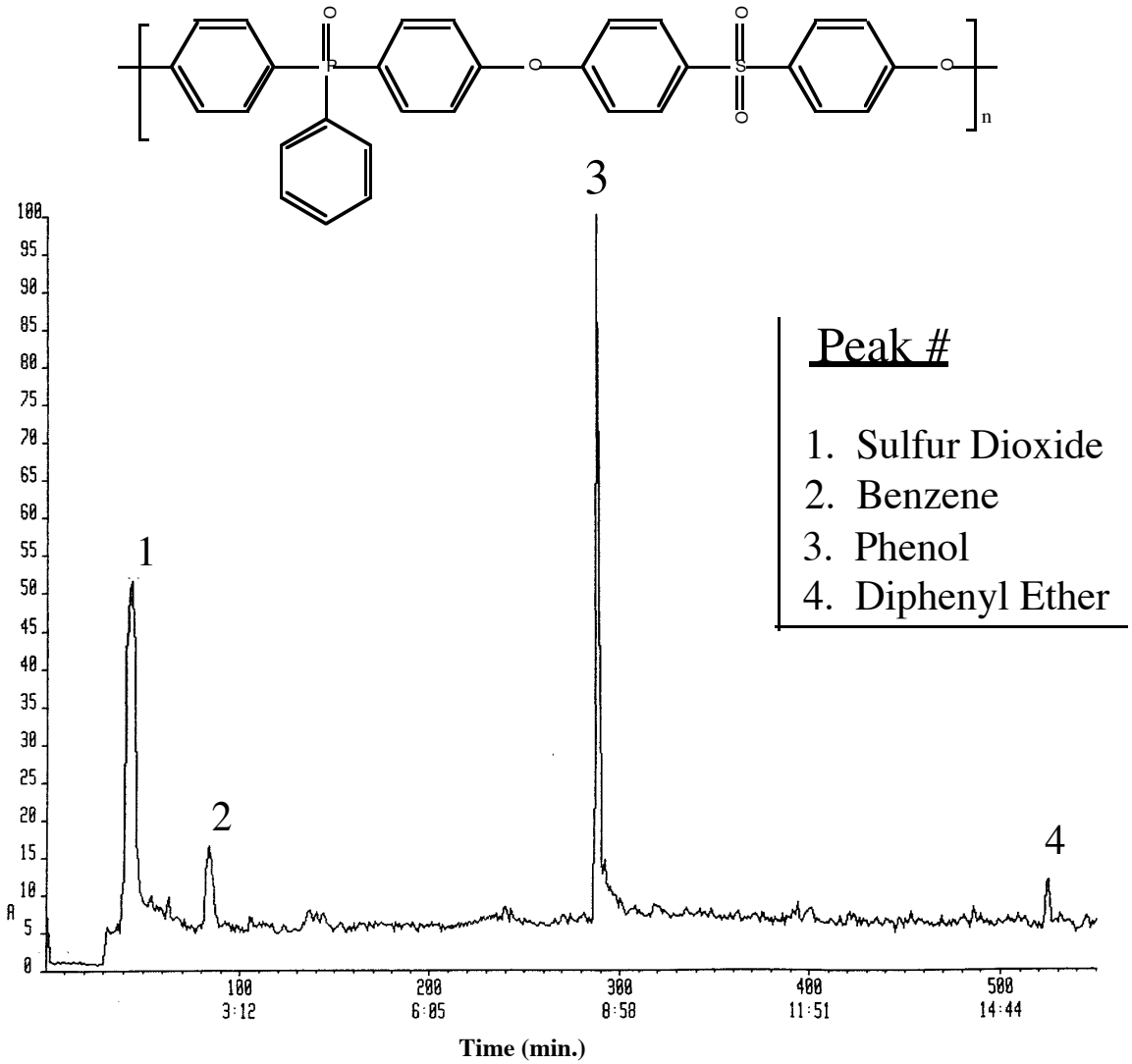

Figure 4.5.3 Gas chromatographic analysis of BFPPO-SO_2 degraded at 550°C in a helium atmosphere

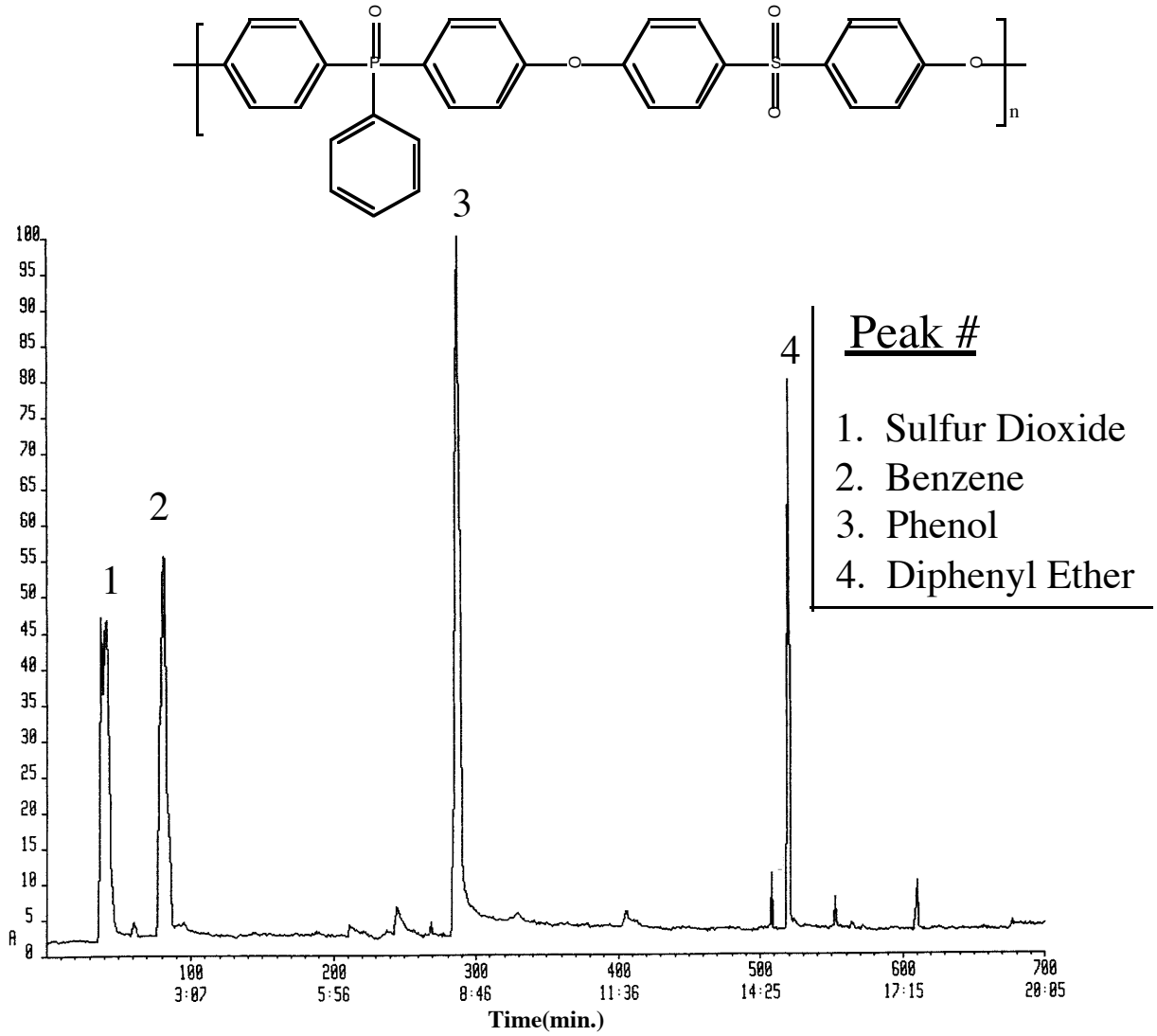

Figure 4.5.4 Gas chromatographic analysis of BFPPO-SO_2 degraded at 700°C in a helium atmosphere

There appears to not be a significant difference between the degradation products of these polymers at 550 and 700°C. By analyzing the byproducts it is possible to deduce how the two polysulfones may have degraded under these specific conditions. For example, at 550°C in helium Victrex produced the following volatiles; phenol, SO_2, chlorobenzene, diphenylether, and dibenzofuran. Figure 4.5.5 shows a possible route how these volatile degradation products may be generated from the degradation of Victrex under an inert atmosphere.

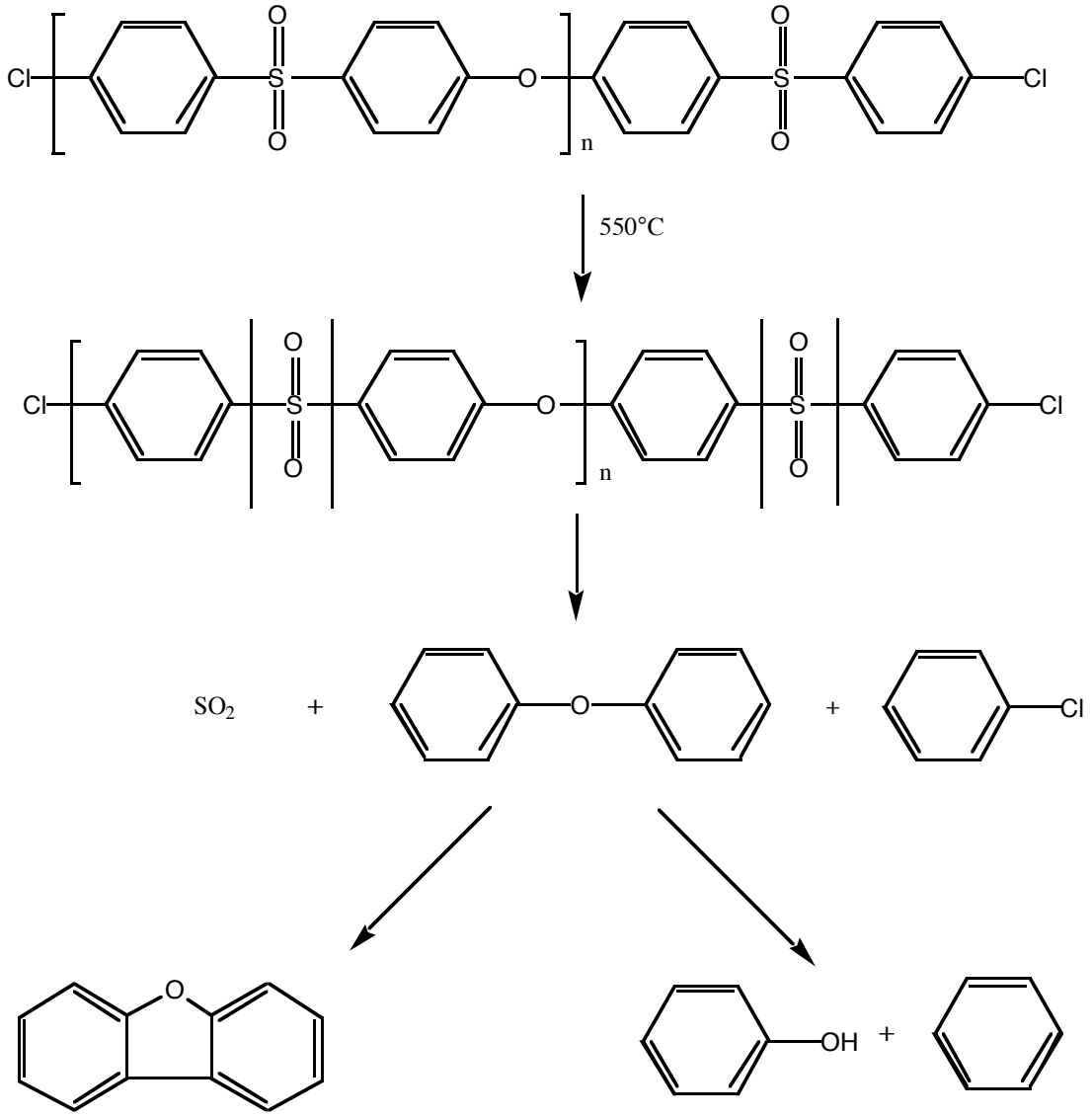

Figure 4.5.5 Schematic of how the volatile degradation products may be generated from the degradation of Victrex poly(ether sulfone).

A similar degradation scheme may be deduced from the volatile degradation products of the poly(arylene ether phosphine oxide sulfone)s. For example, at 700°C in helium BFPPO-SO_2 produced the following volatiles; phenol, SO_2, benzene, and diphenylether. This schematic is shown in Figure 4.5.6 below.

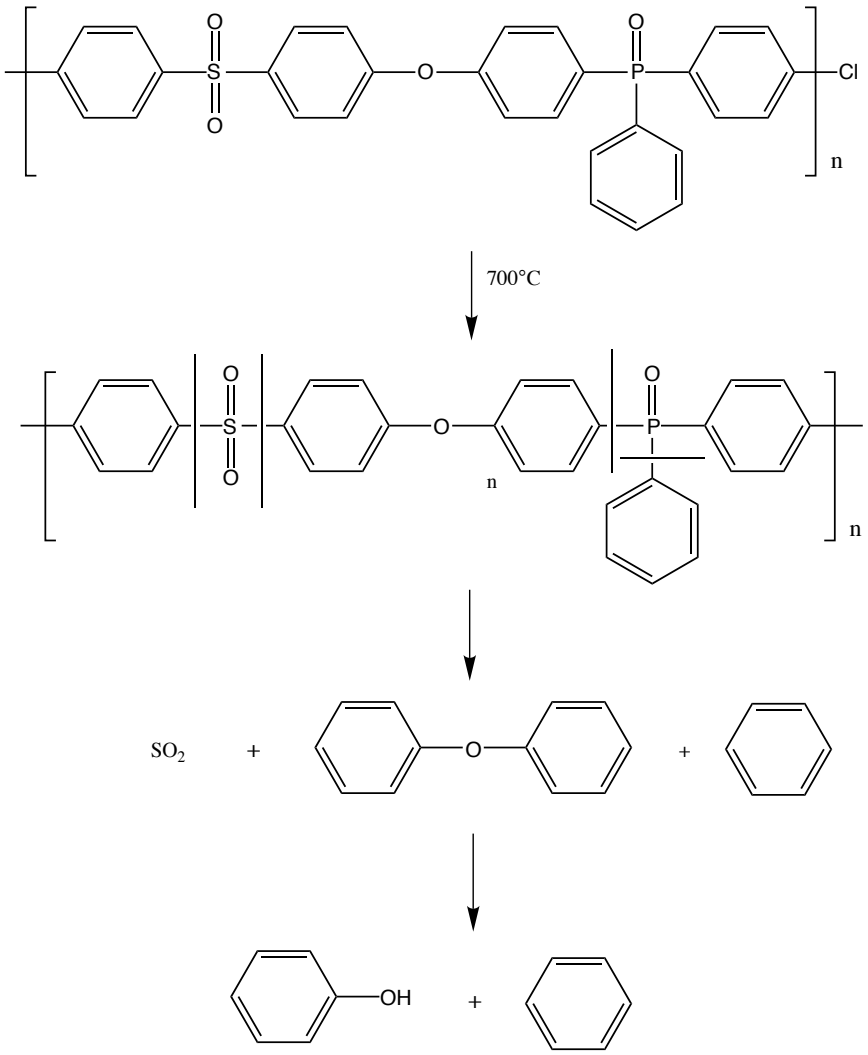

Figure 4.5.6 Schematic of how the volatile degradation products may be generated from the degradation of BFPPO-SO_2.

The degradation pattern of these polymers in an air environment was also analyzed. This provides information about the initial degradation of the polymer in the presence of oxygen. The gas chromatograms of the volatile degradation products of Victrex and BFPPO-SO_2 are shown in Figures 4.5.7-4.5.10 and every major peak was successfully identified.

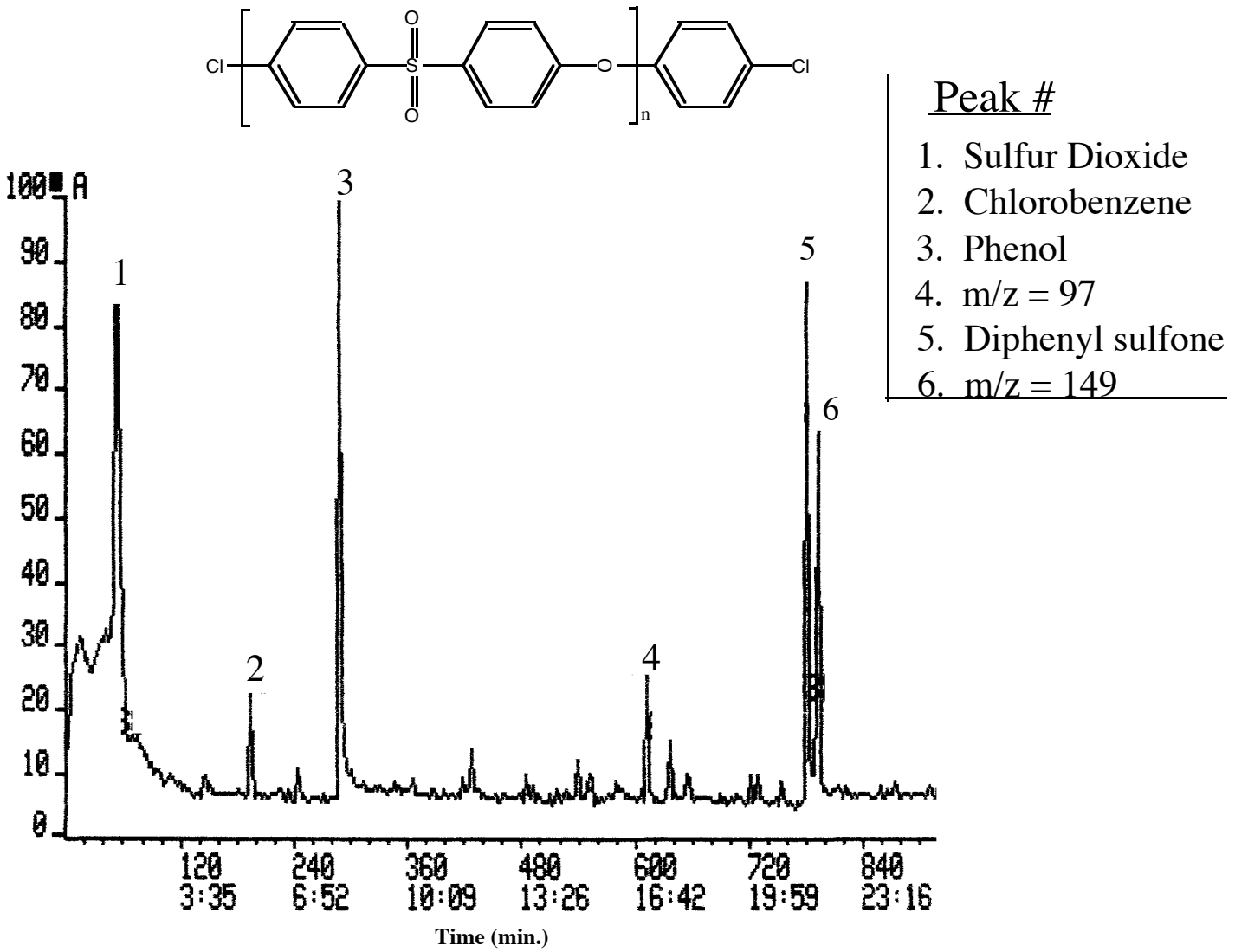

Figure 4.5.7 Gas chromatographic analysis of Victrex degraded at 550°C in an air atmosphere

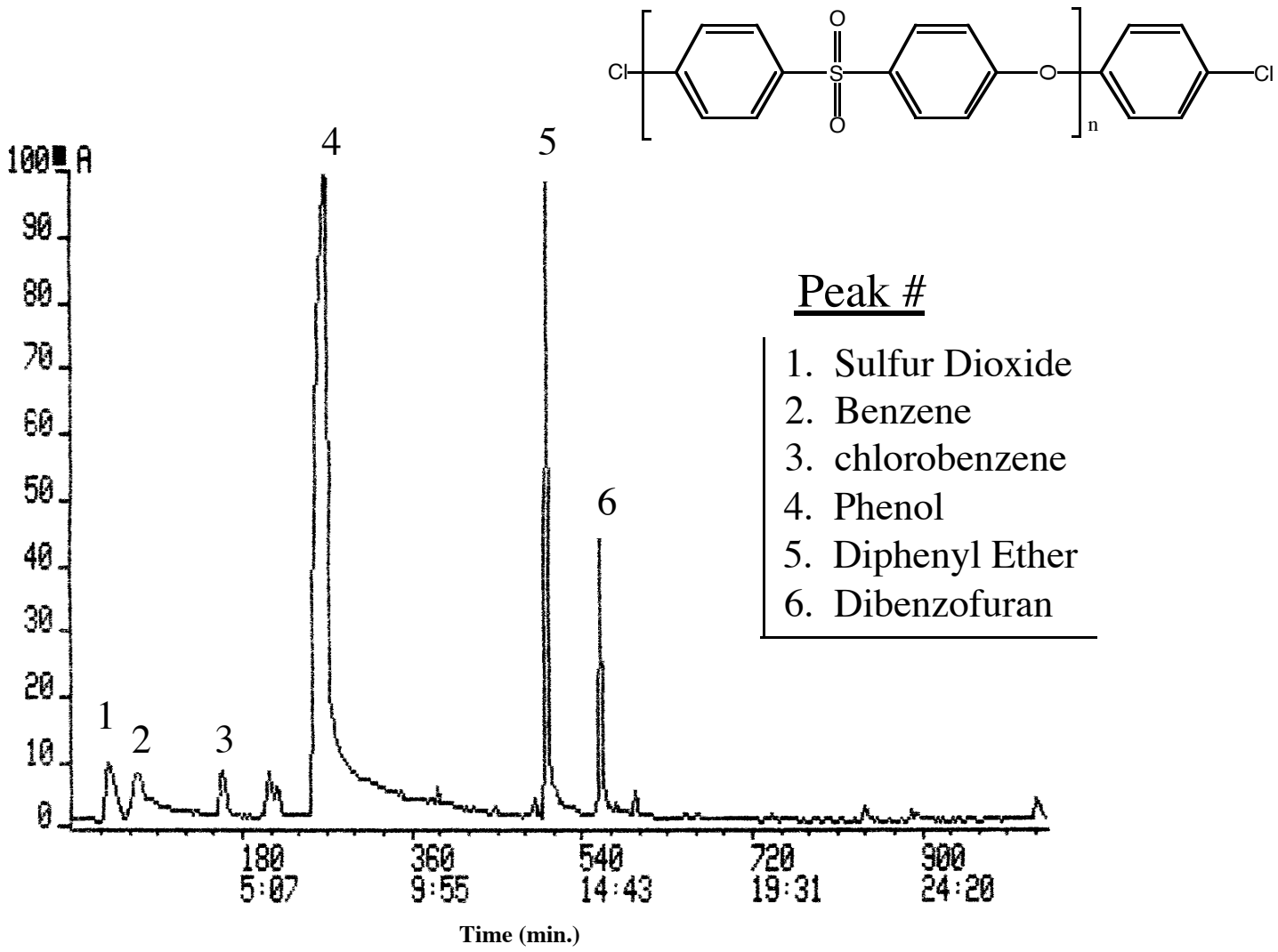

Figure 4.5.8 Gas chromatographic analysis of Victrex degraded at 700°C in an air atmosphere

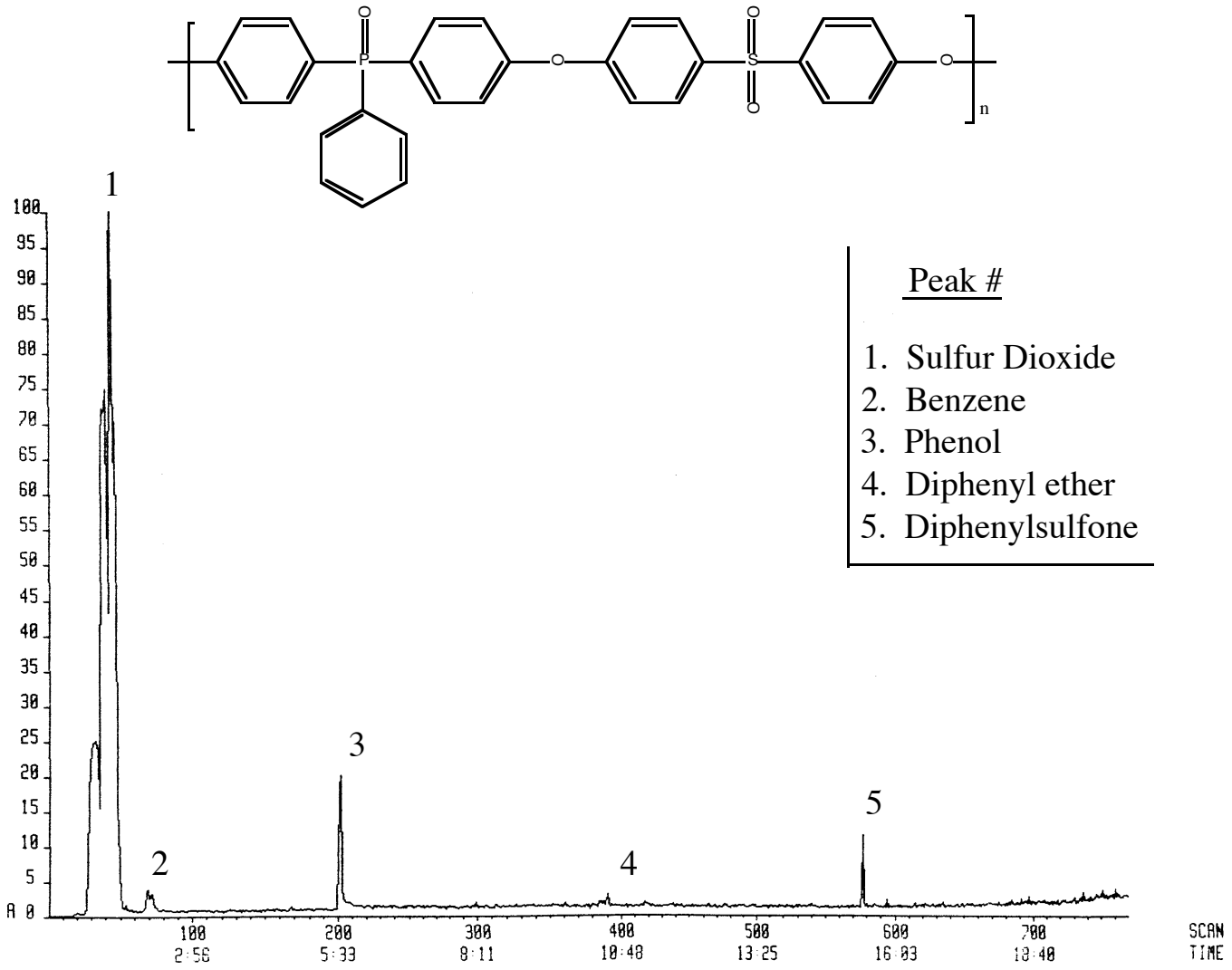

Figure 4.5.9 Gas chromatographic analysis of BFPPO-SO_2 degraded at 550°C in an air atmosphere

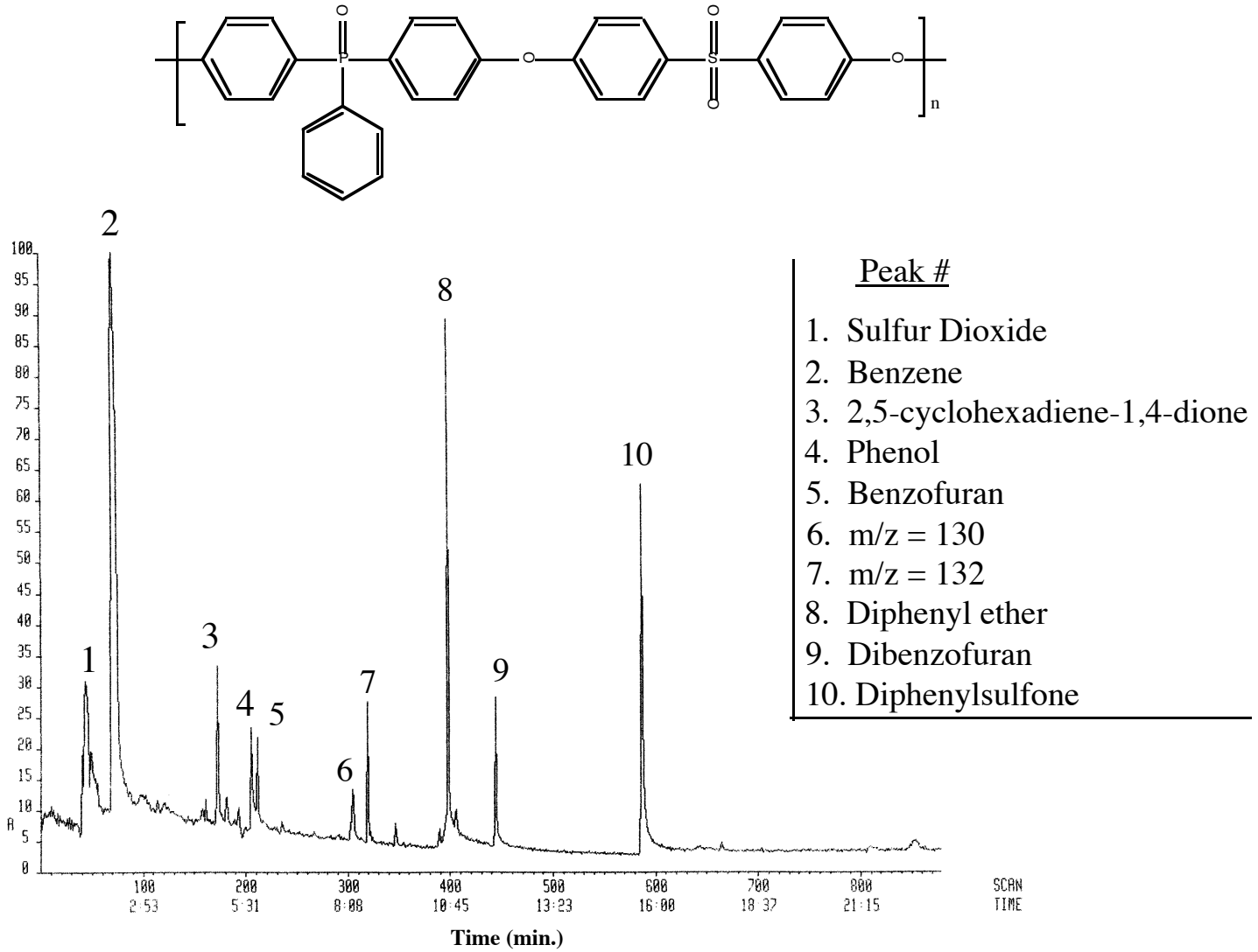

Figure 4.3.10 Gas chromatogram of BFPPO-SO2 degraded at 700°C in an air atmosphere

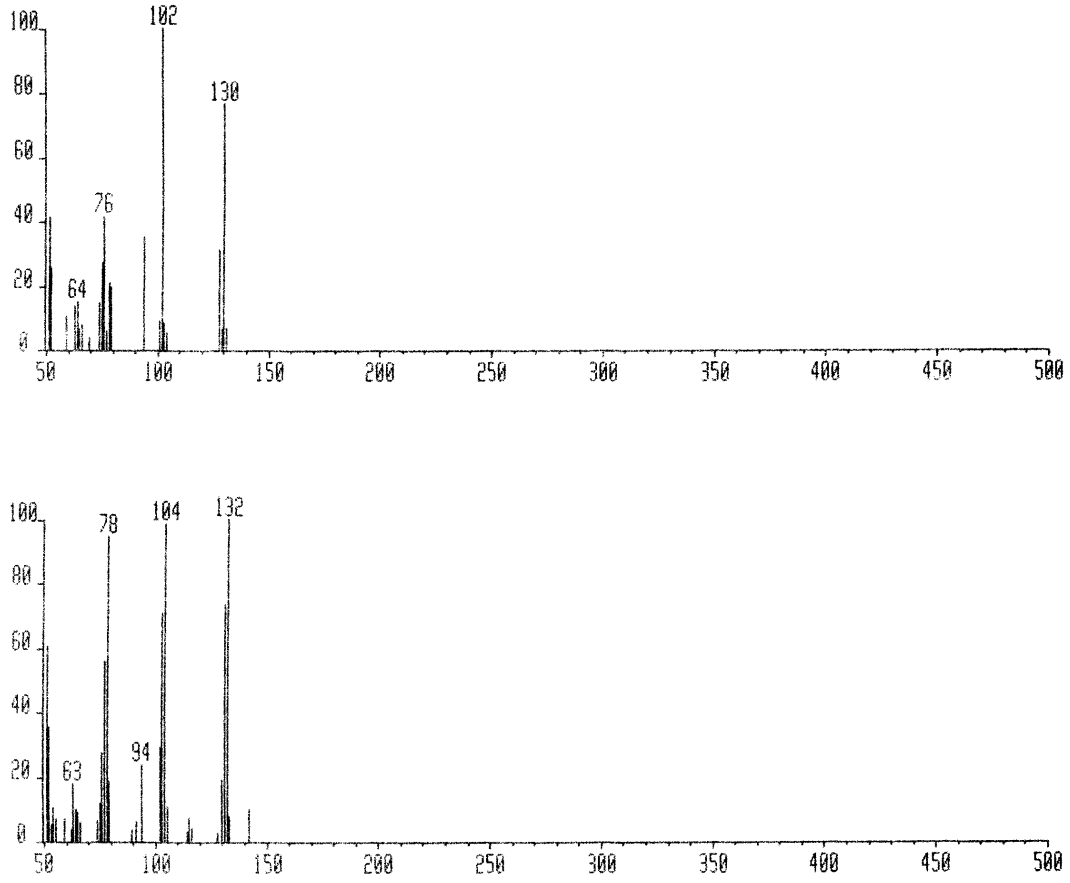

Figure 4.5.11 Mass spectrum of unidentified components in Figure 4.5.10

There appears to not be any significant difference between the initial degradation, of the polysulfones analyzed, due to the presence of oxygen. Therefore, the degradation schemes shown in Figures 4.3.5 and 4.3.6 may also be applicable to these polysulfones degraded in the presence of oxygen. The fact that Victrex does not have a char yield in air at 800°·C (dynamic TGA 10°C min) or isothermally at 550 or 600°C indicates that the polymer completely degrades into volatile byproducts. These volatile byproducts would be expected to further feed an ongoing fire. Whereas if a char is produced not only does the char insulate the underlying polymer from the fire but because of its highly crosslinked network nature does not further volitalize and continue to activate the fire front. It is important to note that there is not any significant amount of a volatile compound containing phosphorus! This also indicates that under these conditions the phosphorus remains in the char indicating a condensed phase mechanism for flame inhibition. In addition, priliminary research *via* ESCA indicates that there is a graphatic layer on the surface of the char for polymers exposed to 550°C for 3 hours. ESCA also shows that this char is also composed of a compound with a binding energy similar to that of P_2O_5. Solid state ^{31}P NMR gives a major peak at O ppm which is further evidence that a type of phosphorus acid structure exists in the char.

4.6 Synthesis of Potential Non-linear Optical Materials Based on Poly(arylene ether phosphonium Ionomers)

Poly(arylene ether)s can be designed to be amorphous, optically clear materials with hydrolytic and thermal stability, as well as good electrical and mechanical properties. As a result, these materials are being investigated for use in second order non-linear optical applications. Materials possessing second order non-linear optics may be used in applications including wave guides, optical switching, sensors, and data storage devices (135, 141-146). Although current polymers have sufficient second order signal (SHG), they are not always practical for device applications because of limitations in the stability of chromophore orientation following electric field poling. Thus, thermal stability of the polymer hosts, including low T_g values, may allow reorientation at temperatures as low as 25°C, where as some commercial applications may require long term stability at temperatures as high as 80-150°C or higher (154).

Polymeric NLO materials are often described as guest-host materials. Thus, the polymer is the host material and the chromophore the guest. Currently, there are two basic types of guest-host NLO systems, for example, the first is where the chromophore is physically blended into the polymeric host (2, 135, 147, 148). The schematic of this system is below in Figure 4.6.1.

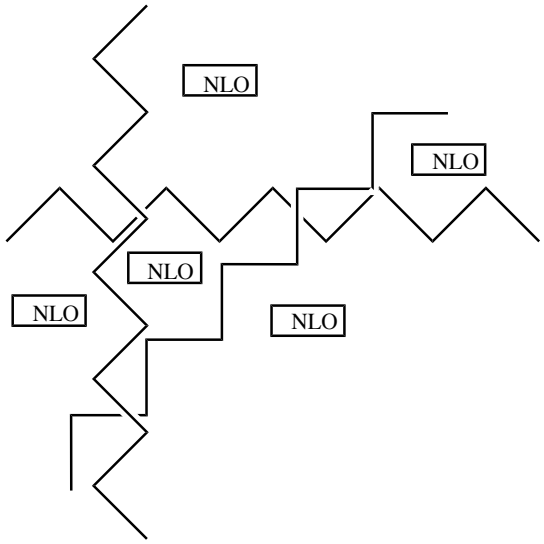

NLO = non-linear optical chromophore

Figure 4.6.1 Schematic of an NLO system where the chromophore is physically blended into a polymeric host.

The chromophores in these systems are usually designed to be miscible with the polymer host, so that macrophase separation does not occur. The advantage of this approach is that it is economical and simple. However, there are limitations related to the concentration of chromophore that can be blended into the polymer host without either macrophase separation or substantial plasticization (T_g reduction). Therefore, much current NLO research has focused on covalently bonding chromophores to the backbone of rigid thermally stable high Tg polymers (154-161). A schematic of these systems is shown below in Figure 4.6.2.

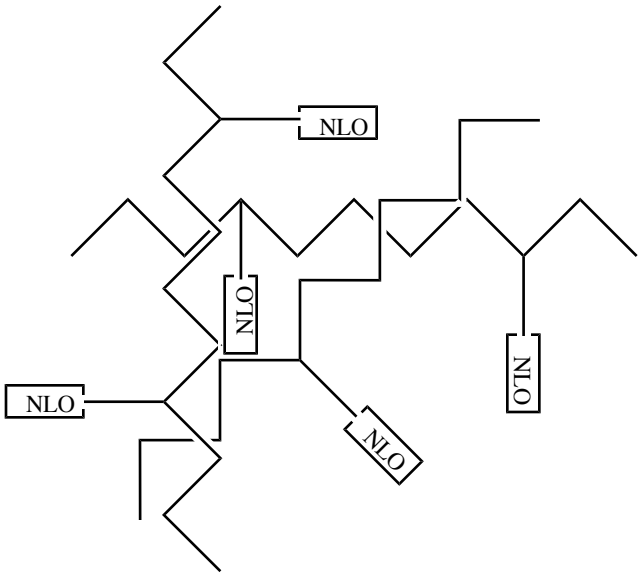

NLO = non-linear optical chromophore

Figure 4.6.2 Schematic of an NLO system where the chromophore is covalently bonded to a polymeric host.

The high T_g and rigid nature of these polymers would be predicted to minimize reorientation of the chromophores orientation after poling. Some of these materials show reasonable SHG stability at 25°C and even 100°C (154). However, the drawback to these high T_g systems is that in order to obtain SHG stability at these temperatures a polymer with a T_g of between 300-350°C is required. It usually follows that chromophores with high $\beta\mu$ values (a measure of the chromophore's ability to generate second harmonics) are not stable at temperatures near the T_g of the high temperature hosts. Consequently, a different approach was initiated in this thesis for the synthesis of high temperature thermally stable polymers for second order non-linear optics. This research focused on the effect of ionically bonding an NLO chromophore to a polymeric backbone upon the physical and optical properties. The schematic of this NLO material is shown below in Figure 4.6.3. Such an approach has not heretofore been proposed or demonstrated in the literature. Very recent work suggests some interest (172).

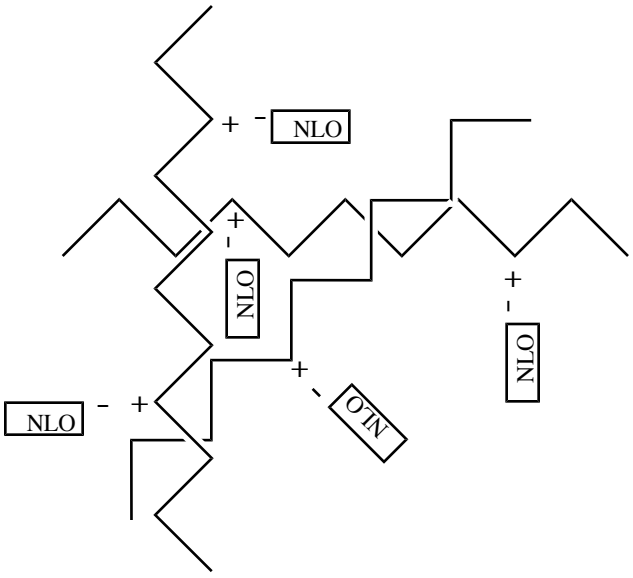

Figure 4.6.3 Schematic of an NLO system where the chromophore is ionically bonded to a polymeric host.

The polymer of choice was a ductile 30 Kg/mole poly(arylene ether phosphine oxide). This polymer produces a tough transparent film which also contains a potentially reactive phosphine oxide moiety. This phosphine oxide functional group can be chemically modified to a phosphonium salt and ion exchange reactions may be employed to subsequently ionically bond a NLO chromophore. This backbone modification and ion exchange reactions are described below.

4.6.1 Synthesis of High Molecular Weight Poly(arylene ether aryl phosphine)

The phosphine oxide moiety of a 30K poly(arylene ether) based on bisphenol-A and BFPPO was successfully reduced using phenylsilane (173, 174). It was possible to control the reaction so that after various reaction times different amounts of the reduced phosphine product were produced. These polymers gave colorless, creasable solvent cast films. The polymer structure was confirmed by ^{1}H and ^{31}P NMR. In the 100% reduced sample only the low field phosphine peak was observed. The NMR spectra are shown in Figures 4.6.1.2 and 4.6.1.3.

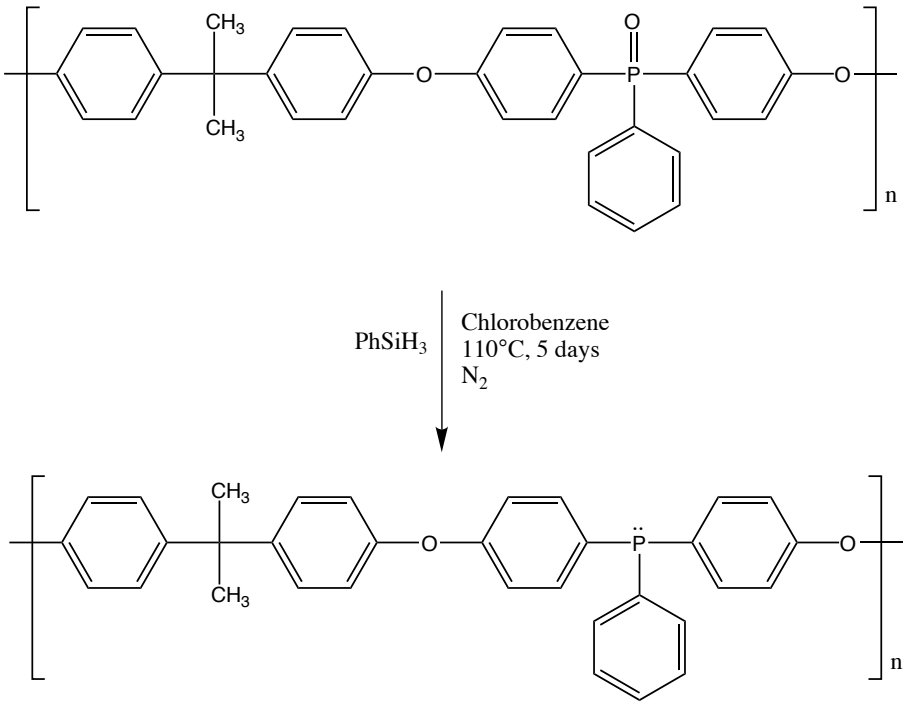

Scheme 4.6.1.1 Synthesis of bisphenol-A based poly(arylene ether aryl phosphine)

The reaction could be followed to completion by analyzing the reaction using ^{31}P NMR. As shown in Figure 4.6.1.3, the ratio of the integration of the phosphine peak/phosphine oxide peak ratio could be used to establish the percent conversion.

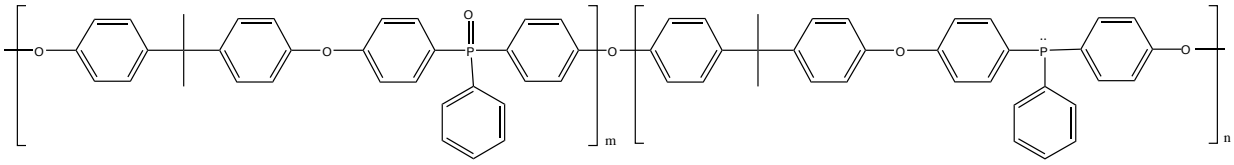

Figure 4.6.1.1 Molecular structure of a partially reduced poly(arylene ether phosphine oxide)

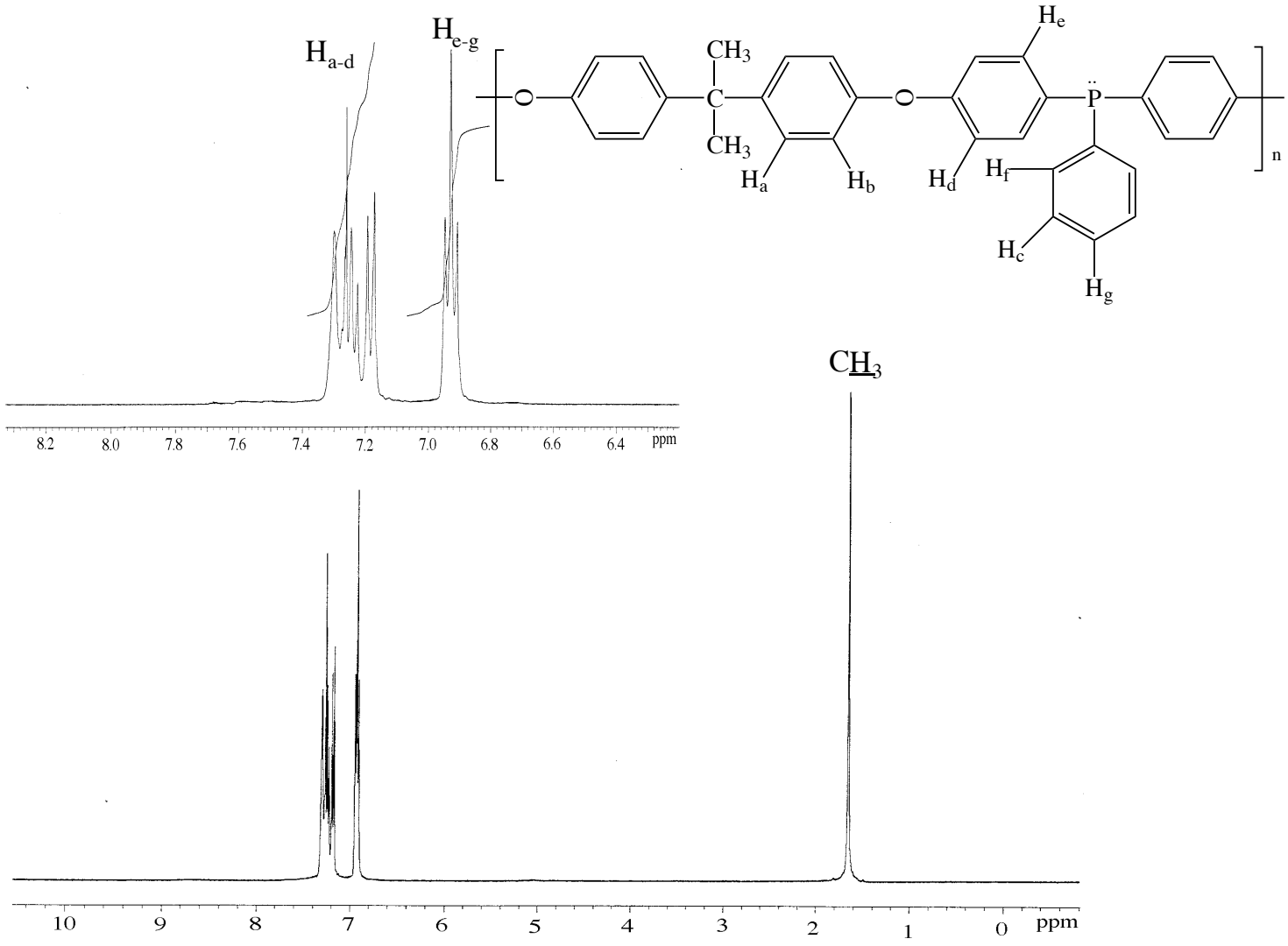

Figure 4.6.1.2 ^{1}H NMR spectrum of bisphenol-A based poly(arylene ether arylphosphine) in $CDCl_3$

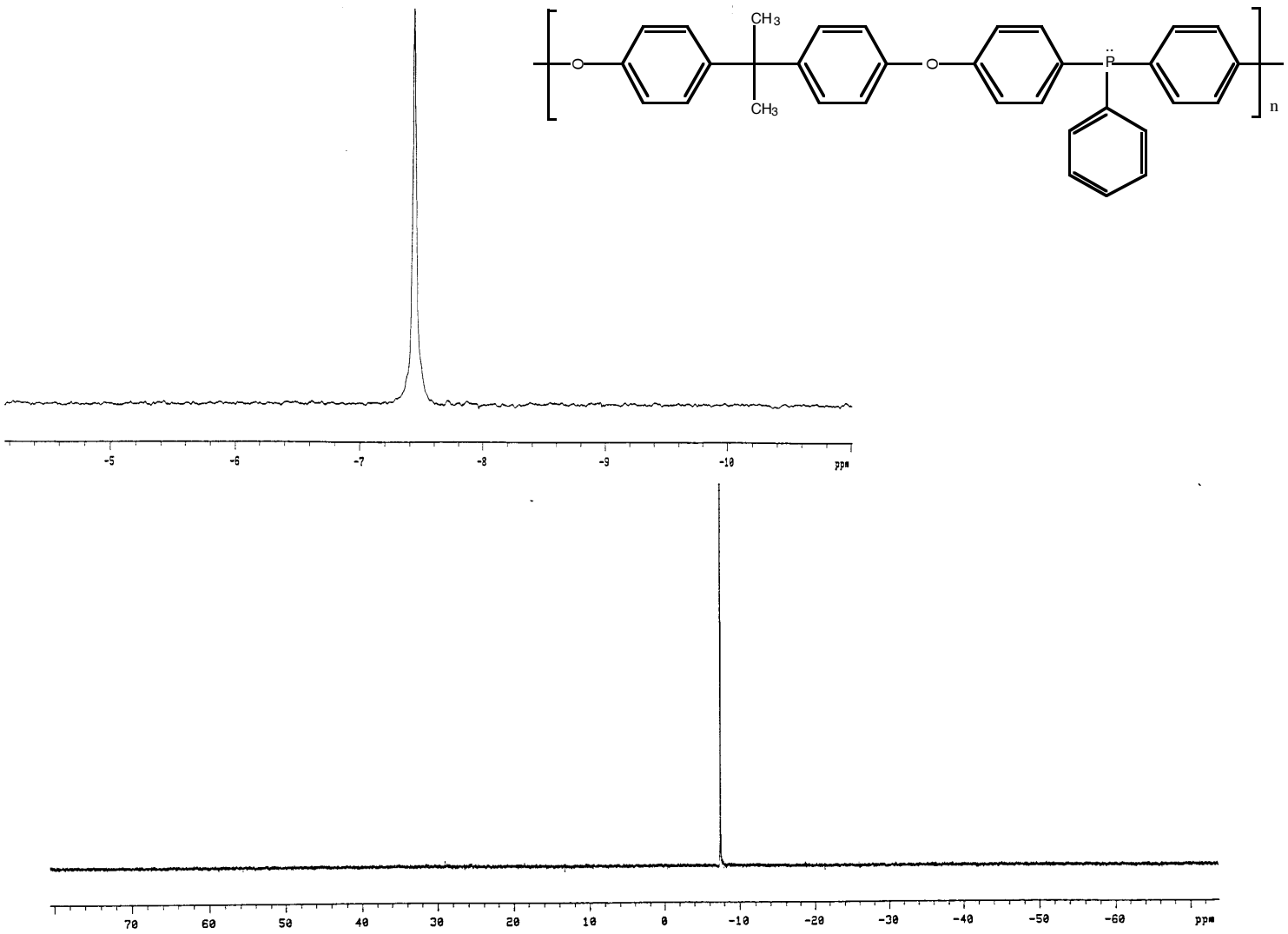

Figure 4.6.1.3 ^{31}P NMR spectrum of bisphenol-A based poly(arylene ether phosphine) in chlorobenzene

4.6.2 Synthesis of Poly(arylene ether phosphonium bromide ionomers)

Poly(arylene ether phosphonium bromide) was synthesized by reacting the poly(arylene ether phosphine) described above with bromobenzene and $NiBr_2$. The reaction was conducted in benzonitrile for 3 hours at 210°C under inert conditions (175). During the work up of the reaction care was taken to ensure all $NiBr_2$ was removed by stirring in warm deionized water for 24 hours. The reaction scheme is shown below in Scheme 4.6.2.1. The polymer structure was confirmed by ^{1}H and ^{31}P NMR and these spectra are shown in Figures 4.6.2.1 and 4.6.2.2. There is a large water peak in the NMR spectrum which is related to the ionic nature of these polymers and difficulties in completely drying the system. In addition, because the poly(arylene ether phosphine) used contained 22% phosphine oxide, the phosphorus NMR shows two peaks, one that corresponds to the phosphonium bromide and another down field that corresponds to the phosphine oxide.

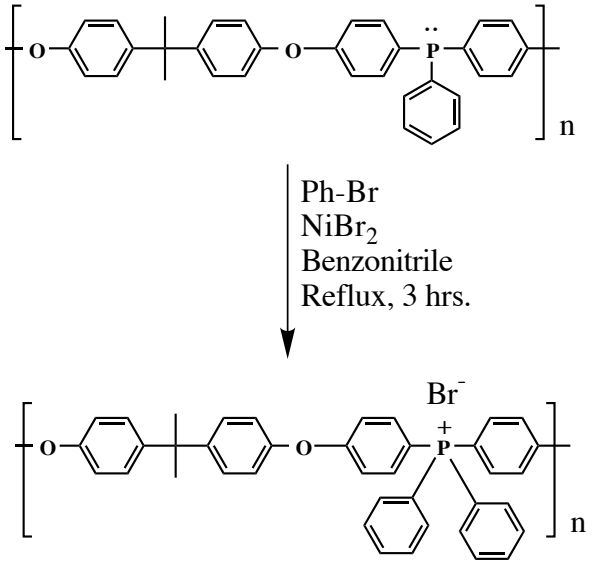

Scheme 4.6.2.1 Synthesis of poly(arylene ether phosphonium bromide)

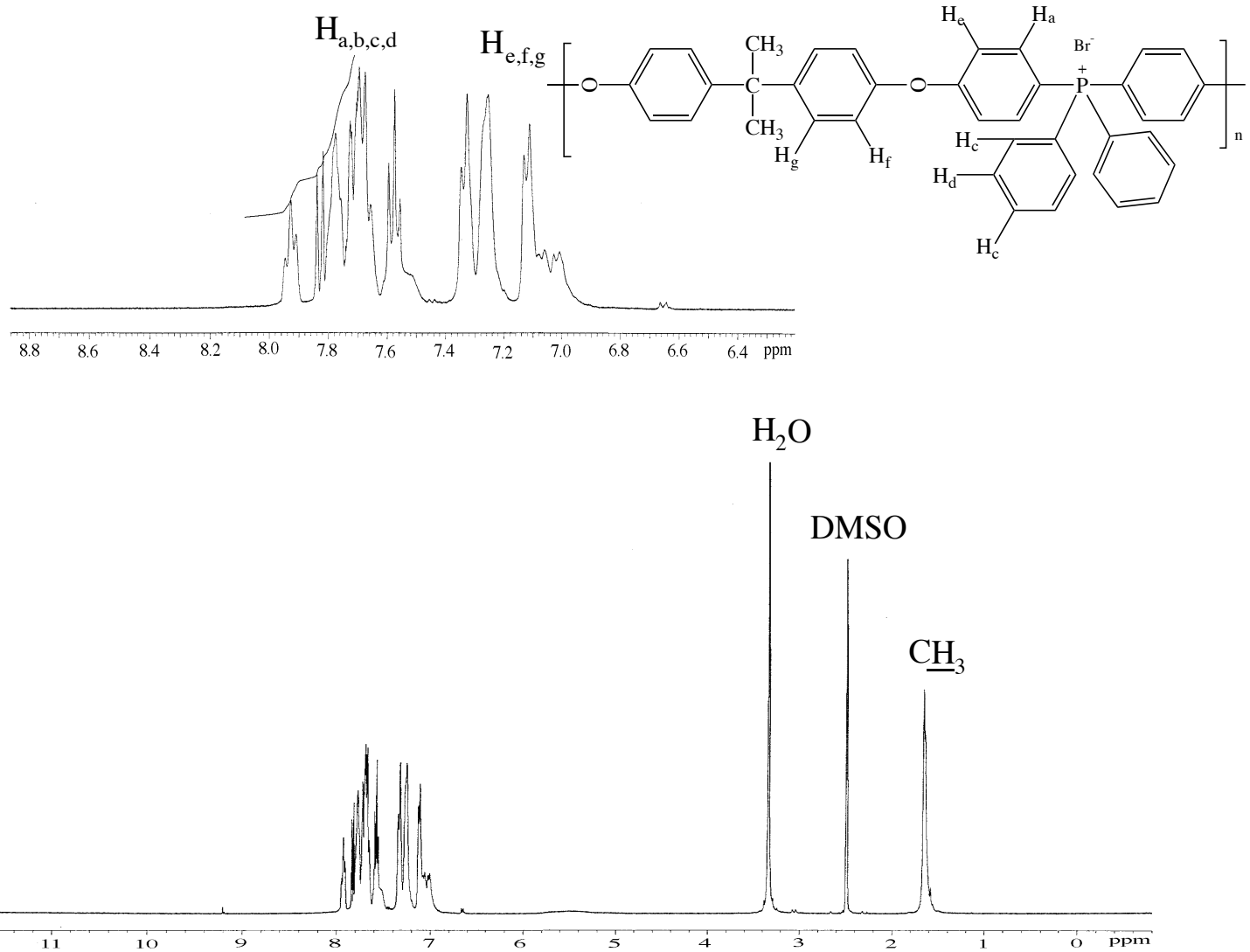

Figure 4.6.2.1 ^{1}H NMR spectrum of bisphenol-A based poly(arylene ether phosphonium bromide) ionomer in DMSO

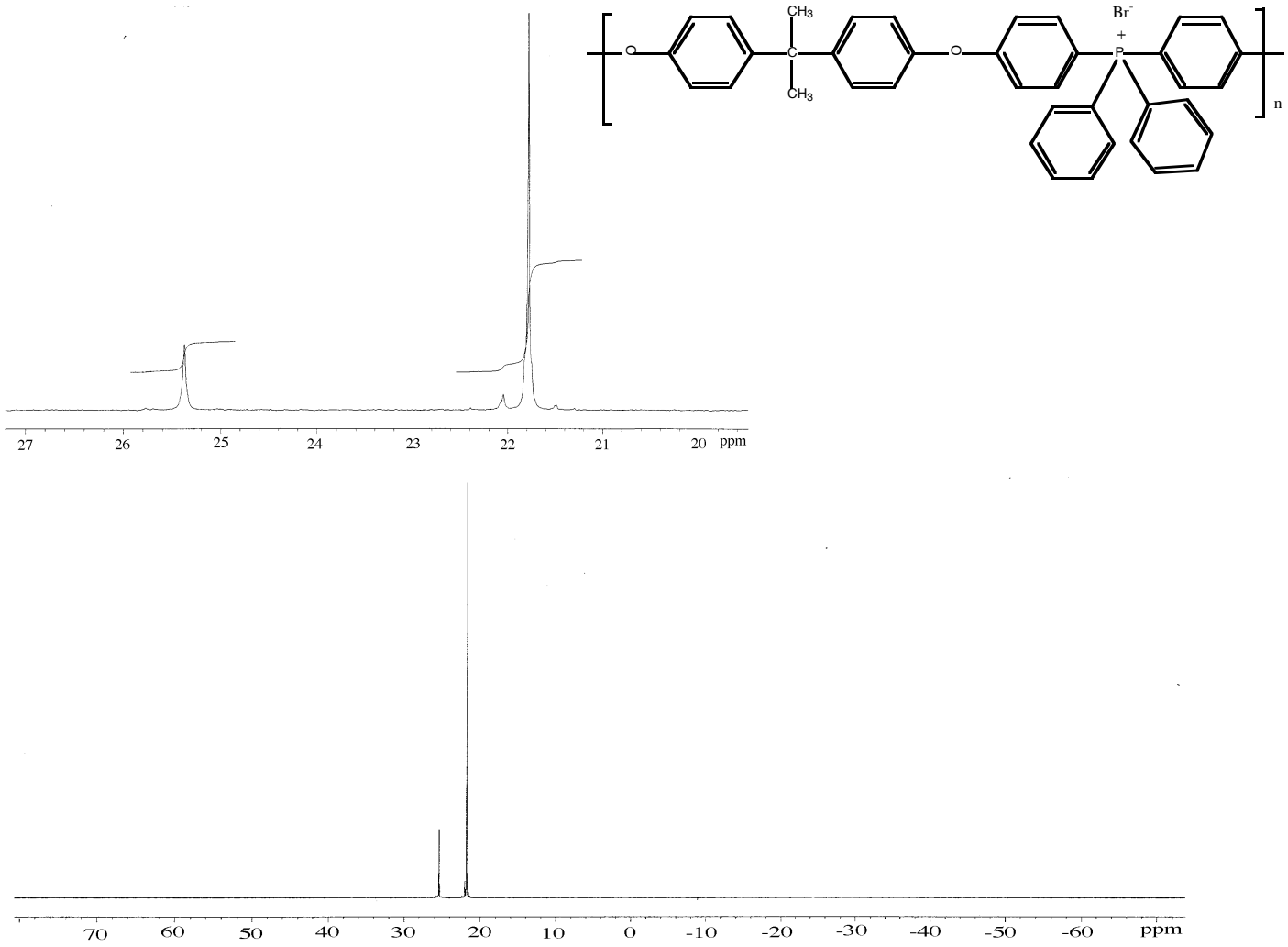

Figure 4.6.2.2 ^{31}P NMR spectrum of bisphenol-A based poly(arylene ether phosphonium bromide) ionomer in benzonitrile

4.6.3 Synthesis of Poly(arylene ether phosphonium) NLO Ionomers

Poly(arylene ether phosphonium bromide) was reacted with 4-[4-(dimethylamino) phenylazo]benzenesulfonic acid, sodium salt (methyl orange) or 4-[4-dimethylaminophenylazo]benzenecarboxylic acid, sodium salt (methyl red) in order to synthesize second order non-linear optical polymers. As shown in Figure 4.6.3.1 the polymeric backbone contained 78% phosphonium bromide and 22% phosphine oxide. This composition was a compromise to avoid the excessively brittle films which were noted when higher amounts of chromophore were utilized. The reaction was conducted at room temperature in DMSO for 1.5 hours and the product was isolated by precipitation into deionized water. This reaction is essentially an ion exchange process and the reaction is highly favored to the right. Equimolar amounts of the basic phosphonium and methyl orange or methyl red were added to the reaction and the product contained quantitative amounts of chromophore after purification by stirring in excess water. The reaction was monitored using ^{1}H and ^{31}P NMR, as shown in Figures 4.6.3.1 and 4.6.3.2. The ^{31}P NMR signal did not shift with different counterions, but other techniques including extraction and GPC were employed to determine if the chromophore was simply blended in or ionically bonded to the polymeric backbone. The down field peak in the phosphorus NMR of Figure 4.6.3.3 is due to the residual 22% phosphine oxide.

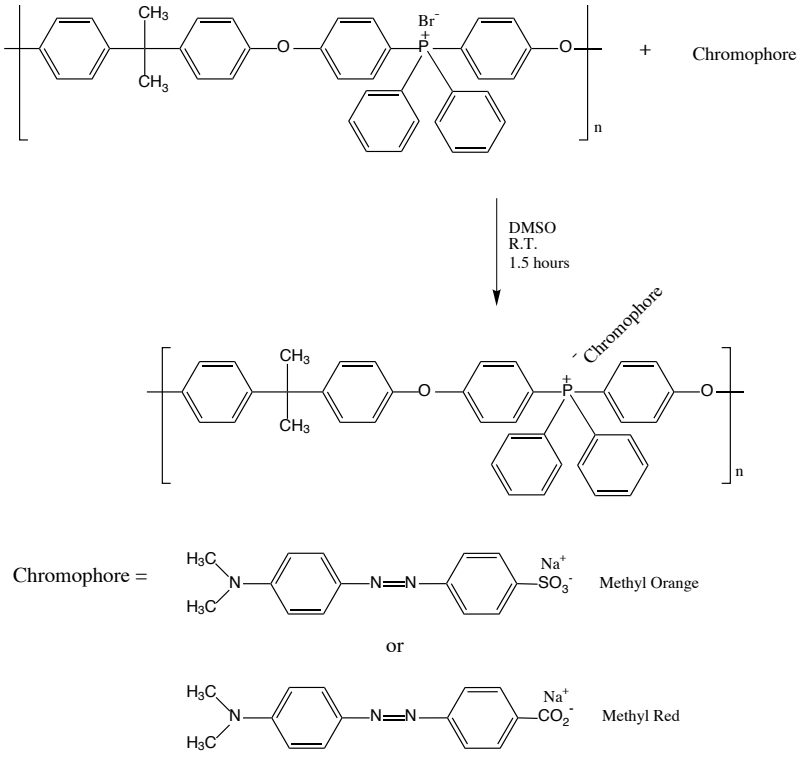

Scheme 4.6.3.1 Synthesis of poly(arylene ether phosphonium) NLO ionomers

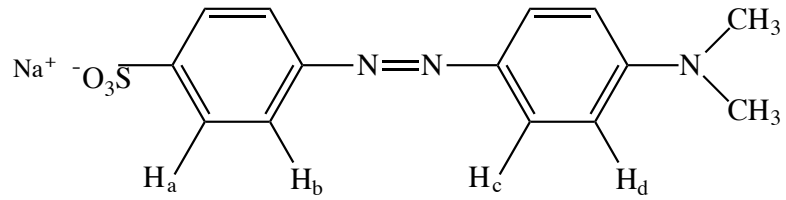

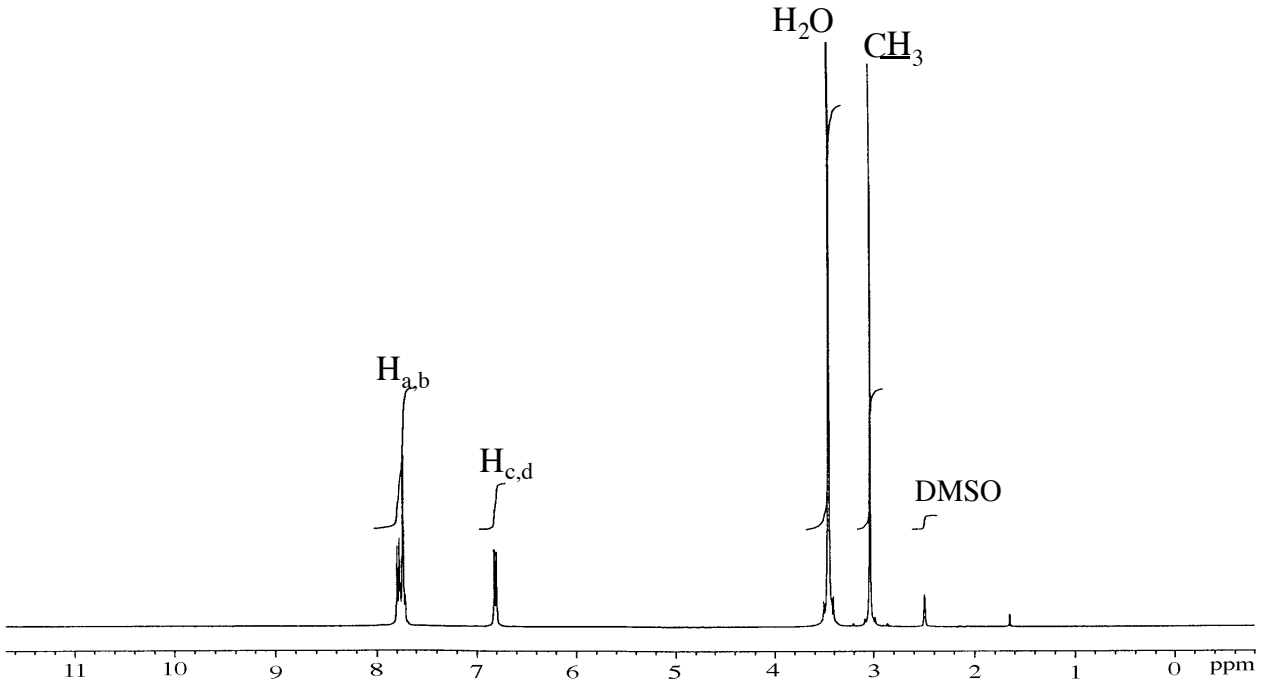

Figure 4.6.3.1 ^{1}H NMR spectrum of methyl orange in DMSO

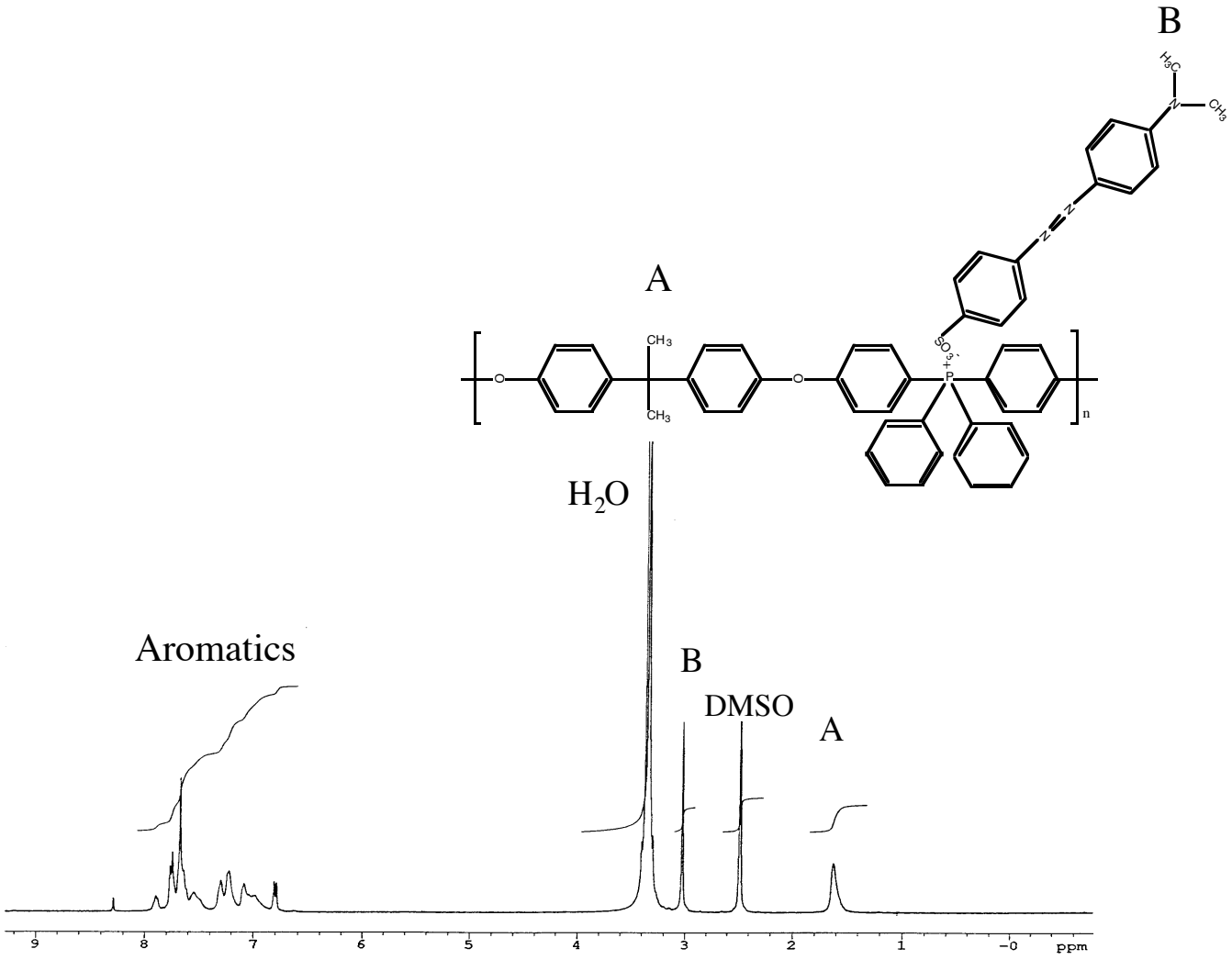

Figure 4.6.3.2 ^{1}H NMR of methyl orange based NLO ionomer material in DMSO

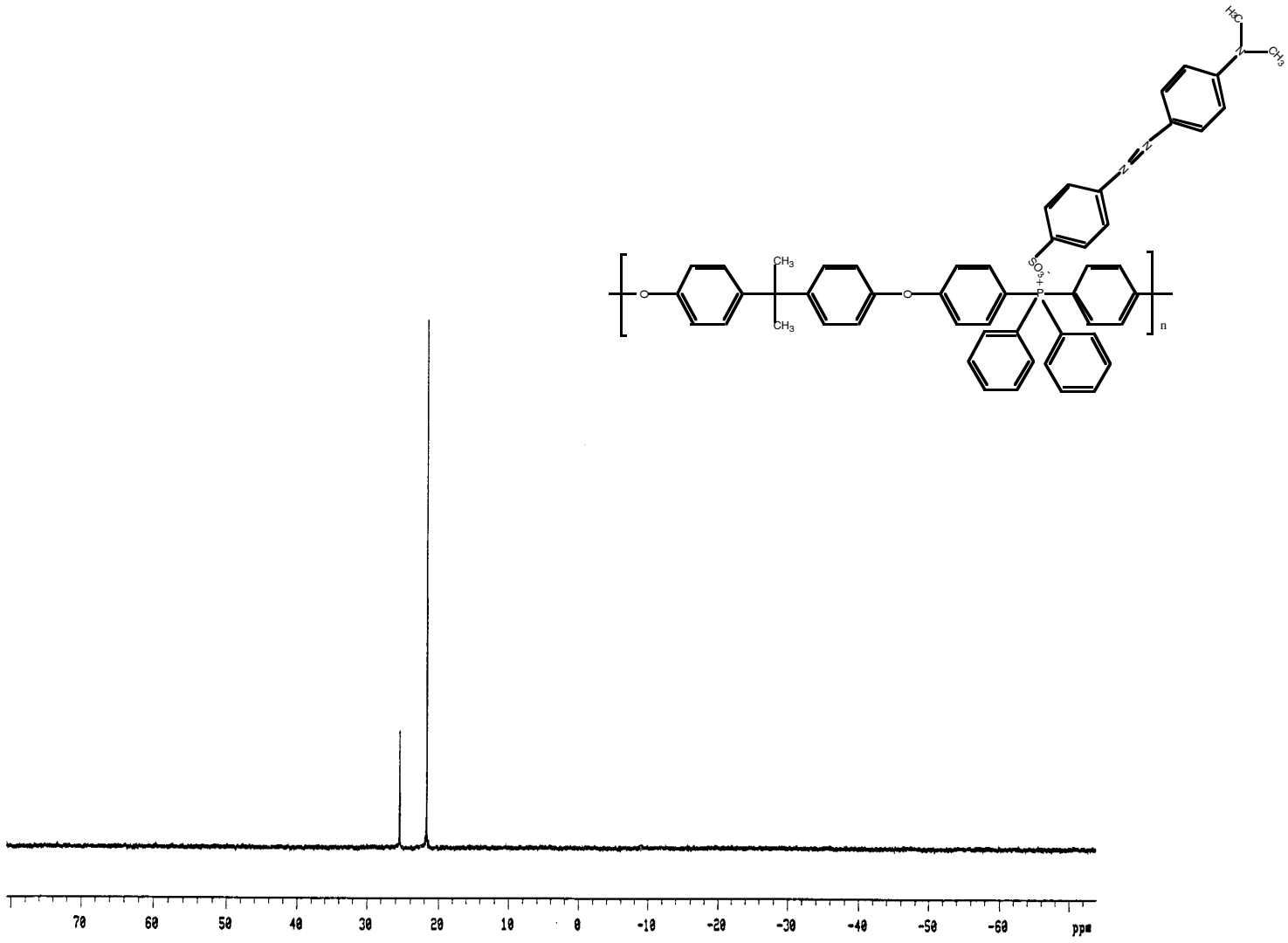

Figure 4.6.3.3 ^{31}P NMR spectrum of methyl orange based NLO ionomer material in DMSO

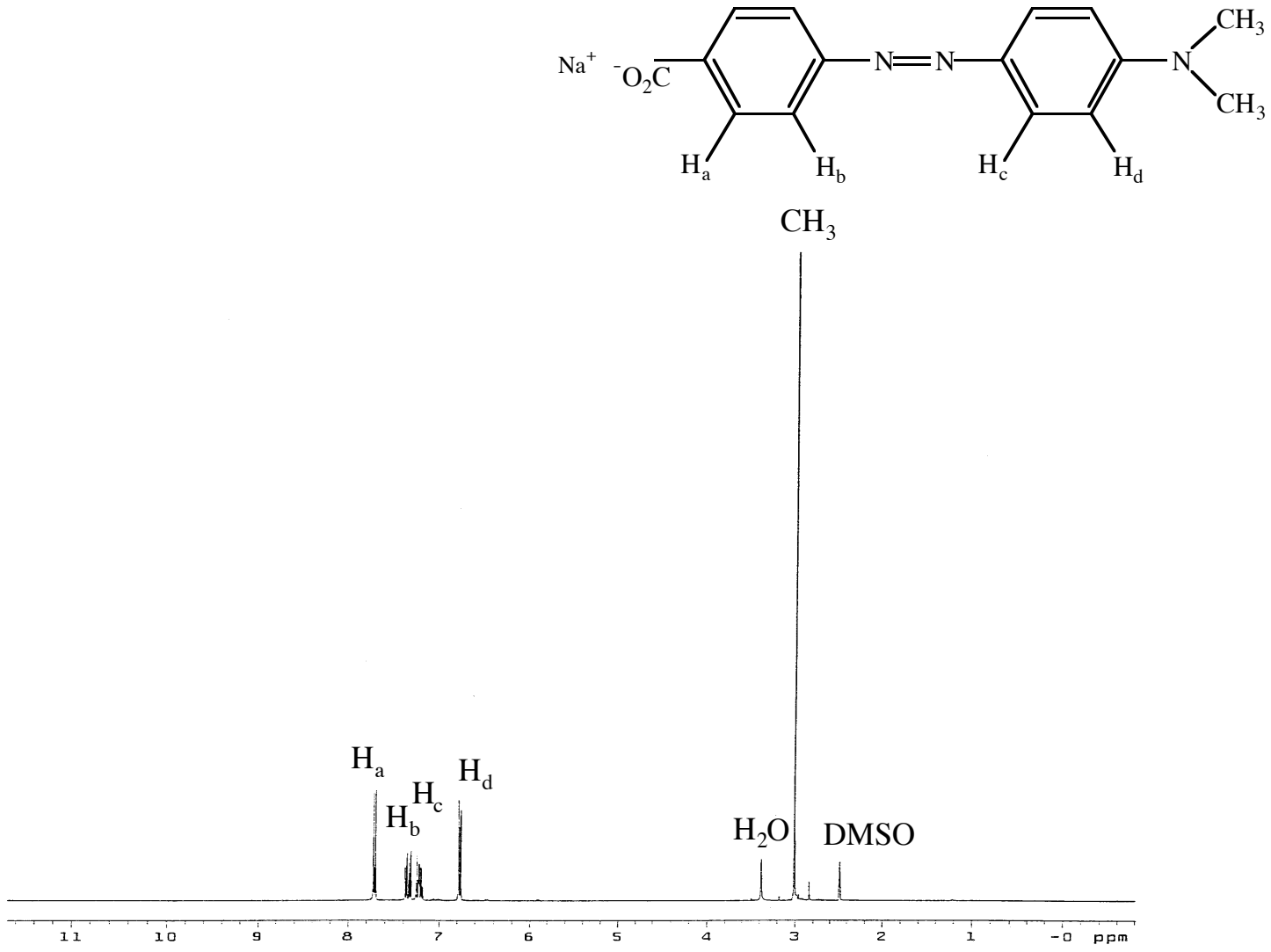

Figure 4.4.3.4 ^{1}H NMR spectrum of methyl red in DMSO

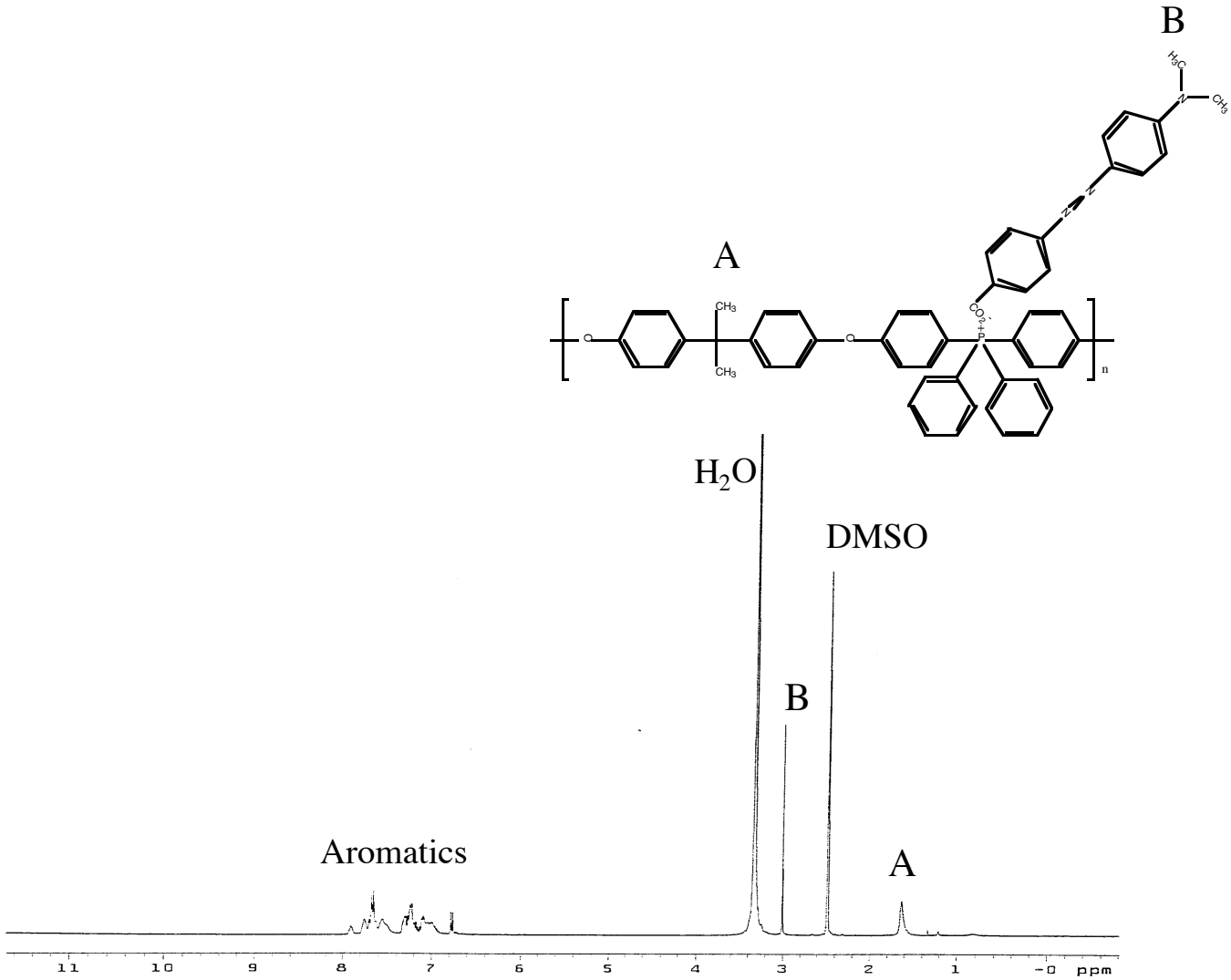

Figure 4.6.3.5 ^{1}H NMR spectrum of methyl red based NLO ionomer material in DMSO

The percent chromophore incorporation could be monitored by ^{1}H NMR. As shown in Figure 4.6.3.6, the integration of the dimethylamino/isopropylidene peak ratio could be used to establish the amount of chromophore incorporation.

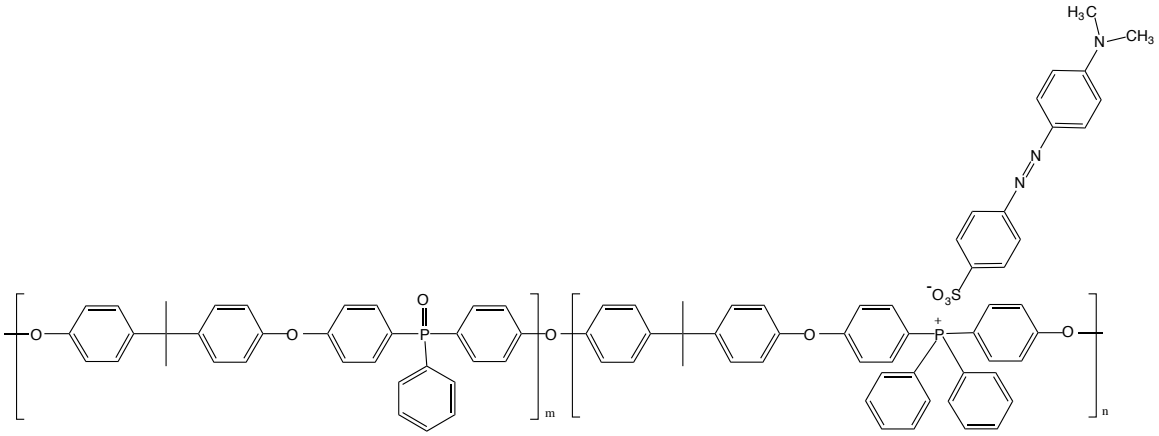

Figure 4.6.3.6 Illustration of how the percent incorporation of chromophore was calculated

The percentage of chromophore incorporated was determined to precisely match the percentage of quartenary phosphorus in the polymeric backbone. This, along with GPC data below indicates that the ion exchange reaction was quantitative as desired.

4.7 Characterization of Modified Poly(arylene ether phosphonium ionomers)

4.7.1 Molecular Weight Analysis of High Molecular Weight NLO Ionomers

GPC was utilized to prove that the chromophore was not just a physical blend but, was rather ionically attached to the polymeric backbone. Table 4.7.1.1 shows the effect of the addition of chromophore on the molecular weight of the polymer.

Table 4.7.1.1 The effect of chromophore side chain addition upon polymeric molecular weight

Polymer	M_n (Kg/mole)	M_w (Kg/mole)
Poly(arylene ether phosphonium bromide	24	52
NLO Polymer with methyl orange as chromophore	31	78

It is concluded that the increase in molecular weight is due to the chromophore being bonded to the backbone of the polymer. The combination of NMR and GPC confirms that the chromophore is bonded to the backbone of the phosphonium polymer.

4.7.2 Thermal Analysis

TGA indicates that while the NLO materials have a lower thermal stability than the phosphonium bromide polymer, it is stable briefly in air to 300°C. Differential scanning calorimetry (DSC) indicates that the polymeric phosphonium bromide and the two different derived NLO systems have the same glass transition at 214°C, which suggests a multiphase, possibly micellar morphology.

Table 4.7.2.1 Effect of side chain NLO chromophore addition on the thermal properties of polymeric phosphonium ionomer cast films

Polymer	TGA(°C)* Initial Wt. loss in air	TGA(°C)* 5% Wt. loss in air	T_g(°C)**
Poly(arylene ether phosphonium bromide	375	437	214
NLO Polymer with methyl orange as chromophore	320	355	214
NLO Polymer with methyl red as chromophore	317	350	214

* Scan rate of 10°C/min
** Determined from second heat rate of 10°C/min

The NLO material degrades at a lower temperature than the base thermoplastic due to the fact that the chromophore is not as thermally stable as the polymer backbone. However, as determined by TGA, these NLO polymers are briefly stable at temperatures in excess of 300°C. It is

speculated that the fact that T_g of the polymeric phosphonium ionomer does not change with the addition of an ionic side chain may indicate that this is a micellar phase separated system. This is being further investigated by x-ray scattering and microscopy.

4.7.3 UV-Visible Absorption of Modified Poly(arylene ether phosphonium salts)

The UV-Visible spectra of these NLO ionomeric materials were also studied to determine if the ionic bonding of the chromophore had an effect on its UV-Vis absorption. The UV-Vis spectra for both the methyl orange and methyl red based NLO material along with the absorption of the chromophore are shown below in Figures 4.7.3.1 and 4.7.3.2 respectively. The data indicates that the methyl orange and methyl red NLO materials, each with 78 mole% chromophore, have maximum absorption in the visible range at 430 and 414 nm respectively. In addition, the polymeric ionomer has a maximum absorption at 270 nm for the methyl orange based NLO material and 264 nm for the methyl red system. Since these polymers are based on the same polymeric backbone, the only difference between the two materials is the ionically bonded chromophore. There is a 2 nm shift in the peak absorption of the methylred based NLO material compared to the control methyl red chromophore. This may be due to steric interactions between the ionically bonded chromophore and the polymeric backbone. Conversly, the fact that there is not a shift in the UV-Vis spectra of methyl orange and methyl orange ionically bonded to the polymeric host indicates that the close association of the chromophore with the polymer does not increase the excitation energy of methyl orange (i.e. possibly due to steric interactions between the chromophore and polymer) in the potential NLO material.

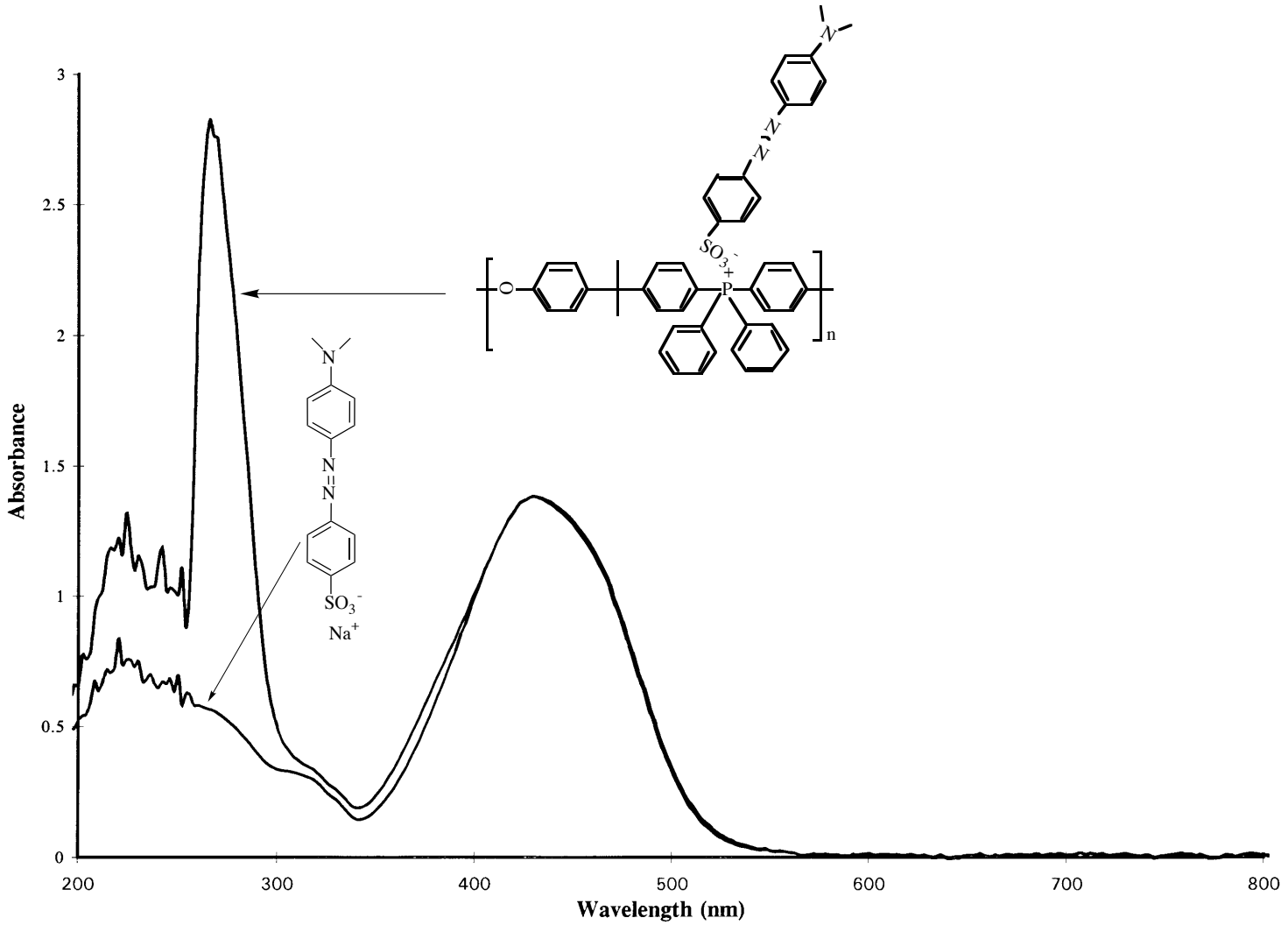

Figure 4.7.3.1 UV-Visible spectra of methyl orange based NLO material

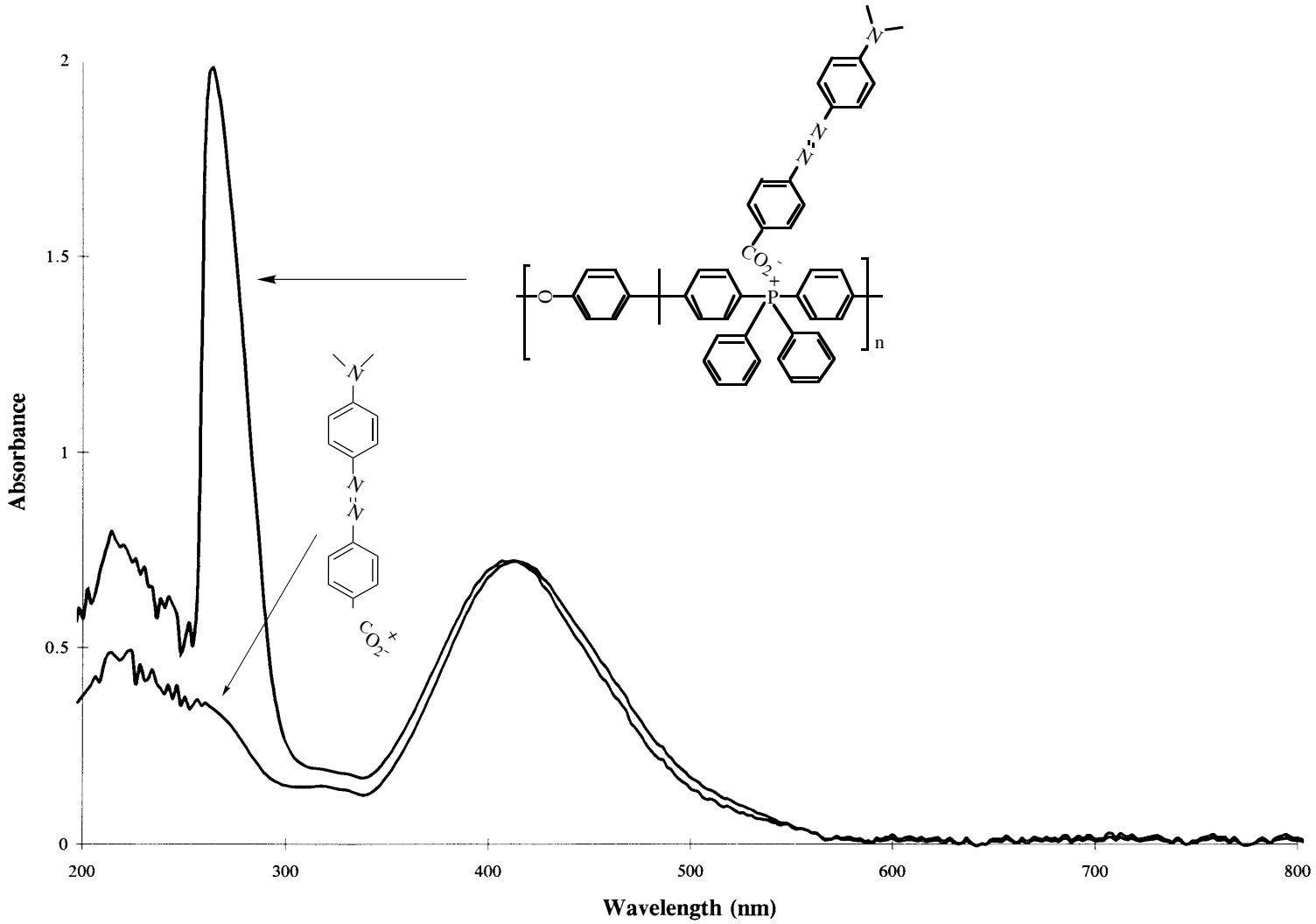

Figure 4.7.3.2 UV-Visible spectra of methyl red based NLO material

4.7.4 Sub-ambient Dielectric Analysis of Poly(arylene ether phosphonium Ionomers)

The dielectric relaxation behavior of the poly(arylene ether phosphonium bromide) and the methyl orange modified poly(arylene ether phosphonium salt) was analyzed to determine if there is a low temperature β transition due to the ionic side chain chromophore. Figure 4.7.4.1 and Figure 4.7.4.2 show the dielectric tan δ versus temperature for the poly(arylene ether phosphonium bromide) thermoplastic. Figure 4.7.4.1 verifies that the single T_g of this material is between 200 and 250°C, depending on the frequency used. These data agrees with that obtained from differential scanning calorimetry. Figure 4.7.4.2 shows the low temperature dielectric behavior of the phosphonium bromide thermoplastic and indicates that this material does not have a low temperature dielectric relaxation. Figure 4.7.4.3 show the low temperature dielectric behavior of the methyl orange modified poly(arylene ether phosphonium salt). These data indicates that only the methyl orange modified poly(arylene ether phosphonium salt) has a low temperature β transition near 0°C. The fact that the starting poly(arylene ether phosphonium bromide) does not have this low temperature relaxation suggests that this low temperature relaxation is probably due to low energy side chain motion.

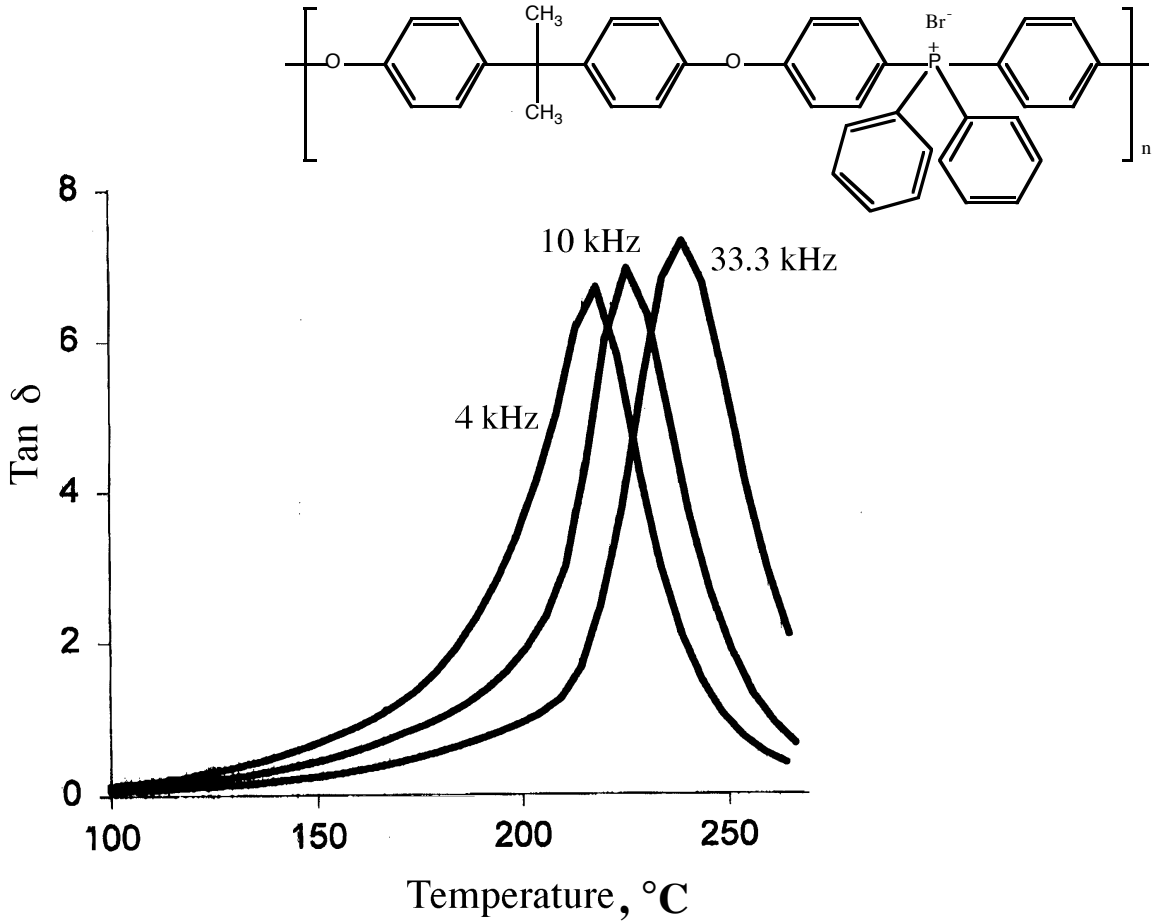

Figure 4.7.4.1 Dielectric analysis of bisphenol-A based poly(arylene ether phosphonium bromide) ionomer

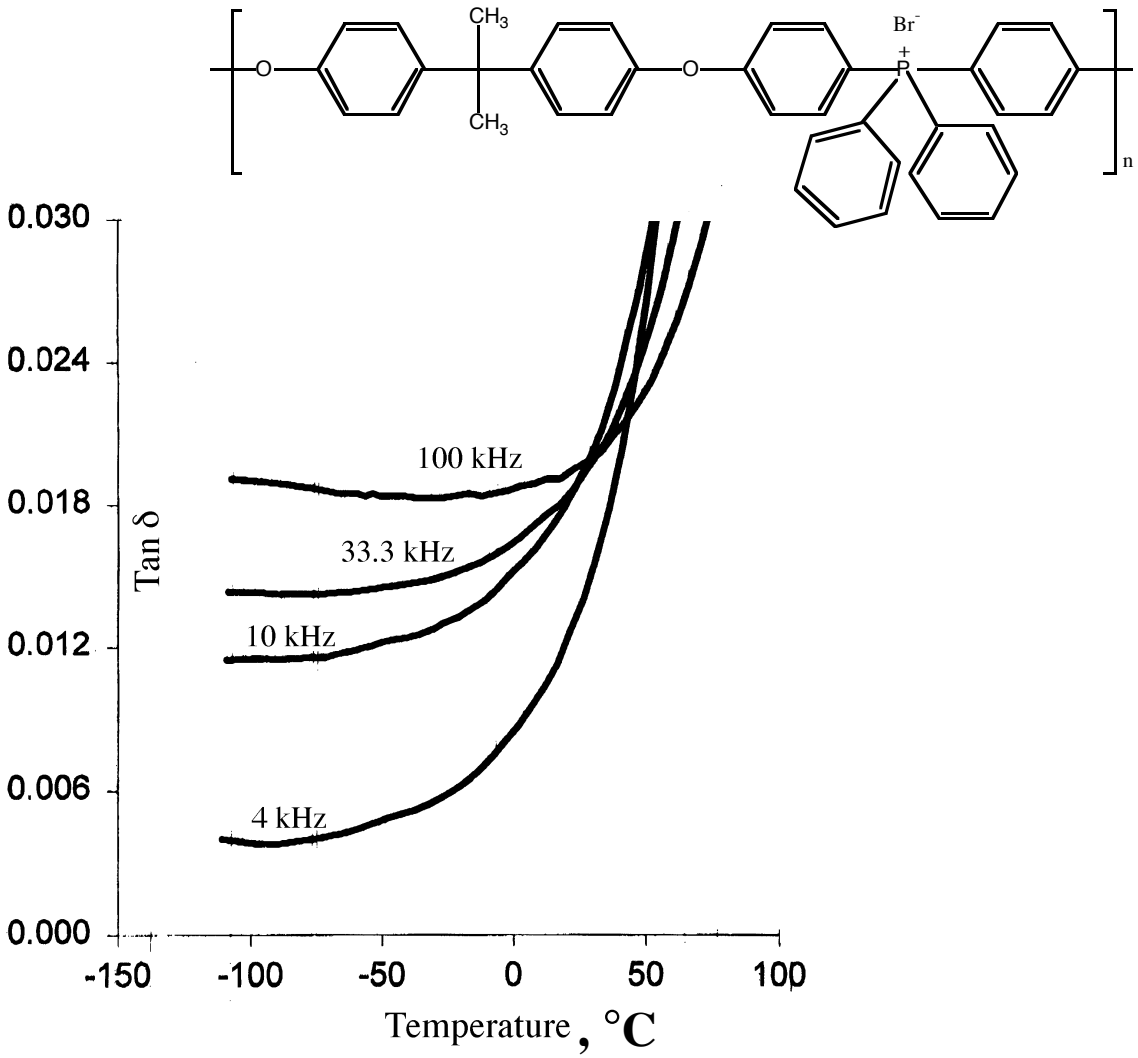

Figure 4.7.4.2 Low temperature dielectric relaxation behavior of bisphenol-A based poly(arylene ether phosphonium bromide) ionomer

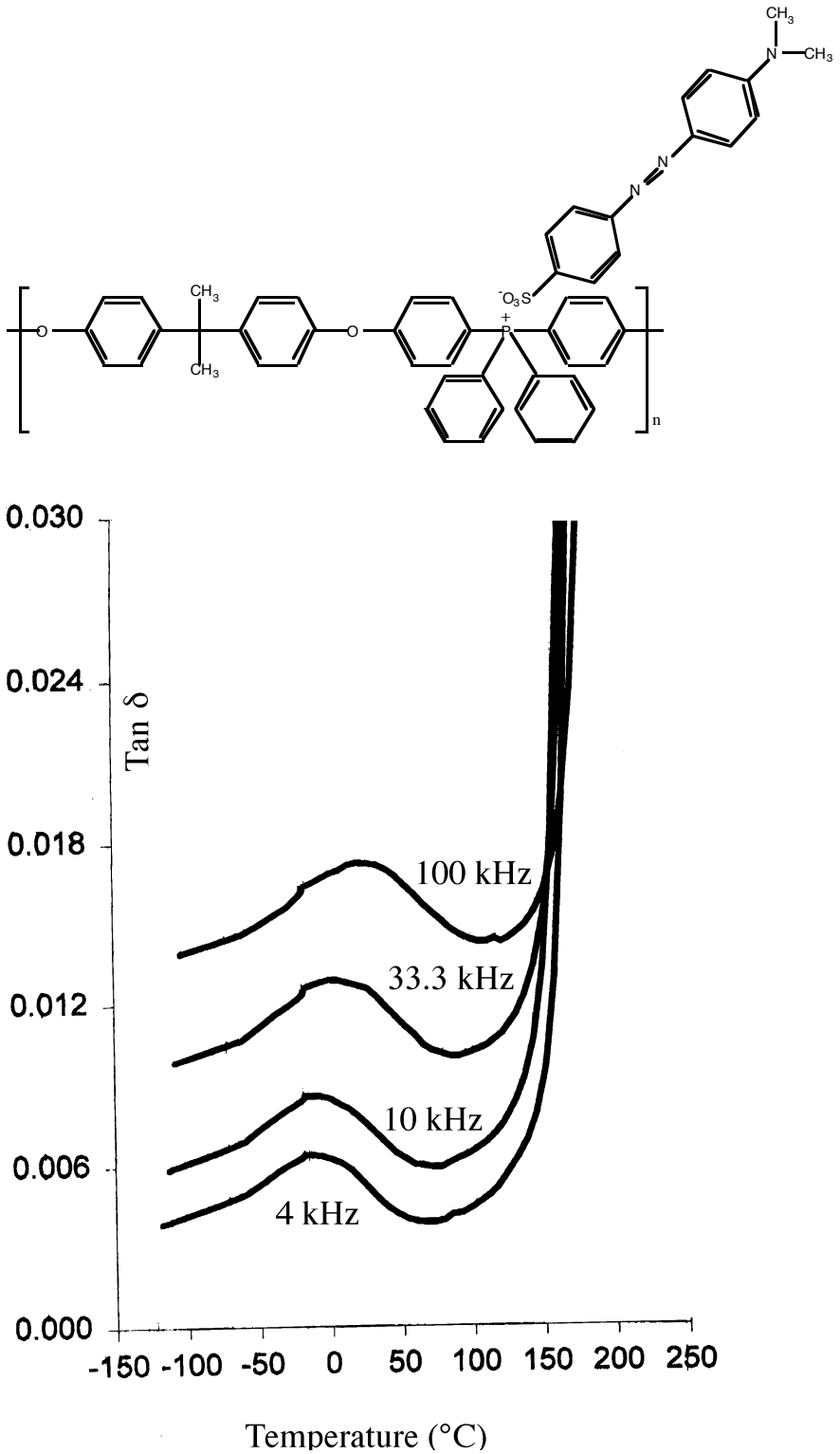

Figure 4.7.4.3 Low temperature dielectric analysis of methyl orange modified poly(arylene ether phosphonium salt)

4.8 Second Harmonic Generation

4.8.1 Background Behind Second Harmonic Generation

Second harmonic generation occurs when light waves of frequency ω interact with a medium to produce higher energy light waves at frequency 2ω. In a NLO polymeric medium the electrons are tightly bound to the nuclei so when the polymer is exposed to a low field the polarization is proportional to the applied field. However, when an intense field is applied the polarization becomes non-linear. This non-linear polarization can be expressed in the equation below (2, 137, 141).

$$P = \chi^{(1)}E + \chi^{(2)}EE + \chi^{(3)}EEE + ...$$

where P is the bulk polarization, E is the field strength and $\chi^{(1)}$, $\chi^{(2)}$, and $\chi^{(3)}$ are the linear, second and third susceptibility tensors in the relationship for the bulk polarization.

In order to generate second harmonics the polymer must contain molecules (chromophores) that have delocalized p electrons with an electron donor and acceptor on opposite ends providing resonance in one direction. The second order polarization in proportional to the electric field squared, therefore , the chromophores must be oriented noncentrosymmetrically, otherwise, in a random oriented medium there will be a cancellation of the net dipole moment of the material (138, 140). The poling method is briefly summarized below.

4.8.2 Poling of Non-linear Optical Polymers

These polymers were poled and all second harmonic generation measurements were made in Prof. H. Lackritz's group at Purdue University. The NLO polymers were spun-cast on an indium tin oxide coated glass substrate from a 10 wt.% DMSO solution. The corona poling method was utilized. Corona poling creates an electric field by generating a discharge at a tip of a needle located above the NLO material (1, 138, 141). Because of this charge the surrounding air becomes ionized and this polarity is directed toward the NLO film and creates a high electric field on the surface . Charges of opposite polarity build up at the metal bottom of the electrode. All second harmonics mentioned in this thesis were generated from material poled at room temperature. It may be significant that this ionic technique was used to pole the novel ionomers in this thesis, as opposed to some other known methods.

4.8.3 Analysis of Second Harmonic Generation (SHG)

The experimentally measured second harmonic intensity was converted to $\chi^{(2)}$ and reported. The reported $\chi^{(2)}$ values are normalized to the point when the poling voltage was turned off. Figure 4.8.3.1 is a plot of the $\chi(2)$ generated as function of time at room temperature for the methyl orange based NLO material.

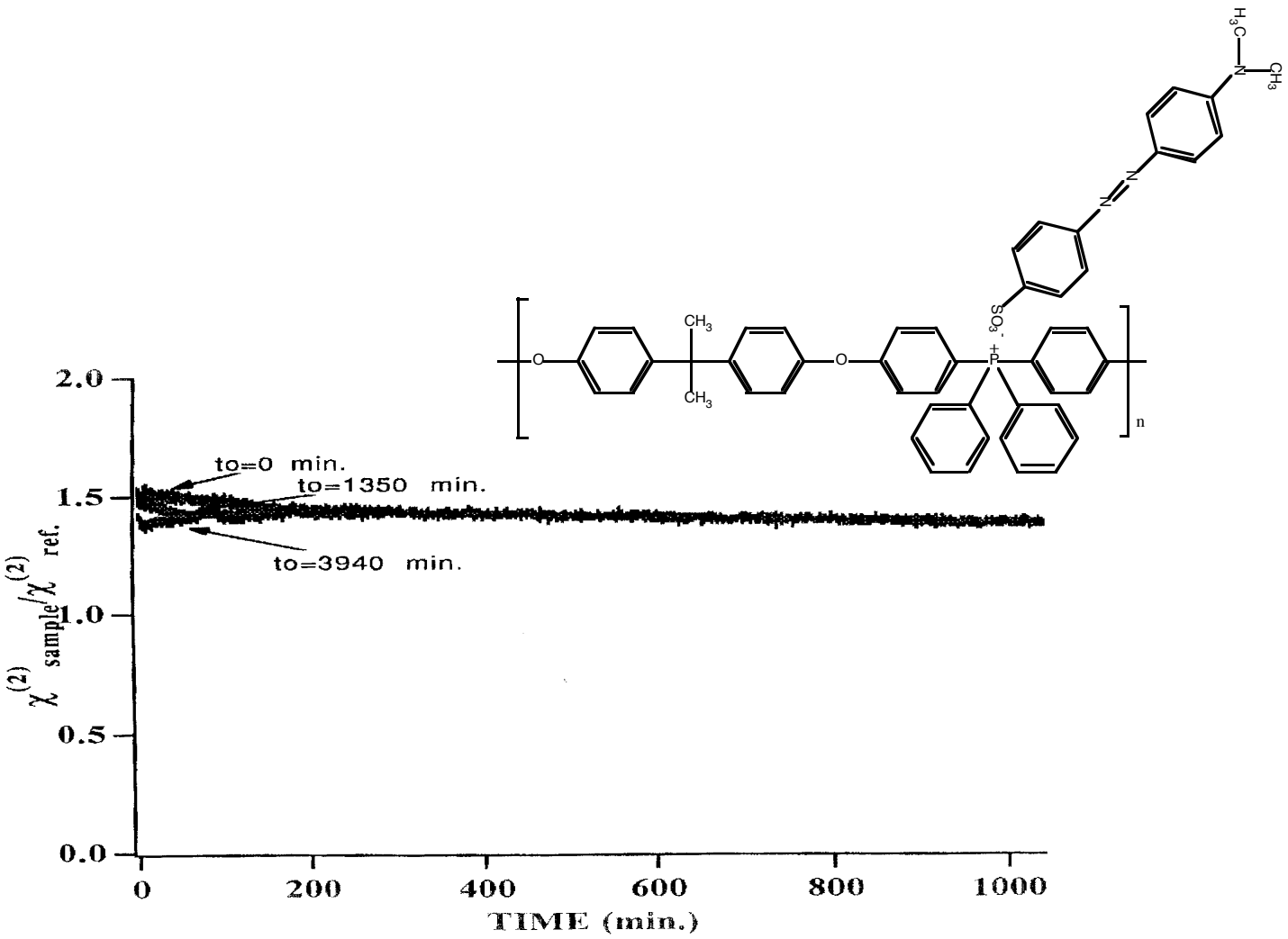

Figure 4.8.3.1 Second harmonic generation of methyl orange based NLO ionomeric material poled at room temperature

This material appears to have a stable SHG over 5000 minutes. This system shows promise of being a material that may undergo low temperature poling while also possessing stable second harmonic generation. The reproducibility of these results and the effect of temperature upon the stability of the second harmonic intensity is currently being analyzed. It is not well understood why the chromophores are able to be poled at room temperature and yet be stable subsequently. Further study is necessary to determine whether the phenomenon is real and if so what is the reason for this unique behavior.

Chapter 5.0, CONCLUSIONS

High molecular weight poly(arylene ether phosphine oxide)s were successfully synthesized via nucleophilic aromatic substitution polycondensation of aromatic bisphenols with 4,4'-bis(fluorophenyl)methyl phosphine oxide and 4,4'bis(fluorophenyl)phenylphosphine oxide in the presence of potassium carbonate and a polar aprotic solvent. The incorporation of the phosphine oxide moiety into the polymeric backbone improved the T_g, Young's modulus and char yield in air, probably as a result of enhanced intermolecular forces and generation of a phosphorus anhydride type structure during degradation. The concentration of phosphorus was also shown to increase both the dynamic and isothermal char yields is air of the poly(arylene ether)s studied. The phosphine oxide containing polymers also appear to show enhanced fire resistance due to their ability to extinguish shortly after ignition. In contrast to their different thermal, mechanical strength, and flammability, incorporation of a phosphine oxide does not appear to alter the sub-ambient damping behavior of the polymers analyzed.

Through GC-MS connected to an online pyrolysis unit, it was possible to analyze the mechanism through which these poly(arylene ether)s thermally degraded. These polymers were thermally degraded under both an inert and air environment. The poly(ether sulfone), Victrex, appeared to have similar degradation volatiles as the poly(arylene ether sulfone). In addition, there did not appear to be any volatile products containing phosphorus. This indicates that under the conditions analyzed that most of the phosphorus remains in the char and may inhibit combustion *via* a condensed phase mechanism.

Novel second order non-linear optical polymers containing ionically bonded chromophore side-chains were synthesized and characterized. These non-linear optical polymers can easily be cast into thin films from DMSO and have T_g values up to 214°C and are briefly stable in air up to 320°C as analyzed utilizing DSC and TGA respectively. Room temperature corona poling of high T_g NLO polymers has also been demonstrated. Low temperature dielectric analysis indicate that these materials possess a sub-ambient β transition.

Chapter 6.0, REFERENCES

1. D.J. Williams, Ed., *Nonlinear Optical Properties of Organic and Polymeric Materials, ACS. Symp. Ser. #233*, American Chemical Society, Washington, D.C., (1983).

2. C.Y.S. Fu, D.B. Priddy, Jr., G.D. Lyle, J.E. McGrath, and H.S. Lackritz, *Mat. Res. Soc. Symp. Proc.* **328,** 547 (1994).

3. R.N. Johnson and A.G. Farnham, *J. Polym. Sci., Polym. Chem. Ed.* **5,** 2415 (1967).

4. B.E. Jennings, M.E.B. Jones, and J.B. Rose, *J. Polym. Sci., Polym. Symp.* **16,** 715 (1967).

5. R.N. Johnson, A.G. Farnham, R.A. Clendinning, W.F. Hale, and C.N. Merriam, *J.Polym. Sci., Polym. Chem. Ed.* **5,** 2375 (1967).

6. A.G. Farnham, L.M. Robeson, and J.E. McGrath, *J. Appl. Polym. Sci. Symp.* **26,** 373 (1975).

7. T.E. Attwood, D.A. Barr, T. King, A.B. Newton, and J.B. Rose, *Polymer* **18,** 359 (1977).

8. R.N. Johnson and A.G. Farnham, *U.S. Patent 4,175,175* to Union Carbide Corp. (1979).

9. B.K. Mandal and S. Maiti, *Eur. Polym. J.* **22,** 447 (1986).

10. S. Maiti and B.K. Mandal, *J. Polym Mater.* **9,** 9 (1992).

11. H.M. Colquhoun, C.C. Dudman, M. Thinass, C.A. O'Mahoney, and D.J. Williams, *J. Chem. Soc. Chem. Comm.* **3,** 336 (1990).

12. M.J. Mullins, E.P. Woo, C.C Chen, D.J. Murray, M.T. Bishop, and K.E. Balon, *Poly. Prepr. (Am. Chem. Soc., Div. Polym. Chem.)* **32,** 174 (1991).

13. D. Xie and H. W. Gibson, *Macromol. Chem.* **197,** 2133 (1996).

14. M. Chen and H. W. Gibson, Mocromolecules 29, 5502 (1996).

15. H.R. Kricheldorf, U. Delius and K.U. Tonnes, *New Polym. Mater.* **1,** 127 (1988).

16. T.E. Attwood, A.B. Newton and J.B. Rose, *Br. Polym. J.* **4,** 391 (1972).

17. J.B. Rose, *NATO ASI Ser., Ser. C* **215,** 207 (1987).

18. I.Y. Chang, *Sci. Adv. Matl. Proc. Eng. Ser.* **33,** 194 (1988).

19. V. Jansons and K. Dahl, *Makromol. Chem., Macromol. Symp.* **51,** 87 (1991).

20. I. Colon, and G.T. Kwiatkowski, *J. Polym. Sci.: Part A-1* **28,** 367, (1990).

21. M. Ueda, and T. Ito, *Polymer* **23,** 297, (1991).

22. R.J. Cotter, Engineering Thermoplastics, A Handbook of Poly(arylene ether)s Gordon and Breach, Postfach, Switzerland, 1995.

23. R.S. Mani and D.K. Mohanty, *Polym. Mater. Sci. Eng. Proc.* **65,** 247 (1991).

24. R.S. Mani, B. Zimmerman, A. Bhatnagar and D.K. Mohanty, *Polymer* **34,** 171 (1993).

25. J.A. Miller, *Aromatic Nucleophilic Substitution*, Elsevier, London, 1968.

26. J. March, *Advanced Organic Chemistry*, McGraw-Hill, Inc., New York, 1977.

27. F.A. Carey and R.J. Sundberg, *Advanced Organic Chemistry, Part A*, Plenum, New York, 1990.

28. V. Perec, J.H. Wang and R.S. Clough, *Makromol. Chem., Macromol. Symp.* **54/55,** 275 (1992).

29. K.L. Rinehart, Jr., Ed., *Aromatic Substitution Reactions*, Prentice-Hall, Inc., Englewood Cliffs, N.J., 1968.

30. R.A. Rossi and R.H. de Rossi, *Aromatic Substitution by the $S_{RN}1$ Mechanism*, American Chemical Society, Washingtion, D.C., 1983.

31. C.G. Swain, J.E. Sheats, and K.G. Harbison, J. *Am. Chem. Soc.* **97,** 783, 796 (1975).

32. E.S. Lewis and E.B. Miller, *J. Am. Chem. Soc.* **97,** 791 (1975).

33. J.F. Bunnett and R.E. Zahler, *Chem. Revs* **49,** 294 (1951).

34. J.D. Roberts, D.A. Semenow, H.E. Simmons, Jr., and L.A. Carlsmith, *J. Am. Chem. Soc.* **78,** 601 (1956).

35. Hoffmann, *Dehydrobenzene and Cycloalkynes*, Academic Press, Inc., New York, 1967.

36. H. M. Colquhoun, *Polym. Prepr.* **25,** (2), 17 (1984).

37. C.D. Smith, Ph.D. Dissertation, Virginia Polytechnic Institute and State University, August (1991).

38. D.J. Riley, A. Gungor, S.A. Srinavasan, M. Sankarapadian, C. Tchatchoua, M.W. Muggli, T.C.Ward, T. Kashiwagi, and J.E. McGrath, *Polym. Eng. Sci.* (Accepted 1996).

39. W.F. Hale, A.G. Farnham, R.N. Johnson and R.A. Clendinning, *Polym. Prepr., Am. Chem. Soc., Div Polym. Chem.* **7,** 503 (1966).

40. R.A. Farnham and W.F. Johnson, *British Patent* 1,078,234 (1965).

41. A.B. Newton and J.B. Rose, *Polymer* **13,** 475 (1972).

42. A.E. Shumeiko and G.D. Titskii, *Zh. Org. Khim.* **14,** 1273 (1978).

43. T.E. Attwood, T. King, I.D. McKenzie, and J.B. Rose, *Polymer* **18,** 365 (1977).

44. T.E. Attwood, T. King, V.J. Leslie, and J.B. Rose, *Polymer* **18,** 369 (1977).

45. T.E. Attwood, D.A. Barr, G.G. Faasey, V.J. Leslie, A.B. Newton, and J.B. Rose, *Polymer* **18,** 354 (1977).

46. W.F. Hale, A.G. Farnham, R.N. Johnson, and R.A. Clendinning, *J. Polym. Sci.: Part A-1* **5,** 2399 (1967).

47. H. Jeong, K. Iwasaki, M. Kakimoto, and Y. Imai, *J.M.S.-Pure Appl. Chem., A31* **12,** 1975 (1994).

48. R.N. Johnson, A.G. Farnham, R.A. Clendinning, W.F. Hale and C.N. Merriam, *paper from Third Biannual Polym. Symp., A.C.S.*, June (1966).

49. M. Tokarzewska, *J. Polym. Sci., Polym. Symp.* **No. 16,** 2433 (1967).

50. M. Tokarzewska, *Polimery* **12,** 512 (1967).

51. M. Tokarzewska, *J. Polym. Sci., Part A* **6,** 777 (1968).

52. M. Tokarzewska, *Polimery* **13,** 304 (1968).

53. H.A. Vogel, *J.Polym. Sci., A-1* **8,** 2035 (1970).

54. R. Viswanathan and J.E. McGrath, *Polym. Prepr., Am. Chem. Soc., Div. Polym. Chem.* **21,** 184 (1980).

55. R. Viswanathan, B.C. Johnson, and J.E. McGrath, *Polymer* **25,** 1827 (1984).

56 P.L. Rinaldi, V.E. Litman, V. Percec, and R.S. Clough, *Macromolecules* **24,** 5889 (1991).

57. M. Novi, G. Petrillo, and M.L. Sartirana, *Tetrahedron Lett* **27,** 6129 (1986).

58. G. Petrillo, M. Novi, G. Garbarino, and C. Dellerba, *Tetrahedron* **42,** 4007 (1986).

59. V. Percec, R.S. Clough, P.L. Rinaldi, and V.E. Litman, *Macromolecules* Submitted.

60. F.R. Hartley Ed. *The Chemistry of Organophosphorous Compounds Vol. 1*, John Wiley and Sons, New York, 1990.

61. F.R. Hartley Ed. *The Chemistry of Organophosphorous Compunds Vol. 2*, John Wiley and Sons, New York, 1992.

62. S. Maiti, S. Banerjee and S.K. Palit, *Prog. Polym. Sci.* **18,** 227 (1993).

63. H.J. Grubbs, Ph.D. Dissertation, Virginia Polytechnic Institute and State University (1993).

64. S. A. Srinivasen, Ph.D. Dissertation, Virginia Polytechnic institute and State University (1994).

65. W.C. Davies, and W.J. Jones, *J. Chem. Soc*., 33 (1929).

66. W.C. Davies, P.L. Pearse, and W.J. Jones, *J.Chem. Soc*., 1262 (1929).

67. P.C. Crofts, and G.M. Kosolapoff, *J. Am. Chem. Soc*. **75,** 3379 (1953).

68. S.O. Grim, W. McFarlane, and E.F. Davidoff, *J. Org. Chem*. **32,** 781 (1967).

69. H. Hoffmann and P. Schellenbeck, *Chem. Ber*. **99,** 1134 (1966).

70. H. Hoffmann and P. Schellenbeck, *Chem. Ber*. **100,** 692 (1967).

71. S.H. Metzger, O.H. Basedow, and A.F. Isbell, *J. Org. Chem*. **29,** 627 (1964).

72. V.V. Kormachev, Yu. M. Mitrasov, and T.G. Kostantinova, *USSR Pat*., 630257 (1978); *Chem., Abstr*. **90,** 39036z (1979).

73. V.V. Kormachev, and Yu. N. Mitrasov, *Fosfororg. Soedin. Polim*. **4,** 23 (1978); *Chem. Abstr*. **92,** 76609a (1980).

74. R.T. Morrisson, and R.N. Boyd, *Organic Chemistry,* 5th ed., Allyn and Bacon, (1987) p.654.

75. C. Screttas, and A.F. Isbell, *J. Org. Chem*. **27,** 2573 (1962).

76. R.C. Srivastava, *J. Chem. Res*. (S), 330 (1985).

77. J.M. Wescott, Ph.D. Thesis, Virginia Polytechnic Institute and State University, (1993).

78. H.J. Kleiner and E. Weiss, *Chem. Abstr*. **105,** 115206a (1986).

79. E. Weiss and H.J.Kleiner, Ger. Pet., DE 3 601 247 (1977).

80. E. Weiss and H.J. Kleiner, *Chem. Abstr*. **107,** 134489c (1987).

81. G.M.Kosolapoff, In *Friedel-Crafts and Related Reactions Vol. IV* G.A. Olah, Ed., Wiley, New York, (1965).

82. L. Horner, H. Winkler, A. Rapp, A. Mentrup, H. Hoffmann, and P. Beck, *Tetrahedron Lett*., 161 (1961).

83. W.C. Davies and P.G. Lewis, *J. Chem. Soc*., 1599 (1934).

84. E. Maccarone, G. Perrini, and M. Torre, *Gazz. Chim. Ital*. **112,** 25 (1982).

85. P.M. Hergenrother, *Angew Chem. Int. Ed. Engl*. 29 (1990).

86. W.C. Kuryla and A.J. Papa Ed., *Flame Retardancy of Polymeric Materials Volume 1*, Marcel Dekker, Inc., New York, 1973.

87. W.C. Kuryla and A.J. Papa Ed., *Flame Retardancy of Polymeric Materials Volume 3*, Marcel Dekker, Inc., New York, 1975.

88. W.C. Kuryla and A.J. Papa Ed., *Flame Retardancy of Polymeric Materials Volume 4*, Marcel Dekker, Inc., New York, 1978.

89. W. L. Hawkins, Ed., *Polymer Stabilization*, Wiley-Interscience, New York, 1972.

90. *Fire Safety Aspects of Polymeric Materials Volume 1*, Technomic Publishing Co. Inc., Connecticut, 1977.

91. G.L. Nelson, Ed., *Fire and Polymers II*, American Chemical Society, Washington, D.C., 1995.

92. S. Maiti, S. Banerjee, and S.K. Palit, *Prog. Polym. Sci.* **18,** 227 (1993).

93. M.S. Lin, B.J. Bulkin, and E.M. Pearce, *J. Polym. Sci.: Polymer Chemistry Ed.* **19,** 2773 (1981).

94. S. Hashimoto, I. Furukawa, and T. Kondo, *J. Polym. Sci.: Polymer Chemistry Ed.* **12,** 2357 (1974).

95. W.C. Kuryla, and A.J. Papa Ed., *Flame Retardancy of Polymeric Materials Volume 5*, Marcel Dekker, Inc., New York, 1979.

96. National Research Council Publication NMAB-4772, *Improved Fire-and Smoke-Resistant Materials for Commercial Aircraft Interiors*, National Academy Press, Washington, D.C., 1995.

97. J. Troitzsch, *Makromol. Chem., Macromol. Symp.* **74,** 125 (1993).

98. R.L. Clough, *J. Polym. Sci.: Polymer Chemistry Ed.* **21,** 767 (1983).

99. D.W. van Krevelen, *Polymer* **16,** 615 (1975).

100. C. Yang and T. Lee, *J. Appl. Polym. Sci.* **34,** 2733 (1987).

101. C. Savides, A. Granzow, and J.F. Cannelongo, *Tech. Pap. Reg. Tech. Conf. Soc. Plast. Eng.* 18 (1975).

102. M.S. Choudhary, J.K. Fink, and K. Lederer, *J. Appl. Polym. Sci.* **30,** 4345 (1985).

103. H.F. Mark, N.M. Bikales, C.G. Overberger, G. Menges, and J.I. Kroschwitz Eds., *Encyclopedia of Polymer Engineering and Science* **7,** 19.

104. N. Ingaki, K. Tomiha, and K. Katsuura, *Polymer* **15,** 335 (1974).

105. H.N. Stokes, *Am. Chem. J.* **19,** 782 (1987).

106. H.R. Allcock, *Inorganic and Organometallic Polymers*, 250, ACS. Symposium Series No. 360. American Chemical Society, Washington, D.C., (1988).

107. D.P. Tate, and T.A. Antowiak, *Kirk-Othmer Encyclopedia of Chemical and Technology,* **10,** 939, 3rd edn. Interscience, New York, (1980).

108. R.E. Singler, G.L. Hangnauer, and R.W. Sicka, *Polymers for Fibers and Elastomers*, 143, ACS. Symposium series. No. 260, Washington, D.C., (1984).

109. H.R. Allcock, *Chem. Eng. News*. 22 (March 18, 1985).

110. R.E. Singler, M.S. Sennett, and R.A. Willingham, *Inorganic and Organometallic Polymers*, 269, ACS. Symposium Series No. 360, American Chemical Society, Washington, D.C., (1988).

111. S. Banerjef, M. Tech. Thesis, Indian Institute of Technology, Kharagpur (1990).

112. E.D. Weil, *Encyclopedia of Polymer Science and Technology* (H.F. Mark, N.M. Bikales, G.C. Overberger, and G. Menges Eds), Vol. 11. p. 96, 2nd edn; and references cited therein, Wiley-Interscience, New York, (1988).

113. E. Steininger and M. Sander, *Kunststoffe* **54,** 507 (1964).

114. E. Steininger and M. Sander, *Ger. Plast.* **54** (8), 11 (1964).

115. F. Millich and L.L. Lambring, *J. Polym. Sci. : Polym. Chem.* **18,** 2155 (1980).

116. Y. Imal, N. Sato, and M. Ueda, *Makromolek. Chem. Rapid Commun.* **1,** 419 (1980).

117. K.S. Kim, *J. Appl. Polym. Sci.* **28,** 1119 (1983).

118. A.C. Haven, *U.S. Pat. 2.716.639* (1955).

119. H.W. Coover, *U.S. Pat. 2.642.413* (1953).

120. H.W. Coover, R.L. McConnell, and N.H. Shearer, *Ind. Eng. Chem.* **52,**412 (1960).

121. A.C. Haven, *U.S. Pat. 2.835.652* (1958).

122. I.C. Popaff and J.P. King, *J. Polym. Sci. B* **1**, 247 (1963).

123. J.R. Caldwell, *U.S. Pat. 3.041.207* (1962).

124. J. Bevillers, A. Munoz, J. Navech, and J.P. Vives, *Compt. Rend.* **261,** 1547 (1965).

125. C.E. Carraher Jr. and D. Winthers, *J. Polym. Sci. Part A-1* **7,** 2417 (1969).

126. B. Tan, Ph.D. Dissertation, Virginia Polytechnic Institute and State University (1997).

127. I.K. Varma and B.S. Rao, *J. Appl. Polym. Sci.* **28,** 2805 (1983).

128. D.J. Riley, S.A. Srinivasan, A. Gungor, C. Tchatchoua, M. Sankarapandian, and J. E. McGrath, *Am. Chem. Soc., Polym. Prepr.* **37,** 489 (1996).

129. I. Wan, Ph.D. Dissertation, Virginia Polytechnic Institute and State University, (1995).

130. D Knauss, Ph.D. Dissertation, Virginia Polytechnic Institute and State University, (1995).

131. M. Sato, Y. Tada, and M. Yorkoyama, *Eur. Polym. J.* **16,** 671, (1980).

132. C.P. Fenimore and F.J. Martin, *Mod. Plast.* **44,** 141 (1966).

133. V. Bsbrauskas and R.D. Peacock, *Fire Safety Journal* **18,** 255 (1992).

134. J.A. Giordmaine The Interaction of Light with Light.

135. W.E. Moerner and S.C. Silence, *Chem. Rev, **94,** 127 (1994).*

136. R.A. Serway and J.S. Faughn, *College Physics 2nd edition,* Saunders College Publishing, Philadelphia, 1989.

137. D.M. Burland, R.D. Miller, and C.A. Walsh, *Chem. Rev.* **94,** 31 (1994).

138. K.J. Drost, A.K. Jen, and V.P. Rao, *ChemTech* 16, (1995).

139. A.F. Garito, Y.M. Cai, H.T. Man, and O. Zamani-Khamiri, *ACS. Symp. Ser.* **337,** 177 (1987).

140. T.J. Marks, and M.A. Ratner, *Angew. Chem. Int. Ed. Engl.* **34,** 155 (1995).

141. P.N. Prasad and D.J. Williams, *Introduction to Nonlinear Optical Effects in Molecules and Polymers*, John Wiley and Sons, Inc., New York, (1991).

142. R.W. Boyd, *Nonlinear Optics*, Academic Press Inc., Boston, (1992).

143. A.K. Jen, K.Y. Wong, V. Rao, K.Drost, and R.M.Mininni, *Mat. Res. Symp. Proc.* **247,** 59 (1992).

144. A.C. Newell and J.V. Moloney, *Nonlinear Optics*, Addison-Wesley Publishing Co., New York, (1992).

145. P.N. Prasad and B.A. Reinhardt, *Chem. Mater.* **2,** 660 (1990).

146. G.P. Agrawal and R.W. Boyd, Eds., *Contemporary Nonlinear Optics*, Academic Press Inc., Boston, (1992).

147. H.L. Hampsch, J. Yang, G.K. Wong, and J.M. Torkelson, *Polym. Commun.* **30,** 40 (1989).

148. M. Stahelin, C.A. Walsh, D.M. Burland, R.D. Miller, R.J. Twieg, and W. Volksen, *J. Appl. Phys.* **73,** 8471 (1993).

149. T. Goodson III, S. S. Gong, and C.H. Wang, *Macromolecules* **27,** 4278 (1994).

150. L.A. Sullivan and H.S. Lackritz, *Mat. Res. Soc. Symp. Proc.* **392,** 69 (1995).

151. H.L. Hampsch, J. Yang, G.K. Wong, and J.M. Torkelson, *Macromolecules* **23,** 3648 (1990).

152. H.L. Hampsch, J. Yang, G.K. Wong, and J.M. Torkelson, *Macromolecules* **23,** 3640 (1990).

153. R. Meyrueix and G. Mignani, *SPIE* **1127,** 160 (1989).

154. T. Verbiest, D.M. Burland, M.C. Jurich, Y.U. Lee, R.D. Miller, W. Volksen, *Science* **268,** 1604 (1995).

155. C.Y.S. Fu, H.S. Lackritz, D.B. Priddy, Jr., and J.E. McGrath, *Macromolecules* **29,** 3470 (1996).

156. C. Zhao, C. Park, P.N. Prasad, Y. Zhang, S. Ghosal, and R. Burzynski, *Chem. Mater.* **7,** 1237 (1995).

157. N. Nemoto, F. Miyata, Y. Nagase, J. Abe, M. Hasegawa, and Y. Shirai, *Macromolecules* **29,** 2365 (1996).

158. Z. Liang, Z. Yang, S. Sun, B. Wu, L.R. Dalton, S.M. Garner, S. Kalluri, A. Chen, and W.H. Steier, *Chem. Mater.* **8,** 2681, (1996).

159. H. Jiang, A.K. Kakkar, A. Lebuis, H. Zhou, and G.K. Wong, *J. Mater. Chem.* **6,** 1075 (1996).

160. M. Trollsas, C. Orrenius, F. Sahlen, U.W. Gedde, T. Norin, A. Hult, D. Hermann, P. Rudquist, L. Komitov, S.T. Lagerwall, and J. Lindstron, *J. Am. Chem. Soc.* **118,** 8542 (1996).

161. M.A. Firestone, J. Park, N. Minani, M.A. Ratner, T.J. Marks, W. Lin, and G.K. Wong, *Macromolecues* **28,** 2247 (1995).

162. D. Yu, A. Gharavi, and L. Yu, *Macromolecules* **29,** 6139 (1996).

163. K. Kajikawa, H. Nagamori, H. Takezoe, A. Fukuda, S. Ukishima, Y. Takahashi, M. Iijima, and E. Fukada, *Jpn. J. Appl. Phys. 2, Lett.* **30,** 1737 (1991).

164. F. Fuso, A.B. Padias, and H.K. Hall, Jr., *Macromolecules* **24,** 1710 (1991).

165. W. Kohler, D.R. Robello, P.T. Dao, C.S. Willand, and D.J. Williams, *J. Chem. Phys.* **93,** 9157 (1990).

166. H.K. Hall, Jr., T. Kuo, and T.M. Leslie, *Macromolecules* **22,** 3525 (1989).

167. G.D. Green, J.I. Weinschenk, III, J.E. Mulvaney, and H.K. Hall, Jr., *Macromolecules* **20,** 722 (1987).

168. G.D. Green, H.K. Hall, Jr., J.E. Mulvaney, J. Noonan, and D.J. Williams, *Macromolecules* **20,** 716 (1987).

169. G.H. Hsiue, J.K. Kuo, R.J. Jeng, J.I. Chen, X.L. Jiang, S. Marturunkakul, J. Kumar, and S.K. Tripathy, *Chem. Mater.* **6,** 884 (1994).

170. S. Ducharme, J.C. Scott, R.J. Twieg, and W.E. Moerner, *Phys. Rev. Lett.* **66,** 1846 (1991).

171. D. Jungbauer, B. Reck, R. Twieg, D. Yoon, C. Willson, and Swalen, *J. Appl. Phys. Lett.* **56,** 2610 (1990).

172. N. Venkatasubramanian, D. Dean, and F.E. Arnold, *Am. Chem. Soc. Polym. Prepr.* **38,** 354 (1996).

173. E. Bonaplata, M.S. Thesis, Virginia Polytechnic Institute and State University, (1994).

174. E. Bonaplata, H. Ding, B.E. Hanson, and J.E. McGrath, *Polymer* **36,** 3035 (1995).

175. H. Ghassemi, M, Curtis, E. Bonaplata, and J.E. McGrath, *Polym. Prepr.* **37,** 420 (1996).

176. M. Konas, T.M Moy, M.E. Rogers, A.R. Shultz, T.C. Ward, and J.E. McGrath, J. Poly. Sci., Poly. Phys. 33, 1429 (1995).

177. D.B. Priddy, Jr. and J.E. McGrath, *Polymer Preprints* **33,** 231 (1992).

178. A. Bhatnagar, Ph.D. Thesis, Michigan Technological University, (1995).

179. T.E. Attwood, P.C. Dawson, J.L. Freeman, L.R.J. Hoy, J.B. Rose, and P.A. Staniland, *Polymer* **22,** 1096 (1981).

180. C.D. Smith, H. Grubbs, H.F. Webster, A. Gungor, J.P. Wightman, and J.E. McGrath, *High Performance Polymers* **3,** (1991).

181. E.M. Pearce, S.C. Lin, M.S. Lin, and S.N. Lee, *Eastern Analytical Symposium in Thermal Methods in Polymer Analysis 187* (1978).

182 D.M. Knauss and J.E. McGrath, In *ACS Symposium Series No 599, Fire and Polymers II: Materials and Tests for Hazard Prevention,* G.L. Nelson, Ed. (1994).

183. I.Y. Wan, J.E. McGrath, and T. Kashiwagi, In *ACS Symposium Series No 599, Fire and Polymers II: Materials and Tests for Hazard Prevention*,G.L. Nelson, Ed. (1994).

184. B. Hartman and G.F. Lee, *J. Appl. Polym. Sci.* **23,** 3639 (1979).

Chapter 7.0, VITA

Daniel Joseph Riley was born in Lompoc, California on July 26, 1971. He grew up in Santa Ynez, California where he graduated from high school in 1989 and subsequently joined Cypress College to pursue a career in science. He transferred to Radford University in 1991 where he graduated with Magna Cum Laude with a B.S. in chemistry in 1993. He was awarded the American Chemical Society, Blue-Ridge Division award for excellence in chemistry. The author then entered the graduate program in chemistry at Virginia Polytechnic Institute and State University in 1993, where he obtained his Doctoral Degree in 1997. As a graduate student he presented papers in both regional and national meetings. Mr. Riley married Michele Leigh Nelson on July 15, 1995. Immediate plans for Daniel include employment with Ashland Chemical in Columbus, Ohio as a polymer research chemist.